Phenomenological Aspects of Noncommutative Standard Model

A thesis submitted in partial fulfillment of
the requirements for the degree of

DOCTOR OF PHILOSOPHY

by

Selvaganapathy J
(Roll No. 2012PHXF0015G)

Under the guidance of
Dr. Prasanta Kumar Das (Supervisor)
and
Dr. Partha Konar (Co-supervisor)

DEPARTMENT OF PHYSICS
BIRLA INSTITUTE OF TECHNOLOGY AND SCIENCE, PILANI
May - 2018

Dedicated to my parents

and

family members

BIRLA INSTITUTE OF TECHNOLOGY AND SCIENCE, PILANI
(RAJASTHAN)

CERTIFICATE

This is to certify that the thesis entitled **Phenomenological Aspects of Noncommutative Standard Model** submitted by **Selvaganapathy J**, ID No 2012PHXF0015G for award of Ph.D. of the Institute embodies original work done by him under our supervision.
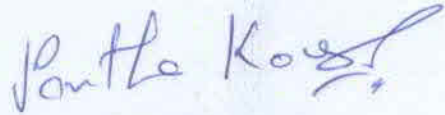

Signature of the Supervisor

Name: Dr. PRASANTA KUMAR DAS

Designation: Associate Professor

Affiliation: BITS PILANI

Date: 16/05/18

Signature of the Co-Supervisor

Name: Dr. PARTHA KONAR

Designation: Associate Professor

Affiliation: Physical Research Laboratory, Ahmedabad

Date: 16/05/18

Abstract

The Standard Model(SM) of Particle Physics has so far been extremely successful, with a recent major triumph in discovering and constraining the properties of the last missing bit of the SM, the Higgs boson. Apart from some discrete and isolated hints, it is broadly evasive, lacking any clinching evidence yet supporting the physics beyond the standard model (BSM) experiment at Large Hadron Collider (LHC) at the TeV energy scale, exploration of which is one of the primary motives for post-Higgs LHC. On the other side, it is widely admitted that the Standard Model is valid only up to a scale of several hundred GeV i.e it is at most a very good description for low energy effective theory which, in fact, falls short to explain several outstanding issues both in terms of theoretical construction and elegance as well as experimental observations.

The idea of field theories on the noncommutative (NC) spacetime is rather primeval, yet fascinate by introducing a fundamental length scale in the model consistent with the symmetry. These ideas are further revived after realization of their possible connection with quantum gravity, where noncommutativity is perceived as an outcome of certain string theory embedded into a background magnetic field. Just like the quantization in phase space, the spacetime coordinate in the noncommutative spacetime gets replaced by an operator $\hat{x}_\mu$ which satisfy the commutation relation

$$[\hat{x}_\mu, \hat{x}_\nu] = i\Theta_{\mu\nu} = i\frac{c_{\mu\nu}}{\Lambda^2}.$$

where $\Theta_{\mu\nu}$ is an antisymmetric matrix tensor, which has the dimension of area reflecting the extent to which the spacetime is fuzzy i.e. noncommutative. $c_{\mu\nu}$ is the anti-symmetric constant c-number matrix which gives a preferred directionality and also a non-vanishing contribution results in deviating from exact Lorentz invariance is broken at all scale Λ, the scale of spacetime noncommutativity. The construction of the noncommutative standard model relies on two important blocks: Moyal-Weyl(MW) $\star$-product of field functions on ordinary spacetime and the Seiberg-Witten(SW) maps. In the SW map, the field variables and the gauge transformation parameter are defined by a formal power series expansion of the fields in terms of Θ. By means of Weyl-Moyal star product and Seiberg-Witten maps, the noncommutative standard model to order $\mathcal{O}(\Theta)$ have been constructed as the effective theory: the minimal Nonconcommutative Standard Model(mNCSM) in which the SM vertices are modified and the non-minimal Nonconcommutative Standard Model(nmNCSM) in which besides those modified SM vertices, several new interactions also appear which are not present in the standard model.

Since the Lorentz invariance including the rotational invariance around the beam axis is broken by the spacetime noncommutativity(which defines a preferred direction), the azimuthal distribution of the cross-section will no longer be isotropic due to its strong ϕ dependence. This azimuthal anisotropy, absent in most of the beyond the standard models (BSM), can be used to single out spacetime non-commutativity from other class of BSM physics by looking at processes at the TeV energy colliders. Besides the fact that the SM vertices get modified in NC space-time, new interactions (e.g. triple neutral gauge boson coupling) also emerge. These vertices as well as directional features incorporated as new features, present and future colliders certainly can provide an opportunity to verify these new physics at TeV scale as well constrain different parameters and the NC scale Λ.

Although theoretically the value of Λ is not known, however if this effective scale lies somewhere between hundreds of GeV to few TeV range, then it can be probed by the ongoing proton-proton Large Hadron Collider or the upcoming electron-positron linear collider. Now most of existing collider searches of spacetime noncommutativity were made in the context of electron-positron collider, only few were available in the context of LHC. Also the effect of earth rotation was not considered in most of the phenomenological searches for the sake of simplicity, which however needs to be taken into account in order to make any serious phenomenological investigation. The present thesis is an effort to fill those gaps and it aims

1. To widen our understanding of the magnitude of the noncommutative scale Λ by looking at processes both at LHC and LC with and without considering the effect of earth rotation into the analysis and have better understanding of the structure of spacetime at high energy.

2. To see how the anisotropic behaviour of the cross-section arising due to the violation of Lorentz invariance can throw light in understanding the structure of spacetime at high energy.

Thesis is organized as follows. In chapter 1, we give a brief review of the Standard model of particle physics, discuss about its gauge structure, particle content and the Higgs mechanism. We discuss about several limitations of the SM: Theoretical question (e.g. hierarchy problem, baryon asymmetry, generation problem etc) and Experimental finding (neutrino oscillation, dark matter etc) of and the necessity of having the beyond the standard model physics(BSM).

In chapter 2, we give a brief introduction of space-time noncommutativity, discuss about the Weyl-Moyal and Seiberg-Witten approach for doing NC phenomenology, and discuss about the construction of minimal and non-minimal noncommutative standard model(NCSM).

In chapter 3, we investigate the higgstralung process $e^+e^- \rightarrow Zh$ process at the LC in the nmNCSM.

We calculate the cross-section using the the Feynman rules to all orders of the noncommutative parameter $\Theta_{\mu\nu}$, with special emphasis on including the effect of earth rotation on the orientation of the NC tensor $\Theta_{\mu\nu}$ on the cross-section and the azimuthal distribution etc corresponding to the machine energy varying from 0.5 TeV to 3 TeV for $\Lambda \geq 0.5$ TeV.

In chapter 4, we study the Drell-Yan process at the Large Hadron Collider in the noncommutative spacetime. We calculate the production cross section to the first order in $\Theta_{\mu\nu}$. An outstanding feature from this nonminimal noncommutative standard model not only modifies the couplings over the SM production channel, but also allows additional nonstandard vertices which can play a significant role and in the Drell-Yan process, one also needs to account for the gluon fusion process i.e. the presence of $g - g - \gamma$ and $g - g - Z$ vertices at the tree level. We find some of the characteristic signatures such as oscillatory azimuthal distributions, are an outcome of the momentum-dependent effective couplings and explore the noncommutative scale $\Lambda \geq 0.4$ TeV, considering different machine energy ranging from 7 TeV to 13 TeV.

In chapter 5, we study the top quark pair production in the noncommutative spacetime in LC. Using the $\mathcal{O}(\Theta)$ Feynman rule, we obtained the cross section and the azimuthal distribution of the top quark pair production and investigated their sensitivies on the $\Theta_{\mu\nu}$ distribution of the pair top quark pair production and investigated their sensitivies in the case of space-time(ST) noncommutativity, space-space(SS) noncommutativity and space-time & space-space noncommutativity. In the case of space-space noncommutivity, the fact that $(\sigma_{SS} - \sigma_{SM}) \leq 0.02\sigma_{SM}$, gives rise the lower bound on the NC scale $\Lambda \geq 0.65$ TeV. In the presence of earth rotation, the time-averaged cross section $\langle \sigma(t) \rangle_T$ attains its maximum value corresponding to the orientation angle $\eta = \pi/2$ (η, the orientation angle of the NC vector w.r.t the earth axis of rotation(fixed direction)). The azimuthal $\left\langle \frac{d\sigma(t)}{d\phi} \right\rangle_T$ vs ϕ distribution, completely flat in the SM, shows peaks and troughs in the case of NCSM corresponding $\eta = \pi/2$ and $\Lambda = 0.65$ TeV at $E_{com} = 1$ TeV. The oscillatory behaviour of the azimuthal distribution and the diurnal behaviour of the top-quark production cross section over the period of a complete day and night can be an useful tool in isolating spacetime noncommutativity from other class of BSM models. In chapter 6, we summarize our thesis work and conclude.

Declaration of Academic Integrity

I, **Selvaganapathy J**, S/o Mr. M. Jaganathan, declare that this written submission represents my ideas in my own words and where others ideas or words have been included, I have adequately cited and referenced the original sources. I also declare that I have adhered to all principles of academic honesty and integrity and have not misrepresented or fabricated or falsified any idea/data/fact/source in my submission. I understand that any violation of the above will be cause for disciplinary action as per rules of regulations of the Institute.

Selvaganapathy J

Acknowledgement

Contents

List of Tables

List of Figures

Nomenclature

Physical constants

Quantity	Symbol	Value
speed of light in vacuum	c	$299,792,458\,m/s$
Planck constant	h	$6.62607 \times 10^{-34}\,Js$
Planck constant, reduced	$\hbar$	$1.0545 \times 10^{-34}\,Js$
electron charge magnitude	e	$1.6021 \times 10^{-19}\,C$
conversion constant	$\hbar c$	$197.326\,MeV\,fm$
conversion constant	$(\hbar c)^2$	$0.3893\,GeV^2\,mbarn$
electron mass	m_e	$0.510\,MeV/c^2$
proton mass	m_p	$938.272\,MeV/c^2$
fine-structure constant	$\alpha = e^2/4\pi\epsilon_0\hbar c$	$1/137.035$
Fermi coupling constant	$G_F/(\hbar c)^3$	$6.6740 \times 10^{-11}\,m^3 Kg^{-1} s^{-2}$
weak-mixing angle	$\sin^2\theta(M_Z)$	0.2312
$W^\pm$ boson mass	M_W	$80.385\,GeV/c^2$
Z^0 boson mass	M_Z	$91.187\,GeV/c^2$
strong coupling constant	$\alpha_s(M_Z)$	0.1181
Top quark mass	M_t	$172.44\,GeV/c^2$
Higgs mass	M_H	$125.09\,GeV/c^2$

Mathematical sets

$\mathcal{R}^n$	Real n dimensional flat space(Euclidean)	Adj	Adjoint
Σ	String world sheet in $\mathcal{R}^{10}$	$\{\,\}$	Set
D_p	Dirichlet p space dimensional brane	$\sum$	Sum
$\mathcal{M}$	Spacetime manifold	$\prod$	Product
$\mathcal{F}$	Noncommutative finite internal space	$\mathcal{I}$	Ideal
$\mathbb{C}^\infty$	complex-valued infinite smooth function	$\triangle$	Difference
$Diff()$	Diffeomorphism	e_μ^a	Four dimensional Vierbein
$\mathcal{U}$	Noncommutative spacetime Gauge group	ω_μ^{ab}	Spin connection
$\mathbb{R}$	Real Numbers	$\mu(...)$	Map
$\mathbb{C}$	Complex Numbers	$W(f)$	Weyl operator of f
$\mathbb{H}$	Quaternions	$\triangleleft$	Operation on left hand side
$\mathbb{I}$	Identity(Unit matrix)	$\triangleright$	Operation on right hand side
$\mathcal{H}$	Hilbert space	$\mathcal{O}$	order of
$\|.\|$	Norm	$\theta^{\mu\nu}$	Noncommutative tensor
$\in$	Belongs to	$\widehat{R}$	Manin plane R Matrix
$\ltimes$, $\rtimes$	Multiplication from left,from right	$\square$	D'Alembertian
$\oplus$, $\otimes$	Matrix addition, Multiplication	γ_E	Euler-Mascheroni constant
$L^2(\mathcal{M}, S)$	Spinor manifold(spin1/2)	Λ	Noncommutative scale
$Aut()$, $Inn()$	Automorphism, Innermorphism	$\mathcal{T}$	SU(N) generator
$iso()$,	Isomorphism	Y	Hypercharge
$\subset$	Proper subset	y	Rapidity
$\forall$	For all	Q	Charge
Tr	Trace	α, α_s	QED,QCD fine structure constant
$\star$	Star product		

Abbreviation

ADD	Arkani-Hamed-Dimopoulos-Dvali
BSM	Beyond the Standard Model
CBH	Campbell-Baker-Hausdroff
CHARM-II	CERN-Hamburg-Amsterdam-Rome-Moscow
CKM	Cabibbo-Kobayashi-Maskawa
CL	Confidence Level
CLIC	Compact Linear Collider
CMBR	Cosmic Microwave Background Radiation
CMS	Compact Muon Solenoid
CP	Charge conjugation-Parity
CTEQ6L	Co-ordinated Theoretical-Experimental Project on QCD version 6 Leading Order
DM	Dark Matter
DY	Drell-Yan
GCP	Gauge Consistency Principle
GEP	Gauge Equivalence Principle
GUT	Grand Unification Theory
GWS	Glashow-Weinberg-Salam
ISR	Initial State Radiation
LEP	Large Electron-Positron Collider
LC	Linear Collider
LHC	Large Hadron Collider
LSND	Liquid Scintillator Neutrino Detector
mNCSM	minimal Noncommutative Standard Model
MSW	Mikheyev-Smirnov-Wolfenstein

MW	Moyal-Weyl
NEMO	Neutrino Ettore Majorana Observatory
NCG	Noncommutative Geometry
nmNCSM	non-minimal Noncommutative Standard Model
NCPS	Noncommutative Phase Space
NCQED	Noncommutative Quantum Electrodynamics
NCQM	Noncommutative Quantum Mechanics
NCS	Noncommutative Space
NS-B	Neveu-Schwarz-B field
OPAL	Omni-Purpose Apparatus at LEP
PBW	Poincare-Birkhoff-Witt
PDF	Parton Distribution Function
PMNS	Pontecorvo-Maki-Nakagawa-Sakata
QM	Quantum Mechanics
RS	Randall-Sundrum
SHE	Spin Hall Effect
SLAC	Stanford Linear Accelerator Center
SM	Standard Model
SNO	Sudbury Neutrino Observatory
SSB	Spontaneous Symmetry Breaking
SSM	Standard Solar Model
SSNC	Space-Space Noncommutative
STNC	Space-time Noncommutative
SW	Seiberg-Witten
TEXONO	Taiwan EXperiment On NeutrinO
TGB	Triple Gauge Boson
UV/IR	Ultra-Violet/Infra-Red
VIP	Violation of the Pauli exclusion principle
XFEL	X-ray Free Electron Laser

Keywords

Standard Model, Beyond the standard model, Open String dynamics, Quantum spacetime, Space-time noncommutativity, Seiberg-Witten map, Canonical deformed space, Moyal-Weyl star product, Filk-Feynmann planar diagram, Goldstone theorem, Higgs mechanism, Vacuum stability, Higgs mass hierarchy, Atmospheric neutrino anomaly, Solar neutrino problem, Extra dimension, Noncommutative gauge theory, Heisenberg-Pauli QED, Snyder space, Pointless geometry, Landau Problem, Neveu-Schwartz B-field, Bosonic strings theory, Spin manifold, Hilbert space, Riemannian spin manifold, Quaternions, Krein space, Lorentzian geometry, Twisted Poincare symmetry, Noncommutative QED, Charge quantization, Lorentz violation, UV/IR mixing, Translational invariant $1/p^2$ model, minimal NCSM, Non-minimal NCSM, Triple gauge boson interaction, Multi-objective Weighted sum optimization, Status of the Noncommutative phenomenology, Higgsstrahlung, Earth rotation effect, Drell-Yan, top anti-top pair production, Time averaged azimuthal anisotropy, Diurnal variation, Space-time noncommutativity, Space-space noncommutativity.

List of Publications

1. *Tsallis statistics and role of a stabilized radion in supernovae SN1987A Cooling.*
   Prasanta Kumar Das, **Selvaganapathy J**, C.Sharma, T.K.Jha and V.SunilKumar,IJMP A28,1350152 (2013),(arXiv:1210.7407).

2. *Probing spacetime noncommutativity in the top quark pair production at e^+e^- collider.*
   Ravi S Manohar, **Selvaganapathy J** and Prasanta Kumar Das, IJMP A29, 1450156 (2014).

3. *Search for associated production of Higgs boson with Z boson in the NCSM at linear colliders.*
   Selvaganapathy J, Prasanta Kr. Das and Partha Konar, IJMP A30,1550159(2015),(arXiv:1509.06478).

4. *Drell-Yan as an avenue to test noncommutative standard model at large hadron collider.*
   Selvaganapathy J, Prasanta Kr. Das and Partha Konar, Phys.Rev.D93:116003(2016),(arXiv:1602.02997).

5. *q-deformed statistics and the role of a light dark matter fermion in the supernovae SN1987A cooling.*
   Atanu Guha, **Selvaganapathy J** and Prasanta Kr. Das, Phys. Rev. D 95,015001(2017),(arXiv:1509.05901).

6. *Spacetime noncommutativity and $e^+e^- \xrightarrow{\gamma,Z} t\bar{t}$ process at the TeV energy collider.*
   Selvaganapathy J and Prasanta Kr. Das , Submitted to J. Phys. Commun.

This thesis is based on following publications

1. *Search for associated production of Higgs boson with Z boson in the NCSM at linear colliders.*
   Selvaganapathy J, Prasanta Kr. Das and Partha Konar, IJMP A30,1550159(2015).

2. *Drell-Yan as an avenue to test noncommutative standard model at large hadron collider.*
   Selvaganapathy J, Prasanta Kr. Das and Partha Konar, Phys.Rev.D93:116003,(2016).

3. *Spacetime noncommutativity and $e^+e^- \xrightarrow{\gamma,Z} t\bar{t}$ process at the TeV energy collider.*
   Selvaganapathy J and Prasanta Kr. Das , Submitted to J. Phys. Commun.

Chapter 1

The Standard Model of Particle Physics

" Science is shaped by ignorance. Great questions themselves evolve, of course, because their answers spawn new and better questions in turn". - David Gross

1.1 Introduction

The standard model (SM) of elementary particles which describes how the elementary particles interact with each other has been consistently developed over the last five decades and became compatible with the experimental results all the way around. The basic building blocks of the SM i.e. the particles, are classified into two classes due to their spin: fermions and bosons. Neutrinos, Leptons and Quarks are the fermionic matter particle which has spin $\frac{1}{2}$ angular momentum. On the other hand, there are two types of bosonic matter particles i.e spin 1 vector boson e.g. Photon(γ), $W^{\pm}$ and Z bosons and spin 0 scalar bosons e.g. Higgs boson (h). In addition, there are eight spin 1 vector bosons called gluons. Bosons are force carriers between fermionic matter particles.

The standard model accommodate three types of interaction (i) Strong interaction: Gluons are the force carriers between quark interaction, (ii) Electromagnetic(EM) interaction: Photon (γ) is responsible for electromagnetic(EM) interaction between quarks and leptons. (iii) Weak interaction: $W^{\pm}$ and Z bosons are responsible for weak interaction between neutrinos, leptons and quarks. Note that neutrinos do not take part in electromagnetic and strong interactions. These gluons, photon(γ), weak bosons $W^{\pm}$ and Z bosons are all known as gauge bosons. The last one is called Higgs interaction. The Higgs interaction with the SM particles is responsible for mass of the SM particle. Note that neutrinos remains massless in the SM.

The Standard model is a theory based on the local $SU(3)_c \otimes SU(2)_L \otimes U(1)_Y$ gauge symmetry group which makes the theory a gauge invariant one.

1.1.1 Symmetry

A symmetry operation is the some sort of transformation on the physical system which leaves the system unchanged and it leads to the conservation of particular physical quantities. If U is a symmetry operation on the system described by the Hamiltonian H, then H is invariant if and only if $UHU^\dagger = H$. According to Noether's theorem, the parameter of U is a constant of motion. The simplest incarnation of Noethers theorem, which states that whenever we have a continuous symmetry of Lagrangian, there is an associated conservation law.

Symmetry		Conserved quantities
Space translation	$\longleftrightarrow$	Linear momentum
Time translation	$\longleftrightarrow$	Energy
Rotation	$\longleftrightarrow$	Angular momentum
Gauge transform	$\longleftrightarrow$	Charge

Table 1.1: Symmetry operation and law of conservation

It is an universal property of the nature which plays a crucial role in condensed matter physics, Particle physics, String theory, Astrophysics and Cosmology etc. Steven Weinberg interpreted this symmetry as,

"A law of nature can be said to respect a certain symmetry if that law remains the same when we change the point of view from which we observe natural phenomena in certain definite ways. The particular set of ways that we can change our point of view without changing the law defines the symmetry."

The symmetry transformations are described by the distinct group elements of appropriate symmetry group. Predominantly, symmetries can be classified into two types: (i) discrete symmetry and (ii) continuous symmetry.

- Discrete Symmetries: The symmetry transformation parameters can take discrete values. For example, Parity P , Charge Conjugation C and Time Reversal T. The electromagnetic interactions and the strong interactions preserve C , P and T symmetry separately, whereas in weak interaction C, P and CP symmetries are not preserved. According to the CPT theorem we

know that all interactions has to be invariant under the combined transformation given by C, P and T, regardless their order.

- Continuous Symmetries: The symmetry transformation parameters take continuous values. There are several types of continuous symmetries. For example, space-time symmetries and internal symmetries are the class of continuous symmetries which play an important role in particle physics.

  - Space-time symmetries: Symmetry transformations that act on the space-time. Typical examples are translations, rotations, etc. The invariance of time translation, space translation and space rotation exhibits the homogeneity of time, space and isotropy of the space respectively in nature.

  - Internal Symmetries: The internal symmetries, not the space-time symmetries, are related to the gauge symmetries which are responsible for interactions/forces in the gauge theory. The typical examples are electromagnetic charge is responsible for electromagnetic forces, weak-Isospin symmetry for weak force and Color symmetry for strong force etc. The internal symmetry operations are the phase transformation of the fields. If the phase is independent of space-time then it is called the global phase transformation (global symmetry) and if the phase is dependent on space-time, then it is called the local phase transformation(local symmetry). Customarily these internal symmetries are described by Lie groups.

1.2   Gauge theory

The gauge field theory provides an insight about the fundamental interactions of the SM particles. The interaction between matter fermion is realized as a some kind of phase transformation on the matter field i.e.$\psi' = U \ \psi$ where $U = \exp(-iq\theta/\hbar c)$ is "unitary". θ is the phase parameter, q, the matter charge(it can be hypercharge or isotopic charge or color charge), act as the generator of the gauge transformation [1].

1.2.1   Global and Local gauge theory

The unitary transformation matrix $U = \exp(\frac{-iq\theta}{\hbar c})$: is a representation of abelian $U(1)$ group. Similarly, $U = \exp(\frac{-igT^i\epsilon^i}{\hbar c})$ is a representation of the non-abelian $SU(2)$ group with T^i being its

generators and ϵ^i are the transformation parameters. Depending on whether the transformation parameter(s) θ (in case of $U(1)$) and ϵ^i (in case of $SU(2)$) are function of spacetime coordinate (x^μ) or not, the transformation will be called local or global. We will be working with $\hbar = 1$, $c = 1$ throughout the thesis.

$U(1)$ global and local gauge symmetry

$U(1)$ **global gauge symmetry**: In quantum gauge theory, the global gauge symmetry requires only conservation laws which do not require any other new gauge field or forces, because global symmetry preserves the symmetry in all spacetime points as a constant. Consider the lagrangian of a free Dirac fermion of mass m

$$\mathcal{L}_0 = \bar{\psi}\left(i\gamma^\mu\partial_\mu - m\right)\psi$$

Consider the global $U(1)$ transformation $\psi \longrightarrow \psi' = U\psi = e^{-iq\theta}\psi$, where θ is independent of spacetime coordinates and q is the Noether charge (group generator) of the particle.

Now the above lagrangian is invariant under the global $U(1)$ transformation i.e. $\mathcal{L}_0(\psi) = \mathcal{L}'_0(\psi \to \psi')$. The conserved Noether current is $j^\mu = q\bar{\psi}\gamma^\mu\psi$, and q is the Noether $U(1)$ charge q of the particle.

$U(1)$ **local gauge symmetry**: The matter fermion ψ transforms under the local $U(1)$ transformation as $\psi \longrightarrow \psi' = U\psi = e^{-iq\theta(x)}\psi$. One finds that $\mathcal{L}'_0 = \mathcal{L}_0 + q\bar{\psi}\gamma^\mu\psi\,\partial_\mu\theta(x)$ i.e. $\mathcal{L}_0 \neq \mathcal{L}'_0$. So, $\mathcal{L}_0$ is not invariant under the local gauge transformation. To make it gauge invariant, we modify the derivative ∂_μ as $D_\mu = \partial_\mu + iqA_\mu$ (called the covariant derivative), where A_μ is the $U(1)$ gauge field. Accordingly, the lagrangian becomes

$$\overline{\mathcal{L}_0} = \mathcal{L}_0 - j_\mu A_\mu$$

where $j^\mu = q\bar{\psi}\gamma^\mu\psi$. This can made gauge invariant by introducing a 4-gauge potential $A_\mu(x)$ and the following transformation under the local $U(1)$ gauge transformation

$$A_\mu(x) \to A'_\mu(x) = A_\mu(x) - \partial_\mu\theta(x)$$

. The theory which describes electron-photon interaction is known as Quantum Electrodynamics(QED). It is described by the lagrangian,

$$\mathcal{L}_{QED} = \bar{\psi}\left(i\gamma^\mu D_\mu - m\right)\psi - \frac{1}{4}F^{\mu\nu}F_{\mu\nu}$$

where $F_{\mu\nu} = \partial_\mu A_\nu - \partial_\nu A_\mu$. Here A_μ is the photon field, $F_{\mu\nu}$ is the photon field strength tensor and ψ the fermionic matter field corresponds to electron.

$SU(2)$ **and** $SU(3)$ **local gauge symmetry**

In the same way the strong interaction (quark-gloun interaction) and the weak interaction (quark,lepton interaction with $W^{\pm}$ and Z bosons) can be formulated as a $SU(3)$ gauge theory and a $SU(2)$ gauge theory, respectively. In general, the lagrangian of a $SU(N)$ gauge theory (with $N = 2, 3$) can be written as

$$\mathcal{L} = \bar{\Psi}\left(i\gamma^{\mu}D_{\mu} - m\right)\Psi - \frac{1}{4}F^{\mu\nu a}F^{a}_{\mu\nu}$$

where the matter field transform as $\Psi \longrightarrow \Psi' = U\Psi = e^{-ig\sum_a T^a\theta^a(x)}\Psi$ (where $a = 1, 2, ...N^2 - 1$) and the gauge field as

$$A'_{\mu}(x) = UA^{\mu}(x)U^{\dagger} + \frac{i}{g}\left(\partial_{\mu}U\right)U^{\dagger}; \quad F'_{\mu\nu}(x) = UF_{\mu\nu}(x)U^{\dagger}$$

Here the $SU(2)$ generator $T^a = \frac{\tau^a}{2}$ (τ^a, $a = 1, 2, 3$,the Pauli matrices) and the $SU(3)$ generator $T^b = \frac{\lambda^b}{2}$ (λ^b, $b = 1, 2, ...8$, the Gell-Man matrices). Here $F_{\mu\nu}(x) = T_a F^a_{\mu\nu}(x); \quad A_{\mu}(x) = T_a A^a_{\mu}(x);$ where

$$F^a_{\mu\nu}(x) = \partial_{\mu}A^a_{\nu}(x) - \partial_{\nu}A^a_{\mu}(x) - g\epsilon^{akl}A_{k\,\mu}A_{l\,\nu},$$

and the co-variant derivative $D_{\mu} = \partial_{\mu} + igT_a A^a_{\mu}(x)$. Here ϵ^{akl} is the fully anti-symmetric tensor. In the gauge kinetic part, the cubic and quartic term in A appears naturally in this Yang-Mills gauge theory due to the term $g\epsilon^{akl}A_{k\,\mu}A_{l\,\nu}$ which are required in order have gauge invariance into the theory.

1.2.2 Goldstone theorem

Global symmetries are not natural symmetries. It may be either broken or approximate or is the leftover symmetry of spontaneous broken local symmetry. The Goldstone theorem states that "If the continuous symmetry of a lagrangian (describing a theory) is spontaneously broken, then it will be accompanied by the existence of a massless scalar boson (called Goldstone boson) in that theory. The number of massless Goldstone bosons is equal to the number of such broken symmetries [2].

1.3 Spontaneous Symmetry Breaking (SSB)

The gauge symmetry keeps the gauge bosons massless. Similarly, the chiral symmetry protects the chiral fermions from getting any mass. However, the weak vector bosons $W^{\pm}$ and Z^0 which have been found at high energy colliders, are found to be massive. To generate masses of the vector bosons in a gauge invariant manner while retaining the the renormalizability of the theory, one need to break

the symmetry spontaneously (SSB) at the vacuum level, while maintaining gauge invariance at the lagrangian level [3]. To see how a continuous symmetry is spontaneously broken, let us use a complex scalar field $\Phi(=\frac{1}{\sqrt{2}}(\phi_1 + i\phi_2))$ with the potential

$$V(\Phi, \Phi^\dagger) = \mu^2 \Phi^\dagger \Phi + \lambda \left(\Phi^\dagger \Phi\right)^2.$$

Note that the constant λ in the potential has to be positive. Else $V(\Phi)$ will become negative for
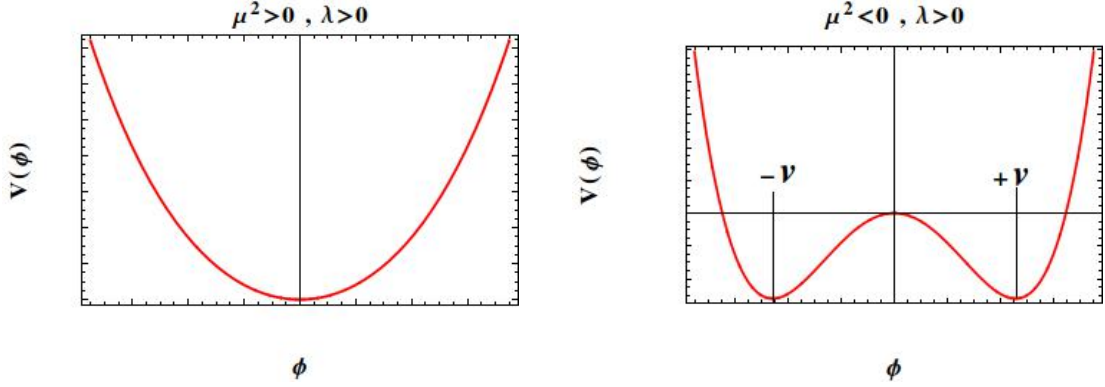
Figure 1.1: Spontaneous symmetry breaking and Higgs potential

sufficiently large Φ and hence the potential will be unbounded from below. With $\lambda > 0$, there are two cases: (i) $\mu^2 > 0$ and (ii) $\mu^2 < 0$

- Case (i): $\mu^2 > 0$. The mass of the scalar boson is positive and the state with $\Phi^\dagger = \Phi = 0$ corresponds to a stable equilibrium and it is the ground state.

- Case (ii): $\mu^2 < 0$, which is a special case: the mass (i.e. $= i\sqrt{2}\mu$) of the scalar boson is found to be imaginary.

Now, the potential is invariant under the global phase transformation as define by $\Phi \longrightarrow \Phi' = e^{-iq\theta}\Phi$. The minimum of the potential lies at $\Phi_0 = \pm\sqrt{\frac{-\mu^2}{2\lambda}} = \pm\frac{v}{\sqrt{2}}$, where v is a positive definite since $\mu^2 < 0$. Although, the potential above is unstable around $\Phi = 0$, but is rotationally symmetric. Any fluctuation around the minimum would break the symmetry. Now in quantum field theory, physical particles are interpreted as quantum fluctuations around their ground state. Here the ground state is located somewhere in the rim of the Mexican hat type of potential(shown in Fig 1.1), which is infinitely degenerate since it is a continuous circle of minima.

Introducing two new field(real) variables $h(x) = \phi_1 - v$ and $\xi = \phi_2$ such that $\langle 0|h(x)|0\rangle = 0$ and $\langle 0|\xi(x)|0\rangle = 0$, which are the quantum fluctuations around the vacuum, one can rewrite Φ as

$$\Phi = \frac{1}{\sqrt{2}}(\phi_1(x) + i\phi_2(x)) = \frac{1}{\sqrt{2}}(h(x) + v + i\xi(x)) \simeq \frac{1}{\sqrt{2}}(h(x) + v)e^{i\xi(x)/v},$$

6

and substituting this in the Lagrangian $\mathcal{L} = (\partial_\mu \Phi)^\dagger \partial^\mu \Phi - \mu^2 \Phi^\dagger \Phi - \lambda \left(\Phi^\dagger \Phi\right)^2$, we find

$$\mathcal{L} = \frac{1}{2}\partial_\mu \left([v + h(x)]e^{-i\xi(x)/v}\right) \partial^\mu \left([v + h(x)]e^{i\xi(x)/v}\right) - \frac{\mu^2}{2}\left(v + h(x)\right)^2 - \frac{\mu^2}{4v^2}\left(v + h(x)\right)^4$$

$$= \frac{1}{2}\partial_\mu h \partial^\mu h + \frac{1}{2}\partial_\mu \xi \partial^\mu \xi + \mu^2 h^2 + \left(\frac{h^2}{2v^2} + \frac{h}{v}\right)\partial_\mu \xi \partial^\mu \xi + \frac{\mu^2}{4v^2}\left(4vh^3 + h^4\right) - \frac{\mu^2 v^2}{4}$$

The Lagrangian consists of the following particle spectrum: a scalar particle of mass $m_h = \sqrt{-2\mu^2}$ which is positive (since $\mu^2 < 0$) and a massless scalar boson $\xi(x)$ (i.e. $m_\xi = 0$) called the Goldstone boson.

1.3.1 Higgs mechanism

This is a kind of SSB mechanism for generating the mass of the vector boson. The mass terms arises naturally due to the interaction of the particles with the vacuum but the theory is still remains normalizable [4]. Below we discuss the Higgs mechanism in the case of abelian and non-abelian gauge symmetries, respectively.

Abelian Higgs mechanism

To start with let us consider the Lagrangian of the scalar QED (the theory which describes the interaction of photons with charged scalar bosons) given by

$$\mathcal{L}_{scalar} = (D^\mu \Phi)^\dagger (D_\mu \Phi) - \mu^2 \Phi^\dagger \Phi - \lambda \left(\Phi^\dagger \Phi\right)^2 - \frac{1}{4}F^{\mu\nu}F_{\mu\nu}.$$

where $D_\mu = \partial_\mu + iqeA_\mu$ and the field transformation are given given by $\Phi' = U\Phi = e^{-iq\,\theta(x)}\Phi$ and $A'_\mu(x) = A_\mu(x) - \frac{q}{e}\partial_\mu \theta(x)$. One can rewrite the above lagrangian (scalar QED) in terms of $h(x)$ and $\xi(x)$ (setting $q = -1$) as

$$\mathcal{L} = \frac{1}{2}\left[\left(\partial_\mu + ieA_\mu\right)\left([v + h(x)]e^{-i\xi(x)/v}\right)\right]\left[\left(\partial^\mu - ieA_\mu\right)\left([v + h(x)]e^{i\xi(x)/v}\right)\right] - \frac{\mu^2}{2}\left(v + h(x)\right)^2$$

$$- \frac{\mu^2}{4v^2}\left(v + h(x)\right)^4 - \frac{1}{4}F^{\mu\nu}F_{\mu\nu}$$

$$= \frac{1}{2}\partial_\mu h \partial^\mu h + \mu^2 h^2 + \frac{1}{2}\partial_\mu \xi \partial^\mu \xi + \frac{e^2 v^2}{2}A_\mu A^\mu - \frac{1}{4}F^{\mu\nu}F_{\mu\nu} - evA^\mu \partial_\mu \xi + ...$$

So, we have one massive scalar $h(x)$ of mass $m_h = \sqrt{2\mu^2}$, one massless Goldstone boson ξ and a massive vector particle A_μ of mass $m_A = ev$, where v is the vacuum expectation value. The last term (off-diagonal mass term) in the lagrangian is unphysical as it means that the massless ξ Goldstone boson converts into the gauge field A_μ and needs to be removed from the theory [5]. We can redefine

the gauge field A_μ by absorbing the Goldstone boson as follows,

$$\frac{1}{2}\partial_\mu\xi\partial^\mu\xi + \frac{e^2 v^2}{2}A_\mu A^\mu - \frac{1}{4}F^{\mu\nu}F_{\mu\nu} - ev A^\mu \partial_\mu\xi = \frac{e^2 v^2}{2}\left(A_\mu - \frac{1}{ev}\partial_\mu\xi\right)\left(A^\mu - \frac{1}{ev}\partial^\mu\xi\right)$$

Writing the the local gauge transformation parameter as $\theta(x) = -\xi/v$, one find that the gauge field transforms as

$$A'_\mu = A_\mu - \frac{1}{ev}\partial_\mu\xi,$$

and the scalar field becomes

$$\Phi \longrightarrow e^{-i\xi(x)/v}\Phi = e^{-i\xi(x)/v}\left(\frac{1}{\sqrt{2}}(h(x)+v)e^{i\xi(x)/v}\right) \equiv \frac{1}{\sqrt{2}}(h(x)+v)$$

One thus gets rid of the unwanted massless scalar Goldstone boson $\xi(x)$ and generates the mass of the gauge field A'_μ by combining spontaneous symmetry breaking with local gauge invariance.

Non-abelian Higgs mechanism

For the non-abelian $SU(2)$ group, the three generators $T^a = \tau^a/2$ satisfies $\left[T^a, T^b\right] = i\epsilon^{abc}T_c$ where ϵ^{abc} is the fully anti-symmetric tensor and T^a are traceless hermitian two dimensional Pauli matrices. The complex scalar Φ is a $SU(2)$ doublet and it transforms under the local $SU(2)$ gauge transformation as

$$\Phi' = U\Phi = e^{ig\sum_a T^a\theta^a(x)}\Phi \quad \text{where} \quad \Phi = \frac{1}{\sqrt{2}}\begin{pmatrix}\phi_1 + i\phi_2 \\ \phi_3 + i\phi_4\end{pmatrix}$$

The $SU(2)$ gauge field $A_\mu(x) = T_a A^a_\mu(x)$, the field strength tensor $F^a_{\mu\nu}(x) = \partial_\mu A^a_\nu(x) - \partial_\nu A^a_\mu(x) - g\epsilon^{akl}A_{k\,\mu}A_{l\,\nu}$; the $SU(2)$ covariant derivative $D_\mu = \partial_\mu + igT^a A^a_\mu(x)$, $a = 1, 2, 3$. which required to construct the $SU(2)$ gauge invariant lagrangian for the complex scalar Φ. After spontaneous symmetry breaking with unitary gauge (i.e. by choosing $\theta^a(x) = -\xi^a(x)/v$ at each point in spacetime), we get

$$\Phi = \frac{1}{\sqrt{2}}\begin{pmatrix}0 \\ h(x)+v\end{pmatrix}.$$

The ξ^a is the Goldstone boson are which are equivalently ϕ_1, ϕ_2 and ϕ_4. The minimum of the scalar potential is $\sum_{i=1}^4 \phi_i^2 = v^2$, where v is the radius of the $4d$ sphere constructed out of $\phi_1, ...\phi_4$. So the Goldstone boson can move freely on the sphere. The expectation value of the Goldstone bosons (ϕ_1, ϕ_2, ϕ_4) are zero. Without loss of generality, we may align our vacuum in the ϕ_3 direction. The above three Goldstone bosons, which were appeared in the spontaneous symmetry breaking mechanism

because of three broken generator of the $SU(2)$ group, are now eaten by the non-abelian gauge fields and become massive which is given by

$$\mathcal{L}_{gaugemass} = \left(\frac{gv}{2}\right)^2 W_\mu^+ W_\mu^- + \frac{1}{2}\left(\frac{gv}{2}\right)^2 A_\mu^3 A_\mu^3,$$

where $W_\mu^\pm = \frac{1}{\sqrt{2}}\left(A_\mu^1 \mp iA_\mu^2\right)$ is the charged weak bosons of mass $m_W = gv/2$. This Higgs mechanism [6,7] generate the same mass for all the three gauge field $W_\mu^\pm$ and A_μ^3.

Glashow, Weinberg and Salam model(GWS) and the Higgs mechanism

The GWS model is a local $SU(2)_L \otimes U(1)_Y$ gauge invariant theory which unifies the electromagnetic and weak interactions [8–10]. We next study the SSB mechanism in the Higgs sector of the $SU(2)_L \otimes U(1)_Y$ gauge theory. To start with we write down the local $SU(2)_L \otimes U(1)_Y$ invariant lagrangian of a complex scalar doublet $\Phi(x)$

$$\mathcal{L}_{scalar} = (D^\mu \Phi)^\dagger (D_\mu \Phi) - \mu^2 \Phi^\dagger \Phi - \lambda \left(\Phi^\dagger \Phi\right)^2$$

where here Y is the hypercharge ($= Q - T^3$) of the particle, with T_3 the 3rd components of the weak iso-spin and Q the total electromagnetic charge. In the lagrangian, the covariant derivative is defined as $D_\mu = \partial_\mu + igT_a A_\mu^a + ig'Y B_\mu$, and the complex scalar field Φ

$$\Phi = \begin{pmatrix} \phi^+ \\ \phi^0 \end{pmatrix} = \frac{1}{\sqrt{2}} \begin{pmatrix} \phi_1 + i\phi_2 \\ \phi_3 + i\phi_4 \end{pmatrix}$$

Considering $\langle 0|\phi_i|0\rangle = 0, i = 1,2,3$ and $\langle 0|\phi_4|0\rangle = v$, we next define the Higgs field $h(x) = \phi_3(x) - v$ ($h(x)$ and $(\xi_1, \xi_2, \xi_3) \equiv (\phi_1, \phi_2, -\phi_4)$ (the three Goldstone bosons). If the symmetry is preserved, then the vacuum should be invariant under the symmetry transformation. So, if T is the generator of the symmetry transformation i.e.

$$U\langle 0|\phi|0\rangle = e^{-i\sum_a T^a \xi^a(x)}\langle 0|\phi|0\rangle \equiv \langle 0|\phi|0\rangle,$$

requires $T^a\langle 0|\phi|0\rangle = 0$, where $a = 1,2...$ We next study the action of the four $SU(2)_L \otimes U(1)_Y$ generators on the vacuum of the theory i.e.

$$T^1\langle 0|\phi|0\rangle = \frac{1}{2}\begin{pmatrix} 0 & 1 \\ 1 & 0 \end{pmatrix}\begin{pmatrix} 0 \\ \frac{v}{\sqrt{2}} \end{pmatrix} = \begin{pmatrix} \frac{v}{2\sqrt{2}} \\ 0 \end{pmatrix} \neq 0$$

Similarly, one also finds that $T_2\langle 0|\phi|0\rangle \neq 0$, $T_3\langle 0|\phi|0\rangle \neq$ and $Y\langle 0|\phi|0\rangle \neq$ i.e. all the four generators breaks the symmetry invariance of the vacuum. As a result, we have one massive scalar and three

9

massless vector bosons eat three Goldstone boson and became massive, while photon remains massless. The counting of gauge degrees of freedom demands that at least one generator should leave the vacuum invariant and it can be linear combination of generators i.e. $T^3 + Y$.

$$(T^3 + Y)\langle 0|\phi|0\rangle = \frac{1}{2}\left\{\begin{pmatrix} 1 & 0 \\ 0 & -1 \end{pmatrix} + \begin{pmatrix} 1 & 0 \\ 0 & 1 \end{pmatrix}\right\}\begin{pmatrix} 0 \\ \frac{v}{\sqrt{2}} \end{pmatrix} = \begin{pmatrix} 1 & 0 \\ 0 & 0 \end{pmatrix}\begin{pmatrix} 0 \\ \frac{v}{\sqrt{2}} \end{pmatrix} = 0$$

while the orthogonal combination $(T^3 - Y)$ of the linear combination of the generator breaks the invariance of the vacuum i.e.

$$(T^3 - Y)\langle 0|\phi|0\rangle = \frac{1}{2}\left\{\begin{pmatrix} 1 & 0 \\ 0 & -1 \end{pmatrix} - \begin{pmatrix} 1 & 0 \\ 0 & 1 \end{pmatrix}\right\}\begin{pmatrix} 0 \\ \frac{v}{\sqrt{2}} \end{pmatrix} = \begin{pmatrix} 0 & 0 \\ 0 & -1 \end{pmatrix}\begin{pmatrix} 0 \\ \frac{v}{\sqrt{2}} \end{pmatrix} \neq 0$$

We see that there are three broken generators and one unbroken generator i.e.

$$(T^1, T^2, K(= T^3 - Y))\langle 0|\phi|0\rangle \neq 0 \quad \text{and} \quad Q(= T^3 + Y)\langle 0|\phi|0\rangle = 0$$

So the GWS gauge group $G_{GWS} = SU(2)_L \otimes U(1)_Y$ with $3+1$ generators is broken into the subgroup $U(1)_{EM}$ with one Q_{EM} generator which is known as electromagnetic charge generator. We find

$$(iT^1\xi^1 + iT^2\xi^2 + iK\xi^3 + I(h(x) + v))/v \begin{pmatrix} 0 \\ \frac{v}{\sqrt{2}} \end{pmatrix} = \frac{1}{\sqrt{2}}\begin{pmatrix} \xi_1 + i\xi_2 \\ (h + v) - i\xi_3 \end{pmatrix} = \frac{1}{\sqrt{2}}\begin{pmatrix} \phi_1 + i\phi_2 \\ \phi_3 + i\phi_4 \end{pmatrix} = \Phi$$

In terms of the Goldstone bosons, $\Phi(x)$ can be rewritten as

$$\Phi = \exp(i\sum_a T^a \xi^a(x)/v)\begin{pmatrix} 0 \\ \frac{h(x)+v}{\sqrt{2}} \end{pmatrix}$$

Using the unitary gauge(choosing $\theta^a(x) = -\xi^a(x)/v$), the gauge transformation as $A_\mu^a \longrightarrow A_\mu^{a'} = A_\mu^a$, $B_\mu \longrightarrow B_\mu$, the scalar field becomes

$$\Phi' \longrightarrow \Phi = \begin{pmatrix} 0 \\ \frac{h(x)+v}{\sqrt{2}} \end{pmatrix}$$

The gauge boson become massive because of their interaction with the Higgs vacuum i.e

$$|D_\mu\Phi|^2 \Longrightarrow |(igT_a A_\mu^a + ig'Y B_\mu)\Phi|^2$$

All of the electroweak gauge bosons acquires mass, except the fact that photon remains massless. The mass term of the electro-weak lagrangian can be written as

$$\mathcal{L}_{mass} = \mu^2 h^2 + \frac{1}{8}g^2 v^2 \left[\left(A_\mu^1 \right)^2 + \left(A_\mu^2 \right)^2 + \left(A_\mu^3 \right)^2 \right] + \frac{1}{8}g'^2 v^2 B_\mu B^\mu - \frac{v^2}{4}g' g B_\mu A^{\mu 3}$$

$$= \mu^2 h^2 + \frac{v^2}{8} \left\{ g^2 \left[\left(A_\mu^1 \right)^2 + \left(A_\mu^2 \right)^2 \right] + \left[\left(g A_\mu^3 - g' B_\mu \right)^2 \right] \right\}$$

Writing the charged($W_\mu^\pm$), the neutral weak gauge boson(Z_μ) and the photon(A_μ) as

$$W_\mu^\pm = \frac{A_\mu^1 \mp i A_\mu^2}{\sqrt{2}}, \;\; Z_\mu = \frac{\left(g A_\mu^3 - g' B_\mu \right)}{\sqrt{g'^2 + g^2}}, \;\; A_\mu = \frac{\left(g' A_\mu^3 + g B_\mu \right)}{\sqrt{g'^2 + g^2}},$$

one finds the mass of the charged and the neutral gauges boson as

$$M_W = \frac{g v}{\sqrt{2}}, \;\; M_Z = v \frac{\sqrt{g'^2 + g^2}}{2}, \;\; M_A = 0.$$

The physical photon (A_μ) and weak neutral Z_μ boson field can be expressed as the rotated state of A_μ^3 and B_μ fields. The angle of rotation, called the Weinberg angle (θ_W), is defined by couplings g and g' of $SU(2)_L$ and $U(1)_Y$ gauge groups [3] i.e.

$$\cos \theta_W = \frac{g}{\sqrt{g^2 + g'^2}}, \;\;\; \sin \theta_W = \frac{g'}{\sqrt{g^2 + g'^2}}.$$

The neutral weak and photon fields can be written as

$$Z_\mu = \cos \theta_W A_\mu^3 - \sin \theta_W B_\mu \;\;\; \text{and} \;\;\; A_\mu = \sin \theta_W A_\mu^3 + \cos \theta_W B_\mu$$

Finally the $U(1)_Q$ coupling is identified as

$$e = g' \cos \theta_W = g \sin \theta_W$$

This is the unification of weak and electromagnetic interaction as obtained in the GWS model electroweak theory. LEP discovered the weak neutral and charged boson of mass $M_Z = 91.1875 \pm 0.0021$ GeV and $M_W = 80.399 \pm 0.025$ GeV, the values as close to the one as predicted by the Weinberg-Salam (or GWS) model with $\sin^2 \theta_W \simeq 0.23$. Finally, the proton-proton Large Hadron Collider discovered [11] the neutral scalar Higgs scalar boson of mass around $m_h = 125.09 \pm 0.23$ GeV [12].

1.4 The Standard Model

The Standard Model is based on $SU(3)_C \otimes SU(2)_L \otimes U(1)_Y$ gauge group which is broken into the gauge group $SU(3)_C \otimes U(1)_Q$ after the Higgs mechanism. The strong interaction, which doesn't participate in the symmetry breaking mechanism, is represented by the $SU(3)_C$ gauge group and the gauge fields are called gluon(G_μ^a). The gluon fields which preserves the color symmetry, are massless.

SM Fields	$SU(3)_C$	$SU(2)_L$	$U(1)_Y$	$U(1)_Q$
e_R	**1**	**1**	-1	-1
$l_L = \begin{pmatrix} \nu_L \\ e_L \end{pmatrix}$	**1**	**2**	$-1/2$	$\begin{pmatrix} 0 \\ -1 \end{pmatrix}$
u_R	**3**	**1**	$2/3$	$2/3$
d_R	**3**	**1**	$-1/3$	$-1/3$
$q_L = \begin{pmatrix} u_L \\ d_L \end{pmatrix}$	**3**	**2**	$1/6$	$\begin{pmatrix} 2/3 \\ -1/3 \end{pmatrix}$
$\Phi = \begin{pmatrix} \phi^+ \\ \phi^0 \end{pmatrix}$	**1**	**2**	$1/2$	$\begin{pmatrix} 1 \\ 0 \end{pmatrix}$
A_μ^a	**1**	**3**	0	$(\pm 1, 0)$
B_μ	**1**	**1**	0	0
G_μ^b	**8**	**1**	0	0

Table 1.2: The Standard Model fields and the charge defined as $Q = T_3 + Y$

The representation of standard model particles are shown in the table 1.2.

The SM fermions come in three generations. Quarks($u, d, ...b$) take part in strong, weak and electromagnetic interaction, the charged leptons(e^-, μ^-, τ^-) take part in weak and electromagnetic interaction, while neutrinos take part in the weak interaction. Neutrinos are found to be massless in the SM, as they don't have any right-handed partner in the SM. But other (charged)leptons and quarks which have right handed partner in the SM are $SU(2)_L$ singlet. The Yukawa term gives the mass for leptons and quarks through interaction with the vacuum. The $SU(3)_C \otimes SU(2)_L \otimes U(1)_Y$ gauge covariant derivative which one requires while describing interaction of the SM fermions with the strong, weak and e.m. gauge field can be written as

$$D_\mu = \partial_\mu + i g_s \frac{\lambda^b}{2} G_\mu^b + i g \frac{\tau^j}{2} A_\mu^j + i g' Y B_\mu$$

Here $b = 1, 2, 3, ..., 8$ and $j = 1, 2, 3$. g_s, g and g' are $SU(3)_C, SU(2)_L$ and $U(1)_Y$ gauge couplings respectively. The generators λ^b correspond to the 3×3 Gellmann matrices, while τ^j, the 2×2 Pauli matrices. The typical fermion interactions are obtained from $\mathcal{L} = \overline{\psi} i \slashed{D}_\mu \psi$. Finally, one can write the Standard Model Lagrangian is [3]

$$\mathcal{L} = -\frac{1}{4}G^b_{\mu\nu}G^{b\mu\nu} - \frac{1}{4}W^j_{\mu\nu}W^{j\mu\nu} - \frac{1}{4}B_{\mu\nu}B^{\mu\nu} + \sum_{n=1}^{3}\bar{l}_{nL}\gamma^\mu\left(i\partial_\mu - \frac{g}{2}\tau^j A^j_\mu - g'YB_\mu\right)l_{nL}$$

$$+ \sum_{n=1}^{3}\left\{\bar{e}_{nR}\gamma^\mu\left(i\partial_\mu - g'YB_\mu\right)e_{nR} + \bar{q}_{nL}\gamma^\mu\left(i\partial_\mu - \frac{g_s}{2}\lambda^b G^b_\mu - \frac{g}{2}\tau^j A^j_\mu - g'YB_\mu\right)q_{nL}\right\}$$

$$+ \sum_{n=1}^{3}\left\{\bar{u}_{nR}\gamma^\mu\left(i\partial_\mu - \frac{g_s}{2}\lambda^b G^b_\mu - g'YB_\mu\right)u_{nR} + \bar{d}'_{nR}\gamma^\mu\left(i\partial_\mu - \frac{g_s}{2}\lambda^b G^b_\mu - g'YB_\mu\right)d'_{nR}\right\}$$

$$+ |\left(i\partial_\mu - \frac{g}{2}\tau^j A^j_\mu - g'YB_\mu\right)\Phi|^2 - \mu^2\Phi^\dagger\Phi - \lambda\left(\Phi^\dagger\Phi\right)^2$$

$$- \sum_{m,n}\left(\Gamma^u_{mn}\bar{q}_{mL}\Phi^c u_{nR} + \Gamma^d_{mn}\bar{q}_{mL}\Phi d'_{nR} + \Gamma^e_{mn}\bar{l}_{mL}\Phi e_{nR} + h.c\right) \tag{1.1}$$

The charged leptons and down type of quarks get mass from the scalar field Φ through the Yukawa terms in equation 1.1. The down up type quarks get mass by introducing the conjugate scalar field of Φ (in conjugate representation of $SU(2)_L$)

$$\Phi^c = i\tau_2\Phi^* = \begin{pmatrix}\phi^0 \\ -\phi^-\end{pmatrix} = \frac{1}{\sqrt{2}}\begin{pmatrix}h(x) + \upsilon \\ 0\end{pmatrix}$$

Here Γ^i_{mn} is the $m \times n$ Yukawa coupling matrix($i = u, d, e$), $m.\ n = 1, 2, 3$ is generation index and it is a diagonal matrix. For example $\Gamma^u_{11} = \lambda_u, \Gamma^u_{22} = \lambda_c, \Gamma^d_{33} = \lambda_t...$ and $\Gamma^e_{11} = \lambda_e..., \Gamma^e_{33} = \lambda_\tau$, where λs are the Yukawa coupling constants. One obtain the fermion mass as

$$\Gamma^u_{11}\bar{q}_{1L}\Phi^c u_{1R} = \lambda_u\bar{u}_L\left(\frac{1}{\sqrt{2}}(h(x) + \upsilon)\right)u_R = m_u\bar{u}_L u_R + \frac{m_u}{\upsilon}\bar{u}_L h(x)u_R$$

where the mass of the u quark is $m_u = \lambda_u\upsilon/\sqrt{2}$. Similarly, the top($t$) quark mass $m_t = \lambda_t\upsilon/\sqrt{2}$ and the electron mass $m_e = \lambda_e\upsilon/\sqrt{2}$ etc. The mass of the particles are proportional to the electroweak symmetry breaking scale υ. The gauge kinetic terms are

$$B_{\mu\nu} = \partial_\mu B_\nu - \partial_\nu B_\mu, \quad W^j_{\mu\nu} = \partial_\mu A^j_\nu - \partial_\nu A^j_\mu - g\epsilon^{jkl}A_{\mu k}A_{\nu l}$$

$$G^a_{\mu\nu} = \partial_\mu G^a_\nu - \partial_\nu G^a_\mu - g_s f^{abc}G_{\mu b}G_{\nu c}$$

Here f^{abc} and ϵ^{kl} are the fully anti-symmetric structure constants. From the above SM, one finds the charged and the neutral current interaction as

$$\mathcal{L}_{weak} = \frac{g}{\sqrt{2}}(W^+_\mu J^-_\mu + W^-_\mu J^+_\mu) + \frac{e}{\sin\theta_W\cos\theta_W}J^\mu_Z Z_\mu + eJ^\mu_{em}A_\mu$$

where $W^\pm_\mu$ are the charged weak bosons and Z_μ and A_μ are the neutral weak boson and photon, respectively. The charged weak current $J^{\mu-}$ is defined as

$$J^{\mu-} = \sum_i\left[\bar{u}_n\gamma^\mu\frac{(1 - \gamma_5)}{2}d_n + \bar{\nu}_n\gamma^\mu\frac{(1 - \gamma_5)}{2}e_n\right]$$

where $n(=1,2,3)$ denotes the generation index. Similarly, the neutral current is given by

$$J_{em}^\mu = \sum_f Q_f \overline{f} \gamma^\mu f$$

$$J_Z^\mu = \sum_f \left[g_L^f \overline{f}_L \gamma^\mu f_L + g_R^f \overline{f}_R \gamma^\mu f_R \right]$$

$$= \sum_f \left[\left(\frac{g_L^f + g_R^f}{2} \right) \overline{f} \gamma^\mu f + \left(\frac{g_R^f - g_L^f}{2} \right) \overline{f} \gamma^\mu \gamma_5 f \right].$$

Here $f = \nu_e, e, u$ and d corresponds to the first generation fermion and $f_L = (1 - \gamma_5)/2$, $\quad f_R = (1 + \gamma_5)/2$, $Q_f = T_3^f - Y^f$. Several coupling constant and parameters appearing in the SM lagrangian are defined in Table 1.3

$g_{L,R}^f = T_3(f_{L,R}) - Q_f \sin^2 \theta_W$	
$g_L^\nu = \frac{1}{2}$	$g_R^\nu = 0$
$g_L^e = \frac{-1}{2} + \sin^2 \theta_W$	$g_R^e = \sin^2 \theta_W$
$g_L^u = \frac{1}{2} - \frac{2}{3} \sin^2 \theta_W$	$g_R^u = -\frac{2}{3} \sin^2 \theta_W$
$g_L^d = \frac{-1}{2} + \frac{1}{3} \sin^2 \theta_W$	$g_R^d = \frac{1}{3} \sin^2 \theta_W$

Table 1.3: Standard model fermionic couplings

1.5 Limitation of the standard model

Although the standard model has been extremely successful in terms of experimental discoveries, it has both theoretical and experimental limitations, some of which are briefly described below.

- Theoretical questions:

  – Stability of the vacuum: The sign of the bosonic and fermionic contributions in β-function of the Higgs quartic coupling λ would significantly affect the behaviour of the effective Higgs potential and the stability of the vacuum [16–18]. Current experimental studies conclude that the electroweak vacuum is metastable.

  – Higgs hierarchy problem: The large quantum corrections [19] pushes the Higgs mass to the highest energy scale of the theory. Since the Higgs boson is an elementary scalar in nature, no symmetry can protect the Higgs boson mass from finding such a huge quantum correction. One needs an extreme fine-tuning to obtain the desired mass of the Higgs boson at 125 GeV.

– Fermion mass hierarchy and number of generations:

The mass of the quarks and leptons are directly proportional to the Yukawa coupling. We do not have any clue about, why the SM has wide spectrum of couplings for SM fermions and how many generations it could accommodate?

- Experimental questions

  – Anomalous magnetic dipole moment of muon: At present Brookhaven E821 and Fermilab experiment E989, the$(g-2)$ result deviates $3\sigma - 4\sigma$ from SM : this corresponds to physics beyond the Standard Model(BSM) [13].

  – B-meson decay:

  Nearly $2\sigma - 4\sigma$ deviation from the SM prediction in R_D and R_{D^*} anomaly (for the B meson decays $B \to Dl\nu$ and $B \to D^*l\nu$ [29–31]) and the 5σ deviation from the SM prediction reported in for the decay $b \to sl^+l^-$, $l = \mu, \tau$ [32], which points towards the BSM physics.

- Phenomena questions

  – Neutrino oscillation: Neutrino oscillation, a result of non-zero neutrino mass and mixing angle, was established [20–28] in a series of oscillation experiments. In the SM there is no right handed neutrino, since only the left handed neutrino takes part in the parity violating weak interaction. Hence, one cannot explain neutrino mass within the SM. One requires BSM models i.e. Neutrino models with right handed neutrino, to accommodate such tiny neutrino mass.

  – Matter-antimatter asymmetry: The present universe is made up of matter predominantly. The standard model predicts that matter and antimatter should have been created in nearly equal amounts in the early stage of the universe [14], however it cannot explain the excess of matter over the antimatter. The matter-antimatter asymmetry in the leptonic sector is known as leptogenesis, while the analogous mechanism for baryons is known as baryogenesis. The Leptogenesis and the baryogenesis requires BSM physics.

  – Dark matter and Dark energy: According to Cosmological observations, only 4% of the total matter-energy content of the Universe are the luminous matter, which the Standard Model can explain. For the remaining, 23% are dark matter, while the remaining 73% are dark energy which is attempted to explain in terms of vacuum energy of the standard

model. But the SM do not have any suitable dark matter candidate [34, 35]. One requires BSM physics in order to have dark matter particles. [33, 36].

– Gravity: The SM doesn't include gravity. Even if we add the particle called graviton(which is responsible for gravitational interaction [15]) in four dimension, it has interaction with the SM particle of strength $\alpha_G \simeq 10^{-39}$, which is negligible. However, if one work in extra-dimensional ($4 + d$, d being the number of extra compact spatial dimension) models, the cumulative effect of Kaluza-Klein graviton towers in the gravitational interaction with the standard model particles, may be of electro-weak strength, which can be probed in the TeV energy hadron or linear collider [37–48].

1.6 Looking for theory beyond the Standard Model

1.6.1 Supersymmetry

However the standard model provides the very precise description of nature at sub-TeV scale as an effective low energy description of the complete theory. One can address many of above mentioned problems by invoking new symmetry in the standard model with the space-time being $3+1$-dimensional and the fundamental scale of gravity being the 4-dimensional Planck scale $M_{Planck} = 10^{19}$ GeV. One such symmetry is the supersymmetry. In supersymmetry, each standard model particles has superpartner which differs by $1/2$ integral spin, for example, electron (fermion spin $1/2$) has selectron as a superpartner which has spin 0 (scalar), gluon (vector boson spin 1) has gluino (fermion spin $1/2$) etc. In the limit of exact supersymmetry where the coupling and mass of the particles corresponding super-
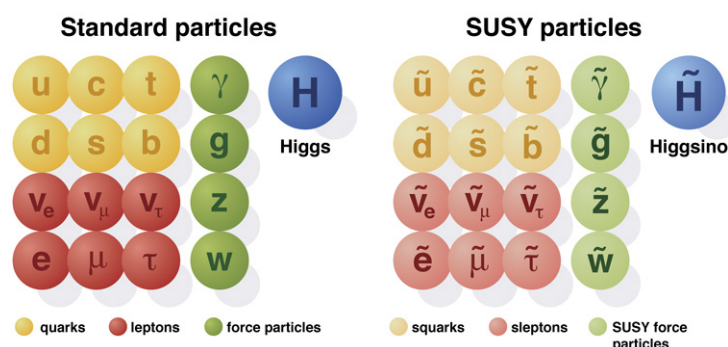
Figure 1.2: (Source: Wikipedia), Supersymmetry standard model

particles are equal, but it cannot be true that we haven't observe such degenerate superpartners of SM

particle so far in experiments. Thus supersymmetry, if it exist, must be a broken symmetry of nature at around TeV scale (require) and all superpartners must be heavier than their known counterparts.

The hierarchy problem is resolved in the limit of exact supersymmetry where the coupling and mass of this bosons and it's corresponding fermions (supersymmetric partner of the boson) are equal, the two quadratic divergences gets canceled because of the extra minus sign which appears in the fermionic loop, there remaining controllable logarithmically divergent [36]. Once supersymmetry is broken, there is an additional soft broken term comes with logarithmically divergent. Supersymmetry also provides the unification of the gauge couplings at GUT scale naturally. In the dark matter point of view, light supersymmetric particles (LSP) can be a natural dark matter candidates. These are the additional features of the supersymmetric theory.

1.6.2 Large Extra dimension:

Among the BSM models, the models based on extra spatial dimension(s) were found to be quite interesting as they solve the Higgs hierarchy problem quite elegantly as the scale of $4 + d$-dimensional gravity is turned out to be 10^3 GeV instead of 10^{19} GeV, a scale which can be probed by the current or the upcoming TeV energy colliders.

In 1998, Nima Arkani-Hamed, Savas Dimopoulos and Gia Dvali (ADD) [39] first proposed the model based on "large extra (compactified) dimensions", and tried to solve the gauge hierarchy (also known as the higgs hierarchy) problem but it raised the new hierarchy problem between the compactification scale of the large extra dimension and the electroweak scale. In 1999, Lisa Randall and Raman Sundrum(RS) [41] proposed warped extra-dimensional model to resolve the gauge hierarchy problem.

Kaluza-Klein model: The idea that the world can be higher-dimensional(i.e. more than of dimension four), was first suggested in 1914 by Nordstrom and gained popularity as a theory of unification of gravity and electromagnetism after the pioneering work by Kaluza(1921) [37] and Klein(1926) [38]. In the original Kaluza-Klein model, the world was assumed to be $4 + 1$-dimensional. The fifth spatial dimension (denoted by the fifth coordinate x^5) is compactified on a circle S^1 of radius R_c with $x^5 = R_c\theta$, θ being the angular coordinate. So the 5-dimensional world is $M^4 \otimes S^1$ and the corresponding Einsteins equation manifests the 5-dimensional general coordinate invariance. In the limit $R_c = 0$, one recovers the 4-dimensional Einsteins equations of general relativity and the Maxwell equations of electromagnetism.

ADD model: In 1998, N. Arkani-Hamed, S. Dimopoulos and G. Dvali (ADD) proposed a model based on large extra dimensions [39]. In the ADD model the world is $D = 4 + d$-dimensional, where d is
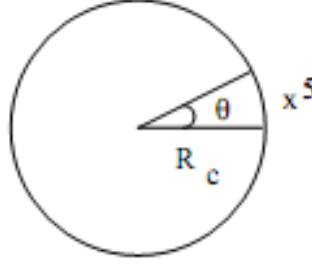
Figure 1.3: Fifth dimension in Kaluza-Klein model

the number of extra compactified spatial dimensions. The 4-dimensional Planck scale is related to the $4 + d$-dimensional Planck scale M_D as follows

$$M_{pl}^2 \approx R_c^d M_D^{2+d}$$

where R_c is the common size of each of the d extra dimensions. Setting the fundamental scale of gravity $M_D = 1$ TeV, we find $R_c \approx 10^{\frac{30}{d} - 17}$cm. In Table 1.4, we have shown R_c for different number of extra spatial dimensions(d) [40]. Obviously, $d = 1$ case is ruled out; else deviation from Newtonian

d	1	2	3	4	5	6
R_c(cm)$\sim$	10^{15}	10^{-1}	10^{-5}	10^{-9}	10^{-11}	10^{-12}

Table 1.4: The size of the extra spatial dimension(R_c) is shown as a function of d

gravity would be observable at the solar system length scale, which has not been seen so far. Thus, the minimum number of extra spatial dimension is $d = 2$. Now, in the ADD scenario, the fundamental scale of gravity is $M_D = 1$ TeV and the standard model is an effective theory valid up to this TeV scale. The quadratic correction changes the Higgs mass by a factor of 100 (much smaller that 10^{19}). This thus solves the hierarchy problem. This model has a lot of interesting phenomenological collider and astrophysical features which have been studied at a length and are available in the literatures.

Randall-Sundrum(RS) model: In 1999, Lisa Randall and Raman Sundrum(RS) proposed a model based on one (warped) extra dimension to solve the Higgs hierarchy problem [41]. According to this model, the fifth dimension of size r_c is S^1/Z_2 orbifold and the 5-dimensional metric is given by

$$ds^2 = e^{-2\sigma(\theta)}\eta_{\mu\nu}dx^\mu dx^\nu - r_c^2 d\theta^2$$

The 5th coordinate $y = r_c\theta$, where $0 \geq \theta \geq \pi$. Randall and Sundrum fixed two D_3 branes: one at $y = 0$ (gravity(hidden) brane) and the other at $y = \pi r_c$ (standard model (visible) brane), respectively. The

exponential factor $e^{-2\kappa r_c \theta}$, appearing in the metric is known as the warp factor. Here r_c is the distance between the two branes and it can be related to the vacuum expectation value (vev) of some modulus field $T(x)$. The modulus field $T(x)$ corresponds to the fluctuation of the metric over the background geometry given by r_c. Replacing r_c by the modulus field $T(x)$, we can rewrite the RS metric at the orbifold point $\theta = \pi$ as

$$ds^2 = e^{-2\kappa T(x)\pi}\eta_{\mu\nu}dx^\mu dx^\nu = g_{\mu\nu}^{vis}\eta_{\mu\nu}dx^\mu dx^\nu$$

where $g_{\mu\nu}^{vis} = e^{-2\kappa T(x)\pi}\eta_{\mu\nu} = \left(\frac{\phi(x)}{f}\right)^2 \eta_{\mu\nu}$. Because of this warping on the visible brane, any scale (e.g. of the order of M_{pl}) on the visible brane, gets warped and produce a TeV scale which thus solves the hierarchy problem. Here $f^2 = \frac{24M_{5pl}^3}{\kappa}$, where M_{5pl} is the 5-dimensional planck scale. One is left with a scalar field $\hat{\phi}(x)(= \phi(x) - \langle\phi\rangle)$, which is known as the radion field. The radion $\phi(x)$, stabilized by the Goldberger and Wise mechanism [42], possesses a lot of interesting phenomenological consequences, which are available in the literature [43–48].

1.6.3 Spacetime Noncommutative theory

The physics of D_p-branes (p being the number of spatial dimension) shows that there is an alternative way of viewing spacetime. In string theory, D_p-branes are the extended dynamical objects. When the open strings propagates through spacetime, its end points are required to lie on a D_p-brane while satisfying the Dirichlet boundary conditions. In the presences of Neveu-Schwarz(NS) B-field, D_p-brane indicates that the string theory contains a fuzziness/noncommutativity of spacetime at a much larger length scale than the string scale which is inversely proportional to the strength of the NS B-field [67]. The strength of the noncommutative scale(Λ) can lie from the Planck scale to the TeV scale. If one performs experiments with the machine energy scale(TeV) equals to the NS B-field scale, then the stringy nature could be revealed with the spacetime noncommutativity.

$$[\hat{x}_\mu, \hat{x}_\nu] = i(B^{-1})_{\mu\nu}$$

In 1936 Heisenberg suggested extending noncommutativity to the coordinates to remove the infinities appearing in Quantum Field Theory(QFT). The divergence appearing in QFT is due to point interaction of the particle. Hence the space-time point is replaced by a "cell" of size l_p (Planck length) and thus the spacetime becomes noncommutative [57, 58]. The spacetime co-ordinates become operators and can be expressed as

$$[\hat{x}_\mu, \hat{x}_\nu] = i\Theta_{\mu\nu} = \frac{i}{\Lambda^2}\mathcal{C}_{\mu\nu}$$

Here $\mathcal{C}_{\mu\nu}$ is the anti-symmetric tensor. The new Heisenberg spacetime uncertainty principle can be written as

$$\triangle\hat{x}_i\triangle\hat{x}_j \geq l_p^2 \quad \text{where} \quad l_p^2 = \tfrac{1}{2}|\Theta_{ij}|.$$

This new principle limits the measurements of position observables near the Planck scale which avoids the formation of black hole at the time of measurements [60, 61].The noncommutative field theory connects the gravity from the spacetime uncertainty principle. Now to study the field theory in a non-commutative spacetime one consider the Moyal-Weyl(MW) $\star$ products instead of the ordinary products among the field variables [102, 103]. The $\star$ product between two smooth function f and g is defined as

$$(f \star g)(x) = f(x) \star g(x) = f(x)exp\left(\frac{i}{2}\overleftarrow{\partial}_\mu \Theta^{\mu\nu}\overrightarrow{\partial}_\nu\right)g(x)$$

Seiberg and Witten realized that there should be a mapping between commutative fields and noncommutative fields which could give a noncommutative gauge theory with any gauge group representation. The map is called the Seiberg-Witten(SW) map [67]. In the Seiberg-Witten approach is that it can be applied to any arbitrary gauge theory (which includes the standard model) where matter can be in an arbitrary representation.

$$\widehat{\Psi}(x, A, \Theta) = \psi(x) + \Psi^{(1)} + \Psi^{(2)} + ...$$
$$\widehat{V}_\mu(x, A, \Theta) = V_\mu(x) + V_\mu^{(1)} + V_\mu^{(2)} + ...$$
$$\widehat{\lambda}(x, A, \Theta) = \alpha(x) + \lambda^{(1)} + \lambda^{(2)} + ...$$
$$\Psi^{(1)} = -\frac{1}{2}\Theta^{\alpha\beta}\left(R_\psi(V_\alpha)\partial_\beta - \frac{i}{4}\left[R_\psi(V_\alpha), R_\psi(V_\beta)\right]\right)\psi$$
$$V_\mu^{(1)} = \frac{1}{2}\Theta^{\alpha\beta}\left\{(\partial_\alpha V_\mu + F_{\alpha\mu}), V_\beta\right\}$$
$$\lambda^{(1)} = \frac{1}{4}\Theta^{\alpha\beta}\left\{V_\beta, \partial_\alpha\lambda\right\}$$

Using the SW approach, Calmet et.al [69] first constructed the standard model using the noncommutative gauge invariance, which is popularly known as the minimal noncommutative standard model (mNCSM). In this model, the triple photon vertex doesn't appear. Melic et.al [70, 71] put forward another version of NCSM where such a triple gauge boson(photon) vertex appears naturally. This is the non-minimal version of the NCSM (in abbreviation nmNCSM). Note that in the mNCSM or in the nmNCSM we don't require to introduce any extra fields: the particle content of these models is the same in the SM. This is discussed in detail in the next chapter.

Chapter 2

The Noncommutative Standard Model

"The string vibrates in ten dimensions because it requires generalized Ramanujan modular functions in order to remain self-consistent. In other words, physicists have not the slightest understanding of why ten and 26 dimensions are singled out as the dimension of the string" - Michio Kaku.

2.1 Historical introduction

The history of the noncommutative theory starts together with the development of quantum field theory. In late 1927, Heisenberg and Pauli were working on quantum theory of electrodynamics, which was before Dirac formulate the relativistic electron theory. They found that, the perturbation terms are led to infinite energies for a given state and also it has infinite energy difference between states [49–52]. In 1930, Oppenheimer pointed out those divergences possibly come from the self-interaction of the electron and it could be removed by non-relativistic limit [53]. In the same year, Lew Landau and Rudolf Peierls tried to reformulate the Heisenberg-Pauli's QED to address the cause of divergence in the many-body configuration space [54,55]. But it didn't remove the divergence from the theory, interestingly it turned out that the Schrodinger equation allows negative energy solution like Dirac equation. Heisenberg believed if one could able to construct the vacuum electromagnetic field configuration with vanishing energy and momentum then the electron self energy could vanish which was missing in the Landau and Peierls configuration space [56]. In 1936, Heisenberg realized that the divergence appearing in QED is due to point interaction of the particle. He suggested to extend noncommutativity to the coordinates to remove the infinities appearing in Quantum Field Theory(QFT). Following Heisenberg's suggestion, Snyder (1947) proposed a minimal length idea (which leads to quantization of spacetime) that would remove the divergences presented in the interaction of matter and field [57, 58]. In his the-

21

ory, Snyder redefines the position and momentum operators as a noncommutative one and they take on discrete values. Therefore a position uncertainty arises naturally. In the same year, Yang formulated the Snyder space for curved spacetime [59]. However, the translational invariance of the theory is broken explicitly in the Snyder's approach. In the late forties, the commutative renormalization program succeeded in the removal of infinities. After a long time in 1990, S. Doplicher, K. Fredenhagen and J. E. Roberts found that though the quantum gravity explains the quantum nature of the gravity but the usual concepts of space-time are inadequate, when we do measurement of distance between two particles is of the order of the Planck length. Hence they showed that the space-time are noncommutative or in other words they has to be quantized [60, 61]. In 1996, Filk investigated the field theories and their properties on quantum spaces [62]. Wess et.al studied deformed algebras on quantum space [63–66]. The seminal work of Seiberg, Witten(1999) and Minwalla(2000) suggests that the noncommutative gauge field theories are the low energy limit of certain class of string theories [67, 68]. Finally in 2002, the standard model on noncommutative spacetime were constructed by X. Calmet, B. Jurco, P. Schupp, J. Wess and M. Wohlgenannt [69], and then it has thoroughly studied on 2005 by B. Melic, J. Trampetic et.al [70, 71]. At the same year, Sorin Marculescu has extended the noncommutative standard model [75]. In 2009, M. M. Ettefaghi extended the standard model with singlet scalar and fermionic particle as cold dark matter in noncommutative space-time [76].

The Field theoretic standard model is basically an algebraic theory, the theory of gravitation is a geometric theory. So we can not quantize the gravity with the rules developed in the framework of quantum field theory because the spacetime coordinates behaves like the dynamical variables in the general theory of relativity. Von Neumann(1934) who first studied mathematically the quantum "space" which is in analogous to the quantum mechanical phase space [77]. According to Heisenberg spacetime uncertainty principle, it is meaningless to talk about point like interaction instead the phase space point could be replaced by "cells" called "Planck cells". The corresponding geometry theory has described as the "pointless geometry" which was later labeled as "noncommutative geometry". In 1980 Alain Connes, Matilde Marcolli, Woronowicz and Drinfeld has constructed a noncommutative geometry by introducing the spectral triples [78–85, 95]. Alain Conne's work provides the mathematical foundation of the quantum field theories in noncommutative spacetime. In the 1996, Alain Connes and Ali Chamseddine developed a unified theory of gravity and standard model in the framework of noncommutative geometry [86]. In the year of 2006 and 2007, J. W Barrett, R. A. Martin, T. Krajewski and C. A. Stephan attempted for the Lorentzian version of the noncommutative geometry standard model of particle physics [87–93]. The Lorentzian noncommutative geometry has developed by Nicolas Franco and

Michal Eckstein. In this case the geometry no longer remains Reimannian, it will turn into Lorentzian geometry and the Hilbert space structure becomes Krein space [96]. Later in 2013, C. A. Stephan extended the noncommutative standard model with the additional $U(1)_X$ gauge group with explicit $U(1)_X$ group particles based on Alain Connes spectral triple approach [94].

2.2   Motivation for Noncommutative(NC) theory

There are two different approaches to construct the gauge theories on noncommutative space: (i) Seiberg-Witten deformed space approach and (ii) Alain Connes quantum(noncommutative) geometry approach. Both theories are formulated from the first principle of gravity. There are several unanswered theoretical questions in Lorentzian notion about quantization of spacetime which motivates predominantly to study noncommutative spacetime. In Sec 2.3, we have discussed about Doplicher, Fredenhagen and Roberts noncommutative deformed theory. Then we followed the deformed noncommutative approach in the framework of Seiberg-Witten map and have discussed about noncommutative standard model. Finally, discussed about status of the Noncommutative phenomenology in Sec 2.9.

- **Motivation-I: Landau Problem**

  Consider the motion of a particle of mass M and charge q in a constant magnetic field $\vec{B}(= (0, 0, B))$, the magnetic field points along the z direction. Landau first investigated this problem in the context of eigenstates and eigenvalues [97]. Without any loss of generality, we can choose the following gauge $\vec{A} = (0, xB, 0)$ and write down the Hamiltonian as

  $$H = \frac{1}{2M}(P_x^2 + P_z^2 + (P_y - \frac{qxB}{c})^2)$$

  Here P_y and P_z are the momentum operators with eigenvalues $\hbar k_y$ and $\hbar k_z$ and they commute with the Hamiltonian operator H. The motion is restricted in $x - y$ plane, so the state in the z direction is not quantized. Then the energy of the harmonic oscillator get shifted with angular frequency $\omega_c = qB/Mc$ and is given by

  $$E_n = \hbar\omega_c(n + \frac{1}{2}) \quad n \geq 0.$$

  The eigen function in the coordinate space is

  $$\langle x, y | n, k_y \rangle = \frac{1}{\sqrt{2\pi\hbar}} e^{ik_y y} \phi_n(x - \frac{c\hbar k_y}{qB})$$

where ϕ_n is the normalized harmonic oscillator wave functions in coordinate space. The energy levels are discrete with the energy difference equal to

$$\triangle E = \hbar\omega_c = \frac{\hbar qB}{Mc}.$$

This clearly shows that the energy difference is directly proportional to the strength of the magnetic field B. At very strong magnetic field ($B \to \infty$), energy separation becomes infinite and only the lowest Landau level (zero point energy) of the oscillator is occupied. The reason is that the coordinates x and y are canonical conjugates in the coordinate space. Those are noncommutative at strong magnetic field i.e.

$$[x, y] = -i\frac{\hbar c}{qB}$$

We can verify by calculating the matrix element of the spacetime commutator of the Landau state $|n, k\rangle$ and $|m, k'\rangle$ as shown below, where n and m are the Landau levels.

$$\langle n, k|[x, y]|m, k'\rangle = \langle n, k|xy|m, k'\rangle - \langle n, k|yx|m, k'\rangle$$
$$= \langle n, k|xy|m, k'\rangle - \langle m, k'|yx|n, k\rangle^*$$
$$= f(nk, mk') - f^*(mk', nk)$$

Using the complete set of states, we find

$$f(nk, mk') = \sum_{l,p}\langle n, k|x|l, p\rangle\langle l, p|y|m, k'\rangle$$

Concentrating on lowest Landau level ($n = m = l = 0$) at strong magnetic field, the wave function becomes $\langle x, y|0, k\rangle = \frac{1}{\sqrt{2\pi\hbar}}e^{iky}\phi_0(x - \frac{c\hbar k}{qB})$. The normalized oscillator wave function ϕ_0 is given by

$$\phi_0 = \left(\frac{M\omega}{\pi\hbar}\right)^{1/4} e^{-\frac{M\omega}{2\hbar}(x - \frac{ck}{qB})^2}$$

The commutator matrix element can be calculated by using

$$f(0k, 0k') = \int \langle 0, k|x|0, p\rangle\langle 0, p|y|0, k'\rangle dp,$$
$$\langle 0, k|x|0, p\rangle = \delta(k - p)\frac{cp}{qB},$$
$$\langle 0, p|y|0, k'\rangle = i\hbar\delta(p - k').$$

Thus the commutator of the canonical conjugate coordinates is obtained in the coordinate space and is given by

$$\langle 0, k|[x, y]|0, k'\rangle = -i\frac{\hbar c}{qB}\langle 0, k|0, k'\rangle.$$

which suggests that space-time coordinates are noncommuting coordinates.

- **Motivation-II: Quantum gravity**

According to Heisenberg uncertainty principle the simultaneous measurement of the dynamical observable A and B can be done with the accuracy of natural unit $\hbar$. One can not achieve the accuracy which is lesser than the natural unit $\hbar$ by any of the experiment. If the dynamical observables commute with each other, then there won't be any uncertainty when we measure the observable. The simultaneous measurement of the accuracy up to 100% can be achieved by experiment. S. Doplicher, K. Fredenhagen and J. E. Roberts [61] found a difficulty in simultaneous measurement of position at very short distance by its very nature. While probing the length between two particles, one has to deposit energy in that spacetime region. The probing energy is inversely proportional to the probing length i.e $E = hc/\lambda \approx hc/l$. If we try to probe the fundamental length $l \approx l_{Planck} = \sqrt{\frac{\hbar G}{c^3}}$, the bailed energy is given by

$$E = hc\sqrt{\frac{c^3}{\hbar G}}$$

One can compare the Schwarzschild solution for black hole which is given by

$$R_s = \frac{2GM}{c^2} = 2\sqrt{\frac{\hbar G}{c^3}} = 2l_{Planck}.$$

Here M denotes the Planck mass $\left(M = M_{Planck} = \sqrt{\frac{\hbar c}{G}}\right)$. Therefore, the deposited energy is good enough to curve the spacetime and it generates the black hole with the event horizon of size $R_s/2$. One may introduce the spacetime uncertainty principle

$$\triangle x_\mu \triangle x_\nu \geq l_{Planck}^2$$

to avoid the appearance of black hole while probing the spacetime points. Therefore the limitation brings the gravity and spacetime noncommutativity together quite naturally.

2.3 Deformed space approach

According to the non-vanishing spacetime commutator, the ordinary field theory has to reformulate on noncommutative spacetime. This is possible when the algebra of functions on a manifold defined by Gelfand-Naimark-Segal theorem [95].Thus the manifold itself includes all information of functions of noncommutative algebra. The deformed approach was mainly developed by S. Doplicher, K. Fredenhagen and J. E. Roberts in which the fields were treated as functions of the noncommutative spacetime coordinates [61]. Later Filk modified the theory based on the product of functions

of noncommutative variable [62]. This product can also be realized by noncommutative product of functions of commutative variables. The fundamental symmetry of the spacetime can be realized by twisted Poincare symmetry [98, 99, 101], the twisted product can be identified as simplest product of Moyal-Weyl star product [102, 103].

2.3.1 Moyal space NC field theory

Points are replaced by maximal ideals and coordinates on the compact manifold $\mathcal{M}$ are replaced by coordinate functions in $\mathbb{C}(\mathcal{M})$ and the vector fields are replaced by derivations of the algebra. Consider the algebra of noncommutative coordinate function $\widehat{\mathcal{A}}$ on canonical Minkowski space

Points	$\longrightarrow$	Maximal ideals
$x \in \mathcal{M}$	$\longmapsto$	Ideal $J = \{f | f(x) = 0\} \subset \mathbb{C}(\mathcal{M})$
Coordinates	$\longrightarrow$	Coordinate functions
Vector field	$\longrightarrow$	Derivation of the algebra
Geometry	$\longrightarrow$	Algebraic geometry

Table 2.1: Algebraic geometry

$$\widehat{\mathcal{A}} = \frac{\mathbb{C}\langle\langle \widehat{x}^1, ..., \widehat{x}^n \rangle\rangle}{\mathcal{I}},$$

where $\mathcal{I}$ is the ideal and equal to commutation relation for the coordinate functions. Here the ideal is $\mathcal{I} \equiv [\widehat{x}_i , \widehat{x}_i] = i\theta_{ij}(\widehat{x})$. Similarly for commutative algebra of functions

$$\mathcal{A} = \frac{\mathbb{C}\langle\langle x^1, ..., x^n \rangle\rangle}{[x^i, x^j]} \equiv \mathbb{C}[[x^1, ...x^n]], \qquad i.e \ [x^i, x^j] = 0$$

Here we have to map both the algebras by an isomorphism. Let us define noncommutative algebra with *dot* product ($\widehat{\mathcal{A}}_{\widehat{x}}, .$) and commutative algebra with $\star$ product ($\mathcal{A}_x, \star$), then the algebra isomorphism map,

$$W : \qquad \widehat{\mathcal{A}}_{\widehat{x}} \sim \mathcal{A}_x^\star \qquad \text{Vector space isomorphism:} \qquad \widehat{V}_r \sim V_r$$

where V_r is the r-polynomial degree of vector space which has N commuting variables. This type of vector space isomorphism is exists, if and only if the noncommutative algebra $\widehat{\mathcal{A}}$ satisfies the Poincare-Birkhoff-Witt property (PBW) i.e the dimension of the subspace of homogeneous polynomials should be the same as for commuting coordinates. The basis of symmetrically ordered polynomials can be written as:

$$1, \widehat{x}_i, \frac{1}{2}(\widehat{x}_i\widehat{x}_j + \widehat{x}_j\widehat{x}_i)... \quad i < j$$

26

Using the vector space isomorphism map, we map the polynomials

$$f(x) \longleftrightarrow \widehat{f}(\widehat{x})$$

by a map of the basis. By definition, two polynomials $\widehat{f}(\widehat{x})$ and $\widehat{g}(\widehat{x})$ can be multiplied

$$\widehat{f}(\widehat{x}).\widehat{g}(\widehat{x}) = \widehat{fg}(\widehat{x})$$

Now we can map the polynomials back to a polynomial in $\mathcal{A}_x^\star$

$$\widehat{fg}(\widehat{x}) \mapsto f(x) \star g(x)$$

This defines the star product of two polynomial functions. It is bilinear and associative but noncommutative.

$$f(x) \star g(x) = \mu \left(e^{\frac{i}{2} h \theta^{\alpha\beta} \partial_\alpha \otimes \partial_\beta} f(x) \otimes g(x) \right)$$

where μ is the multiplication map. The $\star$ is the well-known Moyal-Weyl product. It can be extended to $\mathbb{C}^\infty$ functions without loss of bilinearity and associativity. One write

$$f(x) \star g(x) - g(x) \star f(x) = \frac{ih}{2} \theta^{\mu\nu} \left((\partial_\mu f(x))(\partial_\nu g(x)) - (\partial_\mu g(x))(\partial_\nu f(x)) \right) + \mathcal{O}(h^2),$$

This is the Poisson structure on a differentiable manifold $\mathcal{M}$ with $\star$ product deformation of the algebra of smooth function $\mathbb{C}^\infty(\mathcal{M})$ from $\mathcal{M}$ to $\mathbb{C}$. The star product ($\star : \mathbb{C}^\infty \times \mathbb{C}^\infty \to \mathbb{C}^\infty$) is a bidifferential operator which is a differential operator on both of its arguments. The zeroth order $\star$ product is the usual commutative product of functions. Now we can evaluate the $\star$ commutator

$$[x^\mu \overset{\star}{,} x^\nu] = x^\mu \star x^\nu - x^\nu \star x^\mu = x^\mu x^\nu + \frac{i}{2} \theta^{\mu\nu} - x^\nu x^\mu - \frac{i}{2} \theta^{\nu\mu} = i\theta^{\mu\nu}, \quad h = 1.$$

Here $\theta^{\mu\nu}$ is an anti-symmetric tensor. Hermann Weyl gave a prescription [102] for canonical quantization: he showed how to associate an operator with a classical function of the canonical variables. Say f and g are some smooth functions and their corresponding Weyl operators are $W(f)$ and $W(g)$, defined as,

$$W(f) = \tfrac{1}{\sqrt{(2\pi)^3}} \int d^4k e^{ik\widehat{x}} \widetilde{f}(k) \qquad W(g) = \tfrac{1}{\sqrt{(2\pi)^3}} \int d^4p e^{ip\widehat{x}} \widetilde{g}(p)$$

We use the following Campbell-Baker-Hausdorff(CBH) formula to define the operator $\star$ product

$$i.e \ \ e^\lambda e^\mu \simeq exp \left(\lambda + \mu + \frac{1}{2}[\lambda, \mu] + \frac{1}{12}[\lambda, [\lambda, \mu]] + \frac{1}{12}[\mu, [\lambda, \mu]] + ... \right)$$

Using this we get,

$$W(f).W(g) = W(f \star g) = \frac{1}{(2\pi)^3} \int d^4k d^4p e^{i(k+p)\hat{x}} e^{-\frac{i}{2}k_\mu \theta^{\mu\nu} p_\nu} \widetilde{f}(k)\widetilde{g}(p)$$

The non-commutativity is realized with the $\star$ products in Groenewold-Weyl-Moyal plane

$$(f \star g)(x) = f(x) \star g(x) = f(x) exp\left(\frac{i}{2}\overleftarrow{\partial}_\mu \theta^{\mu\nu} \overrightarrow{\partial}_\nu\right) g(x)$$

In this Moyal space, Noncommutative field theories are obtained by replacing the ordinary products by $\star$ product as defined below

$$(f \star g)(x) = \frac{1}{(2\pi)^N} \int d^N k d^N p e^{ik\hat{x}} \widetilde{f}(k) e^{-\frac{i}{2}k_\mu \theta^{\mu\nu} p_\nu} e^{ip\hat{x}} \widetilde{g}(p)$$

Note that the star product is a nonlocal one. It can also be written as integral kernal

$$(f \star g)(x) = \frac{1}{(2\pi)^N} \int \int \widetilde{f}(x + \frac{1}{2}\theta k)\widetilde{g}(x + p)e^{ip\hat{x}} d^N k d^N p$$

This product is well defined on the space of smooth rapidly decreasing functions.

2.3.2 Classification of noncommutative structure

The quotient algebra $\widehat{\mathcal{A}}$, defined by ideal $\mathcal{I}$, is generated by commutation relations. We can define

$$\mathcal{I} := \{c\widehat{a}, \widehat{r}.\widehat{a}, \widehat{a}.\widehat{r} \,|\, \forall c \in \mathbb{C}, \forall \widehat{r} \in \widehat{\mathcal{A}}\},$$

where $\widehat{a} = \widehat{x}^i.\widehat{x}^j - \widehat{x}^j.\widehat{x}^i - i\theta^{ij}(\widehat{x})$. We can classify the noncommutativity based on structure of the ideal ∞ as three types, which are classified most commonly by $\theta^{ij}(\widehat{x})$. They can be chosen as constant or linear or quadratic. The first one is the class of canonical deformation and later two are under non-canonical deformation.

1. Canonical structure

$$[\widehat{x}^\mu, \widehat{x}^\nu] = i\theta^{\mu\nu},$$

where $\theta^{\mu\nu} \in \mathbb{R}$ is an antisymmetric matrix and $\theta^{\mu\nu}$ is constant and another case it can be dynamic also.

2. Non-canonical deformation

   - Linear or Lie algebra structure

   $$[\widehat{x}^\mu, \widehat{x}^\nu] = i\lambda_\rho^{\mu\nu} \widehat{x}^\rho$$

   where $\lambda_\rho^{\mu\nu} \in \mathbb{C}$ are the structure constant, it has classified into two different approaches

- Fuzzy sphere [104, 105]

- κ-spacetime deformation [107, 108]

- Quadratic or q-deformed structure [106, 109, 110]

$$[\widehat{x}^\mu, \widehat{x}^\nu] = i\theta^{\mu\nu}_{\kappa\rho}\widehat{x}^\kappa\widehat{x}^\rho = \left(\frac{1}{q}\widehat{R}^{\mu\nu}_{\kappa\rho} - \delta^\mu_\rho\,\delta^\nu_\kappa\right)\widehat{x}^\kappa\widehat{x}^\rho$$

where $\widehat{R}^{\mu\nu}_{\kappa\rho} \in \mathbb{C}$. This $\widehat{R}$-matrix corresponding to quantum groups which obeys Hopf algebra.

The constants $\theta^{\mu\nu}$-dynamic, $\lambda^{\mu\nu}_\rho$-structure constant and $\theta^{\mu\nu}_{\kappa\rho}$ satisfies the PBW property.

2.3.3 Constant θ deformation

In the noncommutative space, the coordinate and momentum are the operators and momentum operators would commute each other but position operators won't commute. This space is called non-commutative space. If the momentum operators also won't commute then it called as noncommutative phase space. Thus the noncommutative operators can be represented in two different ways [112].

- NC space. Space-space noncommuting and momentum-momentum commuting representation

$$\hat{x}_i = x_i - \frac{1}{2\hbar}\theta_{ij}p^j \qquad \hat{p}_i = p_i$$

$$[\hat{x}_i, \hat{x}_j] = i\theta_{ij} \qquad [\hat{x}_i, \theta_{ij}] = 0 \qquad [\hat{p}_i, \hat{p}_j] = 0 \qquad [\hat{x}_i, \hat{p}_j] = i\hbar\delta_{ij}$$

- NC Phase space. Space-space noncommuting and momentum-momentum noncommuting representation

$$\hat{x}_i = \alpha x_i - \frac{1}{2\hbar\alpha}\theta_{ij}p^j \qquad \hat{p}_i = \alpha p_i + \frac{1}{2\hbar\alpha}\widetilde{\theta}_{ij}x^j$$

$$[\hat{x}_i, \hat{x}_j] = i\theta_{ij} \qquad [\hat{x}_i, \theta_{ij}] = 0 \qquad [\hat{p}_i, \hat{p}_j] = \widetilde{\theta}_{ij} \qquad [\hat{p}_i, \widetilde{\theta}_{ij}] = 0 \qquad [\hat{x}_i, \hat{p}_j] = i\hbar\delta_{ij},$$

where $\widetilde{\theta}$ is totally antisymmetric on NC Phase space. Here α is a scaling constant related to the NC phase space. Now $\widetilde{\theta} \to 0$ as $\alpha \to 1$, which means NC phase space turns into NC space.

Derivatives on $\mathcal{A}_\theta$

Derivatives on quantum spaces can be constructed by using proper mapping between commutative and noncommutative functions. One can introduce the derivatives on $\mathcal{A}_\theta$ based on the $\star$-product

formulation as given below. First we can use map ϕ on $f \in \mathcal{F}$ and we get $f \in \mathcal{A}_\theta$ and take $\star$-derivative of $f \in \mathcal{A}_\theta$. Similarly in another way, we take derivative on $f \in \mathcal{F}$ and take map ϕ with $\star$.

$$
\begin{array}{ccc}
f \in \mathcal{F} & \overset{\phi}{\longmapsto} & f \in \mathcal{A}_\theta \\
\partial_\mu \downarrow & & \downarrow \partial_\mu^\star \\
(\partial_\mu f) \in \mathcal{F} & \overset{\phi}{\longmapsto} & (\partial_\mu^\star \triangleright f) \in \mathcal{A}_\theta
\end{array}
$$

This defines $\partial_\mu^\star$ acting on $f \in \mathcal{A}_\theta$ i.e.

$$
\partial_\mu^\star \triangleright f := (\partial_\mu f)
$$

We can list the properties of the $\star$-derivatives by using the above map. The partial derivative on the NC coordinate operator is

$$
\partial_\mu^\star \triangleright x^\rho = \delta_\mu^\rho
$$

This turns out usual definition of a derivative and the $\star$-product of two functions is a function again

$$
\partial_\mu^\star \triangleright (f \star g) = (\partial_\mu(f \star g))
$$

For the $\star$-product with x-independent θ is that

$$
(\partial_\mu(f \star g)) = (\partial_\mu f) \star g + f \star (\partial_\mu g)
$$

2.3.4 Twisted Poincare symmetry in the canonical structure

Poincare algera:

Let us consider the Poincare Lie algebra $g = iso(3,1)$ of translation operator P_μ(momentum) and Lorentz generator $M_{\mu\nu}$ which is

$$
[P_\mu, P_\nu] = 0, \quad [P_\rho, M_{\mu\nu}] = i(\eta_{\rho\mu}P_\nu - \eta_{\rho\nu}P_\mu),
$$

$$
[M_{\mu\nu}, M_{\rho\sigma}] = -i(\eta_{\mu\rho}M_{\nu\sigma} - \eta_{\mu\sigma}M_{\nu\rho} - \eta_{\nu\rho}M_{\mu\sigma} + \eta_{\nu\sigma}M_{\mu\rho}
$$

Hopf algebra can be constructed for Poincare Lie algebra by enveloping on iso$(3,1)$ which is $\mathcal{U}(\text{iso}(3,1))$ [98, 99]. The required conditions are

1. Leibniz rule (Co-product):$\Delta(P_\mu) = P_\mu \otimes I + I \otimes P_\mu; \quad \Delta(M_{\mu\nu}) = M_{\mu\nu} \otimes I + I \otimes M_{\mu\nu}$

2. Co-unit: $\varepsilon(P_\mu) = \varepsilon(M_{\mu\nu}) = 0$

3. Antipode: $S(P_\mu) = -P_\mu; \quad S(M_{\mu\nu}) = -M_{\mu\nu}$

Twisted Poincare algera:

Now we can construct the twisted Poincare Lie algebra by using the canonical twist $\mathcal{F} \in \mathcal{U}(g) \otimes \mathcal{U}(g)$

$$\mathcal{F} = e^{\frac{i}{2}\theta^{\mu\nu}P_\mu \otimes P_\nu} \quad \mathcal{F} \in \mathcal{U}_{\mathcal{F}}(g)$$

The twist has to satisfy the cocyle property. Further the structure of the coproduct gets modified in deformed case, apart from that all Hopf algebra structures remains unchanged ($\mathcal{U}^{\mathcal{F}}(g) = \mathcal{U}(g)$) i.e.

$$(\mathcal{F} \otimes I)(\Delta \otimes I)\mathcal{F} = (I \otimes \mathcal{F})(I \otimes \Delta)\mathcal{F}$$

Eventually, the deformed Pioncare algebra $iso^{\mathcal{F}}(3,1)$ is the subalgebra of $\mathcal{U}^{\mathcal{F}}(iso(3,1))$ such that if $\{t_i\}$ is a basis of $iso^{\mathcal{F}}(3,1)$, then

- $\{t_i\}$ generates $\mathcal{U}^{\mathcal{F}}(iso(3,1))$

- $\Delta^{\mathcal{F}}(t_i) = t_i \otimes I + f_i^j \otimes t_j; \quad f_i^j \in \mathcal{U}^{\mathcal{F}}(iso(3,1)) \quad i,j = 1...n$

- $[t_i, t_j]_{\mathcal{F}} = C_{ij}^k t_k; \quad C_{ij}^k -$ is the structure constant
  The adjoint action $[t, t']_{\mathcal{F}} := ad_t^{\mathcal{F}} t' = t_{1_{\mathcal{F}}} t' \, S(t_{2_{\mathcal{F}}})$

The generators of $\mathcal{U}^{\mathcal{F}}(iso(3,1))$ is

$$P_\mu^{\mathcal{F}} = P_\mu; \quad M_{\mu\nu}^{\mathcal{F}} = M_{\mu\nu} - \frac{i}{2}\theta^{\rho\sigma}[P_\rho, M_{\mu\nu}]P_\sigma.$$

The Leibniz rule is

$$\Delta^{\mathcal{F}}(P_\mu) = P_\mu \otimes I + I \otimes P_\mu,$$
$$\Delta^{\mathcal{F}}(M_{\mu\nu}^{\mathcal{F}}) = M_{\mu\nu}^{\mathcal{F}} \otimes I + I \otimes M_{\mu\nu}^{\mathcal{F}} + i\theta^{\alpha\beta}P_\alpha \otimes [P_\beta, M_{\mu\nu}].$$

The co-unit and antipode are

$$\varepsilon(P_\mu) = \varepsilon(M_{\mu\nu}^{\mathcal{F}}) = 0; \quad S(P_\mu) = -P_\mu; \quad S(M_{\mu\nu}^{\mathcal{F}}) = -M_{\mu\nu}^{\mathcal{F}} - i\theta^{\rho\sigma}[P_\rho, M_{\mu\nu}]P_\sigma.$$

The adjoint action are

$$[P_\mu, P_\nu]_{\mathcal{F}} = 0; \quad [P_\rho, M_{\mu\nu}^{\mathcal{F}}] = i(\eta_{\rho\mu}P_\nu - \eta_{\rho\nu}P_\mu);$$

$$[M_{\mu\nu}^{\mathcal{F}}, M_{\rho\sigma}^{\mathcal{F}}]_{\mathcal{F}} = -i(\eta_{\mu\rho}M_{\nu\sigma}^{\mathcal{F}} - \eta_{\mu\sigma}M_{\nu\rho}^{\mathcal{F}} - \eta_{\nu\rho}M_{\mu\sigma}^{\mathcal{F}} + \eta_{\nu\sigma}M_{\mu\rho}^{\mathcal{F}}).$$

Thus the adjoint action gives the Jacobi identity for the element of $\mathcal{U}^{\mathcal{F}}(g)$

$$[t, [t', t'']_{\mathcal{F}}]_{\mathcal{F}} + [t', [t'', t]_{\mathcal{F}}]_{\mathcal{F}} + [t'', [t, t']_{\mathcal{F}}]_{\mathcal{F}} = 0 \quad \forall t, t', t'' \in iso^{\mathcal{F}}(3,1)$$

These commutators are not usual commutators, they are twisted commutator in which the twist has the form $\mathcal{F} = e^{\frac{i}{2}\theta^{\mu\nu}P_\mu \otimes P_\nu}$. It is known as Moyal-Weyl $\star$-product of two canonical functions in the deformed space. In ref [100], it is shown that, the star product obeys noncommutative Lorentz symmetry, which means that the star product is invariant under noncommutative Lorentz transformations. Here the field actions are obtained by expanding the star product order by order of $\theta_{\mu\nu}$ and the fields taken in the enveloping algebra via the Seiberg-Witten maps [101]. So one can think that such type of Lorentz symmetry can exist and which may obeys certain Hopf algebra under some sort of general Poincare/Lorentz group which we don't know distinctly.

2.3.5 Noncommutative QED in canonical deformation

The commutative field functions with Moyal-Weyl product($\mathcal{A}_x, \star$) are defines the NCQED action on Moyal-Weyl space as follows,

$$\mathcal{S}_{NCQED} = \int d^4x\, \mathcal{L}(\psi, A) = \int d^4x \left(\overline{\psi} \star (i\slashed{D}) \star \psi - m\overline{\psi} \star \psi - Tr\frac{1}{4e^2}F_{\mu\nu} \star F^{\mu\nu} \right) \qquad (2.1)$$

and the field-strength tensor is

$$F_{\mu\nu} = i[D_\mu \overset{\star}{,} D_\nu] = \partial_\mu A_\nu - \partial_\nu A_\mu - i[A_\mu \overset{\star}{,} A_\nu]$$

Where $[A_\mu \overset{\star}{,} A_\nu] = A_\mu \star A_\nu - A_\nu \star A_\mu$. And the covariant derivative has the form $D_\mu = \partial_\mu - iA_\mu$ and the coupling constant e is defined with gauge field itself. The renormalizability of the NCQED has been found on the noncommutative Moyal space [132]. The NCQED lagrangian 2.1 is invariant under the below mentioned noncommutative gauge transformation:

$$\delta_\lambda \psi(x) = i\left(\lambda \star \psi\right)(x); \qquad \delta_\lambda \overline{\psi}(x) = -i\left(\overline{\psi} \star \lambda\right)(x);$$

$$\delta_\lambda A_\mu(x) = \partial_\mu \lambda(x) - i[A_\mu \overset{\star}{,} \lambda](x); \qquad \delta_\lambda F_{\mu\nu}(x) = i[\lambda \overset{\star}{,} F_{\mu\nu}](x),$$

where $\lambda(x)$ is the local gauge parameter. The ordinary products in QED are replaced by $\star$ product in the case of NCQED, which is shown in equation 2.1. The charges for the fermions are limited to three types and they are 0, $+1$ and -1. The star commutator in the field-strength tensor gives rise the interesting feature for abelian gauge field interaction in NC gauge theory. This means that, the star commutator of the two abelian field won't vanish. Further, it allows triple and quartic abelian A_μ field interaction. The fermionic interaction with the gauge field can be written as

$$\overline{\psi} \star \gamma^\mu A_\mu \star \psi = \overline{\psi}\, \gamma^\mu A_\mu\, \exp(\frac{i}{2}\, p_\rho \theta^{\rho\sigma} q_\sigma)\, \psi,$$

where p and q are the initial and final momenta of the fermions. Here we have used the cyclic permutation property:

$$\int d^4x(f \star g \star h)(x) = \int d^4x((f \star g).h)(x) = \int d^4x(h.(f \star g))(x) = \int d^4x(h \star f \star g)(x)$$

Drawback of NCQED

- The photon can couple with only the $0, \pm 1$ charged matter field. It cannot couple with fractional charged matter fields(quarks) [113, 114]. Because, for charge $Q = +1$, the fundamental representations :

$$\psi \to \psi' = U \star \psi,$$

$$D_\mu \psi = \partial_\mu \psi - iA_\mu \star \psi,$$

For charge $Q = -1$, the anti-fundamental representations($\hat{\psi}$) :

$$\hat{\psi} \to \hat{\psi}' = \hat{\psi} \star U^{-1},$$

$$D_\mu \hat{\psi} = \partial_\mu \hat{\psi} + i\hat{\psi} \star A_\mu.$$

Finally, for charge $Q = 0$ the adjoint representation:

$$\chi \to \chi' = U \star \chi \star U^{-1},$$

$$D_\mu \psi = \partial_\mu \psi - i[A_\mu \overset{\star}{,} \psi].$$

along with the gauge field transformations

$$A_\mu \to A'_\mu = U \star A_\mu \star U^{-1} + iU \star A_\mu \star U^{-1}$$

The gauge kinetic term is given by

$$\mathcal{L}_{gauge} = -\frac{1}{4e^2}Tr\left(F_{\mu\nu} \star F^{\mu\nu}\right)$$

- The minimal coupling interaction

$$D_\mu \psi^{(n)} = \partial_\mu \psi^{(n)} - iq^{(n)}A_\mu \star \psi^{(n)}$$

does not transform covariantly with integral multiple n of unit charge under transformation of the gauge field and $\psi^{(n)} \to U^{(n)} \star \psi^{(n)}$ with $U^{(n)} = e^{iq^{(n)}\lambda}$. Hence the photon field depends on charge n, which would lead to a multitude of photon fields in NCQED. Here the gauge field

A_μ is not physical. By definition $A_\mu \psi^n = eq^{(n)} a_\mu^{(n)} \psi^{(n)}$ with $a_\mu^{(n)} \neq a_\mu^{(m)}$ for $q^{(n)} \neq q^{(m)}$ and $F_{\mu\nu} \psi^n \equiv e\, q^{(n)} f_{\mu\nu}^{(n)} \psi^n$. There is no compelling reason of assigning the same coupling constant e to all gauge fields $a_\mu^{(n)}$. We may assign individual coupling constant to gauge fields and correspondingly we rescale the physical fields as $a_\mu'^{(n)}$ and $f_{\mu\nu}'^{(n)}$. The corresponding NCQED action can be written as

$$\mathcal{S}_{NCQED} = -\frac{1}{2} \int d^4x \, Tr \, \frac{1}{(eQ)^2} F_{\mu\nu} \star F^{\mu\nu} \quad \Rightarrow \mathcal{S}'_{NCQED} = -\frac{1}{2} \int d^4x \, Tr \, \frac{1}{G^2} F_{\mu\nu} \star F^{\mu\nu}$$

where G, a coupling generator, is a function of the charge operator Q and constants g_n, given by

$$G\psi^{(n)} \propto g_n \psi^{(n)} \qquad \text{and} \qquad Tr \frac{1}{G^2} F_{\mu\nu} \star F^{\mu\nu} = \frac{1}{N} \sum_{n=1}^{N} \frac{e^2}{g_n^2} (q^{(n)})^2 f_{\mu\nu}'^{(n)} \star f'^{(n)\mu\nu}.$$

Now in terms of the g_n, the normal coupling constant e can be expressed by

$$Tr \frac{1}{G^2} Q^2 = \sum_{n=1}^{N} \frac{1}{g_n^2} (q^{(n)})^2 = \frac{1}{2e^2}$$

- The $SU(N)$ gauge theory with only $\star$ product is not allowed on noncommutative space-time except $U(N)$ gauge theory. Because

$$[A_\mu^a T^a \overset{\star}{,} A_\mu^b T^b] = \frac{1}{2} \{A_\mu^a \overset{\star}{,} A_\mu^b\}[T^a, T^b] + \frac{1}{2}[A_\mu^a \overset{\star}{,} A_\mu^b]\{T^a, T^b\}$$

The first term in above satisfy the Lie algebra, while for the second term, the coefficient is zero in commutative case, but non zero due to $\star$ product. The closure property of the commutation relation is satisfied in the fundamental representation of $U(N)$ gauge fields, not possible for $SU(N)$ gauge theory. This is why in the noncommutative space-time we can't construct the standard model with the gauge group $U(1)_Y \otimes SU(2)_L \otimes SU(3)_C$.

Chaichian et.al [115,116], proposed a $U(N)$ gauge theory to overcome the charge quantization problem as well as they constructed the standard model on noncommutative spacetime. The gauge group is restricted to $U(N)$ and the symmetry group of standard model achieved by the reduction of $U(1)_\star \otimes U(2)_\star \otimes U(3)_\star$ in to $U(1) \otimes SU(2) \otimes SU(3)$ by the addition of two new scalars, which are known as Higgsac's. The fractional charge of the quarks can be explained in this model quite naturally.

2.4   Principles of noncommutative gauge theory

The noncommutative standard model fields are enveloped by appropriate Lie gauge group with the Moyal-Weyl star product in the Seiberg-Witten scenario. In this approach, the particle content

and the gauge symmetry groups have been maintained as same as the standard model. Seiberg-Witten approach solves the charge quantization problem naturally by mapping the commutative and non-commutative fields(called SW map) while satisfying appropriate principles. The Seiberg-Witten(SW) noncommutative gauge theory is based on three important principles

1. Principles of Covariant coordinates

2. Locality and classical limit

3. Gauge equivalence principle

- **Covariant coordinates**[1]: Consider the following noncommutative gauge transformation of the noncommutative fields

$$\widehat{\delta}\widehat{\psi}(\hat{x}) = i\widehat{\lambda}\,\widehat{\psi}(\hat{x}) \qquad \widehat{\delta}\psi(x) = i\alpha \star \psi(x) \quad \widehat{\psi}, \widehat{\lambda} \in \{(\widehat{\mathcal{A}}_x, .) = (\mathcal{A}_x, \star)\}, \quad \text{where} \quad W(\alpha) = \widehat{\lambda}.$$

Here α is the commutative gauge parameter (i.e zeroth order of the NC gauge parameter(see in next section)). The $\star$ product of a field and coordinate doesn't transform covariantly i.e.

$$\widehat{\delta}_{\widehat{\lambda}}(x \star \psi(x)) = ix \star \alpha(x) \star \psi(x) \neq i\alpha(x) \star x \star \psi(x)$$

We define the covariant NC coordinate $X^\mu = x^\mu + g\theta^{\mu\sigma}A_\sigma$, which leads to the covariant quantity $\hat{\delta}_{\hat{\lambda}}(X \star \psi) = i\alpha \star (X \star \psi)$. Thus the covariant coordinates and gauge potentials transform under the noncommutative NC gauge transformation [63]

$$\widehat{\delta}_{\widehat{\lambda}}X^\mu = i[\alpha \stackrel{\star}{,} X^\mu], \quad g\widehat{\delta}_{\widehat{\lambda}}A^\mu = i\theta^{-1}_{\mu\sigma}[\alpha \stackrel{\star}{,} X^\sigma] + ig[\alpha \stackrel{\star}{,} A^\mu] \quad \text{and}$$

$$ig\,\theta^{\mu\rho}\theta^{\nu\sigma}F_{\rho\sigma} = [X^\mu \stackrel{\star}{,} X^\nu] - i\theta^{\mu\nu}, \quad \widehat{\delta}_{\widehat{\lambda}}F^{\mu\nu} = i[\alpha \stackrel{\star}{,} F^{\mu\nu}].$$

- **Classical limit**: The noncommutatine product of any two field function can be represented as nonlocal $\star$ product. So the locality property is lost in this NC geometry. But it is the valid notion to bring gravity in this algebraic geometry because theory of gravity is nonlocal. The $\star$ product can be written as

$$f \star g = f \cdot g + \sum_{n=1}^{\infty} h^n C_n(f, g)$$

In the limit $h \to 0$ (commutative limit), the nonlocal product becomes point wise product. Similarly the noncommutative fields turns into commutative fields.

---

[1]Note: In this thesis hereafter we use $\widehat{}$ symbol for noncommutative operator and without $\widehat{}$ for commutative operator with $\star$ product, which means the Seiberg-Witen map yet to substitute and then $\star$ operation can be done.

- **Gauge equivalence principle**: The commutative Yang-Mills gauge theory and noncommutative Yang-Mills theory are different by choice of regularization which is Pauli-Villars for first one and point-splitting scheme [111] for later one. This provides us classical gauge invariance $\delta A_i = \partial_i \alpha$ and NC gauge invariance $\hat{\delta}_{\hat{\lambda}} \hat{A}_i = \partial_i \hat{\lambda} + i[\hat{\lambda} \stackrel{\star}{,} \hat{A}_i]$ respectively. In the case of quantum electrodynamics, while the gauge group is abelian in commutative spacetime, it is non-abelian in noncommutative spacetime. So neither commutative nor nocommutative gauge group are going to be isomorphic one to each other, but they are related to each other by a change of variables. This mapping is known as the Seiberg-Witten map [67].

$$\begin{pmatrix} A \\ \alpha \end{pmatrix} \rightarrow \begin{pmatrix} \hat{A}(A) \\ \hat{\lambda}(A) \end{pmatrix}$$

Here the NC gauge parameter $\hat{\lambda}$ is dependent on the gauge field A and also α is connected with $\hat{\lambda}$ by the SW map, otherwise the commutative and nocommutative gauge group would be equivalent, which cannot be true. Hence, the gauge equivalence equations are

$$\hat{\delta}_{\hat{\lambda}} \hat{A}_\mu(A; \theta) = \hat{A}_\mu(A + \delta_\alpha A; \theta) - \hat{A}_\mu(A; \theta) = \delta_\alpha \hat{A}_\mu(A; \theta),$$

$$\hat{\delta}_{\hat{\lambda}} \hat{\Psi}(\psi, A; \theta) = \delta_\alpha \hat{\Psi}(\psi, A; \theta),$$

$$\hat{\delta}_{\hat{\lambda}(\alpha, A)} \hat{\lambda}(\beta, A) = \delta_\alpha \hat{\lambda}(\beta, A).$$

We know that the gauge parameters do commute in the NC gauge theory, but not in the NC case.

$$\delta_\alpha \alpha(x) = \frac{i}{2}[\alpha(x), \alpha(x)] = 0; \quad \hat{\delta}_{\hat{\lambda}(\alpha, A)} \hat{\lambda}(\beta, A) = \delta_\alpha \hat{\lambda}(\beta, A) = \frac{i}{2}[\alpha \stackrel{\star}{,} \beta](x) \neq 0$$

In addition, we require that the gauge parameter has to satisfy gauge consistency principle, which is

$$i \left(\hat{\delta}_\alpha \hat{\lambda}_\beta - \hat{\delta}_\beta \hat{\lambda}_\alpha \right) + [\hat{\lambda}_\alpha \stackrel{\star}{,} \hat{\lambda}_\beta] = i\hat{\lambda}_{-i[\alpha \stackrel{\star}{,} \beta]}.$$

We know that, this consistency principle are even required for commutative infinitesimal gauge transformation as well as in twisted infinitesimal gauge transformation when two gauge fields say A and A' becomes the part of the same gauge orbit.

2.5 Seiberg-Witten(SW) Map

Seiberg-Witten Map overcomes the shortcoming of purely equipped $\star$ product NC gauge theory and enables one to deform commutative gauge theories with essentially arbitrary gauge group

and its representation. The Seiberg-Witten Map is the map between noncommutative fields and commutative fields which is constructed from Gauge Consistency principle(GCP) and Gauge equivalence principle(GEP),where noncommutative fields and gauge transformation parameters are non-local. We impose the enveloping algebra-valued functions on gauge field and gauge parameter with noncommutative parameter θ. Such a procedure allows to construct the standard model and the GUT theory on NC space-time [117].

2.5.1 SW map construction

Let us consider the noncommutative gauge fields $\hat{A}$ and gauge parameters $\hat{\lambda}$ are enveloping algebra valued by an arbitrary gauge group. So we choose a symmetric basis in the enveloping algebra, T^a, $\frac{1}{2}(T^a T^b + T^b T^a)$, ...

$$\hat{\lambda}(x) = \hat{\lambda}_a(x)T^a + \hat{\lambda}_{ab}^1(x) : T^a T^b : + ...$$

$$\hat{A}_\mu(x) = \hat{A}_{\mu\, a}(x)T^a + \hat{A}_{\mu\, ab}^1(x) : T^a T^b : + ...$$

The solution of the GEP and GCP can be found to each order of the NC parameter θ. The gauge field, gauge parameter and fermion fields are the functions of the covariant NC coordinates.

$$\hat{\lambda}(\lambda, A, \theta) = \alpha + \sum_{n=1}^{\infty} \lambda^n(\lambda, A, \theta),$$

$$\hat{A}_\mu(A, \theta) = A_\mu + \sum_{n=1}^{\infty} A_\mu^n(A, \theta),$$

$$\hat{\psi}(\psi, A, \theta) = \psi + \sum_{n=1}^{\infty} \psi^n(\psi, A, \theta).$$

Consider the infinitesimal NC gauge transformation of the guage fields, fermion fields and gauge parameter,

$$\hat{\delta}_{\hat{\lambda}}\hat{A}_\mu = \partial_\mu \hat{\lambda} - i\left[\hat{A}_\mu \stackrel{\star}{,} \hat{\lambda}\right]; \quad \hat{\delta}_{\hat{\lambda}}\hat{F}_{\mu\nu} = i\left[\hat{\lambda} \stackrel{\star}{,} \hat{F}_{\mu\nu}\right]; \quad \hat{\delta}_{\hat{\lambda}}\hat{\Psi} = i\hat{\lambda} \star \hat{\Psi}.$$

The Bianchi identity can be written as

$$[D_\sigma \stackrel{\star}{,} F_{\mu\nu}] + [D_\mu \stackrel{\star}{,} F_{\nu\sigma}] + [D_\nu \stackrel{\star}{,} F_{\sigma\mu}] = 0.$$

Expanding the gauge equivalence principle up to order θ for gauge parameter, we get

$$\triangle\lambda^{(1)} : i\left(\delta_\alpha \lambda_\beta^{(1)} - \delta_\beta \lambda_\alpha^{(1)}\right) + [\lambda_\alpha^{(1)}, \beta] + [\alpha, \lambda_\beta^{(1)}] - \lambda_{[\alpha \stackrel{\star}{,} \beta]}^{(1)} = -\frac{i}{2}\theta^{\mu\nu}\left\{\partial_\mu \alpha, \partial_\nu \beta\right\}.$$

The solution of this linear inhomogeneous equation can be evaluated by using Moyal-Weyl $\star$ product

$$\lambda_\alpha^{(1)} = -\frac{1}{4}\theta^{\mu\nu}\{A_\mu, \partial_\nu\alpha\}$$

This is not an unique solution. We could find the solution for homogeneous equation when we assume $\triangle\lambda^{(1)} = 0$. The general solution would be the addition of homogeneous and inhomogeneous solution [67, 120, 121]

$$\lambda_\alpha^{(1)} = \theta^{\mu\nu}\left(\frac{1}{4}\{\partial_\mu\alpha, A_\nu\} + iC_\alpha^{(1)}[\partial_\mu\alpha, A_\nu]\right).$$

The ambiguity of the gauge parameter to the first order, parametrized by $C_\alpha^{(1)}$, is an arbitrary coefficient. Next we determine the SW map for $\hat{\psi}$ to $\mathcal{O}(\theta)$. From the gauge equivalence principle of the fermion field ψ, we get $\hat{\delta}_\alpha\hat{\psi}(\psi, A, \theta) = i\hat{\lambda}\star\hat{\psi}$ and hence,

$$\hat{\delta}_\alpha\psi^1 = i\alpha\,\psi^1 + i\lambda^1\,\psi - \frac{1}{2}\theta^{\mu\nu}\partial_\mu\alpha\,\partial_\nu\psi \quad \Rightarrow \triangle_\alpha\psi^{(1)} := \hat{\delta}_\alpha\psi^1 - i\alpha\,\psi^1 = i\lambda^1\,\psi - \frac{1}{2}\theta^{\mu\nu}\partial_\mu\alpha\,\partial_\nu\psi$$

On substituting the first order gauge parameter and adding the homogeneous solution, we get the general solution as

$$\psi^{(1)} = \theta^{\mu\nu}\left(\frac{1}{2}A_\mu\partial_\nu\psi + \frac{i}{4}A_\mu A_\nu\psi - C_\alpha^{(1)}A_\mu A_\nu\psi + \frac{C_\psi^{(1)}}{2}F_{\mu\nu}\psi\right)$$

Similarly, the SW map for gauge field up to order θ gives rise

$$A_\xi^{(1)} = \theta^{\mu\nu}\left(\frac{1}{4}\{F_{\mu\xi} + \partial_\mu A_\xi, A_\nu + iC_\alpha^{(1)}[D_\xi A_\mu, A_\nu] - 2iC_A^{(1)}D_\xi F_{\mu\nu}\right)$$

But in the NC standard model the Higgs scalar field has different SW map. Because they do not commute with $U(1)$ and $SU(3)$. So the Yukawa term $\overline{\hat{\psi}}_L \star \hat{\phi} \star \hat{\psi}_R$ can have different gauge transformation with scalar Higgs field, where $\hat{\psi}_L$ and $\hat{\psi}_R$ are the left handed doublet and right handed singlet, respectively. The Higgs field which needs to transform on both sides while retaining the gauge invariance with the appropriate gauge parameter which is given by

$$\hat{\delta}_{\lambda\lambda'}\hat{\phi}(\phi, A, A', \theta) = i\hat{\lambda}(\lambda, A, \theta)\star\hat{\phi} - i\hat{\phi}\star\hat{\lambda}'(\lambda', A, \theta).$$

The solution for the scalar hybrid SW map is

$$\phi^1(\phi, A, A', \theta) = \frac{1}{2}\theta^{\mu\nu}A_\nu(\partial_\mu\phi - \frac{i}{2}(A_\mu\phi + \phi A'_\mu)) - \frac{1}{2}\theta^{\mu\nu}(\partial_\mu\phi - \frac{i}{2}(A_\mu\phi + \phi A'_\mu))A'_\nu.$$

The SW map given above is known as θ expanded SW map. One can derive all order θ recursion SW map using Seiberg-Witten differential equation [67, 118, 119, 122]. A new type of SW map arises

because, when we consider the SW map for gravitation field, it starts with second order in θ because first order θ terms vanishes automatically. Therefore in the expanded SW map we need to start with the second order in θ term. Horvat and Trampetic [125, 126, 198] has introduced the θ exact SW map which is expanded in powers of gauge field A_μ and gauge parameter λ. At each order in A_μ, the exact θ expressions can be determined. Here the $\star$ products between gauge field and other fields has different structure. The θ expanded SW map has a control on renormalization by adding appropriate counter term in one loop calculation.

θ exact SW map

First we define the Moyal-Weyl $\star$ product between two functions to all order in θ. There are different $\star$ product rule for abelian and non-abelian gauge fields.

For abelian gauge field:

$$f(x) \star_2 g(x) = [f(x) \stackrel{\star}{,} g(x)] = \frac{\sin\left(\frac{\partial_1 \theta \partial_2}{2}\right)}{\left(\frac{\partial_1 \theta \partial_2}{2}\right)} f(x_1)g(x_2)|_{x_1=x_2=x}$$

$$(f(x)g(x)h(x))_{\star_3} = \left(\frac{\sin\left(\frac{\partial_2 \theta \partial_3}{2}\right)\sin\left(\frac{\partial_1 \theta(\partial_2+\partial_3)}{2}\right)}{\frac{(\partial_1+\partial_2)\theta\partial_3}{2}\frac{\partial_1\theta(\partial_2+\partial_3)}{2}} + \{1 \leftrightarrow 2\}\right) f(x_1)g(x_2)h(x_3)|_{x_i=x}$$

For Non-abelian gauge field:

$$f(x) \circledast g(x) = \frac{exp\left(i\frac{\partial_1 \theta \partial_2}{2}\right) - 1}{\left(\frac{\partial_1 \theta \partial_2}{2}\right)} f(x_1)g(x_2)|_{x_1=x_2=x}$$

θ exact SW map:

$$\widehat{A}_\mu = A_\mu - \frac{1}{2}\theta^{\nu\rho} A_\nu \star_2 (\partial_\rho A_\mu + F_{\rho\mu}) + \mathcal{O}(A^3),$$

$$\widehat{\psi} = \psi - \theta^{\mu\nu} A_\mu \star_2 \partial_\nu \psi + \frac{1}{2}\theta^{\mu\nu}\theta^{\rho\sigma}\{(A_\rho \star_2 (\partial_\sigma A_\mu + F_{\sigma\mu})) \star_2 \partial_\nu \psi + 2A_\mu \star_2 (\partial_\nu(A_\rho \star_2 \partial_\sigma \psi))$$

$$- A_\mu \star_2 (\partial_\rho A_\nu \star_2 \partial_\sigma \psi) - (A_\rho \partial_\mu \psi(\partial_\nu A_\sigma + F_{\nu\sigma}) - \partial_\rho \partial_\mu \psi A_\nu A_\sigma)_{\star_3}\} + \mathcal{O}(A^3)\psi,$$

$$\widehat{\Lambda} = \lambda - \frac{1}{2}\theta^{\mu\nu} A_\mu \star_2 \partial_\nu \lambda + \mathcal{O}(A^2)\lambda.$$

Solution for charge quantization

The SW map is the Taylor expanded ordinary gauge fields on order by order expansion in θ. Therefore even when we introduce a few more noncommutative gauge fields, the SW map would identify the correct number of ordinary commutative fields. Now, the covariant derivative

$$D_\mu \hat{\psi}^{(n)} = \partial_\mu \hat{\psi}^{(n)} - ieq^{(n)} \hat{A}_\mu \star \hat{\psi}^{(n)}$$

does not transform in the covariant manner under $\delta_{\hat{\lambda}} \hat{\psi}^{(n)} = ieq^{(n)} \star \hat{\psi}^{(n)}$, as there is only one gauge field $\hat{A}_\mu$. But if we introduce n gauge fields $\hat{A}_\mu^{(n)}$ ie..

$$D_\mu \hat{\psi}^{(n)} = \partial_\mu \hat{\psi}^{(n)} - ieq^{(n)} \hat{A}_\mu^{(n)} \star \hat{\psi}^{(n)}$$

and transform covariantly under $\hat{\delta}_{\hat{\lambda}}\hat{\psi}^{(n)} = ieq^{(n)} \star \hat{\psi}^{(n)}, \quad \hat{\delta}_{\hat{\lambda}}\hat{A}_\mu = \partial_\mu\hat{\lambda}^{(n)} + ieq^{(n)}[\hat{\lambda}^{(n)} \stackrel{\star}{,} \hat{A}_\mu^{(n)}]$. It may appear that the theory has too many degree of freedom, as we have introduced many new gauge fields now. The SW-map reduces the no of degrees of freedom. It is realized that these n noncommutative gauge fields has the same classical limit A_μ:

$$\hat{A}_\mu^{(n)} = A_\mu - eq^{(n)}\frac{1}{4}\theta^{\rho\sigma}\{A_\rho\,,\,\partial_\sigma A_\mu + F_{\sigma\mu}\} + \mathcal{O}(\theta^2)$$

2.6   Renormalizability problem(UV/IR mixing)

In 1999, Shiraz Minwalla, Mark Van Raamsdonk and Nathan Seiberg [68, 198] studied the perturbative dynamics of noncommutative scalar field theories on $\mathcal{R}^d$, and found an intriguing mixing of the UV and the IR, popularly known as the UV/IR mixing. The UV/IR mixing plagues into the NC ϕ^4 theory makes it non-renormalizable because of the nonlocal star product between scalar fields in Moyal-Weyl space. Let us start with the Moyal-Weyl quantization of scalar field. The NC operator of the classical function $\phi(x)$ in dimension $d = 4$ is given as

$$\Phi(\hat{x}) := \frac{1}{(2\pi)^4}\int d^4p \int d^4x\, e^{ip\hat{x}}e^{-ipx}\phi(x) = \frac{1}{(2\pi)^4}\int d^4p \int d^4x\, e^{-ipx}\widehat{T}(p)\phi(x),$$

where the operator $\widehat{T}(p) := e^{ip\hat{x}}$ and it's properties are described as follows

$$\widehat{T}^\dagger(p) = \widehat{T}(-p)$$
$$\widehat{T}(p)\widehat{T}(q) = \exp(-\frac{i}{2}\,p\theta q)\,\widehat{T}(p+q)$$
$$tr\,\widehat{T}(p) = \prod_\mu \delta(p_\mu) = (2\pi)^4\delta^{(4)}(p)$$

The trace of the NC operator $\Phi(\hat{x})$ provides the classical field $\phi(x)$

$$\phi(x) = \frac{1}{(2\pi)^2}\int d^4p\, e^{ipx}tr(\Phi(\hat{x})\widehat{T}^\dagger(p)),$$

and it's Fourier transform is defined as

$$\widetilde{\phi}(p) = \frac{1}{(2\pi)^2}\int d^4x e^{-ipx}\phi(x).$$

Thus the trace of the NC operator $\Phi(\hat{x})$ can be written as

$$tr(\Phi(\hat{x})) := \frac{1}{(2\pi)^2}\int d^4p\, e^{-ipx}\widetilde{\phi}(p)\,tr(\widehat{T}(p)).$$

The star product between the classical fields can be written as

$$(\phi \star \phi)(x) = \frac{1}{(2\pi)^2}\int d^4p\, e^{ipx}\, tr\left[\Phi_1(\hat{x})\Phi_2(\hat{x})\widehat{T}^\dagger(p)\right]$$

40

$$= \int dx_1 dx_2 \, K(x; x_1, x_2)\phi(x_1)\phi(x_2),$$

with

$$K(x; x_1, x_2) = \frac{1}{(2\pi)^4} \int d^4p \prod_\mu \delta(x^\mu - x_1^\mu + \frac{1}{2}\theta^{\mu\nu} p_\nu) \, \exp(ip_\nu(x - x_2)^\nu)$$

$$= \frac{1}{\pi^4 |det\,\theta|} \exp\{2i[(x - x_1)^\mu (\theta^{-1})_{\mu\nu}(x - x_2)^\nu]\}.$$

Here $\theta_{\mu\nu}$ is non-degenerate and it admits an inverse. The oscillations in the phase of K suppress parts of the integration region. In the momentum space we can define the star products of classical fields as follows

$$(\phi \star \phi)(x) = \frac{1}{(2\pi)^4} \int d^4p_1 \int d^4p_2 \, e^{i(p_1+p_2)\,x} \widetilde{\phi}_1(p_1)\widetilde{\phi}_1(p_1)e^{-\frac{i}{2}p_1\theta p_2}$$

$$= \prod_{i=1}^{2} \left[\frac{1}{(2\pi)^2} \int d^4p_i e^{ip_i\,x} \widetilde{\phi}_i(p_i) \right] e^{-\frac{i}{2}\sum_{i<j} p_{i\,\mu}\theta^{\mu\nu}p_{j\,\nu}}$$

This phase factor is invariant under cyclic permutation of the momentum indices, because the constraints is related to the momentum conservation. This deformed interaction admits

$$tr(\Phi^\dagger(\widehat{x})\Phi(\widehat{x}))^2 = \int d^4p_1...d^4p_4 \, \widetilde{\phi}(p_1)...\widetilde{\phi}(p_4) \, \delta^{(4)}(p_1 + ... + p_1) \, e^{-\frac{i}{2}\sum_{i<j}^{4} p_{i\,\mu}\theta^{\mu\nu}p_{j\,\nu}}$$

The cyclic symmetry of the star($\star$) product

$$\int d^4x(\phi_1 \star \phi_2 \star ... \star \phi_n)(x) = \int d^4x(\phi_2 \star ... \star \phi_n \star \phi_1)(x)$$

Also, we can replace one of the $\star$ products by . products

$$\int d^4x(\phi_1 \star \phi_2 \star ... \star \phi_n)(x) = \int d^4x(\phi_1 \star ... \star \phi_i)(x)\,(\phi_{i+1} \star ... \star \phi_n)(x)$$

Next we write down the scalar action of the ϕ^4 scalar theory in the NC space-time as follows

$$\mathcal{S}_\phi = \int d^4x \left(\frac{1}{2}\partial_\mu\phi \star \partial^\mu\phi + \frac{1}{2}m^2\phi \star \phi + \frac{\lambda}{4!}\phi \star \phi \star \phi \star \phi \right)$$

Consider the 1PI two point function. We have two types of one loop Feynman diagram due to additional phase factor: one is planar diagram, while the other is non-planar diagram. The corresponding one loop correction is given by

$$\Gamma^{(2)}_{1\,planar} = \frac{g^2}{3(2\pi)^4} \int \frac{d^4k}{k^2 + m^2}$$

$$\Gamma^{(2)}_{1\,nonplanar} = \frac{g^2}{6(2\pi)^4} \int \frac{d^4k}{k^2 + m^2} e^{ik\theta p}$$

41
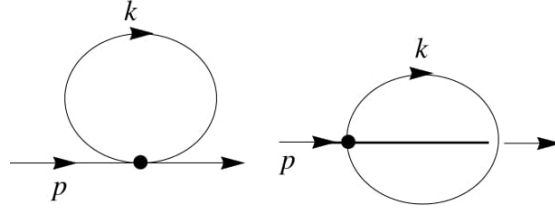
Figure 2.1: One loop Planar and non-planar diagram

The one loop planar diagram corresponding to the mass correction in the commutative theory, diverges quadratically at high energies. The non-planar loop has the vertex with the phase factor which is due to pointless like interaction in the NC theory. One can parametrize the integrals by using Schwinger parameterization,we get

$$\frac{1}{k^2 + m^2} = \int_0^\infty d\alpha \, e^{-\alpha(k^2+m^2)}$$

The k integrals are now Gaussian, and may be evaluated to yield

$$\Gamma^{(2)}_{1\,planar} = \frac{g^2}{48\pi^2} \int \frac{d\alpha}{\alpha^2} e^{-\alpha m^2}$$

$$\Gamma^{(2)}_{1\,nonplanar} = \frac{g^2}{96\pi^2} \int \frac{d\alpha}{\alpha^2} e^{-\alpha m^2 - \frac{p\circ p}{\alpha}}$$

Here we have introduced new notation

$$p \circ q \equiv -p_\mu \theta^2_{\mu\nu} q_\nu = |p_\mu \theta^2_{\mu\nu} q_\nu|$$

The dimension of $p \circ p$ is length squared. In order to regulate the small α divergence in the above equation, we multiply the integrands by Pauli-Villars regulator $\exp(-1/(\Lambda^2 \alpha))$ and we get

$$\Gamma^{(2)}_{1\,planar} = \frac{g^2}{48\pi^2} \int \frac{d\alpha}{\alpha^2} e^{-\alpha m^2 - \frac{1}{\Lambda^2 \alpha}}$$

$$\Gamma^{(2)}_{1\,nonplanar} = \frac{g^2}{96\pi^2} \int \frac{d\alpha}{\alpha^2} e^{-\alpha m^2 - \frac{p\circ p + \frac{1}{\Lambda^2}}{\alpha}}$$

Therefore,

$$\Gamma^{(2)}_{1\,planar} = \frac{g^2}{48\pi^2} \left(\Lambda^2 - m^2 \ln(\frac{\Lambda^2}{m^2}) + \mathcal{O}(1) \right)$$

$$\Gamma^{(2)}_{1\,nonplanar} = \frac{g^2}{96\pi^2} \left(\Lambda^2_{eff} - m^2 \ln(\frac{\Lambda^2_{eff}}{m^2}) + \mathcal{O}(1) \right)$$

where

$$\Lambda^2_{eff} = \frac{1}{1/\Lambda^2 + p \circ p}$$

42

In the limit $\Lambda \to \infty$, the non-planar diagram corresponding to the one loop graph remains finite. It is regulated by the spacetime noncommutativity. In this limit the effective cutoff $\Lambda^2_{eff} = \frac{1}{p \circ p}$ goes to infinity when either $\theta \to 0$ or $p \to 0$. So the IR divergence appears naturally by oscillation phase factor. In addition, the planar and the non-planar contribution to mass correction diverges at the cutoff scale $\Lambda \to \infty$(UV) as well as NC scale $\theta \to 0$(IR). These type of divergence problem are known as UV/IR mixing. In ref [189], it has shown that if the interaction Hamiltonian density is translational invariant and invariant under twisted Poincare symmetry then the star product and twisted statistics are inherent for removal of UV/IR mixing in the absence of gauge fields. But interaction only with the star product and usual statistics of the fields are not invariant under twisted Poincare symmetry.

The following three proposals are pursued that the usual star product and usual statistics but which are deals translational invariant in order to overcome the UV/IR mixing by adding suitable terms [127].

1. Broken translation invariant: [130]

    The counter term: It is of the form $\widetilde{x}^2 \phi^2$ (a harmonic oscillator-like potential), where $\widetilde{x} = \theta_{\mu\nu} x^\nu$

2. Minimalist translation invariant: [131]

    The counter term: A non-local term of the form $\frac{\mu}{\theta^4} \left(\int d^4 x \phi(x) \right)^2$.

3. Translation invariant: [132]

    The counter term: A non-local term of the form $\phi \frac{a^2}{\theta^2 \Box} \phi$

2.6.1 Translational invariant $1/p^2$ model

NC Scalar theory:

In 2008, Gurau, Magnen, Rivasseau and Tanasa [132] has proposed a model to cure the IR divergence by adding a non-local counter term $\phi \frac{1}{\theta^2 \Box} \phi$. They proposed a solution for the UV/IR problem while maintaining the translation invariance. The scalar action in the Euclidean space is

$$\mathcal{S} \equiv \int_{\mathbb{R}^4} d^4 x \left[\frac{1}{2} \left(\partial^\mu \phi \star \partial_\mu \phi + m^2 \phi \star \phi - \phi \star \frac{a^2}{\Box} \phi \right) + \frac{\lambda}{4!} \phi \star \phi \star \phi \star \phi \right],$$

where the parameter a is dimension-full and it has the form $a = a'/\theta$ where a' represents a real dimensionless constant. The 4-dimensional operator $1/\Box$ denotes the Green function which is of the form $4 - d$ Laplacian $\Box \equiv \partial^\mu \partial_\mu$ and in momentum space it is $-1/k^2$. Thus the propagator in momentum space is defined as

$$G(k) = \frac{1}{k^2 + m^2 + \frac{a^2}{k^2}}.$$

The integral factor of the one-loop correction to the propagator (corresponding to the Feynman diagrams in 2.1) is given by

$$\Pi(p) = -\frac{\lambda}{6} \int_{\mathbb{R}^4} \frac{d^4k}{(2\pi)^4} \frac{2 + \cos(k\tilde{p})}{k^2 + m^2 + \frac{a^2}{k^2}} \equiv \Pi^{\text{plan}} + \Pi^{\text{n-pl}}(p) \quad \text{where} \quad \cos(k\tilde{p}) = \frac{1}{2} \sum_{\eta = \pm 1} e^{i\eta k \tilde{p}}$$

In above, we have used $\tilde{p}_\mu \equiv \theta_{\mu\nu} p^\nu$. The propagator term(in the denominator) can be written as

$$\frac{1}{k^2 + m^2 + \frac{a^2}{k^2}} = \frac{k^2}{\left(k^2 + \frac{m^2}{2}\right)^2 - M^4} = \frac{1}{2} \sum_{\zeta = \pm 1} \frac{1 + \zeta \frac{m^2}{2M^2}}{k^2 + \frac{m^2}{2} + \zeta M^2},$$

where $M^2 \equiv \sqrt{\frac{m^4}{4} - a^2}$. The Schwinger exponential parametrization is given by

$$\Pi^{\text{n-pl}}(p) = -\frac{\lambda}{24} \sum_{\eta = \pm 1} I(p) \quad \text{and} \quad I(p) \equiv \sum_{\zeta = \pm 1} \left(1 + \zeta \frac{m^2}{2M^2}\right) \int \frac{d^4k}{(2\pi)^4} \frac{e^{i\eta k \tilde{p}}}{k^2 + \frac{m^2}{2} + \zeta M^2}.$$

For $m > 0$, $a \neq 0$ and $\left(\frac{m^2}{2} + \zeta M^2\right)$ is a positive, then the above parameterization yields

$$\frac{1}{k^2 + \frac{m^2}{2} + \zeta M^2} = \int_0^\infty d\alpha \, e^{-\alpha(k^2 + \frac{m^2}{2} + \zeta M^2)}.$$

The integral over k provides

$$I(p) = \sum_\zeta \left(1 + \zeta \frac{m^2}{2M^2}\right) \int \frac{d^4k}{(2\pi)^4} \int_0^\infty d\alpha \exp\left[-\alpha\left(k^2 - \frac{i\eta k \tilde{p}}{\alpha}\right) - \alpha\left(\frac{m^2}{2} + \zeta M^2\right)\right]$$

$$= \sum_\zeta \frac{1 + \zeta \frac{m^2}{2M^2}}{(4\pi)^2} \int_0^\infty \frac{d\alpha}{\alpha^2} \exp\left[-\frac{\tilde{p}^2}{4\alpha} - \alpha\left(\frac{m^2}{2} + \zeta M^2\right)\right].$$

The integral result in terms of the modified Bessel function $K_{-1} = K_1$ is given by [123]

$$I_{\text{regul.}}(p, \Lambda) = \sum_\zeta \frac{1 + \zeta \frac{m^2}{2M^2}}{(2\pi)^2} \sqrt{\frac{\frac{m^2}{2} + \zeta M^2}{\tilde{p}^2}} K_1\left(\sqrt{\tilde{p}^2\left(\frac{m^2}{2} + \zeta M^2\right)}\right).$$

Note that $\tilde{p}^2 \neq 0$ and is finite if $\theta \neq 0$ and $p \neq 0$. The IR behaviour of the model can be studied in the limit $\tilde{p}^2 \to 0$. For small $z \left(= \sqrt{\tilde{p}^2\left(\frac{m^2}{2} + \zeta M^2\right)}\right)$, one can write $\frac{1}{z} K_1(z)$ as

$$\frac{1}{z} K_1(z) = \frac{1}{z^2} + \frac{1}{2} \ln z + \frac{1}{2}\left(\gamma_E - \ln 2 - \frac{1}{2}\right) + \frac{z^2}{16}\left(\ln z + \gamma_E - \ln 2 - \frac{5}{4}\right) + \mathcal{O}(z^4)$$

Here γ_E is the Euler-Mascheroni constant. Thus, for $\tilde{p}^2 \ll 1$,

$$\Pi^{\text{n-pl}}(p) = \frac{-\lambda}{6(4\pi)^2}\left[\frac{4}{\tilde{p}^2} + m^2 \ln\left(\tilde{p}^2 \sqrt{\frac{m^4}{4} - M^4}\right) + \left(M^2 + \frac{m^4}{4M^2}\right) \ln \sqrt{\frac{\frac{m^2}{2} + M^2}{\frac{m^2}{2} - M^2}}\right] + \mathcal{O}(1).$$

44

The quadratic IR divergence appears in the above result and this is also accompanied by a sub leading logarithmic IR divergence. For $a \to 0$ (i.e. $M^2 \to \frac{m^2}{2}$) emphasize the the naïve model given in [68]. By introducing a cutoff Λ and replacing $\tilde{p}^2 \to \tilde{p}^2 + \frac{1}{\Lambda^2}$ in $\Pi^{\text{n-pl}}(p)$, one can regularize the planar propagator and in the limit $\tilde{p}^2 \to 0$ one finds

$$\left(\Pi^{\text{plan}}\right)_{\text{regul.}}(\Lambda) = \frac{-\lambda}{3(4\pi)^2}\left[4\Lambda^2 + m^2 \ln\left(\frac{1}{\Lambda^2}\sqrt{\frac{m^4}{4} - M^4}\right) + \left(M^2 + \frac{m^4}{4M^2}\right)\ln\sqrt{\frac{\frac{m^2}{2} + M^2}{\frac{m^2}{2} - M^2}}\right] + \mathcal{O}(1).$$

Eventually the $1/p^2$ model proves the renormalizability of the noncommutative scalar theory up to one-loop and also the renormalizability of two and higher loop nocommutative field theory shown in [127].

NC Gauge theory:

The addition of non-local term in the NC action has reduced the tension about renormalizability of the ϕ^4 theory significantly. Further this approach motivated the searches for an analogon U(1) gauge theory [128, 129]. Here the new non-local term $(a'/(D^2\widetilde{D}^2))$ were introduced in the action which satisfy the gauge invariant as well. Where $\widetilde{D} = \theta^{\mu\nu}D_{\mu\nu}$ and $D_{\mu\nu}$ is the covariant. The gauge fixing action is BRST invariant but the interaction term $(a'/(D^2\widetilde{D}^2) \star F^{\mu\nu})$ introduces an infinite number of gauge boson interaction. So it is very difficult to compute the loop diagrams in a particular order. In the ref [128] these problems were circumvented by introducing a new antisymmetric field of mass dimension two. But the physical meaning of the new dynamic antisymmetric field is not understood till now. In order to solve UV/IR mixing, instead of looking for non-local term, there is an alternative approach in the NC theory which are θ-exact and θ-expanded SW map.

The advantage in the SW approach over the Weyl-Moyal approach is that it can be applied to any gauge theory and matter can be in an arbitrary representation. Reasonable progress has been made in NCQED using SW map as far as it's quantum structure, perturbative renormalization is concerned [191–202]. In particularly, the UV/IR mixing arises in an arbitrary non-abelian noncommutative gauge theory has been studied [191, 192, 194, 197–202]. Using SW expansion of the NC fields, Bichl *et al.* [192] show that the self-energy of photon in NCQED is renormalizable to all orders in θ. Anomalies and renormalizability of SW θ-expanded NCSM are studied in [193, 195, 196]. The two-point functions for photon and neutrino are discussed in [197, 199–202] by θ-exact SW map. By calculating the one loop self-energy correction to the massless fermion up to order $\mathcal{O}(\theta)$, the ref [199] shows that the UV/IR mixing effects can be made under control. In the SW map, the first several orders of the expansion can be written in a simple form by introducing certain generalized star products [203, 204]. Such an expansion enables one to treat all orders of θ at once in each interaction vertex, thereby allows one to compute non-perturbative results [197].

2.7 Noncommutative Standard model

The SW map solves the charge quantization problem and it provides the $SU(N)$ gauge group representation by enveloping the Lie algebra. In the classical limit, noncommutative theory turns into commutative theory when $\theta^{\mu\nu} \to 0$. We have to treat $\theta^{\mu\nu}$ as a universal constant tensor, just like the speed of light in special theory of relativity on commutative space. In order to construct the standard model on NC spacetime, we have to satisfy the gauge consistency principle of tensor product of respective two gauge groups. Therefore the SM gauge group $G : U(1)_Y \otimes SU(2)_L \otimes SU(3)_C$ accommodate the "master gauge potential" and the "master gauge parameter".

$$\rho(V_\mu) = g'\rho(Y_{SM})\mathcal{A}_\mu + g\sum_i \rho(T_L^i)B_\mu^i + g_s\sum_a \rho(T_s^a)G_\mu^a$$

$$\rho(\Lambda) = g'\rho(Y_{SM})\alpha(x) + g\sum_i \rho(T_L^i)\alpha_i^L(x) + g_s\sum_a \rho(T_s^a)\alpha_a^s(x)$$

and the Seiberg-Witten(SW) map:

$$\widehat{V}_\rho = V_\rho - \frac{1}{4}\theta^{\mu\nu}\left\{V_\mu \ , \ \partial_\nu V_\rho + F_{\nu\rho}\right\} + ...$$

$$\widehat{\Lambda} = \Lambda + \frac{1}{4}\theta^{\mu\nu}\left\{V_\mu \ , \ \partial_\nu\Lambda\right\} + ...$$

To construct the noncommutative standard model, what one needs to do is as follows [69–71]

- Replace the ordinary products with the $\star$ product.

- Substitute the noncommutative fields for each corresponding commutative one.

- Perform the trace for each standard model field representation with respect to the gauge group.

Now the action of the NCSM can be written as follows [69]:

$$
\begin{aligned}
S_{NCSM} = &\int d^4x \sum_{i=1}^3 \overline{\widehat{\Psi}}_L^{(i)} \star i\widehat{\slashed{D}}\widehat{\Psi}_L^{(i)} + \int d^4x \sum_{i=1}^3 \overline{\widehat{\Psi}}_R^{(i)} \star i\widehat{\slashed{D}}\widehat{\Psi}_R^{(i)} \\
&- \int d^4x \frac{1}{2g'}\mathbf{tr_1}\widehat{F}_{\mu\nu} \star \widehat{F}^{\mu\nu} - \int d^4x \frac{1}{2g}\mathbf{tr_2}\widehat{F}_{\mu\nu} \star \widehat{F}^{\mu\nu} - \int d^4x \frac{1}{2g_S}\mathbf{tr_3}\widehat{F}_{\mu\nu} \star \widehat{F}^{\mu\nu} \\
&+ \int d^4x \left(\rho_0(\widehat{D}_\mu\widehat{\Phi})^\dagger \star \rho_0(\widehat{D}^\mu\widehat{\Phi}) - \mu^2\rho_0(\widehat{\Phi})^\dagger \star \rho_0(\widehat{\Phi}) - \lambda\rho_0(\widehat{\Phi})^\dagger \star \rho_0(\widehat{\Phi}) \star \rho_0(\widehat{\Phi})^\dagger \star \rho_0(\widehat{\Phi}) \right) \\
&+ \int d^4x \left(-\sum_{i,j=1}^3 \mathcal{W}^{ij}\left((\bar{\widehat{L}}_L^{(i)} \star \rho_L(\widehat{\Phi})) \star \widehat{e}_R^{(j)} + \bar{\widehat{e}}_R^{(i)} \star (\rho_L(\widehat{\Phi})^\dagger \star \widehat{L}_L^{(j)}) \right) \right) \\
&- \sum_{i,j=1}^3 \mathcal{G}_u^{ij}\left((\bar{\widehat{Q}}_L^{(i)} \star \rho_{\bar{Q}}(\widehat{\bar{\Phi}})) \star \widehat{u}_R^{(j)} + \bar{\widehat{u}}_R^{(i)} \star (\rho_{\bar{Q}}(\widehat{\bar{\Phi}})^\dagger \star \widehat{Q}_L^{(j)}) \right)
\end{aligned}
$$

$$- \sum_{i,j=1}^{3} \mathcal{G}_d^{ij} \left((\bar{\widehat{Q}}_L^{(i)} \star \rho_Q(\widehat{\overline{\Phi}})) \star \widehat{d}_R^{(j)} + \bar{\widehat{d}}_R^{(i)} \star (\rho_Q(\widehat{\overline{\Phi}})^\dagger \star \widehat{Q}_L^{(j)}) \right) \Bigg),$$

with $\overline{\Phi} = i\tau_2 \Phi^*$ and τ_2 is the usual Pauli matrix. The matrices $\mathcal{W}^{ij}$, $\mathcal{G}_u^{ij}$ and $\mathcal{G}_d^{ij}$ are the Yukawa couplings. We know that the SM Higgs scalar has hybrid SW map and is given by $\hat{\Phi} = \hat{\Phi}(\Phi, V, V')$. It transforms covariantly under gauge transforms with the field functionals of the two gauge field V and V' (responsible for left handed and right handed fermion fields coupled with the Higgs scalar field). The Higgs field $\hat{\Phi}$ in the NC spacetime is given by

$$\hat{\Phi} \equiv \hat{\Phi}[\Phi, V, V']$$
$$= \Phi + \frac{1}{2}\theta^{\alpha\beta} V_\beta \left(\partial_\alpha \Phi - \frac{i}{2}(V_\alpha \Phi - \Phi V'_\alpha) \right) + \frac{1}{2}\theta^{\alpha\beta} \left(\partial_\alpha \Phi - \frac{i}{2}(V_\alpha \Phi - \Phi V'_\alpha) \right) V'_\beta + \mathcal{O}(\theta^2)$$

,which is an example of hybrid map. The covariant transformation is given as $\delta\hat{\Phi}(\Phi, V, V') = i\hat{\Lambda} \star \hat{\Phi} - i\hat{\Phi} \star \hat{\Lambda}$. The following scalar representation can be chosen for yukawa terms. Note that the gauge invariance doesn't restrict the choice of the Higgs field representation [71]. The representations are

$$\rho_0(\hat{\Phi}) = \hat{\Phi}[\Phi, \frac{1}{2}g'\mathcal{A}_\mu + gB_\mu^a T_L^a, 0]$$
$$\rho_\psi(\hat{\Phi}) = \hat{\Phi}[\Phi, \mathcal{R}_{\psi_L}(V), \mathcal{R}_{\psi_R}(V)]$$
$$\rho_\psi(\hat{\Phi}_c) = \hat{\Phi}[\Phi_c, \mathcal{R}_{\psi_L}(V), \mathcal{R}_{\psi_R}(V)] \quad \text{Where} \quad \Phi_c = i\tau_2 \Phi^*$$

The representation R_ψ for the SM multiplet ψ are listed in Table(2.2). Here $\mathcal{R}_\psi(f(V_\mu)) = f(\mathcal{R}_\psi(V_\mu))$ for any function f.

Ψ	$\mathcal{R}_\psi(V_\nu)$
e_R	$-g'\mathcal{A}_\nu(x)$
$L_L = \begin{pmatrix} \nu_L \\ e_L \end{pmatrix}$	$-\frac{1}{2}g'\mathcal{A}_\nu(x) + gB_{\nu a}(x)T_L^a$
u_R	$\frac{2}{3}g'\mathcal{A}_\nu(x) + g_S G_{\nu b}(x)T_S^b$
d_R	$-\frac{1}{3}g'\mathcal{A}_\nu(x) + g_S G_{\nu b}(x)T_S^b$
$Q_L = \begin{pmatrix} u_L \\ d_L \end{pmatrix}$	$\frac{1}{6}g'\mathcal{A}_\nu(x) + gB_{\nu a}(x)T_L^a + g_S G_{\nu b}(x)T_S^b$

Table 2.2: Standard model gauge representation of the fermionic fields. Here $T_L^a = \tau^a/2$ and $T_S^b = \lambda^b/2$.

The simplest choice of Higgs scalar representation ρ_0 brings the NCSM and SM very closely:

$$\rho_0(\hat{\Phi}) = \hat{\Phi}[\Phi, \frac{1}{2}g'\mathcal{A}_\mu + gB_\mu^a T_L^a, 0].$$

In NCSM, the leptons and quarks have different scalar representation in Yukawa terms because the neutrinos do not have mass due to absence of the right handed neutrino. One can choose the leptonic representation as follows

$$\rho_L(\hat{\Phi}[\Phi, V_\mu, V'_\nu]) = \hat{\Phi}[\Phi, -\frac{1}{2}g'\mathcal{A}_\mu + gB_\mu^a T_L^a, \, g'\mathcal{A}_\nu]$$

where $V_\mu = -\frac{1}{2}g'\mathcal{A}_\mu + gB_\mu^a T_L^a$ and $V'_\nu = g'\mathcal{A}_\nu$. In the Yukawa term, we need different representation for up and down type of quarks and are given as follows

$$\rho_Q(\hat{\Phi}[\Phi, V_\mu, V'_\nu]) = \hat{\Phi}[\Phi, \frac{1}{6}g'\mathcal{A}_\mu + gB_\mu^a T_L^a + g_S G_\mu^a T_S^a, \frac{1}{3}g'\mathcal{A}_\nu - g_S G_\nu^a T_S^a],$$

$$\rho_{\bar{Q}}(\hat{\Phi}[\Phi, V_\mu, V'_\nu]) = \hat{\Phi}[\Phi, \frac{1}{6}g'\mathcal{A}_\mu + gB_\mu^a T_L^a + g_S G_\mu^a T_S^a, -\frac{2}{3}g'\mathcal{A}_\nu - g_S G_\nu^a T_S^a].$$

Spontaneous Symmetry breaking

Let us first consider the scalar action in the NCSM

$$S_\Phi = \int d^4x \left[\rho_0(\mathcal{D}_\mu\widehat{\Phi})^\dagger \rho_0(\mathcal{D}_\mu\widehat{\Phi}) - \mu^2 \rho_0(\widehat{\Phi})^\dagger \star \rho_0(\widehat{\Phi}) - \lambda(\rho_0(\widehat{\Phi})^\dagger \star \rho_0(\widehat{\Phi})) \star (\rho_0(\widehat{\Phi})^\dagger \star \rho_0(\widehat{\Phi})) \right]$$

where $\mathcal{D}$ is SM covariant derivative. The SM minimization of the doublet scalar field and the NCSM scalar field minimization are same and it obeys the following steps as given below [69]

- To find the potential minima attained for constant fields neglecting the derivative terms and star product terms.

- The terms in the hybrid SW map like $\theta^{\alpha\beta} V_\alpha V_\beta \Phi$ leads to corrections to Higgs vacuum expectation value(vev).

- We should consider the field value $V_\alpha = 0$, i.e. $\widehat{\Phi} = \phi$ when fixing the Higgs vev.

- The gauge degrees of freedom allows to choose the unitary gauge for Higgs scalar field
$\phi = \frac{1}{\sqrt{2}} \begin{pmatrix} 0 \\ h + v_h \end{pmatrix},$

where $v_h(= \sqrt{-\mu^2/\lambda})$ is the vev and $\mu^2 < 0$. To the leading order in θ expansion, we use $\rho_0(\hat{\Phi}) = \phi + \rho_0(\phi^1) + \mathcal{O}(\theta^2)$ and get

$$\mathcal{S}_{Higgs} = \int d^4x \left((D_\mu^{SM}\phi)^\dagger D^{SM\mu}\phi - \mu^2\phi^\dagger\phi - \lambda(\phi^\dagger\phi)(\phi^\dagger\phi) \right)$$

$$+ \int d^4x \left((D_\mu^{SM}\phi)^\dagger \left(D^{SM\mu}\rho_0(\phi^1) + \frac{1}{2}\theta^{\alpha\beta}\partial_\alpha V^\mu \partial_\beta \phi + \Gamma^\mu \phi \right) \right)$$

$$+\left(D_\mu^{SM}\rho_0(\phi^1)+\frac{1}{2}\theta^{\alpha\beta}\partial_\alpha V_\mu\partial_\beta\phi+\Gamma_\mu\phi\right)^\dagger D^{SM\mu}\phi$$

$$+\frac{1}{4}\mu^2\theta^{\mu\nu}\phi^\dagger(F_{\mu\nu})\phi-\lambda i\theta^{\alpha\beta}\phi^\dagger\phi(D_\alpha^{SM}\phi)^\dagger(D_\beta^{SM}\phi)\Bigg)+\mathcal{O}(\theta^2),$$

where $F_{\mu\nu}=g'f_{\mu\nu}+gF_{\mu\nu}^L$,

$$\Gamma_\mu=-iV_\mu^1=i\frac{1}{4}\theta^{\alpha\beta}\{g'\mathcal{A}_\alpha+gB_\alpha,g'\partial_\beta\mathcal{A}_\mu+g\partial_\beta B_\mu+g'f_{\beta\mu}+gF_{\beta\mu}^L\},$$

and

$$\rho_0(\phi^1)=-\frac{1}{2}\theta^{\alpha\beta}(g'\mathcal{A}_\alpha+gB_\alpha)\partial_\beta\phi+i\frac{1}{4}\theta^{\alpha\beta}(g'\mathcal{A}_\alpha+gB_\alpha)(g'\mathcal{A}_\beta+gB_\beta)\phi.$$

The Higgs boson mass is defined as $M_h=\sqrt{-2\,\mu^2}$. The masses of the electroweak bosons is generated by the so-called Higgs mechanism

$$M_{W^\pm}=\frac{gv}{2}\quad\text{and}\quad M_Z=\frac{\sqrt{g^2+g'^2}}{2}v.$$

Here the physical mass eigenstates of the electroweak bosons $W^\pm$, Z and A are defined by

$$W_\mu^\pm=\frac{B_\mu^1\mp iB_\mu^2}{\sqrt{2}},\quad Z_\mu=\frac{-g'\mathcal{A}_\mu+gB_\mu^3}{\sqrt{g^2+g'^2}}\quad\text{and}\quad A_\mu=\frac{g\mathcal{A}_\mu+g'B_\mu^3}{\sqrt{g^2+g'^2}}.$$

We can rewrite the gauge field $\mathcal{A}_\mu$ and B_μ^3 in terms of physical photon field A_μ and massive neutral Z boson

$$B_\mu^3=\frac{g\,Z_\mu+g'\,A_\mu}{\sqrt{g^2+g'^2}}\quad\text{and}\quad\mathcal{A}_\mu=\frac{g\,A_\mu-g'\,Z_\mu}{\sqrt{g^2+g'^2}}$$

which helps one to find the interactions of Higgs and physical gauge fields besides the usual SM interactions.

2.7.1 Noncommutative standard model: Scalar sector

In the Higgs action, the order θ terms has enormous interaction with Higgs and gauge field. We examine here the single Z boson and W^+W^- interaction with Higgs up to order θ. The last term of the $\mathcal{S}_{Higgs}$ gives [71],

$$\frac{1}{2}\theta^{\alpha\beta}\int d^4x\,\phi^\dagger\left(\frac{1}{2}\mu^2\,F_{\alpha\beta}-2i\lambda\,\phi(D_\alpha^{SM}\phi)^\dagger D_\beta^{SM}\right)\phi$$

$$=\frac{1}{8}\theta^{\alpha\beta}\left\{ig^2\int d^4x(h+v)^2[\mu^2+\lambda(h+v)^2]W_\alpha^+W_\beta^-\right.$$

$$\left.+\frac{g}{\cos\theta_W}\int d^4x(h+v)^2[-\mu^2(\partial_\alpha Z_\beta)+2\lambda(h+v)(\partial_\alpha h)Z_\beta]\right\},$$

by making the using of the field strength tensor

$$F_{\mu\nu} = \begin{pmatrix} eA_{\mu\nu} + \frac{g}{2\cos\theta_W}(1 - 2\sin^2\theta_W)Z_{\mu\nu} & \frac{g}{\sqrt{2}}W^+_{\mu\nu} \\ \frac{g}{\sqrt{2}}W^-_{\mu\nu} & -\frac{g}{2\cos\theta_W}Z_{\mu\nu} \end{pmatrix}$$

$$-\frac{ig^2}{2}\begin{pmatrix} W^+_\mu W^-_\nu - W^+_\nu W^-_\mu & \sqrt{2}(B^3_\mu W^+_\nu - W^+_\mu B^3_\nu) \\ -\sqrt{2}(B^3_\mu W^-_\nu - W^-_\mu B^3_\nu) & -W^+_\mu W^-_\nu + W^+_\nu W^-_\mu \end{pmatrix}.$$

The μ^2 integration term get vanishes because of Stokes theorem. So we get

$$\frac{1}{8}\theta^{\alpha\beta}\lambda\int d^4x\, h(h+v)(h+2v)\left\{ig^2(h+v)W^+_\alpha W^-_\beta + 2\frac{g}{\cos\theta_W}(\partial_\alpha h)Z_\beta\right\}.$$

The scalar triple and quartic interaction doesn't have $\mathcal{O}(\theta)$ correction in the NCSM and also there is no hZZ, $hhZZ$ interaction in $\mathcal{O}(\theta)$ correction. Other two Higgs action terms has multiple field interaction of gauge and Higgs scalar in the order of $\mathcal{O}(\theta)$.

2.7.2   Noncommutative Standard model: Fermionic sector

The action corresponding to the Yukawa terms which generates masses for the fermions,

$$\mathcal{S}_{Yukawa} = \int d^4x \left(-\sum_{i,j=1}^3 \mathcal{W}^{ij}\left((\bar{\widehat{L}}_L^{(i)} \star \rho_L(\widehat{\Phi})) \star \widehat{e}_R^{(j)} + \bar{\widehat{e}}_R^{(i)} \star (\rho_L(\widehat{\Phi})^\dagger \star \widehat{L}_L^{(j)})\right)\right.$$

$$-\sum_{i,j=1}^3 \mathcal{G}_u^{ij}\left((\bar{\widehat{Q}}_L^{(i)} \star \rho_{\bar{Q}}(\widehat{\bar{\Phi}})) \star \widehat{u}_R^{(j)} + \bar{\widehat{u}}_R^{(i)} \star (\rho_{\bar{Q}}(\widehat{\bar{\Phi}})^\dagger \star \widehat{Q}_L^{(j)})\right)$$

$$\left.-\sum_{i,j=1}^3 \mathcal{G}_d^{ij}\left((\bar{\widehat{Q}}_L^{(i)} \star \rho_Q(\widehat{\Phi})) \star \widehat{d}_R^{(j)} + \bar{\widehat{d}}_R^{(i)} \star (\rho_Q(\widehat{\Phi})^\dagger \star \widehat{Q}_L^{(j)})\right)\right)$$

Here $\widehat{\Phi}[\Phi, V, V']$ is already defined earlier. L_L^i stands for the left-handed leptonic doublet and e_R^i for a leptonic singlet of the ith generation. Q_L^i stands for a left-handed quark doublet of the ith generation, u_R^i for a right-handed up-type quark singlet of the ith generation and d_R^i stands for a right-handed down-type quark singlet of the ith generation.

Using the biunitary transformations, one can diagonalize the Yukawa coupling matrices [71]

$$\mathcal{G}_d = \frac{\sqrt{2}}{v}S_d\,M_d\,T_d^\dagger, \quad \mathcal{G}_u = \frac{\sqrt{2}}{v}S_u\,M_u\,T_u^\dagger.$$

After diagonlization, we get the diagonal 3×3 mass matrices M_d and M_u. One has to redefine the quark fields by biunitary transformation so as to make it the mass eigenstates

$$\bar{d}_L^{(i)}S_d^{(ij)} \to \bar{d}_L^{(j)}, \quad T_d^{\dagger(ij)}\widehat{d}_R^{(j)} \to \widehat{d}_R^{(i)}, \quad \bar{u}_L^{(i)}S_u^{(ij)} \to \bar{u}_L^{(j)}, \quad T_u^{\dagger(ij)}\widehat{u}_R^{(j)} \to \widehat{u}_R^{(i)}.$$

This redefinition of the fields introduces the quark mixing matrix $V = S_u^\dagger S_d$ which gives the Cabibbo Kobayashi Maskawa(CKM) matrix [72–74] in the Standard Model charged current sector.

$$V_f = \begin{cases} 1 & \text{for } f = \ell \ (e, \mu, \tau), \\ V \equiv V_{CKM} & \text{for } f = q \ (u, d, ...b), \end{cases}$$

where ℓ and q denote leptons and quarks, respectively. Note that there is no mixing in the lepton sector due to absence of the right handed neutrinos.

The minimal modification of the Standard Model is possible by introducing the right handed neutrinos, which comprises neutrino masses. There would be neutrino mixing matrix instead of unit matrix mentioned above.

The leading order Yukawa expansion is

$$\begin{aligned}
\mathcal{S}_{Yukawa} = \mathcal{S}_{Yukawa}^{SM} - \int d^4x \bigg(& \sum_{i,j=1}^3 \mathcal{W}^{ij} \bigg((\bar{L}_L^i \phi) e_R^{1j} + (\bar{L}_L^i \rho_L(\phi^1)) e_R^j \\
& + (\bar{L}_L^{1i} \phi) e_R^j + i\frac{1}{2}\theta^{\alpha\beta} \partial_\alpha L_L^i \partial_\beta \phi e_R^j + \bar{e}_R^i (\phi^\dagger L_L^{1j}) \\
& + \bar{e}_R^i (\rho_L(\phi^1)^\dagger L_L^j) + \bar{e}_R^{1i} (\phi^\dagger L_L^j) + i\frac{1}{2}\theta^{\alpha\beta} \partial_\alpha e_R^i \partial_\beta \phi^\dagger L_L^j \bigg) \\
& - \sum_{i,j=1}^3 \mathcal{G}_u^{ij} \bigg((\bar{Q}_L^i \bar{\phi}) u_R^{1j} + (\bar{Q}_L^i \rho_{\bar{Q}}(\bar{\phi}^1)) u_R^j + (\bar{Q}_L^{1i} \bar{\phi}) u_R^j \\
& + i\frac{1}{2}\theta^{\alpha\beta} \partial_\alpha Q_L^i \partial_\beta \bar{\phi} u_R^j + \bar{u}_R^i (\bar{\phi}^\dagger Q_L^{1j}) + \bar{u}_R^i (\rho_{\bar{Q}}(\bar{\phi}^1)^\dagger Q_L^j) \\
& + \bar{u}_R^{1i} (\bar{\phi}^\dagger Q_L^j) + i\frac{1}{2}\theta^{\alpha\beta} \partial_\alpha u_R^i \partial_\beta \bar{\phi}^\dagger Q_L^j \bigg) \\
& - \sum_{i,j=1}^3 \mathcal{G}_d^{ij} \bigg((\bar{Q}_L^i \phi) d_R^{1j} + (\bar{Q}_L^i \rho_Q(\phi^1)) d_R^j + (\bar{Q}_L^{1i} \phi) d_R^j \\
& + i\frac{1}{2}\theta^{\alpha\beta} \partial_\alpha Q_L^i \partial_\beta \phi d_R^j + \bar{d}_R^i (\phi^\dagger Q_L^{1j}) + \bar{d}_R^i (\rho_Q(\phi^1)^\dagger Q_L^j) \\
& + \bar{d}_R^{1i} (\phi^\dagger Q_L^j) + i\frac{1}{2}\theta^{\alpha\beta} \partial_\alpha \bar{d}_R^i \partial_\beta \phi^\dagger Q_L^j \bigg) \bigg) + \mathcal{O}(\theta^2)
\end{aligned}$$

Charged current interaction

Here we give the complete expressions of the electroweak charged currents to order $\mathcal{O}(\theta)$ [69]

$$\mathcal{L}_{cc} = \begin{pmatrix} \bar{u} & \bar{c} & \bar{t} \end{pmatrix}_L V_{CKM} J_1 (1 - \gamma_5) \begin{pmatrix} d \\ s \\ b \end{pmatrix}_L + \begin{pmatrix} \bar{d} & \bar{s} & \bar{b} \end{pmatrix}_L V_{CKM}^\dagger J_2 (1 - \gamma_5) \begin{pmatrix} u \\ c \\ t \end{pmatrix}_L$$

with

$$J_1 = \frac{1}{\sqrt{2}} g W\!\!\!\!/^+ + (\frac{1}{2}\theta^{\mu\nu}\gamma^\alpha + \theta^{\nu\alpha}\gamma^\mu)$$

$$\left(\left(-\frac{\sqrt{2}}{4} Y g' g(\cos\theta_W \partial_\mu A_\nu - \cos\theta_W \partial_\nu A_\mu - \sin\theta_W \partial_\mu Z_\nu + \sin\theta_W \partial_\nu Z_\mu) W_\alpha^+ \right) \right.$$

$$+ g\frac{\sqrt{2}}{8} \left(\partial_\mu W_\nu^+ - \partial_\nu W_\mu^+ \right.$$

$$\left. -2ig \left(\cos\theta_W Z_\mu W_\nu^+ + \sin\theta_W A_\mu W_\nu^+ - \cos\theta_W W_\mu^+ Z_\nu - \sin\theta_W W_\mu^+ A_\nu \right) \right) \cdot$$

$$(-2i\partial_\alpha + 2Y g' \sin\theta_W Z_\alpha - 2Y g' \cos\theta_W A_\alpha + g\cos\theta_W Z_\alpha + g\sin\theta_W A_\alpha)$$

$$-\frac{\sqrt{2}}{8} g^2 \left(\cos\theta_W \partial_\mu Z_\nu - \cos\theta_W \partial_\nu Z_\mu + \sin\theta_W \partial_\mu A_\nu - \sin\theta_W \partial_\nu A_\mu \right.$$

$$\left. \left. -2ig(W_\mu^+ W_\nu^- - W_\nu^+ W_\mu^-) \right) W_\alpha^+ \right)$$

and

$$J_2 = \frac{1}{\sqrt{2}} g W\!\!\!\!/^- + (\frac{1}{2}\theta^{\mu\nu}\gamma^\alpha + \theta^{\nu\alpha}\gamma^\mu)$$

$$\left(\left(-\frac{\sqrt{2}}{4} Y g' g(\cos\theta_W \partial_\mu A_\nu - \cos\theta_W \partial_\nu A_\mu - \sin\theta_W \partial_\mu Z_\nu + \sin\theta_W \partial_\nu Z_\mu) W_\alpha^- \right) \right.$$

$$+ g\frac{\sqrt{2}}{8} \left(\partial_\mu W_\nu^- - \partial_\nu W_\mu^- \right.$$

$$\left. -2ig \left(\cos\theta_W W_\mu^- Z_\nu + \sin\theta_W W_\mu^- A_\nu - \cos\theta_W Z_\mu W_\nu^- - \sin\theta_W A_\mu W_\nu^- \right) \right) \cdot$$

$$(-2i\partial_\alpha + 2Y g' \sin\theta_W Z_\alpha - 2Y g' \cos\theta_W A_\alpha - g\cos\theta_W Z_\alpha - g\sin\theta_W A_\alpha)$$

$$-\frac{\sqrt{2}}{8} g^2 \left(\cos\theta_W \partial_\mu Z_\nu - \cos\theta_W \partial_\nu Z_\mu + \sin\theta_W \partial_\mu A_\nu - \sin\theta_W \partial_\nu A_\mu \right.$$

$$\left. \left. -2ig(W_\mu^+ W_\nu^- - W_\nu^+ W_\mu^-) \right) W_\alpha^- \right)$$

Here we disregarded the interactions with the gluon in the "electroweak" charged currents. We pick $W\!\!\!\!/^+$ term up to $\mathcal{O}(\theta)$ in $\mathcal{L}_{cc}$ and obtain

$$\left(\bar{u}\ \bar{c}\ \bar{t} \right)_L V_{CKM} \left(\frac{1}{\sqrt{2}} g W\!\!\!\!/^+ + \frac{-ig}{2\sqrt{2}} \theta^{\mu\nu\alpha}(1-\gamma_5)\partial_\mu W_\nu^+ \partial_\alpha \right) \begin{pmatrix} d \\ s \\ b \end{pmatrix}_L = \left(\bar{u}\ \bar{c}\ \bar{t} \right)_L \mathcal{V}_{CKM} \frac{1}{\sqrt{2}} g W\!\!\!\!/^+ (1-\gamma_5) \begin{pmatrix} d \\ s \\ b \end{pmatrix}_L,$$

where $\theta^{\mu\nu\alpha} = \theta^{\mu\nu}\gamma^\alpha + \theta^{\nu\alpha}\gamma^\mu + \theta^{\alpha\mu}\gamma^\nu$ and

$$\mathcal{V}_{CKM}(p,p') \equiv \begin{pmatrix} 1 - \lambda^2/2 + ix_{ud} & \lambda + ix_{us} & A\lambda^3(\rho - i\eta) + ix_{ub} \\ -\lambda + ix_{cd} & 1 - \lambda^2/2 + ix_{cs} & A\lambda^2 + ix_{cb} \\ A\lambda^3(1-\rho-i\eta) + ix_{td} & -A\lambda^2 + ix_{ts} & 1 + ix_{tb} \end{pmatrix}.$$

In above $x_{ab} \equiv p_a{}^\mu \theta_{\mu\nu} p_b'{}^\nu$ for quarks a, b. All the momenta p_a and p_b are taken to be incoming. This is true in Moyal-Weyl approach and Seiberg-Witten approach (with massless quarks), but there are quark mass dependent interaction term in Yukawa NCSM action [133]. So the momentum dependent CKM matrix in NCSM is not complete. Finally, we present the quarks-charged bosons($W^\pm$) interaction up to $\mathcal{O}(\theta)$ i.e. the Feynman rules for the vertices $f_u^{(i)} - f_d^{(j)} - W^+(k)$ and $f_u^{(i)} - f_d^{(j)} - W^-(k)$ to $\mathcal{O}(\theta)$ as follows [71]

$$\frac{i\,e}{2\sqrt{2}\sin\theta_W} \begin{pmatrix} V_f^{(ij)} \\ V_f^{\dagger(ij)} \end{pmatrix} \left\{ \left[\gamma_\mu - \frac{i}{2}\,\theta_{\mu\nu\rho}\,k^\nu\,p_{\rm in}^\rho \right] (1-\gamma_5) \right.$$
$$\left. -\frac{i}{2}\,\theta_{\mu\nu} \left[\begin{pmatrix} m_{f_u^{(i)}} \\ m_{f_d^{(j)}} \end{pmatrix} p_{\rm in}^\nu (1-\gamma_5) - \begin{pmatrix} m_{f_d^{(j)}} \\ m_{f_u^{(i)}} \end{pmatrix} p_{\rm out}^\nu (1+\gamma_5) \right] \right\} .$$

Here i and j are quark generation index. The same Feynman rule is applicable for doublet lepton charge current interaction. Here the quark mixing matrix has to replaced by neutrino mixing matrix when the mass of the neutrinos are non zero.

Neutral currents interaction

We now present the the neutral current expression to order $\mathcal{O}(\theta)$ [69]

$$\mathcal{L}_{nc} = \mathcal{L}_{nc}^{SM} - i\frac{1}{2}\sum_i \bar{u}_L^{(i)} \left(\frac{1}{2}\theta^{\mu\nu}\gamma^\alpha + \theta^{\nu\alpha}\gamma^\mu \right)$$
$$\left(\left(\cos\theta_W\partial_\mu A_\nu - \cos\theta_W\partial_\nu A_\mu - \sin\theta_W\partial_\mu Z_\nu + \sin\theta_W\partial_\nu Z_\mu \right) \right.$$
$$\left(g'Y\partial_\alpha - iY^2g'^2\cos\theta_W A_\alpha + iY^2g'^2\sin\theta_W Z_\alpha - i\frac{1}{2}Yg'g\cos\theta_W Z_\alpha - i\frac{1}{2}Yg'g\sin\theta_W A_\alpha \right)$$
$$+\frac{1}{2}\left(\cos\theta_W\partial_\mu Z_\nu - \cos\theta_W\partial_\nu Z_\mu + \sin\theta_W\partial_\mu A_\nu - \sin\theta_W\partial_\nu A_\mu - 2ig(W_\mu^+ W_\nu^- - W_\nu^+ W_\mu^-) \right)$$
$$\left(g\partial_\alpha - iYg'g\cos\theta_W A_\alpha + iYg'g\cos\theta_W Z_\alpha - \frac{1}{2}ig^2\cos\theta_W Z_\alpha - \frac{1}{2}ig^2\sin\theta_W A_\alpha \right)$$
$$-\frac{i}{2}g^2\left(\partial_\mu W_\nu^+ - \partial_\nu W_\mu^+ - 2ig\left(\cos\theta_W Z_\mu W_\nu^+ + \sin\theta_W A_\mu W_\nu^+ - W_\mu^+\cos\theta_W Z_\nu - W_\mu^+\sin\theta_W A_\nu \right) \right) W_\alpha^- \right) u_L^{(i)}$$
$$-i\frac{1}{2}\sum_i \bar{u}_R^{(i)} \left(\frac{1}{2}\theta^{\mu\nu}\gamma^\alpha + \theta^{\nu\alpha}\gamma^\mu \right) \left(\left(\cos\theta_W\partial_\mu A_\nu - \cos\theta_W\partial_\nu A_\mu - \sin\theta_W\partial_\mu Z_\nu + \sin\theta_W\partial_\nu Z_\mu \right) \right.$$
$$\left. \left(g'Y\partial_\alpha - iY^2g'^2\cos\theta_W A_\alpha + iY^2g'^2\sin\theta_W Z_\alpha \right) \right) u_R^{(i)} - i\frac{1}{2}\sum_i \bar{d}_L^{(i)} \left(\frac{1}{2}\theta^{\mu\nu}\gamma^\alpha + \theta^{\nu\alpha}\gamma^\mu \right)$$
$$\left(\left(\cos\theta_W\partial_\mu A_\nu - \cos\theta_W\partial_\nu A_\mu - \sin\theta_W\partial_\mu Z_\nu + \sin\theta_W\partial_\nu Z_\mu \right) \right.$$
$$\left(g'Y\partial_\alpha - iY^2g'^2\cos\theta_W A_\alpha + iY^2g'^2\sin\theta_W Z_\alpha - i\frac{1}{2}Yg'g\cos\theta_W Z_\alpha - i\frac{1}{2}Yg'g\sin\theta_W A_\alpha \right)$$
$$-\frac{1}{2}\left(\cos\theta_W\partial_\mu Z_\nu - \cos\theta_W\partial_\nu Z_\mu + \sin\theta_W\partial_\mu A_\nu - \sin\theta_W\partial_\nu A_\mu \right.$$

$$-2ig(W_\mu^+ W_\nu^- - W_\nu^+ W_\mu^-)\Big)\Big(g\partial_\alpha - iYg'g\cos\theta_W A_\alpha + iYg'g\cos\theta_W Z_\alpha + \frac{1}{2}ig^2\cos\theta_W Z_\alpha + \frac{1}{2}ig^2\sin\theta_W A_\alpha\Big)$$

$$-\frac{i}{2}g^2\Big(\partial_\mu W_\nu^- - \partial_\nu W_\mu^- + 2ig\left(\cos\theta_W Z_\mu W_\nu^- + \sin\theta_W A_\mu W_\nu^- - W_\mu^-\cos\theta_W Z_\nu - W_\mu^-\sin\theta_W A_\nu\right)\Big)W_\alpha^+\Big)d_L^{(i)}$$

$$-i\frac{1}{2}\sum_i \bar{d}_R^{(i)}\left(\frac{1}{2}\theta^{\mu\nu}\gamma^\alpha + \theta^{\nu\alpha}\gamma^\mu\right)$$

$$\Big(\Big(\cos\theta_W\partial_\mu A_\nu - \cos\theta_W\partial_\nu A_\mu - \sin\theta_W\partial_\mu Z_\nu + \sin\theta_W\partial_\nu Z_\mu\Big)\Big(g'Y\partial_\alpha - iY^2 g'^2\cos\theta_W A_\alpha + iY^2 g'^2\sin\theta_W Z_\alpha\Big)\Big)d_R^{(i)}$$

The gluon interaction with the "electroweak" neutral currents is not considered here. Also in Yukawa NCSM action there is quark mass dependent interaction term. Here we present the Feynman rule for $q - \bar{q} - A_\mu$ and $q - \bar{q} - Z_\mu$ vertices, respectively.

$$i\,e\,Q_f\left[\gamma_\mu - \frac{i}{2}k^\nu\left(\theta_{\mu\nu\rho}p_{\text{in}}^\rho - \theta_{\mu\nu}m_f\right)\right]$$

$$= i\,e\,Q_f\,\gamma_\mu + \frac{1}{2}e\,Q_f\left[(p_{\text{out}}\theta p_{\text{in}})\gamma_\mu - (p_{\text{out}}\theta)_\mu(\not{p}_{\text{in}} - m_f) - (\not{p}_{\text{out}} - m_f)(\theta p_{\text{in}})_\mu\right]$$

and

$$\frac{i\,e}{\sin 2\theta_W}\left\{\left(\gamma_\mu - \frac{i}{2}k^\nu\theta_{\mu\nu\rho}p_{\text{in}}^\rho\right)(c_{V,f} - c_{A,f}\,\gamma_5) - \frac{i}{2}\theta_{\mu\nu}\,m_f\left[p_{\text{in}}^\nu\left(c_{V,f} - c_{A,f}\,\gamma_5\right) - p_{\text{out}}^\nu\left(c_{V,f} + c_{A,f}\,\gamma_5\right)\right]\right\}$$

The neutral current interaction Feynman rule for lepton and quark are same. They differs by charge(Q), vector(C_V) and axial(C_A) coupling constants as defined below

$$C_{V,f} = T_{3\,f_L} - 2Q_f\sin^2\theta_W, \qquad C_{A,f} = T_{3\,f_L}.$$

Note that the NC tensor $\theta^{\mu\nu}$ is antisymmetric in $\mu - \nu$ plane. It has the following property

$$(\theta k)^\mu \equiv \theta^{\mu\nu}k_\nu = -k_\nu\theta^{\nu\mu} \equiv -(k\theta)^\mu \quad \text{and} \quad (k\theta p) = k_\mu\theta^{\mu\nu}p_\nu.$$

Below in Table 2.3, we have displayed the standard model fermions, gauge bosons along with their charge, hypercharge, iso-spin etc.

New sources of CP-violation

In the standard model we have CP violation in leptonic sector and as well as in quark sector. Besides that spacetime noncommutativity introduces a new source of CP violation in the standard model [65, 100, 133]. To see this let us write down the $U(1)$ NCQED field strength tensor as

$$\widehat{F}_{\mu\nu} = \partial_\mu A_\nu - \partial_\nu A_\mu + ig[A_\mu \stackrel{\star}{,} A_\nu].$$

	$SU(3)_C$	$SU(2)_L$	$U(1)_Y$	$U(1)_Q$	T_3
$e_R^{(i)}$	**1**	**1**	-1	-1	0
$L_L^{(i)} = \begin{pmatrix} \nu_L^{(i)} \\ e_L^{(i)} \end{pmatrix}$	**1**	**2**	$-1/2$	$\begin{pmatrix} 0 \\ -1 \end{pmatrix}$	$\begin{pmatrix} 1/2 \\ -1/2 \end{pmatrix}$
$u_R^{(i)}$	**3**	**1**	$2/3$	$2/3$	0
$d_R^{(i)}$	**3**	**1**	$-1/3$	$-1/3$	0
$Q_L^{(i)} = \begin{pmatrix} u_L^{(i)} \\ d_L^{(i)} \end{pmatrix}$	**3**	**2**	$1/6$	$\begin{pmatrix} 2/3 \\ -1/3 \end{pmatrix}$	$\begin{pmatrix} 1/2 \\ -1/2 \end{pmatrix}$
$\Phi = \begin{pmatrix} \phi^+ \\ \phi^0 \end{pmatrix}$	**1**	**2**	$1/2$	$\begin{pmatrix} 1 \\ 0 \end{pmatrix}$	$\begin{pmatrix} 1/2 \\ -1/2 \end{pmatrix}$
W^+, W^-, Z	**1**	**3**	0	$(\pm 1, 0)$	$(\pm 1, 0)$
A	**1**	**1**	0	0	0
G^b	**8**	**1**	0	0	0

Table 2.3: The Standard Model fields are shown. Here $i \in \{1, 2, 3\}$ denotes the generation index. The electric charge is given by $Q = (T_3 + Y)$, which is called the Gell-Mann-Nishijima relation.

Under the charge conjugation(C),parity(P) and the time-reversal(T) transformations, the vector field transforms as follows:

Under C: $A_\mu \to -A_\mu$. If $\quad \theta \to -\theta \quad$ then $\quad \hat{F}_{\mu\nu} \to -\hat{F}_{\mu\nu}$.

Under P: $A_0 \to A_0, \quad A_i \to -A_i, \quad \theta \to \theta$.

Under T: $A_0 \to A_0 \quad A_i \to -A_i \quad$ So if $\quad \theta \to -\theta \quad$ then $\hat{F}_{\mu\nu} \to -\hat{F}_{\mu\nu}$.

It is to be noted that $\theta \to -\theta$ under the CP transformation and hence one can observe CP violation in NC theory. However, the noncommutative theory is a CPT invariant theory.

2.8   Classification of Noncommutative Standard model

The complete action of the noncommutative standard model(NCSM) can be written as

$$S_{NCSM} = S_{fermions} + S_{gauge} + S_{Higgs} + S_{Yukawa}.$$

Expanding $\widehat{F}_{\mu\nu}$ up to order $\theta_{\mu\nu}$, one finds

$$S_{gauge} = -\frac{1}{2} \int d^4x \sum_\rho \mathcal{C}_\rho Tr \{\rho(F^{\mu\nu})\rho(F_{\mu\nu})\}$$

$$+ \theta^{\mu\nu} \int d^4x \sum_\rho \mathcal{C}_\rho Tr \left\{ \left(\frac{1}{4}\rho(F_{\mu\nu})\rho(F_{\rho\sigma}) - \rho(F_{\mu\rho})\rho(F_{\nu\sigma}) \right) \rho(F^{\rho\sigma}) \right\}$$

The first term of S_{gauge}, which is independent of $\theta_{\mu\nu}$, corresponds to the standard model term. The standard model group is the product of irreducible gauge group representation of $U(1)_Y$, $SU(2)_L$ and $SU(3)_c$. The generator of the SM group is $\mathcal{T}^A$ [65]. Here $A = 1, 2, ...12$.

$$\{\rho(\mathcal{T}^A)\} = \{\rho_1(Y) \otimes \mathbf{1}_{\rho_2} \otimes \mathbf{1}_{\rho_3},\, 1 \otimes \rho_2(T_L^a) \otimes \mathbf{1}_{\rho_3},\, 1 \otimes \mathbf{1}_{\rho_2} \otimes \rho_3(T_S^b)\}$$

Here a can take value $1, 2$ and 3, and similarly $b = 1, 2, ...8$. The master field strength tensor with SM representations $\rho = \rho_1 \otimes \rho_2 \otimes \rho_3$ are

$$\rho(F_{\mu\nu}) = g'\rho(Y_{SM})f_{\mu\nu} + g \sum_i \rho(T_L^i)F_{\mu\nu}^i + g_s \sum_a \rho(T_s^a)G_{\mu\nu}^a.$$

First we consider the $\theta_{\mu\nu}$ independent term in the gauge kinetic action.

$$\mathcal{L}_{SM} = -\frac{1}{2}g'^2 \sum_\rho \mathcal{C}_\rho\, d(1_{\rho_2})\, d(1_{\rho_3})\, \rho_1(Y)^2 f_{\mu\nu}f^{\mu\nu} - \frac{1}{2}g^2 \sum_\rho \mathcal{C}_\rho\, d(1_{\rho_3})\, Tr\left(\rho_2(T_L^i)\rho_2(T_L^j)\right)\, F_{\mu\nu}^i F^{j\,\mu\nu}$$

$$- \frac{1}{2}g_s^2 \sum_\rho \mathcal{C}_\rho\, d(1_{\rho_2})\, Tr\left(\rho_3(T_s^a)\rho_3(T_s^b)\right)\, G_{\mu\nu}^a G^{b\,\mu\nu},$$

where $d(1_{\rho_i})$ denotes the dimension of the particular gauge representation ρ of the gauge group fermion multiplets. For example, the dimension of the ρ_1 is equal to 1×1. The above equations are constraint equations to match with the following SM lagrangian

$$\mathcal{L}_{SM} = -\frac{1}{4}f_{\mu\nu}f^{\mu\nu} - \frac{1}{4}F_{\mu\nu}^i F^{i\,\mu\nu} - \frac{1}{4}G_{\mu\nu}^b G^{b\,\mu\nu}.$$

The constraint equations are

$$\frac{1}{2g'^2} = \sum_\rho \mathcal{C}_\rho\, d(1_{\rho_2})\, d(1_{\rho_3})\, \rho_1(Y)^2,$$

$$\frac{1}{2g^2}\delta^{ij} = \sum_\rho \mathcal{C}_\rho\, d(1_{\rho_3})\, Tr\left(\rho_2(T_L^i)\rho_2(T_L^j)\right),$$

$$\frac{1}{2g_s^2}\delta^{ab} = \sum_\rho \mathcal{C}_\rho\, d(1_{\rho_2})\, Tr\left(\rho_3(T_s^a)\rho_3(T_s^b)\right).$$

The matching condition of the NCSM gauge sector shows the structure of the gauge couplings. Here the traces are taken for all the SM fields generators. $\mathcal{C}_\rho(= 1/\mathcal{G}_\rho^2)$ is the coupling generator, where $\mathcal{G}_\rho$ is the SM coupling generator [69]. It operates on the SM fields and produces the coupling eigen values

corresponding to the SM fields, they are equal to $1/g_\rho$. One can write

$$
\mathcal{G}_\rho \begin{pmatrix} e_R \\ L_L \\ u_R \\ d_R \\ Q_L \\ \phi \end{pmatrix} = g_\rho \begin{pmatrix} e_R \\ L_L \\ u_R \\ d_R \\ Q_L \\ \phi \end{pmatrix}.
$$

For example, $\mathcal{G}_\rho e_R = g_1 e_R$, $\mathcal{G}_\rho L_L = g_2 L_L$... $\mathcal{G}_\rho \phi = g_6 \phi$. $g_1, g_2...g_6$ are non zero SM coupling eigen value. Let us evaluate the traces over all the standard model fields, for example:

$$
\frac{1}{2g'^2} = \sum_\rho \mathcal{C}_\rho \, d(1_{\rho_2}) \, d(1_{\rho_3}) \, \rho_1(Y)^2 = \frac{1}{g_1^2}(1)(1)(-1)^2 + \frac{1}{g_2^2}(2)(1)(-1/2)^2 + \frac{1}{g_3^2}(1)(3)(2/3)^2
$$
$$
+ \frac{1}{g_4^2}(1)(3)(-1/3)^2 + \frac{1}{g_5^2}(2)(3)(1/6)^2 + \frac{1}{g_6^2}(2)(1)(1/2)^2
$$

Similarly, repeating the same for others, we finally get the constraint equations with full structure of the coupling constants g_i,

$$
\frac{1}{2g'^2} = \frac{1}{g_1^2} + \frac{1}{2g_2^2} + \frac{4}{3g_3^2} + \frac{1}{3g_4^2} + \frac{1}{6g_5^2} + \frac{1}{2g_6^2}
$$
$$
\frac{1}{g^2} = \frac{1}{g_2^2} + \frac{3}{g_5^2} + \frac{1}{6g_6^2}, \quad \frac{1}{g_s^2} = \frac{1}{g_3^2} + \frac{1}{g_4^2} + \frac{2}{g_5^2}
$$

According to trace of the triple gauge boson kinetic term, the NCSM has been classified into two types as stated below [71]:

1. minimal NCSM (mNCSM)

2. Non-minimal NCSM (nmNCSM)

The main difference between the two models are due to the freedom of the choice of traces in the kinetic terms for gauge fields.

2.8.1 Minimal Noncommutative Standard model

In the mimimal noncommutative standard model(mNCSM), the gauge sector has representation that yields a model as close as possible to the SM without new triple gauge boson couplings. In both mNCSM and nmNCSM models, the scalar and fermionic part of the action won't affect by this

particular choice of trace. The trace of triple gauge boson SM group generators are assumed to be zero and the interaction vanishes automatically. The simplest choice of trace zero $U(1)_Y$ generator is

$$Y = \frac{1}{2} \begin{pmatrix} 1 & 0 \\ 0 & -1 \end{pmatrix}$$

This leaves the gauge invariant action and usual SM gauge interaction without neutral triple gauge boson interaction.

2.8.2 Non-minimal Noncommutative Standard model

The trace is chosen over all particles (having different quantum numbers) on which covariant derivative act. So the trace of $U(1)_Y$ is chosen to be non-zero. The triple gauge boson couplings are defined as follows

$$\kappa_1 = \sum_\rho \mathcal{C}_\rho \, d(1_{\rho_2}) \, d(1_{\rho_3}) \, \rho_1(Y)^3,$$

$$\kappa_2 = \sum_\rho \mathcal{C}_\rho \, d(1_{\rho_3}) \, \rho_1(Y) \, Tr\left(\rho_2(T_L^i)\rho_2(T_L^j)\right),$$

$$\kappa_3 = \sum_\rho \mathcal{C}_\rho \, d(1_{\rho_2}) \, \rho_1(Y) \, Tr\left(\rho_3(T_s^a)\rho_3(T_s^b)\right),$$

$$\kappa_4 = \sum_\rho \mathcal{C}_\rho \, d(1_{\rho_3}) \, \frac{1}{2} Tr\left(\left\{\rho_2(T_L^i), \rho_2(T_L^j)\right\} \rho_2(T_L^k)\right),$$

$$\kappa_5 = \sum_\rho \mathcal{C}_\rho \, d(1_{\rho_2}) \, \frac{1}{2} Tr\left(\left\{\rho_3(T_s^a), \rho_3(T_s^b)\right\} \rho_3(T_s^c)\right).$$

Here the term κ_5 provides the order θ correction in the usual triple gluon vertex. The coefficient of the κ_4 gets zero due to symmetric in gauge field indices and anti-symmetric in NC tensor indices. The above constant parameters κ_1, κ_2 and κ_3 can be evaluated in terms of coupling constant eigen values $g_1, g_2...g_6$ by using Table 2.3. We know that $\mathcal{C}_\rho$ is equal to $1/g_\rho^2$ and hence κ_i has the following form

$$\kappa_1 = -\frac{1}{g_1^2} - \frac{1}{4g_2^2} + \frac{8}{9g_3^2} - \frac{1}{9g_4^2} + \frac{1}{36g_5^2} + \frac{1}{4g_6^2}, \tag{2.2}$$

$$\kappa_2 = \left(-\frac{1}{4g_2^2} + \frac{1}{4g_5^2} + \frac{1}{4g_6^2}\right)\delta^{ij}, \tag{2.3}$$

$$\kappa_3 = \left(\frac{1}{3g_3^2} - \frac{1}{6g_4^2} + \frac{1}{6g_5^2}\right)\delta^{ab}. \tag{2.4}$$

The action for triple gauge boson($\widehat{S}_{3g}$) interaction can explore as follows [134, 135]

$$\widehat{S}_{3g} = \int d^4x \; g'^3 \kappa_1 \theta^{\mu\nu} \left(\frac{1}{4} f_{\mu\nu} f_{\rho\sigma} - f_{\mu\rho} f_{\nu\sigma} \right) f^{\rho\sigma}$$

$$+ \int d^4x \; g'g^2 \kappa_2 \theta^{\mu\nu} \sum_{i,j} \left[\left(\frac{1}{4} f_{\mu\nu} F^i_{\rho\sigma} - f_{\mu\rho} F^i_{\nu\sigma} + \frac{1}{4} F^i_{\mu\nu} f_{\rho\sigma} - F^i_{\mu\rho} f_{\nu\sigma} \right) F^{j\,\rho\sigma} \right.$$

$$\left. + \left(\frac{1}{4} F^i_{\mu\nu} F^j_{\rho\sigma} - F^i_{\mu\rho} F^j_{\nu\sigma} \right) f^{\rho\sigma} \right]$$

$$+ \int d^4x \; g' g_s^2 \kappa_3 \theta^{\mu\nu} \sum_{a,b} \left[\left(\frac{1}{4} f_{\mu\nu} G^a_{\rho\sigma} - f_{\mu\rho} G^a_{\nu\sigma} + \frac{1}{4} G^a_{\mu\nu} f_{\rho\sigma} - G^a_{\mu\rho} f_{\nu\sigma} \right) G^{b\,\rho\sigma} \right.$$

$$\left. + \left(\frac{1}{4} G^a_{\mu\nu} G^b_{\rho\sigma} - G^a_{\mu\rho} G^b_{\nu\sigma} \right) f^{\rho\sigma} \right]$$

$$+ \int d^4x \; g^3 \kappa_4 \theta^{\mu\nu} \sum_{i,j,k} \left(\frac{1}{4} F^i_{\mu\nu} F^j_{\rho\sigma} - F^i_{\mu\rho} F^j_{\nu\sigma} \right) F^{k\,\rho\sigma}$$

$$+ \int d^4x \; g_s^3 \kappa_5 \theta^{\mu\nu} \sum_{a,b,c} \left(\frac{1}{4} G^a_{\mu\nu} G^b_{\rho\sigma} - G^a_{\mu\rho} G^b_{\nu\sigma} \right) G^{c\,\rho\sigma}$$

We use the Weinberg rotation for physical and unphysical gauge field and we gets

$$\begin{pmatrix} Z_\mu \\ \mathcal{A}_\mu \end{pmatrix} = \begin{pmatrix} \cos\theta_W & -\sin\theta_W \\ \sin\theta_W & \cos\theta_W \end{pmatrix} \begin{pmatrix} B^3_\mu \\ A_\mu \end{pmatrix}$$

The interaction of the triple gauge bosons can be written in terms physical fields as follows

$$\mathcal{L}_{\gamma\gamma\gamma} = \frac{e}{4} \sin 2\theta_W K_{\gamma\gamma\gamma} \; \theta^{\mu\nu} \left(F_{\mu\nu} F_{\rho\sigma} F^{\rho\sigma} - 4 F_{\mu\rho} F_{\nu\sigma} F^{\rho\sigma} \right),$$

$$K_{\gamma\gamma\gamma} = \frac{1}{2} gg'(\kappa_1 + 3\kappa_2);$$

$$\mathcal{L}_{\gamma gg} = \frac{e}{4} \sin 2\theta_W K_{\gamma gg} \; \theta^{\mu\nu} \left\{ 2 \left(2 G_{\mu\rho} G_{\nu\sigma} - G_{\mu\nu} G_{\rho\sigma} \right) F^{\rho\sigma} + 8 F_{\mu\rho} G_{\nu\sigma} G^{\rho\sigma} - F_{\mu\nu} G_{\rho\sigma} G^{\rho\sigma} \right\},$$

$$K_{\gamma gg} = \frac{-g_s^2}{2} \left(\frac{g}{g'} + \frac{g'}{g} \right) \kappa_3;$$

$$\mathcal{L}_{Z\gamma\gamma} = K_{Z\gamma\gamma} \theta^{\mu\nu} \left\{ 2 \left(2 F_{\mu\rho} F_{\nu\sigma} - F_{\mu\nu} F_{\rho\sigma} \right) Z^{\rho\sigma} + 8 Z_{\mu\rho} F_{\nu\sigma} F^{\rho\sigma} - Z_{\mu\nu} F_{\rho\sigma} F^{\rho\sigma} \right\},$$

$$K_{Z\gamma\gamma} = \frac{1}{2} \left[g'^2 \kappa_1 + \left(g'^2 - 2g^2 \right) \kappa_2 \right]$$

Other three TGB couplings are uniquely fixed by $K_{\gamma\gamma\gamma}$, $K_{Z\gamma\gamma}$ and $K_{\gamma gg}$

$$K_{ZZ\gamma} = \frac{1}{2} \left(\frac{g}{g'} - 3\frac{g'}{g} \right) K_{Z\gamma\gamma} - \frac{1}{2} \left(1 - \frac{g'^2}{g^2} \right) K_{\gamma\gamma\gamma};$$

$$K_{ZZZ} = \frac{3}{2} \left(1 - \frac{g'^2}{g^2} \right) K_{Z\gamma\gamma} - \frac{g'}{2g} \left(3 - \frac{g'^2}{g^2} \right) K_{\gamma\gamma\gamma}; \quad K_{\gamma gg} = -\frac{g}{g'} K_{Zgg}.$$

According to Bose statistics(Landau-Pomeranchuk-Yang theorem), the triple gauge boson (TGB) interactions are forbidden by in the standard model. However, it arises within the framework of the non-minimal NCSM. Here we can maximize the TGB coupling by solving the three TGB equation including three matching equations.
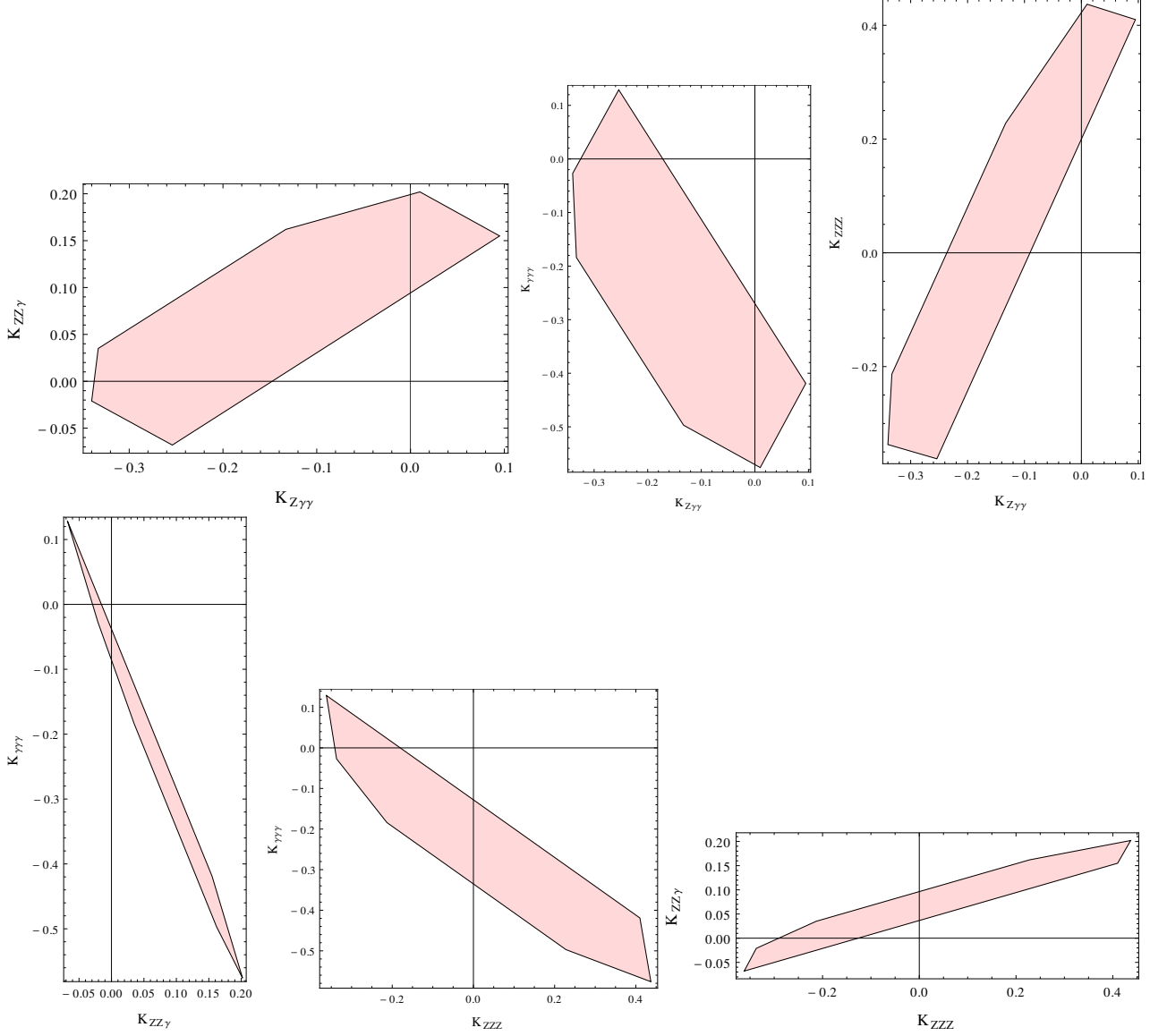
Figure 2.2: The allowed region for **K** values of neutral triple gauge boson couplings in the nmNCSM

The three matching conditions(constraint equations), satisfying $1/g_i^2 > 0$, defines a three dimensional simplex in the six dimensional moduli space spanned by $1/g_1^2, 1/g_2^2, ...1/g_6^2$. The constants κ_1, κ_2 and κ_3 are functions of $1/g_1^2, 1/g_2^2, ...1/g_6^2$. We have obtained the optimum value for three objectives $K_{\gamma\gamma\gamma}, K_{Z\gamma\gamma}$ and $K_{\gamma gg}$ TGB equations with the requirement that three constraint equation and six moduli condition($1/g_i^2 > 0$) by multi-objective Weighted sum optimization method. Later substituting these into other three TGB equation, we get the non vanishing six TGB coupling constants in the nmNCSM. The values for all six coupling constants at the pentahedron vertices are given in Table 2.4. From Table 2.4, we can construct the allowed region for any pair of couplings: $K_{\gamma\gamma\gamma}, K_{Z\gamma\gamma}, K_{Zgg}, K_{ZZ\gamma}, K_{ZZZ}$ and $K_{\gamma gg}$. The range of values for a full set of electroweak coupling constants is given in the figures2.2. Any combination of two TGB coupling constants from the gauge

$K_{\gamma\gamma\gamma}$	$K_{Z\gamma\gamma}$	K_{Zgg}	$K_{ZZ\gamma}$	K_{ZZZ}	$K_{\gamma gg}$
-0.1745	-0.3339	0.054	0.0311	-0.2211	-0.098
-0.027	-0.34	-0.108	-0.021	-0.337	0.197
0.1177	-0.2606	0.217	-0.0645	-0.3605	-0.396
-0.4304	0.089	0.217	0.1585	0.412	-0.396
-0.576	0.01	-0.108	0.202	0.437	0.197
-0.5017	-0.124	0.054	0.1644	0.2414	-0.098

Table 2.4: The **K** values of the triple gauge boson couplings at the vertices of the pentahedron in the nmNCSM at the M_Z scale

sector can never vanish simultaneously due to the constraint set by the value of the SM coupling constants at the M_Z scale. One can derive the interaction between charged W^a fields and neutral fields as follows,

$$\mathcal{L}_{\gamma WW} = \frac{e}{2}\sin 2\theta_W K_{\gamma WW} \quad \theta^{\mu\nu} \left[\left\{ 2(W^+_{\mu\rho}W^-_{\nu\sigma} + W^-_{\mu\rho}W^+_{\nu\sigma}) - (W^+_{\mu\nu}W^-_{\rho\sigma} + W^-_{\mu\nu}W^+_{\rho\sigma}) \right\} F_{\mu\nu} \right.$$
$$\left. + 4F_{\mu\rho}(W^{+\;\rho\sigma}W^-_{\nu\sigma} + W^{-\;\rho\sigma}W^+_{\nu\sigma}) - F_{\mu\nu}W^+_{\rho\sigma}W^{-\;\rho\sigma} \right]$$

$$K_{\gamma WW} = \frac{-g}{2g'}(g^2 + g'^2)\kappa_2$$

$$\mathcal{L}_{ZWW} = \frac{e}{2}\sin 2\theta_W K_{ZWW} \quad \theta^{\mu\nu} \left[\left\{ 2(W^+_{\mu\rho}W^-_{\nu\sigma} + W^-_{\mu\rho}W^+_{\nu\sigma}) - (W^+_{\mu\nu}W^-_{\rho\sigma} + W^-_{\mu\nu}W^+_{\rho\sigma}) \right\} Z_{\mu\nu} \right.$$
$$\left. + 4Z_{\mu\rho}(W^{+\;\rho\sigma}W^-_{\nu\sigma} + W^{-\;\rho\sigma}W^+_{\nu\sigma}) - Z_{\mu\nu}W^+_{\rho\sigma}W^{-\;\rho\sigma} \right] \quad \text{where} \quad K_{ZWW} = -\tan\theta_W K_{\gamma WW}$$

In addition, there are additional $\mathcal{O}(\theta)$ contribution for triple gauge boson($WW\gamma/Z$) interaction presents in Higgs action.

2.9   Status of the Noncommutative phenomenology

In the last two decades, enormous effort have been made to understand the fundamentals of the noncommutative theory. Several efforts in the model-building which leads towards experimental detection of noncommutative effects have been made. Some of the theoretical difficulties were addressed properly and quite improved the understanding in the last few years. Importantly, Poincare symmetry and Renormalizability of the NC theory have been attempted in an authentic manner. The probing energy scale could lie anywhere between the Planck scale to TeV scale. There was a surge of intense

phenomenological activities among experimentalist and phenomenologist, after the construction of the noncommutative standard model.

Noncommutative quantum mechanical experiments:

The quantum field theory on a noncommutative space-time has studied in Ref. [136–139]. Many articles have been devoted to the study of various aspects of quantum mechanics (QM) on a noncommutative space (NCS) and a noncommutative phase space(NCPS), because the main goal of the noncommutative quantum mechanics (NCQM) is to find a measurable spatial noncommutativity effects. We have listed the current lower bound on NC scale in table 2.5, and quantum Hall effect, which are obtained from quantum mechanical experiments like Aharonov-Bohm phase, Aharonov-Caser phase, Hydrogen Lamb shift, Rydberg atom [141].

Experiments	Lower bound on Λ
Lamb shift [140, 174]	≥ 10 TeV
Transitions in the Helium atom [173]	≥ 3 GeV
Aharonov-Bohm phase [142–145]	$\geq 10^{-6}$ GeV
Aharonov-Casher phase [146–148]	$\geq 10^{-7}$ GeV
Noncommutative quantum Hall effect [149–151]	≥ 10 GeV
Spin Hall effect [149, 152, 153]	$\geq 10^{-13}$ GeV
Spin Hall conductivity [154]	$\geq 10^{-12}$ GeV

Table 2.5: Lower bound on NC scale Λ

Noncommutative standard model experiments:

There are two different approaches to study the quantum field theory in the NC space-time. One is the Moyal-Weyl (MW) star product approach and another one is Seiberg-Witten map approach.

Moyal-Weyl (MW) star product approach:

A host of collider searches of spacetime noncommutativity using the MW start product approach is available in the literature. Hewett *et al.* [181, 182] have studied the processes $e^+e^- \rightarrow e^+e^-$ (Bhabha) and $e^-e^- \rightarrow e^-e^-$(Moller) and subsequent studies [183, 184] were done in the context of $e\gamma \rightarrow e\gamma$ (Compton) and $e^+e^- \rightarrow \gamma\gamma$ (pair annihilation), $\gamma\gamma \rightarrow e^+e^-$ and $\gamma\gamma \rightarrow \gamma\gamma$. For a review on NC phenomenology, see [185]. The Noncommutative contribution of neutral vector boson (γ, z) pair production was studied [186] at the LHC and the bound was obtained for the NC scale $\Lambda \geq 1$ TeV under some conservative assumptions. Further study on the pair production of charged gauge bosons $(W^{\pm})$ at

the LHC in the noncommutative extension of the standard model found [187] significant deviation of the azimuthal distribution(oscillation) from the SM one (which is a flat distribution) for $\Lambda = 700 \text{ GeV}$. More recently, t-channel single top quark production was calculated at the LHC, and significant deviation in the cross section can be expected from the standard model for $\Lambda \geq 980 \text{ GeV}$ [188].

Pauli-forbidden transitions:

The twisted Poincare symmetry has deformed the methods of symmetrization and anti-symmetrization of the identical particles. The corresponding fermions and bosons are called as twisted fermions and twisted bosons respectively, which are obeys the twisted statistics. Thus one can expect that there could be a violation of Pauli exclusion principle in the fermionic sector. There are few nuclear and atomic experiments has made searches on Pauli forbidden transitions. As a result, the lifetime of the particular non-Pauli transitions are quite higher than the age of the universe. So if there were Pauli forbidden levels created at the initiation of the universe the probability of the allowed non-Pauli transitions to be less than 10^{-26} or 10^{-28} [190].

Experiment	Type	Bound on Λ (Energy scales)
Borexino [228]	Nuclear	$\geq 10^{24}$ TeV
Kamiokande [229]	Nuclear	10^{23} TeV
NEMO [230]	Atomic	10^5 eV
NEMO-2 [231]	Nuclear	10^{22} TeV
Maryland [232]	Atomic	10 TeV
VIP [233]	Atomic	100 TeV

Table 2.6: Bounds on the noncommutative scale Λ [190].

Seiberg-Witten map approach:

Using this SW map Calmet *et al.* [205,206] first constructed the *minimal* version of the noncommutative standard model (mNCSM in brief). They derived the $\mathcal{O}(\theta)$ Feynman rules of the standard model interactions and found several new interactions which are absent in the standard model. All the above analyses were limited to the leading order in θ. Das *et al.* first analyzed the $e^+e^- \rightarrow \gamma, Z \rightarrow \mu^+\mu^-$ to order θ^2 (without considering the effect of earth's rotation) [207]. There exists another version: the non-minimal version of the NCSM (nmNCSM in brief) where the triple neutral gauge boson coupling arises (absent in the mNCSM) naturally in the gauge sector. This model (nmNCSM) was first formulated by Melic *et al.* [208,209]. Interesting phenomenological studies comprising triple gauge in-

teraction are available in the literature [196, 210–213]. The direct test of space-time noncommutativity comes from the two decays $Z \to \gamma\gamma$, gg (forbidden in the SM at the tree level). Using the experimental bound $\Gamma_{Z\to\gamma\gamma}^{exp} < 1.3 \times 10^{-4}$ GeV and $\Gamma_{Z\to gg}^{exp} < 1.0 \times 10^{-3}$ GeV, Behr *et al.* [210] shows the bound on the NC scale ~ 1 TeV. Taking the SM fields in the enveloping algebra, Calmet *et al.* [214, 215] shows that the bound on the NC scale ~ 10 TeV, a rather weak bound. The invisible Z boson decay in covariant theta-exact NCSM was studied in [216]. Early collider searches of space-time noncommutativity include the work by Kamoshita *et al.* [217, 255]. Das *et al.* (one of the current authors) studied in detail the Bhabha and the Möller scattering [218, 219], muon pair production [207, 220] in the non-minimal NCSM scenario. The noncommutative parameter $\theta_{\mu\nu}$ can be fundamental constant in nature that has a fixed direction in the celestial sphere. Hence, the daily modulation effect of earth's rotation can be observed in the noncommutative phenomenology. The associated Higgs boson production was recently studied associated with the Z boson, taking into account the effect of the Earth's rotation in the nmNCSM. It was found that the azimuthal distribution significantly differs from the standard model result if the NC scale $\Lambda \geq 500$ GeV [221]. The low energy experiments (e.g. modeling of the atomic, QCD-hadronic and astrophysical systems) remains valid at an energy-momentum range significantly lower than Λ. The current bound on the NC scale Λ has been displayed in the Table 2.7 (given in [155]).

 Flavour Physics Precision measurements:

Table 2.7: The key parameters used in the TEXONO, LSND and CHARM-II measurements on $\nu - e$ scattering, and the bounds obtained on the NC scale Λ are shown here. The the bound on the 95% CL lower limits on Λ and the best-fit values in θ^2 are shown [155].

Experiment	ν	$< E_\nu >$	T	Measured $\sin^2\theta_W$	Best-Fit on θ^2 (MeV^{-4})	Λ (95% CL)
TEXONO-HPGe [156]	$\bar{\nu}_e$	$1-2$ MeV	$12-60$ keV	$-$	$(9.27 \pm 6.65) \times 10^{-22}$	> 145 GeV
TEXONO-CsI(Tl) [157]	$\bar{\nu}_e$	$1-2$ MeV	$3-8$ MeV	0.251 ± 0.039	$(0.81 \pm 5.74) \times 10^{-21}$	> 95 GeV
LSND [158]	ν_e	36 MeV	$18-50$ MeV	0.248 ± 0.051	$(0.38 \pm 2.06) \times 10^{-21}$	> 123 GeV
CHARM-II [159]	ν_μ	23.7 GeV	3-24 GeV	} 0.2324 ± 0.0083	$(0.20 \pm 1.03) \times 10^{-26}$	> 2.6 TeV
	$\bar{\nu}_\mu$	19.1 GeV	3-24 GeV		$(-0.92 \pm 4.77) \times 10^{-27}$	> 3.3 TeV

The impact of NC space-time on Quarkonia decay into two photons [222, 223] and $K \to \pi\gamma$ [224] decay (forbidden in the SM) have been investigated in detail. However, the experimental upper bound on such rare decays are too weak to obtain any bound on Λ. In [164] top quark decay has studied and also in [161] the top quark width and W boson polarization have been estimated and the bound on noncommutative scale is given $\Lambda \geq 625$ GeV. The inclusive $b \to s\gamma$ and $b \to sg$ decay studied

in [225, 226]. Non-commutative spacetime lead to CPT violation [227]. One of the strongest experimental supports to CPT symmetry comes from the mass difference of K^0 and $\overline{K}^0$ which is predicted to vanish exactly for CPT-invariant theories. In [234], the data from the KTeV E731 experiment [235] and the experiments on kaons [236, 237] have been used to get bounds on $\Lambda \geq 2$TeV. In [234], CPT measurements on the $g-2$ difference of μ^+ and μ^- [238–241] have been also used to constrain θ. The derivation is similar to the kaon case but, the mass of the muon being considerably smaller than the kaon mass, the lower bound for the energy scale is 10^3 GeV.

Astrophysical measurements:

The impact of neutrino-photon interaction in the noncommutative space-time on the cooling of stars [249], on the primordial nucleosynthesis and ultra-high energy cosmic ray [250, 251] have been studied in detail. Assuming the plasmon decay to a pair of neutrino may contribute substantially to the star energy loss, the author P. Schupp *et al.* [249] obtain a lower bound $\Lambda > 81$ GeV. The non-observation of large neutrino-nucleon cross-section for ultra high energy neutrinos (10^{10} GeV) at observatories gives rise a lower bound on Λ which is as high as 900 TeV [251].

Laser beam experiments and CMB :

In the early universe physics can test by the observation of the polarization in the cosmic microwave background(CMB) which is correlated with the temperature anisotropy.The CMB radiation is expected to be linearly polarized of the order of 10%.This Linearity is a result of the anisotropic Compton scattering around the epoch of recombination. The Compton scattering can generate a linearly polarized wave but it can't generate circular polarized wave. The non-zero backgrounds would produce the circular polarization for the CMB radiation. Therefore, any experiment including the measurement of circular polarization can provide a way to understand more accurately the physics of scattering. It is possible in space-time noncommutative or external magnetic field to generate the circular polarization by the Compton scattering [242, 243].The possibility of the generation of circular polarization can be determined by the Stokes parameter. The circularly polarized laser beam experiment and CMB measurement limits the lower bound on the NC scale $\Lambda \sim 1 - 10$ TeV. Some of the important laser beams are: X-ray free-electron laser (XFEL) facilities [244], optical high-intensity laser facilities such as Vulcan [245], peta-watt laser beam [246] and ELI [247], as well as SLAC E144 using nonlinear Compton scattering [248]. Various experiments like low energy Precision experiment and high energy collider experiments put limits/bound(lower) on the noncommutative scale Λ, which are listed in the Table 2.8.

Table 2.8: Summary of experimental constraints on the noncommutative scale Λ. The quoted bounds for the direct experiments on scattering processes at colliders are at 95% CL [155].

Experiments	Direct Scattering Channels	Λ
High Energy Collider Experiments		
Current Bounds		
LEP-OPAL	$e^- + e^+ \to \gamma + \gamma$ [160]	> 141 GeV
LEP	$e^- + e^+ \to Z \to \gamma + \gamma$ [134]	> 110 GeV
Tevatron	$t \to W + b$ [164]	> 624 GeV
	$t \to W_R + b$ [161]	> 1.5 TeV
Projected Sensitivities		
LHC	$Z \to \gamma + \gamma$ [166]	> 1 TeV
	$p + p \to Z + \gamma \to l^+ + l^- + \gamma$ [168]	> 1 TeV
	$p + p \to W^+ + W^-$ [169]	> 840 GeV
Linear Collider	$e + \gamma \to e + \gamma$ [170]	> 900 GeV
	$e^- + e^- \to e^- + e^-$ [165]	> 1.7 TeV
	$e^- + e^+ \to \gamma + \gamma$ [165]	> 740 GeV
	$\gamma + \gamma \to \gamma + \gamma$ [165]	> 700 GeV
	$e^- + e^+ \to \gamma + \gamma \to Z$ [167]	> 4 TeV
	$e^- + e^+ \to Z + \gamma \to e^+ + e^- + \gamma$ [168]	> 6 TeV
	$e^- + e^+ \to W^+ + W^-$ [169]	> 10 TeV
Photon Collider	$\gamma + \gamma \to l^+ + l^-$ [171]	> 700 GeV
	$\gamma + \gamma \to f + \bar{f}$ [172]	> 1 TeV
Low Energy and Precision Experiments		
Atom Spectrum of Helium [173]		> 3 GeV
Lamb Shift in Hydrogen [174]		> 10 TeV
Electric Dipole Moment of Electron [114, 175]		> 100 TeV
Atomic Clock Measurements [176]		$> 10^8$ TeV
CP Violating Effects in K^0 System [133]		> 2 TeV
C Violating Effects in $\pi^0 \to \gamma + \gamma + \gamma$ [177]		> 1 TeV
Magnetic Moment of Muon [178]		> 1 TeV
Astrophysics and Cosmology Bounds		
Energy Loss via $\gamma \to \nu\bar{\nu}$ in Stellar Clusters [162]		> 80 GeV
Cooling of SN1987A via $\gamma \to \nu\bar{\nu}$ [163]		> 4 TeV
Effects of $\gamma \to \nu\bar{\nu}$ in Primordial Nucleosynthesis [179]		> 3 TeV
Ultra High Energy Astrophysical Neutrinos [180]		> 200 TeV

Chapter 3

Search for associated production of Higgs with Z boson in the noncommutative Standard Model at linear colliders

"What we observe is not nature itself, but nature exposed our method of questioning" - Werner Heisenberg

3.1 Introduction

After the discovery of the Higgs boson (last missing link of the standard model) at CERN LHC on 2012, the main question that has become central in high energy physics phenomenology: Is there any BSM physics and will it show up in the present and future high energy colliders? The SM Higgs boson production is possible in the future electron positron colliders via the process of Higgs-strahlung, WW fusion and ZZ fusion. In the LC the electron and positron collides and produce a virtual Z boson and it decays into Z boson and Higgs boson. This is called Higgs-strahlung and also known as associated production which is dominant mode at LC. The collision energy of the LEP collider was 209 GeV and it gave an important hint on Higgs mass (lower bound) to search the Higgs boson at LHC which is $m_h \geq 114.4$ GeV at 95% CL [252, 253]. Tevatron also has excluded the Higgs mass range between $162 - 166$ GeV at 95% CL [254]. Higgs boson was discovered with the 125 GeV at LHC. ILC planned to have collision energy is 500 GeV and upgraded to 1 TeV. Similarly CLIC collision energy planned upto 3 TeV.

There are several BSM models studied Higgstralung process which are left-right twin Higgs

model (LRTH) [260], minimal dilaton model [261] and Monohar-Wise color octet scalar model [262] etc. In the LRTH model, they have found that the lower bound on LRTH parameters which are the mass of the scalar $m_{\phi_0} = 117.0$ GeV, the symmetry breaking scale $f > 900$ GeV at scalar mixing parameter $M = 150$, the mass of the top quark partner $m_T = 908.5$ GeV and new Vector boson mass is equal to $m_{Z_H} = 2.76$ TeV which is involved in the Higgs-strahlung process. In the dilaton model, the coupling hZZ were studied at 240 GeV LC collider. The coupling is defined as $C_{hZZ}/SM = \cos\theta_s$. There two scenario was considered 1) heavy dilaton and lighter dilaton. In the case of lighter dilaton the cross section for Higgs-strahlung varies 1% with limit $0 < \tan\theta_s < 0.1$.

At the TeV energy scale if the spacetime becomes noncommutative(NC), whether such a NC spacetime can play an important role in Higgs boson production and it's decay? In an earlier work, Das et. al [220, 256] studied the Higgs boson pair production in the noncommutative spacetime. Another interesting process may be the Higgs-strahlung process. The associated Higgs production with Z boson and the vector boson fusion through W or Z bosons are two most significant Higgs production channels in linear collider. Wang et. al., [257] made a preliminary study of the Higgs-strahlung process in the noncommutative spacetime, however they didn't consider the effect of of earth's rotation into their analysis.

3.2   Methodology

In this chapter, we have made a detailed investigation of the Higgs-strahlung process by considering the effect of earth rotation into account.

The tree level Feynman diagram for the Higgs-strahlung process which is a s-channel process is shown below in Fig. 3.1. We use the notation for the incoming electron and positron momenta as p_1
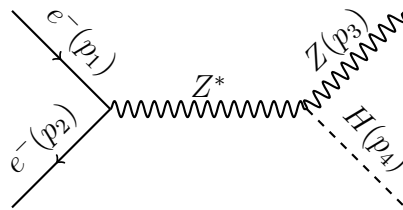
Figure 3.1: *Representative Feynman diagram for the process* $e^-(p_1)e^+(p_2) \xrightarrow{Z^*} Z(p_3)H(p_4)$ *both in SM and NCSM with different structure of couplings. As can be noted from the vertices given in the text, in the very large NCSM scale* $(\Lambda \to \infty)$ *extra tensor structures disappear to reproduce SM couplings.*

and p_2, whereas the outgoing Z boson and Higgs(H) boson momenta are p_3 and p_4, respectively. In

terms of the noncommutative parameter $\Theta_{\mu\nu}$, we use the Feynman rule [257] for $e^- - e^+ - Z$ vertex

$$\frac{-ie}{\sin 2\theta_W}\gamma^\mu\left\{\left(\frac{-1}{2}+2\sin^2\theta_W\right)+\frac{1}{2}\gamma_5\right\}e^{i\left(\frac{p_1\Theta p_2}{2}\right)}, \tag{3.1}$$

and for $Z - Z - H$ vertex

$$\frac{iM_Z^2}{\upsilon}\left\{2\cos\left(\frac{p_3\Theta p_4}{2}\right)\eta^{\mu\nu}+\left[\frac{\cos\left(\frac{p_3\Theta p_4}{2}\right)-1}{4(p_3\Theta p_4)}\right][(\Theta p_4)^\mu\,p_3^\nu+(\Theta p_4)^\nu\,k^\mu]\right\}. \tag{3.2}$$

Neglecting the masses of incoming electrons and positrons, we consider the vertices above contain all orders of $\Theta\left(\propto\frac{1}{\Lambda^2}\right)$ terms. Using these Feynman rules, we find the squared amplitude (spin-averaged) as,

$$\overline{|M|}^2_{NCSM}=\overline{|M|}^2_{SM}\cos^2\left(\frac{p_3\Theta p_4}{2}\right) \tag{3.3}$$

where the quantity $p_3\Theta p_4$ (the argument of cosine function appeared in above) is given by

$$p_3\Theta p_4=\frac{1}{4\Lambda^2}\sqrt{\frac{\lambda\left(s,M_Z^2,M_H^2\right)}{3}}\,f(\theta,\phi)\simeq\frac{1}{4\sqrt{3}}\left(\frac{\sqrt{s}}{\Lambda}\right)^2 f(\theta,\phi),\text{ as }\sqrt{s}\gg M_Z,M_H \tag{3.4}$$

where $f(\theta,\phi)=cos\theta+sin\theta\left(sin\phi+cos\phi\right)$. Here θ, ϕ respectively stands for the polar and the azimuthal angles of the outgoing Z boson. $\lambda\left(s,M_Z^2,M_H^2\right)$ (the Kallen function), in terms of Higgs mass (M_H) and Z boson mass (M_Z) are given by

$$\lambda(s,M_Z^2,M_H^2)=s^2+M_Z^4+M_H^4-2sM_Z^2-2sM_H^2-2M_Z^2M_H^2\;\rightarrow s^2\text{ as }\sqrt{s}\gg M_Z,M_H$$

It is important to note that the oscillatory behaviour that the cross section and other angular dependence of the azimuthal distribution (as we will see later) is due to the presence of the function $f(\theta,\phi)$ defined above.

Note that the SM squared amplitude term gets recovered in $\lim_{\Lambda\to\infty}\overline{|M|}^2_{NCSM}$ and is equal to

$$\overline{|M|}^2_{SM}=\left(\frac{16\pi\alpha M_Z^4\left[\frac{1}{4}+\left(-\frac{1}{2}+2\sin^2\theta_W\right)^2\right]}{\left[(s-M_Z^2)^2+M_Z^2\Gamma_Z^2\right]\upsilon^2\sin^2 2\theta_W}\right)\cdot\left\{\frac{s}{2}+\frac{s}{2M_Z^2}\left(M_Z^2+\frac{\lambda\left(s,M_Z^2,M_H^2\right)}{4s}\right)\right\} \tag{3.5}$$

Since the noncommutative parameter $\Theta_{\mu\nu}$ is considered as fundamental constant in nature, it's direction is fixed with respect to an inertial (non rotating) coordinate system. Now the experiment is done in the laboratory coordinate system located on the surface of the earth and is moving along with the earth's rotation. As a result $\Theta_{\mu\nu}$ ($\vec{\Theta}_E,\;\vec{\Theta}_B$), fixed in the primary co-ordinate system, will also vary with time in the laboratory frame and this must be taken into account while making any serious phenomenological investigations of space-time. The effect of earth's rotation in the non-commutative space-time has explained in appendix 3.6 and [255].

The differential cross-section of the $e^+ e^- \xrightarrow{Z^*} ZH$ scattering is given by

$$\frac{d\sigma}{d\cos\theta d\phi} = \frac{\lambda^{1/2}\left(s, M_Z^2, M_H^2\right)}{64\pi^2 s^2} \overline{|M|^2}_{NCSM} \tag{3.6}$$

and the total cross-section

$$\sigma = \int_0^\pi d\theta \int_0^{2\pi} d\phi \frac{d\sigma}{d\cos\theta\, d\phi} \tag{3.7}$$

In above, the spin-averaged squared-amplitude $\overline{|M|^2}_{NCSM}$ is given by Eqn.3.3 To extract the effect of this lab-rotation coming through noncommutative effect, one takes the average of the cross-section σ or it's distributions over the sidereal day T_{day}. Here, we consider $\langle\sigma\rangle_T = \frac{1}{T_{day}} \int_0^{T_{day}} \sigma\, dt$ and so on [255]. Here $\sigma = \sigma(\sqrt{s}, \Lambda, \eta, \xi, t)$. The cross-section is calculated using the center of mass frame of the $e^+ e^- \xrightarrow{Z^*} ZH$ process in which 4 momenta of the incoming and outgoing particles are given by:

$$p_1 = p_{e^-} = \frac{\sqrt{s}}{2}\left(1, 0, 0, 1\right),\ p_2 = p_{e^+} = \frac{\sqrt{s}}{2}\left(1, 0, 0, -1\right),$$

$$p_3 = p_Z = \left(E_Z,\ k'\sin\theta\,\cos\phi,\ k'\sin\theta\,\sin\phi,\ k'\cos\theta\right),$$

$$p_4 = p_H = \left(E_H,\ -k'\sin\theta\,\cos\phi,\ -k'\sin\theta\,\sin\phi,\ -k'\cos\theta\right).$$

where $k' = \frac{1}{2}\sqrt{\frac{\lambda}{s}}$ and θ is the scattering angle made by the 3-momentum vector p_3 of Z boson with the $\hat{k}$ axis (the 3-momentum direction of the incoming electron e^-) and ϕ is the azimuthal angle. The time dependence in the cross-section or it's distribution enters through the NC parameter $\vec{\Theta}(= \vec{\Theta}_E)$ which changes with the change in $\zeta = \omega t$. The angle ξ which appears in $\vec{\Theta}$ through $\cos(\omega t - \xi)$ or $\sin(\omega t - \xi)$ (the initial phase for time evolution) gets disappeared in the time averaged observables. So one can deduce $\vec{\Theta}$ i.e. the NC scale Λ and the orientation angle η from the time-averaged observables.

3.3 Noncommutative effects on production cross-section and angular distributions

We analyze the Higgs-strahlung process, $e^-(p_1)\, e^+(p_2) \to Z(p_3)\, H(p_4)$ in presence of the noncommutative standard model in TeV energy linear colliders. We assume both the final Z boson and Higgs boson are produced on-shell and reconstructed from their decay products which is not problematic in a linear collider by choosing suitable decay channels. The initial unpolarized electron and positron beams are colliding back to back with half of machine energy without considering any effects

70

from ISR whereas the final particle momenta can be defined in terms of polar (θ) and azimuthal angle (ϕ) as they are produced inside the collider. We further study this process with and without taking into consideration the effect of earth rotation into noncommutative space-time. In this context, we probe the non-commutative scale Λ for the machine energy ranging from 500 GeV to 3000 GeV from the associated production of Higgs with Z boson. Here we utilize the total cross-section rate, azimuthal distribution and rapidity distributions and their time-averaged estimates to discriminate the new physics. In our analysis we have used the Higgs boson mass as 125 GeV and used $(\delta, a) = (\pi/4, \pi/4)$ which corresponds to the location of the OPAL experiment at LEP. In Fig. 3.2 we display the total cross-
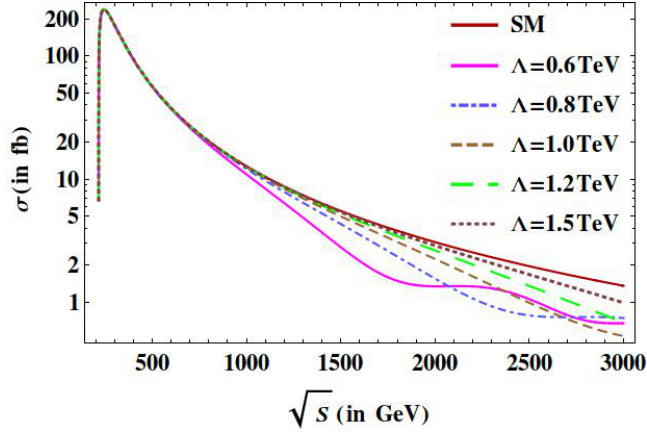
Figure 3.2: *The total cross-section σ (in fb) for associated production of Higgs with Z boson is shown as a function of the machine energy $\sqrt{s}$ (in GeV). Different lines represent the choice of different non-commutative scale Λ which is ranging from 0.6 TeV to 1.5 TeV. The topmost curve (solid line) corresponds to the expected Standard Model production cross-section which is essentially NC cross-section at the limit $\Lambda \to \infty$.*

section as a function of the center of mass energy energy $\sqrt{s}$ for different values of non-commutative scale Λ. The uppermost curve in this plot refers the expected contribution from SM production (which corresponds to the NCSM value at the limit of NC scale $\Lambda \to \infty$ as we already noted down in previous section). While going below in the same plot, the curve next to the topmost one corresponds to the scale $\Lambda = 1.5$ TeV and so on. On the other hand, the lowermost curve corresponds to $\Lambda = 0.6$ TeV. The deviation from the SM plot starts getting manifested at and above $\sqrt{s} = 1$ TeV. For example, at the machine energy $\sqrt{s} = 1.5$ TeV, we see that the overall cross-section gradually increases with the increase in the scale Λ from 0.6 TeV to 1.5 TeV before merging with the SM value for larger NC scale. Expectedly, maximum deviation from that of SM in observed for the lower values of Λ. Also, note that for a given machine energy the NC cross-section is always less than that the corresponding SM value. That is simply followed from the Eq. 3.3. Moreover, one can notice that at higher machine energy the NC cross-sections are not always simply falling with monotonous regularity. The ripple

effect appears and become prominent at some higher machine energy subject to each NC curves. This is an effect of tensor structure coming into the Eq. 3.3. In the next subsection we would explore this as a characteristic feature from NC effects.

3.3.1 Noncommutative correction

To explore and quantify the noncommutative effect manifested in production cross-section and originated from the tensorial structure as in $\Theta_{\mu\nu}$, we define the NC correction with respect to the SM value $\Delta\sigma$ as,

$$\Delta\sigma = \sigma_{NC} - \sigma_{SM}. \tag{3.8}$$

In Fig. 3.3(a), we have demonstrated the variation of $\Delta\sigma$ as a function of the machine energy $\sqrt{s}$ for
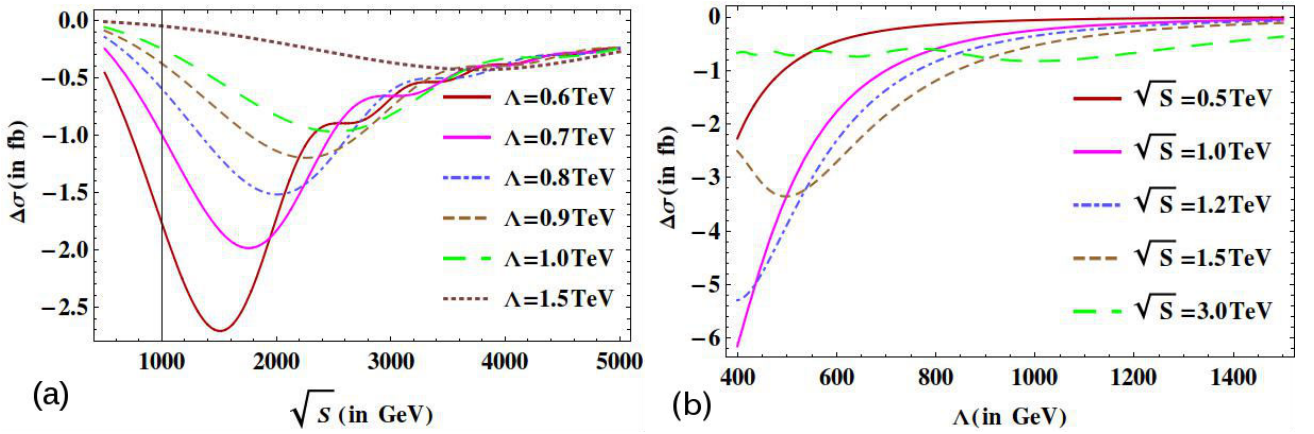
Figure 3.3: *On the left, (a) noncommutative correction to the total cross-section $\Delta\sigma$ (in fb) for associated production of Higgs with Z boson is shown as a function of the linear collider machine energy $\sqrt{s}$ (in GeV) for different Λ ranging from 0.6 TeV to 1.5 TeV. On the right, (b) the same quantity is plotted as a function of NC scale Λ for different machine energy.*

different values of Λ. Now, we can spot it very clearly that $\Delta\sigma$ first decreases (becomes more negative as $\sigma_{NC} < \sigma_{SM}$) with the increase in $\sqrt{s}$ and reaches a minimum for its first trough [1]. Note that the first minimum occurs at $\sqrt{s} = 2 \times (3)^{1/4} \times \Lambda$ (See Eqn.3.4)= $1579(2105)$ GeV corresponding to $\Lambda = 600(800)$ GeV,whereas the second minimum occurs at $\sqrt{s} \approx 2700(3600)$ GeV for the same Λ. After that they decreases with the increase in $\sqrt{s}$ and pass through an oscillatory phase and eventually becomes a flat curve asymptotically meeting at the line $\Delta\sigma = 0$, which is the case for large Λ limit(the

---

[1]However additional subsequent troughs remain sub dominant to be observed in this figure and would be clearly prominent in our next figure where we would consider the relative correction

SM limit). As for example, for $\Lambda = 0.6$ TeV, we find $\Delta\sigma = -2.7$ fb at $\sqrt{s} = 1.5$ TeV and for $\Lambda = 0.6$ TeV, $\Delta\sigma = -0.4$ fb (minimum) at $\sqrt{s} = 4.0$ TeV. As we vary $\Lambda = 0.6$ TeV to $\Lambda = 1.5$ TeV, we see that the height/depth of the trough $\Delta\sigma_{min}$ decreases and it's location (the value of $\sqrt{s}$) also gets changed. In Fig. 3.3(b), we have plotted the variation of the difference $\Delta\sigma$ as a function of the NC scale Λ corresponding to the different machine energy $\sqrt{s} = 0.5, 1.0, 1.2, 1.5$ and 3 TeV, respectively. We see that the deviation decreases with the increase in Λ for a fixed machine energy and for large Λ the NC effect gets disappeared as expected. For $\sqrt{s} = 1$ TeV, $|\Delta\sigma|$ changes by an amount 6 fb as Λ changes from 400 GeV to 1500 GeV.

As noted earlier, we next define the relative correction of this NC cross-section by normalizing the noncommutative correction to the total cross-section by the SM value:

$$\delta_r = \frac{\Delta\sigma}{\sigma_{SM}}. \tag{3.9}$$

In Fig. 3.4, we have shown the variation of δ_r against the machine energy $\sqrt{s}$ for different val-
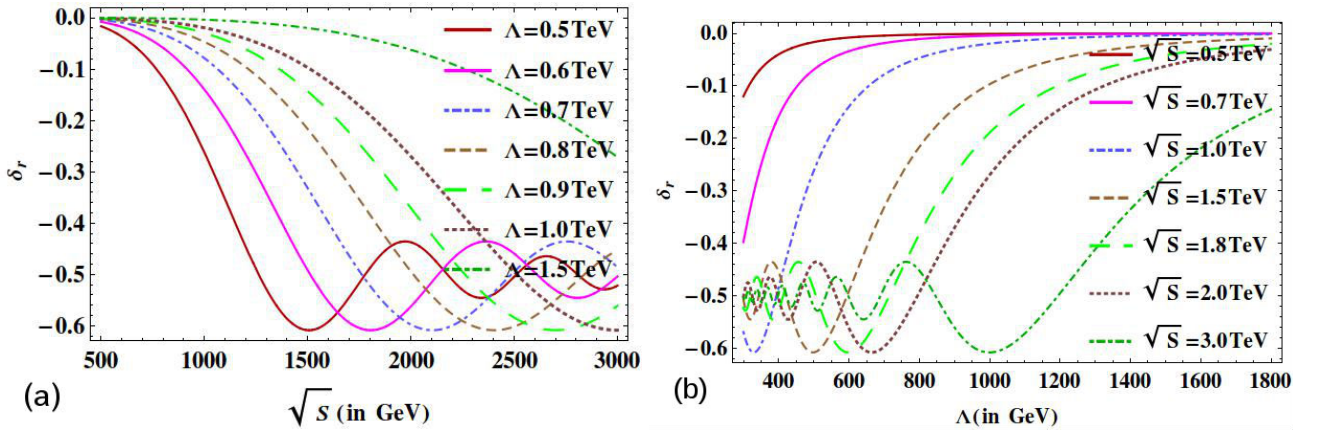
Figure 3.4: *On the left, (a) the ratio δ_r is plotted as a function of $\sqrt{s}$ (in GeV) for different Λ values. On the right, (b) δ_r is shown as a function of Λ (in TeV) for different machine energy.*

ues of Λ (left figure), whereas on the right figure, we have shown the dependence of δ_r against the NC scale Λ for few different machine energy $\sqrt{s}$. From the left figure, we see that δ_r becomes maximum at its first peak when $\sqrt{s} = 1.5, 1.8, 2.1, 2.4, 2.7$ TeV and 3.0 TeV corresponding to $\Lambda = 0.5, 0.6, 0.7, 0.8, 0.9$ TeV and 1.0 TeV. For $\Lambda = 0.5$ TeV at $\sqrt{s} = 1.5$ TeV, the deviation δ_r reaches it's minimum value -0.6085. This is called primary minimum (crest). Similarly the secondary minimum (crest) corresponds to $\delta_r = -0.5456$ and the next to it corresponds to $\delta_r = -0.435$. On the right plot, we have shown how δ_r varies with Λ as the machine energy increases from 0.5 TeV to 3 TeV. For $\Lambda \leq 1$ TeV, we see that for a wide range of machine energies, δ_r converges to -0.5. In

Table 3.1: The NC correction δ_r against the NC scale Λ (in GeV) is shown corresponding to different machine energy $\sqrt{s}$. Primary peak values and corresponding NC scales are shown in bold.

$\sqrt{s} = 500$ GeV		$\sqrt{s} = 1$ TeV		$\sqrt{s} = 1.5$ TeV		$\sqrt{s} = 3$ TeV	
Λ (GeV)	δ_r	Λ (GeV)	δ_r	Λ (GeV)	δ_r	Λ (GeV)	δ_r
100	-0.543	200	-0.515	300	-0.508	600	-0.504
158	**-0.608**	300	-0.569	450	-0.564	700	-0.485
160	-0.607	**330**	**-0.608**	**497**	**-0.608**	800	-0.452
250	-0.229	400	-0.485	600	-0.492	**999**	**-0.608**
300	-0.120	600	-0.139			1100	-0.572
600	-0.008						

Table 3.1, we have displayed the value δ_r for different Λ corresponding to different machine energies. We also listed several values of δ_r for different Λ corresponding to CLIC energy ($\sqrt{s} = 3.0$ TeV). We find that $\delta_r(= -0.608596)$ is maximum corresponding to $\Lambda \sim 1$ TeV.
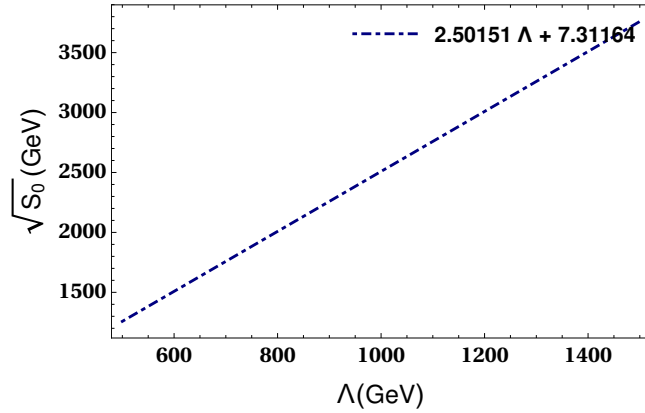
Figure 3.5: *Particle optimal collision energy vs noncommutative scale Λ*

The existing literature (Wang et. al., [257]) also has arrived the same conclusion, but we have showed that the NC correction ($\Delta\sigma$) can't be lesser than -2.7 (0 to -2.7) provided that $\Lambda \geq 600$ GeV and Higgs mass $m_H = 125$ GeV. Here $-^{ve}$ refers NC cross section is less than SM cross section. Further, $\Delta\sigma$ doesn't always increase with $\sqrt{s}$, but it appears as a Kurtosis distribution(negative) [258, 259]. The maximum value of normalized NC correction (δ_r) is $-0.608(2)$ which we get for all values of Λ but it attains a certain collision energy. It implies that there is an optimum collision energy to observe the NC effect in the Higgstralung process. In principle it could be detected when the particle

collision energy is higher than Λ. We have found that the optimal collision energy relation which is slightly differs from ref [257], because we have included the $\sqrt{s} = 3.0$ TeV mechine energy as well as mass of the Higgs boson $m_H = 125$ GeV. The relation is $\sqrt{s_0} = 7.31164 + 2.50151\Lambda$. One can arrive the conclusion from the table 3.1 to probe the reliable lower value of the Λ which are $\simeq 500$ GeV and $\simeq 1000$ GeV at $\sqrt{s} = 1.5$ TeV and $\sqrt{s} = 3.0$ TeV and the optimal collision energy is $\sqrt{s_0} = 1258.07$ GeV and $\sqrt{s_0} = 2508.82$ GeV respectively.

3.3.2 Angular distributions in absence of earth rotation

The angular distribution of the final state scattered particles is a useful tool to understand the nature of new physics. Since the noncommutativity of space-time breaks Lorentz invariance including rotational invariance around the beam axis, this will lead to an anisotropy in the azimuthal distribution of the cross-section i.e. the distribution will depends strongly on ϕ. In the standard model the azimuthal distribution for one of the final particles is found to be flat. However, in the noncommutative standard model(NCSM) due to the presence of the tensor θ-weighted dot product i.e. terms like $p_3\theta p_4 \sim \left(\frac{\sqrt{s}}{\Lambda}\right)^2 (cos\theta + sin\theta (sin\phi + cos\phi))$ (Eqn. 3.4), these distributions are no longer remain flat. We see (Eqs. 3.3, 3.4) that the squared amplitude is a oscillatory function of (θ, ϕ) and is further distorted by an oscillatory function of $(\sqrt{s}, \Lambda)$ (of the form $\sim cos\left\{\left(\frac{\sqrt{s}}{\Lambda}\right)^2 (cos\theta + sin\theta (sin\phi + cos\phi))\right\}$). In Fig. 3.6, we have shown the azimuthal ϕ distributions for different Λ values corresponding to the machine energy $\sqrt{s} = 0.5$, 1.0, 1.5 and 3.0 TeV, respectively. The distribution has several maxima(minima) located at $\phi = 2.4$, 5.4 rad (0.8, 4.0 rad). For a given machine energy (e.g. $\sqrt{s} = 1.0$ TeV), the height of the peaks decreases with the increase in Λ. We see that as the machine energy is increased to 3 TeV, the peaks corresponding to $\Lambda = 0.5$, 0.6, 0.7 TeV located at $\phi = 2.4$, 5.4 rad gets smeared, while the peaks corresponding to $\Lambda = 1.0$, 1.5 TeV still survives. The fluctuation observed at the crest and trough of the figure corresponding to machine energy $\sqrt{s} = 3$ TeV is due to the fact that $\frac{d\sigma}{d\phi}$ is a oscillatory function of ϕ and as well as the oscillatory function of $(\sqrt{s}, \Lambda)$. At higher energy $\frac{d\sigma}{d\phi}$ is dominated by $\sqrt{s}$ and Λ. Next, we define the rapidity of a particle as

$$y = \frac{1}{2}ln\left(\frac{E - P_z}{E + P_z}\right)$$

where E, the energy and P_z, the z-component momentum of the particle (Z boson or the Higgs boson H).

In Fig. 3.7, we have plotted the distribution $d\sigma/dy$ as a function of rapidity y for different cases of machine energies. In the leftmost Figure where the machine energy is fixed at $\sqrt{s} = 0.5$ TeV, we
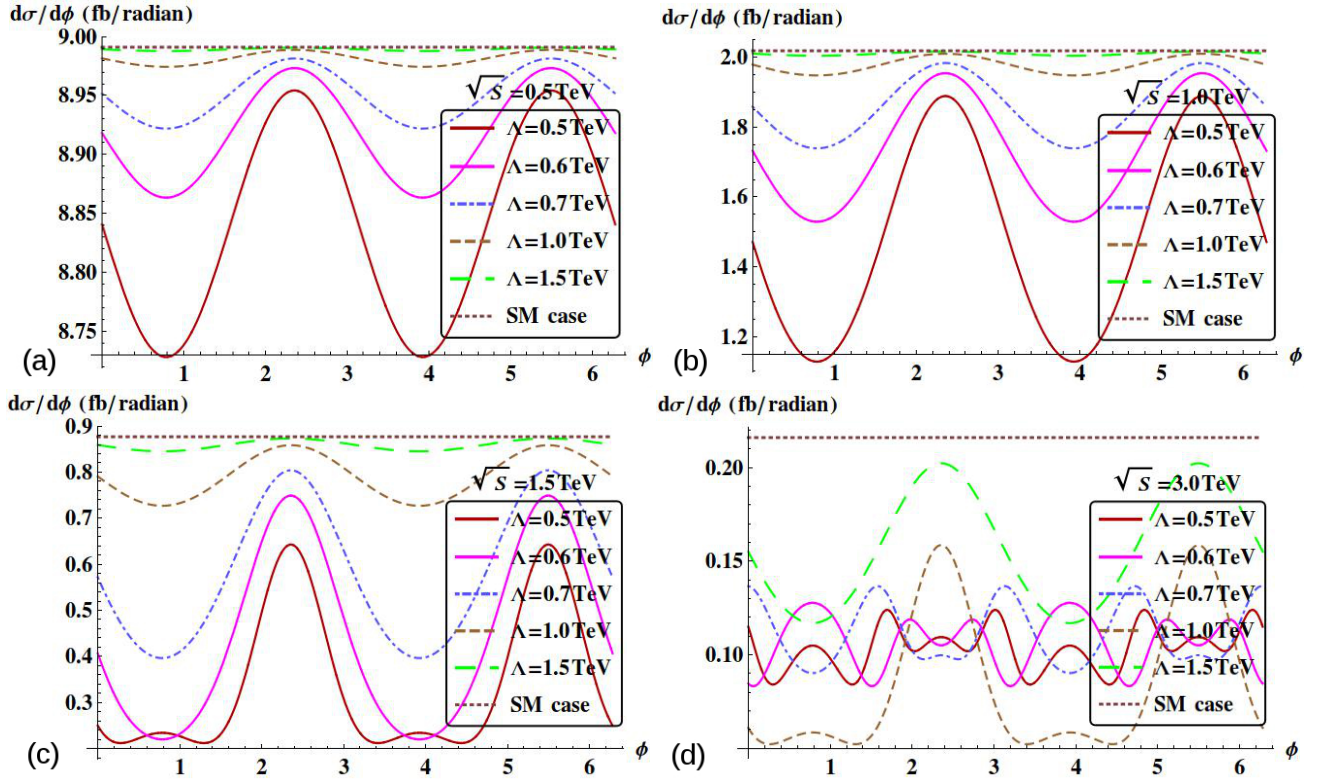
Figure 3.6: *The azimuthal distribution $\frac{d\sigma}{d\phi}$ (in fb/rad) is plotted as a function of ϕ (in rad) for different Λ values. Displayed are four plots (a), (b) and (c) corresponding to different machine energy $\sqrt{s} = 0.5, 1.0, 1.5$ and 3.0 TeV are shown.*

see that the height of the peak (located at $y = 0$) increases with the increase in Λ. The topmost curve corresponds to the SM curve ($\Lambda \to \infty$). As we move towards left (i.e. increase the machine energy from 0.5 TeV to 3.0 TeV, the height of a peak (corresponding to a particular Λ value) decreases and gets flattened. When the machine energy is equal to 3 TeV, the peak at $y = 0$ corresponding to $\Lambda = 0.6$ TeV split into two. Note that the rapidity distribution of Z boson or Higgs particle are the same.
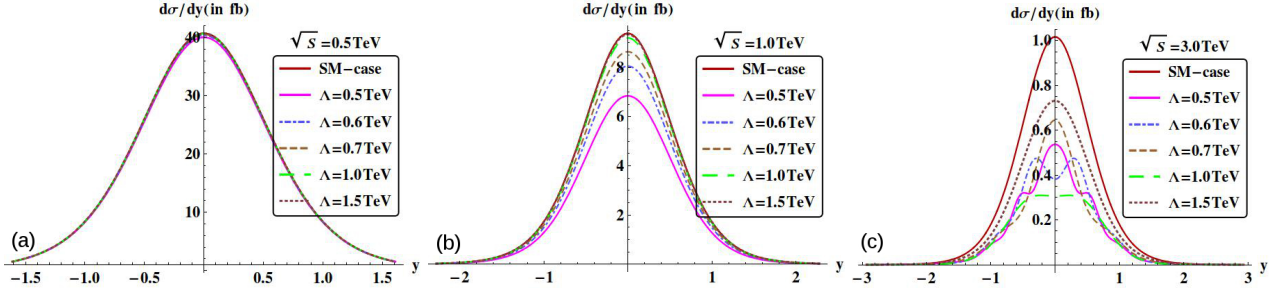
Figure 3.7: *The rapidity distribution $\frac{d\sigma}{dy}$ (in fb) is plotted as a function of the rapidity y for different Λ values. Three plots (a), (b) and (c) are shown corresponding to machine energy $\sqrt{s} = 0.5, 1.0$ and 3.0 TeV, respectively.*

3.4 Consequence of earth rotation on the cross-section and angular distributions

3.4.1 Cross-section, diurnal motion in presence of earth rotation

It was pointed out earlier that one significant aspect for noncommutative effect can be originated from directionality of fundamental NC fix points. The experiment is done in the laboratory frame attached to the earth surface which is rotating, whereas directions related to the NC parameter $\Theta_{\mu\nu}$ has a fixed direction in the celestial sphere. In sec 3.4 we described the notation to parameterize the processes in rotating frame. This rotation can have a direct but sub leading impact in daily modulation on the inherent structure of the interaction couplings. Noncommutative contributions and angular dependence due to additional tensorial were presented in Sec 3.3.1, where this effect was not considered. Now we would like to analyze the effect of earth rotation on the orientation of the NC vector $\vec{\Theta}_E$ and thus on the cross-section and angular distribution of the associated Higgs production. Since the cross-section and the angular distributions are function of time, we made a time-averaged (i.e. averaged over the side-real day T_{day}) estimate of the total cross-section, correction, azimuthal distribution and rapidity distributions to account for this additional effect coming from the new physics. The laboratory coordinate system is being set at $(\delta, a) = (\pi/4, \pi/4)$. Our choice of same lab-system enables one to directly compare the consequence due to the earth rotation. The time-averaged azimuthal distribution and the cross-section are defined as,

$$\left\langle \frac{d\sigma}{d\phi} \right\rangle_T = \frac{1}{T_{day}} \int_0^{T_{day}} \frac{d\sigma}{d\phi} dt = \frac{1}{T_{day}} \int_0^{T_{day}} \int_{-1}^{1} \frac{d\sigma}{dcos\theta \, d\phi} dcos\theta \, dt, \quad (3.10)$$

$$\langle \sigma \rangle_T = \frac{1}{T_{day}} \int_0^{T_{day}} \sigma dt = \frac{1}{T_{day}} \int_0^{T_{day}} \int_{-1}^{1} \int_0^{2\pi} \frac{d\sigma}{d\phi \, dcos\theta} dcos\theta \, d\phi \, dt, \quad (3.11)$$

where $T_{day} = 23\text{h}56\text{m}4.09053\text{s}$, the sidereal day.

In Fig. 3.8 we have shown $\langle\sigma\rangle_T$ against the machine energy $\sqrt{s}$ corresponding to $\eta = 0, \ \pi/4$ and $\pi/2$.
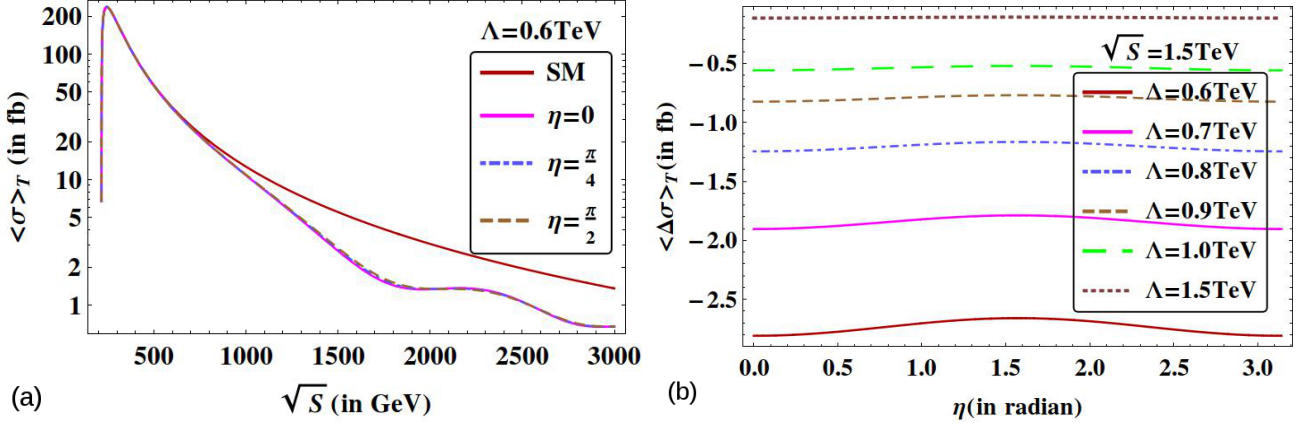
Figure 3.8: *(a) The time-averaged total cross-section $\langle\sigma\rangle_T$ (in fb) for associated production of Higgs with Z boson is shown as a function of the linear collider center of mass energy $\sqrt{s}$. The topmost curve (solid line) corresponds to the expected Standard Model production cross-section which is essentially NC cross-section at the limit $\Lambda \to \infty$. The three other plots (below the SM plot) corresponds to $\eta = 0, \ \pi/4$ and $\pi/2$ and $\Lambda = 0.6$ TeV are found to be almost overlapping. (b) The time-averaged NC correction to the cross-section $\langle\Delta\sigma\rangle_T$ (in fb) is shown as a function of orientation angle η of the NC vector for a fixed machine energy $\sqrt{s} = 1.5$ TeV. The different plots correspond to $\Lambda = 0.6, \ 0.7, \ 0.8, \ 0.9, \ 1.0$ and 1.5 TeV.*

In Fig.3.9a and Fig.3.9b, we have shown $\langle\Delta\sigma\rangle_T$ and $\langle\delta_r\rangle_T$ as a function of $\sqrt{s}$ for $\Lambda = 0.6$ TeV and $\eta = 0, \ \pi/4$ and $\pi/2$, respectively. We see that the curves corresponding to different η are almost overlapping for different machine energy values except near the region $\sqrt{s} = 1.5$ TeV. From the lowermost to the topmost curves η corresponds to $0, \ \pi/4$ and $\pi/2$, respectively. We see that for $\eta = \pi/2$, the deviation $\langle\Delta\sigma\rangle_T$ and the normalized deviation $\langle\delta_r\rangle_T = \langle\Delta\sigma\rangle_T/\langle\sigma_{SM}\rangle_T$ are minimum, yielding $\langle\sigma_{NC}\rangle_T$ is largest for $\eta = \pi/2$. We set $\eta = \pi/2$ in the rest of our analysis. Only one NC scale ($\Lambda = 0.6$ TeV) is chosen for demonstration comparing with the corresponding non-rotation plot in Fig 3.2. The plots corresponding to $\eta = 0, \ \pi$ and $\eta = \pi/2$ are seen to be nearly overlapping with a narrow effect due to different choices of η values. To demonstrate the variation due to this parameter, we next define the NC-correction to the cross-section (time-averaged) as $\langle\Delta\sigma\rangle_T = \langle\sigma_{NC}\rangle_T - \langle\sigma_{SM}\rangle_T$. In Fig. 8(b), we have plotted $\langle\Delta\sigma\rangle_T$ as a function of η corresponding to $\Lambda = 0.6, \ 0.7, \ 0.8, \ 0.9, \ 1.0$ and 1.5 TeV for a fixed machine energy $\sqrt{s} = 1.5$ TeV. The plot shows a peak at $\eta = \pi/2$ which corresponds to the fact that $\langle\sigma_{NC}\rangle_T$ is larger at that value irrespective to the Λ chosen. However this maximum deviation is quite small; around 0.1 fb corresponding to $\Lambda = 0.6$ TeV and even less for larger Λ.

As expected from these results, one finds that the variation of time-averaged quantity $\langle\Delta\sigma\rangle_T$ and
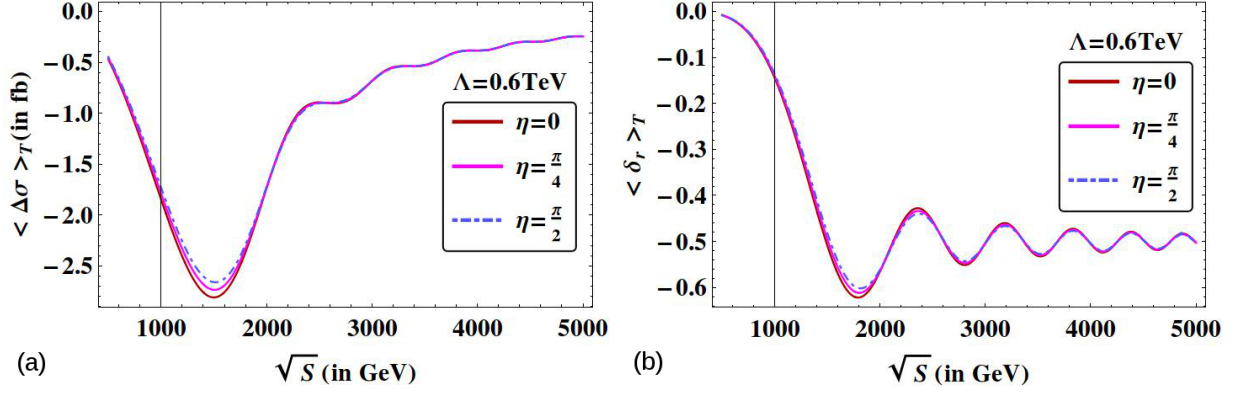
Figure 3.9: *In (a) the time-averaged NC correction to the cross-section $\langle\Delta\sigma\rangle_T$ (in fb) is shown as a function of the machine energy $\sqrt{s}$ (in GeV) for $\Lambda = 0.6$ TeV. The different plots correspond to $\eta = 0, \pi/4, \pi/2$. In (b), the normalized correction $\langle\delta_r\rangle_T$ is shown as a function of $\sqrt{s}$ for the same above set of η values.*

Table 3.2: The NC correction $\langle\delta_r\rangle_T$ against the NC scale Λ is shown corresponding to different machine energy $\sqrt{s}$ and orientation angle of the NC vector $\eta = \pi/2$. Primary peak value and the corresponding NC scales are shown in bold.

$\sqrt{s} = 500\text{GeV}$		$\sqrt{s} = 1000\text{GeV}$		$\sqrt{s} = 1500\text{GeV}$		$\sqrt{s} = 3000\text{GeV}$	
Λ GeV	$\langle\delta_r\rangle_T$	Λ GeV	$\langle\delta_r\rangle_T$	Λ GeV	$\langle\delta_r\rangle_T$	Λ GeV	$\langle\delta_r\rangle_T$
100	-0.541	200	-0.514	300	-0.508	600	-0.504
158	**-0.604**	300	-0.568	450	-0.563	700	-0.485
160	-0.603	**330**	**-0.602**	**497**	**-0.602**	800	-0.456
250	-0.226	400	-0.476	600	-0.483	**999**	**-0.602**
300	-0.118	600	-0.136			1100	-0.563
600	-0.008						

$\langle\delta_r\rangle_T$ with respect to machine energy $\sqrt{s}$ (for different Λ) or Λ (for different $\sqrt{s}$) remains very similar to the plots shown in Fig 3.3 and Fig. 3.4 in absence of the earth rotation with a subleasing shift. We skip the repetition of these plots for the brevity. Magnitude of the shifts for different parameters are better expressed in a representative table similar to the one we discussed in last section. In table 3.2, we have displayed time-averaged $\langle\delta_r\rangle_T$ for different Λ corresponding to different machine energies and $\eta = \pi/2$ after taking consideration of earth rotation effect.

Note, for example, the shift in the ratio $|\langle\delta_r\rangle_T| = 0.604$ form our non-rotating estimate of $|\langle\delta_r\rangle| = 0.608$ for values of $\Lambda = 158$ GeV and $\sqrt{s} = 500$ GeV.

Diurnal modulation in the production signal in our lab frame can also appear as a distinctive

feature of fundamental NC fixed points. This modulation would depend upon η together with the NC scale Λ and machine energy $\sqrt{s}$, although the phase of these oscillation are fixed by the choice of experiment location.
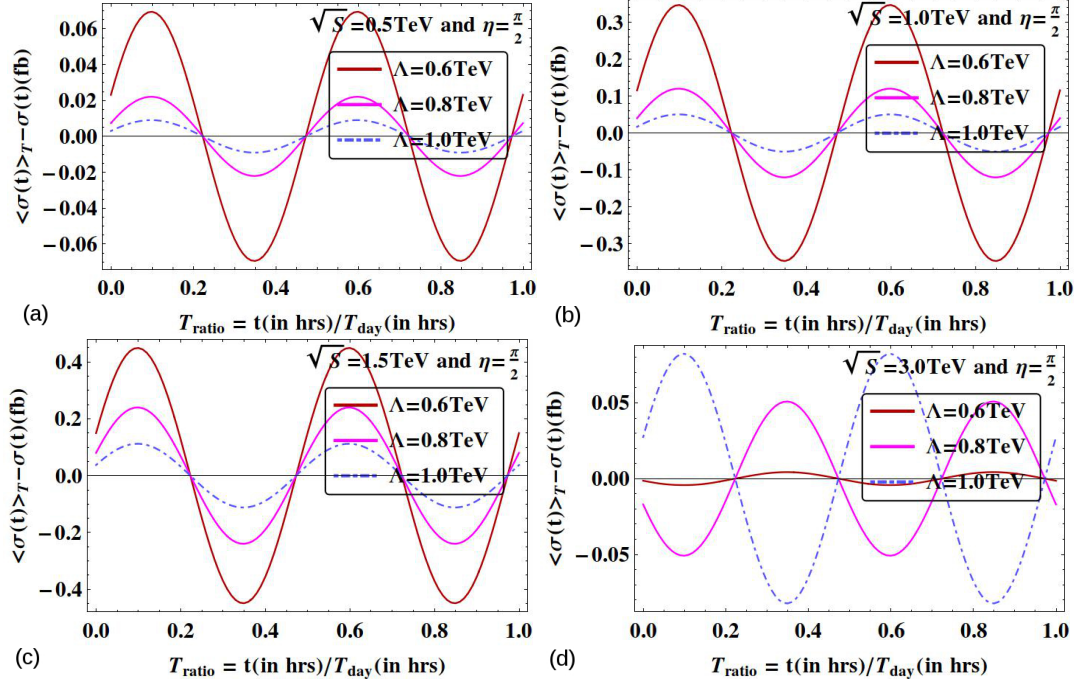
Figure 3.10: *The diurnal modulation $\Delta(t)$ in the production signal is plotted as a function of time fraction of sidereal day $T_{ratio}(= t/T_{day})$ for the machine energy $\sqrt{s} = 0.5$, 1.0, 1.5 and 3.0 TeV, respectively. The NC scale is chosen as $\Lambda = 0.6$, 0.8 and 1.0 TeV and $\eta = \pi/2$.*

To take into account this modulation, we define the quantity $\Delta(t) = \sigma(t) - \langle\sigma(t)\rangle_T$. This is the deviation of the Higgs-strahlung production cross-section $\sigma(t)$ at any time from the time-averaged cross-section $\langle\sigma(t)\rangle_T$ over the period of sidereal day, $T_{day} = 23.934$ hours. In Fig. 3.10, we have plotted $\Delta(t)$ as a function time fraction for the machine energy $\sqrt{s} = 0.5$, 1.0, 1.5 and 3.0 TeV, respectively. In each plot, the NC scale is chosen as $\Lambda = 0.6$, 0.8 and 1.0 TeV and the orientation angle $\eta = \pi/2$. From the figures corresponding to $\sqrt{s} = 0.5$, 1.0, 1.5 TeV, we see that at a given machine energy, as we increase Λ from 0.6 TeV to 1.0 TeV, the fluctuation gets diminished and eventually it becomes zero in the $\Lambda \to \infty$ limit (the SM result). The plots show peaks at $t = 0.35\ \mathrm{T_{day}}$ and $0.85\ \mathrm{T_{day}}$ times of the day, where $T_{day} = 23.934$ hours. For the machine energy $\sqrt{s} = 0.5$, 1.0, 1.5, we see that with the increase although the location of several peaks/dips remains unchanged and the fluctuation pattern remains almost same, however it's magnitude at any particular point of time in a day for a give Λ changes largely. However, for $\sqrt{s} = 3.0$ TeV, we see something different behaviour: there are dips and peaks in the plot corresponding to $\Lambda = 0.6$ TeV and 0.8 TeV at some T_{ratio}, the

same T_{ratio} corresponds to dips and peaks for the $\Lambda = 1.0$ TeV plot i.e. they are out-of-phase. Also interestingly, the height of the peak/dip decreases with the decrease in Λ, contrary to the one found in $\sqrt{s} = 0.5,\ 1.0$ and 1.5 TeV cases.

3.4.2 Angular distributions in presence of earth rotation

The anisotropy emerged from the breaking of Lorentz invariance as mentioned earlier, persists in the time-averaged (averaged over the side-real day T_d) azimuthal distribution of the cross-section $\langle \frac{d\sigma}{d\phi} \rangle_T$ can act as a signature of space-time noncommutativity which is found to be absent in many theories beyond the Standard Model physics. In Fig. 3.11, we have shown the time averaged azimuthal distri-
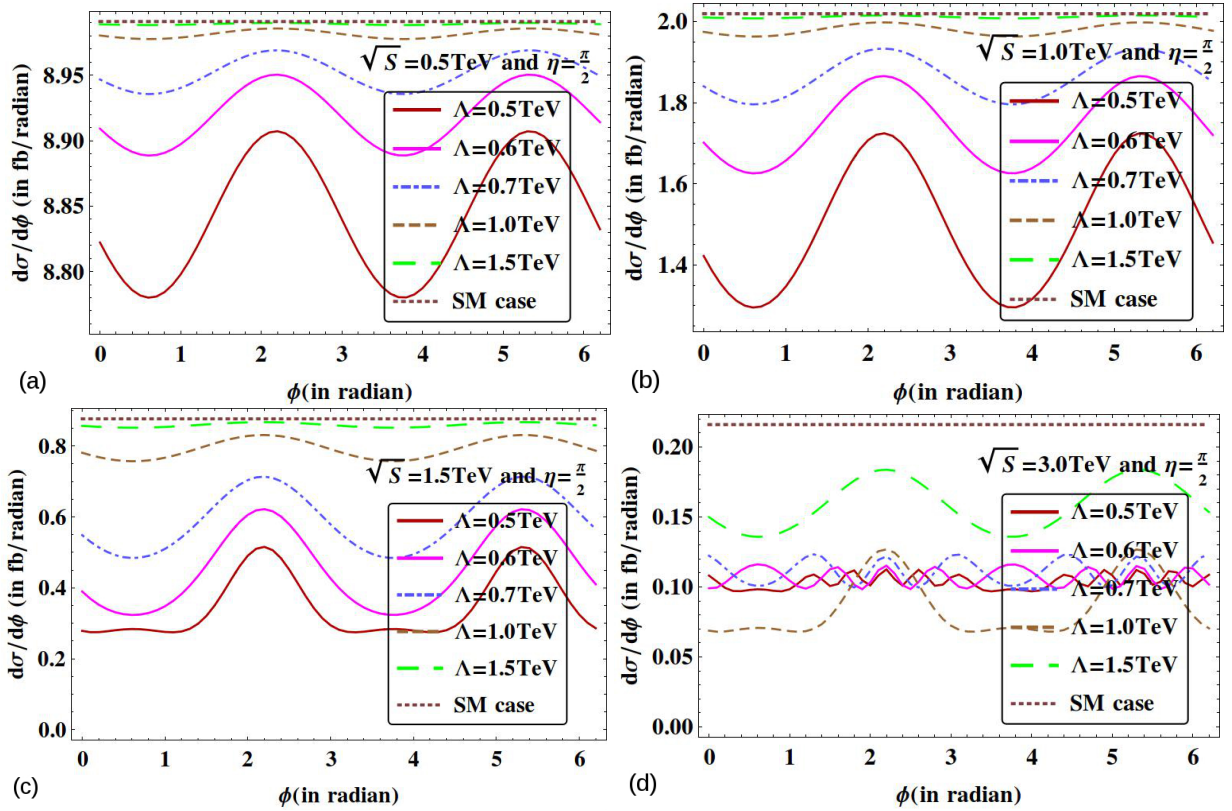
Figure 3.11: *The time-averaged azimuthal distribution of the cross-section $\langle \frac{d\sigma}{d\phi} \rangle_T$ (fb/rad) is shown as a function of the azimuthal angle ϕ (in radian) for $\eta = \pi/2$ and the machine energy $\sqrt{s} = 0.5,\ 1.0,\ 1.5$ and 3.0 TeV (which corresponds to figures a,b,c and d). The different plot in each figure correspond to $\Lambda = 0.5,\ 0.6,\ 0.7,\ 1.0$ and 1.5 TeV.*

bution of the cross-section $\langle \frac{d\sigma}{d\phi} \rangle_T$ corresponding to different values of NC scale $\Lambda = 0.5,\ 0.6,\ 0.7,\ 1.0$ and 1.5 TeV. The machine energy $\sqrt{s}$ is fixed at $0.5, 1.0, 1.5$ and 3.0 TeV, respectively. Each distribution has maxima(crest) and minima(trough) located at $\phi = 2.2,\ 5.4$ rad $(0.8,\ 3.8$ rad). At a fixed machine energy (say $\sqrt{s} = 1.0$ TeV), the height of the peaks decreases with the increase in Λ. For

$\eta = \pi/2$, as the machine energy is increased from 0.5 TeV to 3 TeV, the peaks corresponding to $\Lambda = 0.5,\ 0.6,\ 0.7$ TeV located at $\phi = 2.2,\ 5.4$ rad gets smeared, while the peaks corresponding to $\Lambda = 1.0,\ 1.5$ TeV still survives. The fluctuation observed at the crest and trough of the figure corresponding to machine energy $\sqrt{s} = 3$ TeV is due to the fact that $\langle \frac{d\sigma}{d\phi} \rangle_T$ is a oscillatory function of ϕ and as well as the oscillatory function of $(\sqrt{s}, \Lambda)$. As we see that the behaviour of $\langle \frac{d\sigma}{d\phi} \rangle_T$ at large energy $(\sqrt{s})$ is dominated by the machine energy at a given Λ. In Fig. 3.12, we have also shown the time averaged rapidity distribution $\langle \frac{d\sigma}{dy} \rangle_T$ against the rapidity y of the final state particle for different value of the machine energy and $\eta = \pi/2$. On comparing Fig. 3.12 and Fig. 3.7, we see that the behaviour of
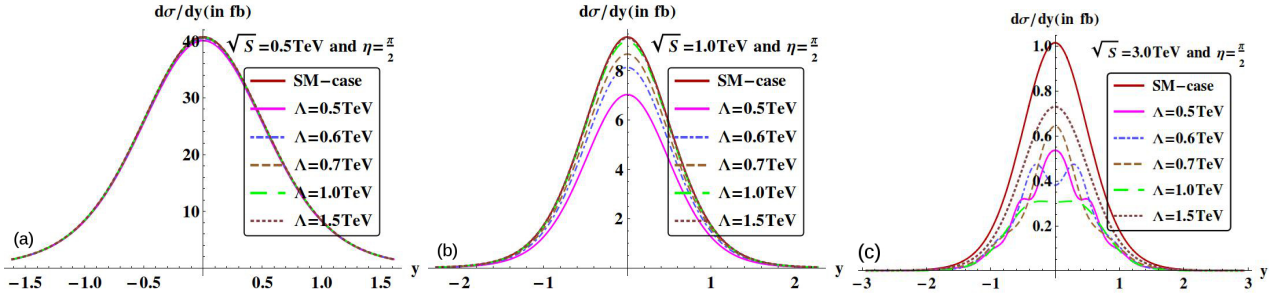
Figure 3.12: *The rapidity distribution $\langle \frac{d\sigma}{dy} \rangle_T$ (in GeV) is shown plotted as a function of the rapidity y for $\eta = \pi/2$ and the machine energy $\sqrt{s} = 0.5,\ 1.0$ and 3.0 TeV (which corresponds to figures a,b and c). The different plot in each figure correspond to $\Lambda = 0.5,\ 0.6,\ 0.7,\ 1.0$ and 1.5 TeV.*

the rapidity distributions in both cases(in the presence and absence of the effect due to earth rotation) are almost identical, although the magnitude differs from each other slightly.

3.5   Summary

In this chapter, we have investigated the associated Higgs production with Z boson at the future TeV energy linear collider. We did our calculation in the framework of the non-minimal noncommutative standard model(nmNCSM) using the Feynman rules involving all orders of the noncommutative parameters $\Theta_{\mu\nu}$ with (or without) considering the effect of earth rotation. We found that the total cross-section $\sigma(e^- e^+ \to ZH)$ departs significantly from the standard model value as the machine energy starts getting larger than 1.0 TeV with the NC contribution found to be lower than the SM one.

We have found that the optimal collision energy relation which is slightly differs from ref [257], because we have included the $\sqrt{s} = 3.0$ TeV mechine energy as well as mass of the Higgs boson $m_H = 125$ GeV. The relation is $\sqrt{s_0} = 7.31164 + 2.50151\Lambda$. One can arrive the conclusion from the table 3.1, 3.2 to probe the reliable lower value of the Λ which are $\simeq 500$ GeV and $\simeq 1000$ GeV

at $\sqrt{s} = 1.5$ TeV and $\sqrt{s} = 3.0$ TeV and the optimal collision energy is $\sqrt{s_0} = 1258.07$ GeV and $\sqrt{s_0} = 2508.82$ GeV respectively.

Considering the effect of earth rotation in our analysis, we find from $\langle \Delta \sigma \rangle_T$ vs η plot that for $\eta = \pi/2$, $\langle \Delta \sigma \rangle_T$ becomes minimum (yielding $\langle \sigma_{NC} \rangle_T$ to maximum for $\Lambda \sim 0.6$ TeV. The time-averaged NC correction $\langle \Delta \sigma \rangle_T$ and the relative correction $\langle \delta_r \rangle_T$ is found to be minimum (a trough) (yielding $\langle \sigma_{NC} \rangle_T$ to maximum) at $\sqrt{s} = 1.5$ TeV for the NC scale $\Lambda = 0.5$ TeV. The trough depth decreases with the increase in Λ and becomes zero as $\Lambda \to \infty$ (the SM value). The diurnal modulation of the NC signal is found to be quite interesting. We plot $\sigma(t) - \langle \sigma \rangle_T$ is plotted as a function of t/T_{day} and is found to have an oscillatory behaviour. At a given energy, the amplitude of oscillation gets damped with the increase in Λ and finally it becomes zero in the limit $\Lambda \to \infty$ (the SM limit). The time-averaged azimuthal distribution $\langle \frac{d\sigma}{d\phi} \rangle_T$ against ϕ for different Λ at different machine energies is found to have a oscillatory behaviour because of the additional terms $p_3 \Theta p_4 \sim \left(\frac{\sqrt{s}}{\Lambda} \right)^2 (cos\theta + sin\theta (sin\phi + cos\phi))$ which content the tensorial effect from noncommutativity. Note that the distribution is completely flat in the standard model. The distribution shows peak at certain ϕ values (similar peaks are observed in the case of no earth rotation) corresponding to different Λ at a machine energy ($\sqrt{s} = 0.5$ TeV to 3.0 TeV), which can be looked at in the linear collider experiment and thus test the idea of space-time noncommutativity in near future.

3.6   Appendix

Since the noncommutative parameter $\Theta_{\mu\nu}$ is considered as fundamental constant in nature, it's direction is fixed with respect to an inertial(non rotating) coordinate system. Now the experiment is done in the laboratory coordinate system, which (located on the earth's surface) is moving by the earth's rotation. As a result $\Theta_{\mu\nu}$ also varies with time which should be taken into account before making any phenomenological investigations.

In order to the study the earth's rotational effect into our analysis in the non-commutative space-time, we follow the notation of Kamoshita's paper [255]. Let $\hat{i}_X$, $\hat{j}_Y$ and $\hat{k}_Z$ (an orthonormal basis) form the primary(non rotating) coordinate system (X-Y-Z) and $\hat{i} - \hat{j} - \hat{k}$ form the laboratory co-ordinate system. The primary(non-rotating) bases vectors can be written as

$$\hat{i}_X = \begin{pmatrix} c_a s_\zeta + s_\delta s_a c_\zeta \\ c_\delta c_\zeta \\ s_a s_\zeta - s_\delta c_a c_\zeta \end{pmatrix}, \hat{j}_Y = \begin{pmatrix} -c_a c_\zeta + s_\delta s_a s_\zeta \\ c_\delta s_\zeta \\ -s_a c_\zeta - s_\delta c_a s_\zeta \end{pmatrix}, \hat{k}_Z = \begin{pmatrix} -c_\delta s_a \\ s_\delta \\ c_\delta c_a \end{pmatrix}.$$
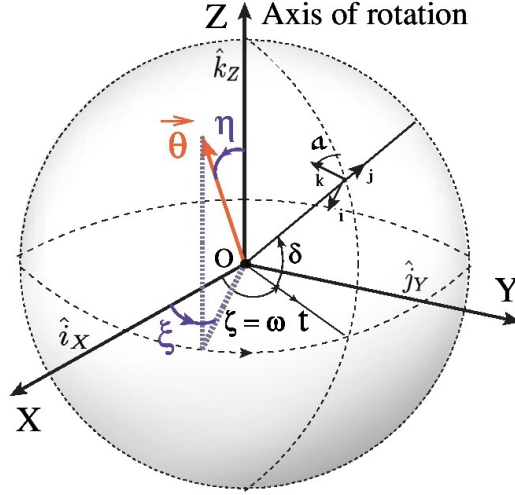
Figure 3.13: *On the left panel the primary coordinate system(X-Y-Z) is shown. The generic NC vector $\vec{\Theta}$ (electric or magnetic type) of $\Theta_{\mu\nu}$ is shown with η and ξ, respectively the polar and the azimuthal angle. On the right panel, the arrangement of laboratory coordinate system $(\hat{i} - \hat{j} - \hat{k})$ for an experiment on the earth in the primary coordinate system (X-Y-Z) is shown. In the above $\zeta = \omega t$ where ω is a constant. Also (δ, a), which defines the location of the laboratory, are constants.*

Here we have used the abbreviations $c_\beta = cos\beta$, $c_a = cosa$, $c_\delta = cos\delta$, $c_\zeta = cos\zeta$ etc. In Fig. 3.13 we have shown the primary$(X - Y - Z)$ and laboratory$(\hat{i} - \hat{j} - \hat{k})$ coordinate system. Note that the earth's axis of rotation is taken along the primary Z axis and (δ, a) defines the location of $e^- - e^+$ experiment on the earth's surface, with $-\pi/2 \le \delta \le \pi/2$ and $0 \le a \le 2\pi$. Because of earth's rotation the angle ζ (see Fig.3.13) increases with time and the detector comes to its original position after a cycle of one complete day, one can define $\zeta = \omega t$ with $\omega = 2\pi/T_{day}$ and $T_{day} = 23h56m4.09053s$. As mentioned earlier, we have taken $(\delta, a) = (\pi/4, \pi/4)$ in our case.

In the primary system, the electric and the magnetic components of the NC parameter $\Theta_{\mu\nu}$ is given by

$$\vec{\Theta}_E = \Theta_E(\sin \eta_E \ \cos \xi_E \ \hat{i}_X + \sin \eta_E \ \sin \xi_E \ \hat{j}_Y + \cos \eta_E \ \hat{k}_Z) \tag{3.12}$$

$$\vec{\Theta}_B = \Theta_B(\sin \eta_B \ \cos \xi_B \ \hat{i}_X + \sin \eta_B \ \sin \xi_B \ \hat{j}_Y + \cos \eta_B \ \hat{k}_Z) \tag{3.13}$$

In the laboratory frame a generic NC vector $\vec{\Theta}_A$ (with $A = \vec{E}, \vec{B}$)can be written as

$$\vec{\Theta}_A = \Theta_A \sin \eta_A \ \cos \xi_A \ \hat{i}_X + \Theta_A \sin \eta_A \ \sin \xi_A \ \hat{j}_Y + \Theta_A \cos \eta_A \ \hat{k}_Z$$
$$= \Theta_{Ax}^{lab}\hat{i} + \Theta_{Ay}^{lab}\hat{j} + \Theta_{Az}^{lab}\hat{k} \tag{3.14}$$

where

$$\Theta_{Ax}^{lab} = \Theta_A \left(s_{\eta_A} c_{\xi_A} (c_a s_\zeta + s_\delta s_a c_\zeta) + s_{\eta_A} s_{\xi_A} (-c_a c_\zeta + s_\delta s_a s_\zeta) - c_{\eta_A} c_\delta s_a) \right)$$

$$\Theta_{Ay}^{lab} = \Theta_A \left(s_{\eta_A} c_{\xi_A} c_\delta c_\zeta + s_{\eta_A} s_{\xi_A} c_\delta s_\zeta + c_{\eta_A} s_\delta \right)$$

$$\Theta_{Az}^{lab} = \Theta_A \left(s_{\eta_A} c_{\xi_A} (s_a s_\zeta - s_\delta c_a c_\zeta) - s_{\eta_A} s_{\xi_A} (s_a c_\zeta + s_\delta c_a s_\zeta) + c_{\eta_A} c_\delta c_a) \right) \tag{3.15}$$

with $\vec{\Theta}_E = (\Theta^{01}, \Theta^{02}, \Theta^{03})$, $\vec{\Theta}_B = (\Theta^{23}, \Theta^{31}, \Theta^{12})$ and $\Theta_E = |\vec{\Theta}_E| = 1/\Lambda_E^2$, $\Theta_B = |\vec{\Theta}_B| = 1/\Lambda_B^2$. Here (η, ξ) specifies the direction of the NC parameter $\Theta_{\mu\nu}$ w.r.t the primary coordinate system with $0 \leq \eta \leq \pi$ and $0 \leq \xi \leq 2\pi$. In above Θ_E and Θ_B corresponds to the energy scale are defined by $\Lambda_E = 1/\sqrt{\Theta_E}$ and $\Lambda_B = 1/\sqrt{\Theta_B}$, the two model parameters, which one can probe for different processes.

Since it is difficult to get the time dependent data, we take the average of the cross section or it's distributions over the sidereal day T_{day} and compare that with the experimental data. Next we introduce several time averaged observables as follows:

$$\left\langle \frac{d^2\sigma}{d\cos\theta \, d\phi} \right\rangle_T = \frac{1}{T_{day}} \int_0^{T_{day}} \frac{d\sigma}{d\cos\theta \, d\phi} dt, \tag{3.16}$$

$$\left\langle \frac{d\sigma}{d\cos\theta} \right\rangle_T = \frac{1}{T_{day}} \int_0^{T_{day}} \frac{d\sigma}{d\cos\theta} dt, \tag{3.17}$$

$$\left\langle \frac{d\sigma}{d\phi} \right\rangle_T = \frac{1}{T_{day}} \int_0^{T_{day}} \frac{d\sigma}{d\phi} dt, \tag{3.18}$$

$$\langle \sigma \rangle_T = \frac{1}{T_{day}} \int_0^{T_{day}} \sigma dt, \tag{3.19}$$

where $\sigma = \sigma(\sqrt{s}, \Lambda, \theta, \phi, t)$ and where $T_{day} = 23\text{h}56\text{m}4.09053\text{s}$, the sidereal day. The time dependence in the cross section or it's distribution enters through the NC parameter $\vec{\Theta}(= \vec{\Theta}_E)$ which changes with the change in $\zeta = \omega t$. The angle ξ appears in $\vec{\Theta}$ through the functions $\cos(\omega t - \xi)$ or $\sin(\omega t - \xi)$ as the initial phase for time evolution, which gets disappeared in the time averaged observables. So one can deduce $\vec{\Theta}_E$ i.e. Λ_E and the angle η_E from the time-averaged observables.

Chapter 4

Drell-Yan production in the noncommutative standard model

"An equation means nothing to me unless it expresses a thought of God" - Srinivasa Ramanujan

4.1 Introduction

With the upgradation of LHC energy (i.e. from 7 TeV to 14 TeV), we have entered a new era of high-energy physics that directly probes Nature at the TeV scale. The strong belief that the SM (which has its own limitation in explaining problems like Higgs mass instability, neutrino mass, baryon asymmetry problem, dark matter etc) is only a low energy effective theory, and there is some physics beyond the standard model(BSM physics) i.e. New Physics has been gaining ground over a couple of years. Depending on the underlying theory, the resonance production of new particles or some kind of angular distribution may lead to novel and distinctive signatures at the TeV energy collider. Looking for signature of new physics through the resonance production of new particle or modification specific angular distribution in the classic Drell-Yan process may give a striking signal at around the TeV scale.

There are several new physics models explored in this area particularly Drell-Yan lepton pair production at LHC. Here I have given few of them which are ADD, RS TeV scale gravity [265–268], spin-2 with non-universal couplings [269] and slepton pair production from neutral current [270]. In the TeV scale gravity models, the contribution of the KK graviton is large compare to the SM, because the gloun gloun mediated sub process dominates over rest of the SM processes. QCD has important role at higher order corrections in the SM (studied upto N^3LO ref [271, 272]) as well as TeV gravity models(studied upto NLO+NLL and NNLO ref [265–268]). In our analysis we haven't consider either

NLO nor NNLO calculation because which are not yet understood properly in the noncommutative theory.

4.2 Methodology

In this chapter, we discuss the Drell-Yan process $p\,p \to l^+\,l^- + X$ (with $l = e\,\mu$) at LHC, mediated by two partonic (quarks, gluons) sub-processes in the NCSM up to $\mathcal{O}(\Theta)$. To make an estimate of the hadronic cross-section $\sigma(p_1, p_2)$ of the Drell-Yan process which is the convolution of the partonic sub-process cross sections $\hat{\sigma}_{ab}(p_1, p_2)$ with the Parton Distributions Functions (PDF) f_a $(a = u, d, ..\overline{u}, ...)$, we work in the QCD Parton Model and its powerful tool, the QCD factorization theorem. One can write the the Drell-Yan cross section as

$$\sigma_{pp\to l^+l^-}(P_1, P_2) = \sum_{ab} \int dx_1 \int dx_2 \, f_a(x_1, \mu^2) f_b(x_2, \mu^2) \, \hat{\sigma}_{ab\to l^+l^-}(p_1, p_2, \alpha_S(\mu^2)). \qquad (4.1)$$

where $p_1 = x_1 P_1$ and $p_2 = x_2 P_2$ are the momenta carried by the two partons. x_1, x_2 are the momentum fractions and P_1 and P_2 are the proton momenta. The PDFs which can be determined experimentally, are universal. They are defined at the factorization scale μ. In this work, we use the CTEQ6L1 parton distribution function in our analysis. In general the factorization scale μ is taken to be equal to the hard
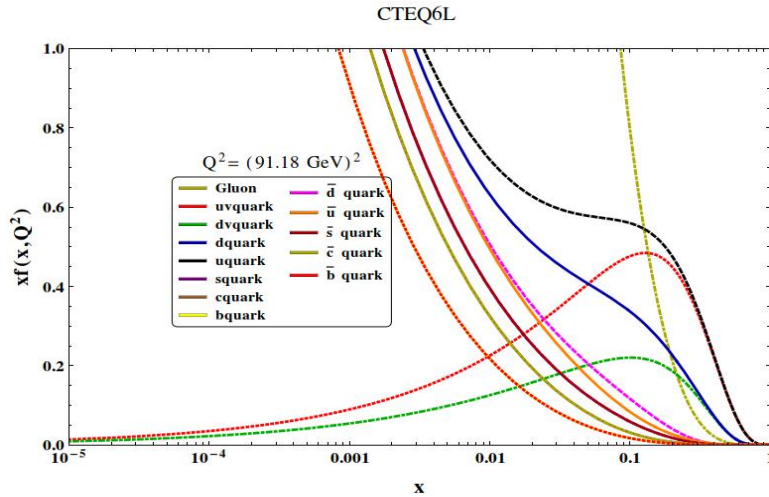
Figure 4.1: Parton distribution function CTEQ6L(Leading Order)

scale Q^2 at which the partonic scattering takes place. We calculate the partonic cross section within the framework of the NCSM discussed in chapter 2 and will convolute the result with the PDF mentioned above. In fact, one need to consider the effect of spacetime noncommutativity in PDF also in order to make the entire analysis consistent. However, the use of usual PDF in the SM is justified, because of

the fact that the energy scale at which the physics in the proton takes place is much lower than the scale of the partonic hard scattering processes. The factorization theorem which separates the hard scattering cross section from the low energy process absorbed in the PDF, ensures this. Hence, in our estimation of the noncommutative scale Λ, the noncom- mutative effects are important for the hard processes and no so important for the physics beyond the partonic scattering process we are interested in.

Now, besides the standard quark-initiated partonic subprocess $q\bar{q} \to \gamma, Z \to l^+l^-$, an additional the gluon-initiated partonic subprocesses $gg \to \gamma, Z \to l^+l^-$ can also contribute to the Drell-Yan production cross section. The Representative Feynman diagrams for these partonic subprocess are shown in Fig. 4.2. For the quark mediated process, the Feynman rules for the vertices $f\bar{f}\gamma$ and $f\bar{f}Z$
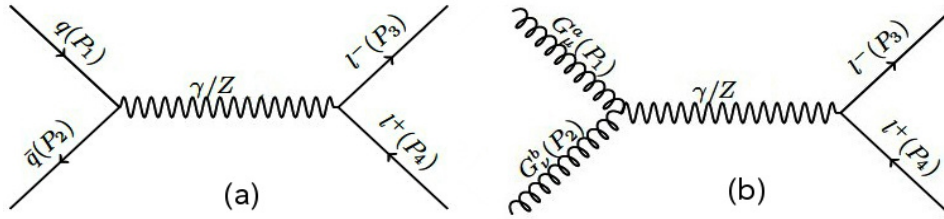
Figure 4.2: Representative Feynman diagrams for the partonic subprocess for quark initiated (a) $q\bar{q} \to \gamma, Z \to l^+l^-$, and gluon initiated (b) $gg \to \gamma, Z \to l^+l^-$. Both of them contributes in Drell-Yan type lepton pair production at the hadron collider considering noncommutative standard model.

(where $f = q, l$) are shown in Appendix 4.5.1. Note that the vertices, besides the SM part, also contain an extra $\mathcal{O}(\Lambda)$-dependent term for which, at the limit $\Lambda \to \infty$, the original SM vertices get recovered. The second gluon mediated partonic-process comprises two new vertices γgg and Zgg, which are not present in the SM and are depicted in Fig. 4.3. Corresponding leading-order Feynman rules in these
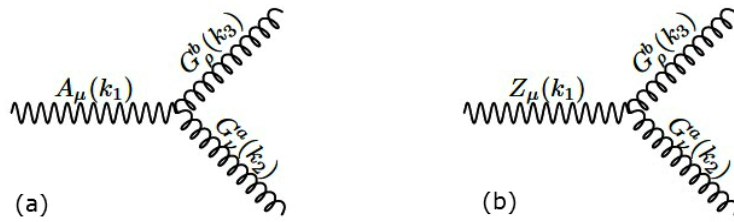
Figure 4.3: Feynman diagrams for additional vertices in the noncommutative standard model which can contribute in Drell-Yan production process at the LHC.

figures are given by,

$$\gamma gg : (-2e)\sin(2\theta_w)K_{\gamma gg}\,\theta_3^{\mu\nu\rho}(k_1, k_2, k_3)\,\delta^{ab} \tag{4.2}$$

$$Zgg : (-2e)\sin(2\theta_w)K_{Zgg}\,\theta_3^{\mu\nu\rho}(k_1, k_2, k_3)\,\delta^{ab}. \tag{4.3}$$

Here, θ_W is the Weinberg angle and the vertex factors $K_{\gamma gg}$ and K_{Zgg} are given by [1].

$$K_{\gamma gg} = \frac{-g_s^2}{2gg'}\left(g'^2 + g^2\right)\zeta_3 , \quad K_{Zgg} = \left(-\tan\theta_w\right)K_{\gamma gg},$$

where g_s, g, g' are being the $SU(3)_C$, $SU(2)_L$ and $U(1)_Y$ coupling strengths, respectively. The tensorial quantity[2] $\theta_3 \equiv \theta_3^{\mu\nu\rho}(k_1, k_2, k_3)$ and the parameter ζ_3 are defined in Appendix 4.5.1.

Note that the triple gauge boson vertices K_{Zgg} and $K_{\gamma gg}$, absent in the standard model (once again, one gets a vanishing θ_3 at the limit $\Lambda \to \infty$), arise in this nonminimal version of NCSM. A direct test of these vertices have been performed [134] by studying the SM forbidden decays $Z \to \gamma\gamma$ and $Z \to gg$. Analyzing the 3-dimensional simplex that bounds possible values for the coupling constants $K_{\gamma\gamma\gamma}$, $K_{Z\gamma\gamma}$ and K_{Zgg} at the M_Z scale, allowed region for our necessary couplings $(K_{Zgg}, K_{Z\gamma\gamma})$ are obtained as ranging between $(-0.108, -0.340)$ and $(0.217, -0.254)$.

4.3 Result and Discussion

To estimate the noncommutative effects in our parton-level calculation, we analytically formulate both subprocesses initiated either by a quark-antiquark pair or by a gluon pair at the leading order. Using the Feynman rules to $\mathcal{O}(\Theta)$ as described above and in Appendix 4.5.1, the squared amplitude (spin-averaged) can be expressed as

$$\overline{|M^2_{NCSM}|}_{ab \to l^+ l^-} = \overline{|\mathcal{M}_\gamma + \mathcal{M}_Z|^2} \quad \text{for, } a, b = q, \bar{q} \text{ or } g, g. \tag{4.4}$$

Detailed analytic expression for each nmNCSM amplitude-square is presented in Appendix 4.5.2. The NC antisymmetric tensor $\Theta_{\mu\nu}$, analogous to the electromagnetic field(photon) strength tensor, has six independent components: three are of the electric type, while three are of the magnetic type. We have chosen $E_i = \frac{1}{\sqrt{3}}$ and $B_i = \frac{1}{\sqrt{3}}$ in our analysis (for more, see Appendix 4.5.3). We have not considered here the effect of the Earth's rotation. Note that in the DY lepton distribution, besides the Lorentz invariant momentum dot product (e.g. $p_1.p_2$ etc), the Θ-weighted dot product (e.g. $p_3\Theta p_4$ as one follows from Appendix 4.5.3) also appears. These terms give rise to nontrivial azimuthal distribution in the Drell-Yan lepton pair production as discussed at the end of our results.

---

[1]Note that, in principle, K_{Zgg} (and $K_{\gamma gg}$) can be zero, in combination with two other couplings, $K_{\gamma\gamma\gamma}$ and $K_{Z\gamma\gamma}$. But all three cannot be zero [134] simultaneously and these other two couplings can be tested at the linear collider with a high degree of precision

[2]We follow the couplings in similar notation as in [134]
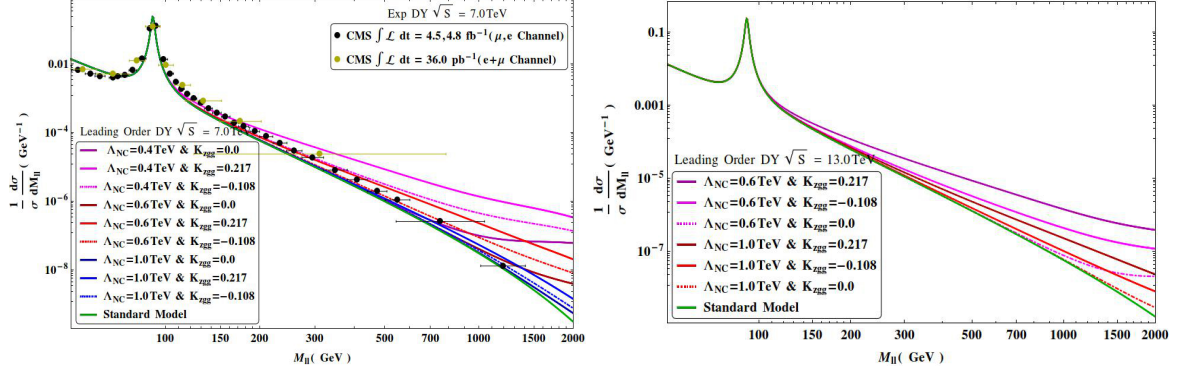
Figure 4.4: Normalized invariant mass distribution $\frac{1}{\sigma}\frac{d\sigma}{dM_{ll}}$ (GeV^{-1}) as a function of the invariant mass M_{ll} (GeV) is shown corresponding to the machine energy (left plot)$\sqrt{s} = 7$ TeV and (right plot) 13 TeV, respectively. Continuous curves of different colors in both plots are shown for the choice of Λ and K_{Zgg} and they converge to the lowermost SM curve in the limit both of these parameters go to zero. In 7 TeV plot, experimental bin-wise data are also shown with central values and error bars.

We estimate the parton-level total cross section and differential distributions for the LHC operated at the energy $\sqrt{S}$,

$$d\sigma_{pp\rightarrow l^+l^-} = \sum_{ab} \int dx_1 \int dx_2\, f_a(x_1, \mu_f^2) f_b(x_2, \mu_f^2)\, d\hat{\sigma}_{ab\rightarrow l^+l^-}(x_1 x_2 S). \tag{4.5}$$

We employ the CTEQ6L1 parton distribution function (PDF) throughout the analysis, setting the factorization scale μ_f at the dilepton invariant mass M_{ll}. After formulating the setup, we are now in a position to describe the numerical results for the Drell-Yan lepton pair production in the presence of spacetime noncommutativity. In Fig. 4.4 we have shown the normalized dilepton invariant mass distribution $\frac{1}{\sigma}\frac{d\sigma}{dM_{ll}}$ (GeV^{-1}) against the invariant mass M_{ll} (GeV) corresponding to the LHC machine energy $\sqrt{s}$ at (left plot) 7 TeV and (right plot) 13 TeV.

The peak at $M_{ll} = 91.18$ GeV corresponds to the Z boson resonance production. Different continuous curves in both plots correspond to the theoretical (SM and nmNCSM) predictions. Note that the additional positive contributions in nmNCSM curves are realized from two sources: the first being the Θ-dependent NC parts supplemented with the SM vertex, and the second being the complete new tree-level process that enhances significantly.

In the 7 TeV (left) plot the dotted curves correspond to the experimental bin wise data provided by the CMS collaboration [263] for the integrated luminosity 4.5 fb^{-1} and 35.9 pb^{-1} which is presented along with the error bar.

The lowermost curve in each plot (see Fig. 4.4) is the SM contribution estimated at the leading order. In this figure, we present different NC contributions based on the two relevant parameters Λ and
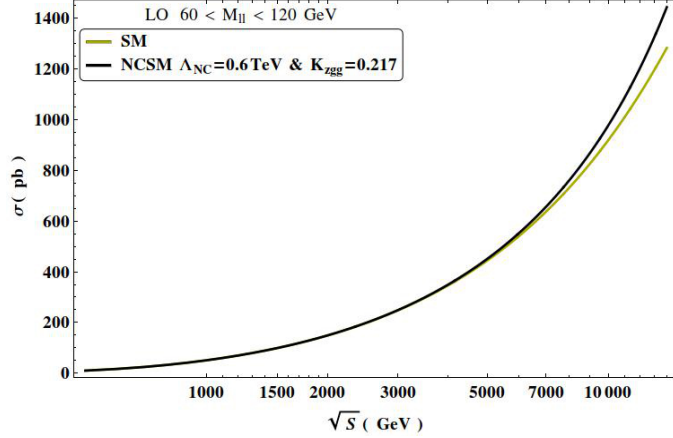
Figure 4.5: The Drell-Yan cross section is shown as a function of the LHC machine energy. In the NCSM, we demonstrate with one of the very optimistic choice like, $\Lambda = 0.6$ TeV and $K_{Zgg} = 0.217$.

K_{Zgg} varying between $(0.4\text{ TeV} - 1\text{ TeV})$ and (-0.108, +0.217), respectively. Justification for these choices has been discussed. Since the parameter K_{Zgg} contributes in square from the gluon-initiated diagram, sign of this parameter is irrelevant. So, both sign contribute positively and the magnitude depending upon the absolute values. Note that $K_{Zgg} = 0$ corresponds to the vanishing coupling of the gluon with Z boson and photon, and the Drell-Yan process in the NCSM arises only from the quark-mediated partonic subprocess $q\bar{q} \to \gamma, Z \to l^+ l^-$ as in Fig. 1(a). The NC scale Λ determines the energy when this BSM effects can be perceived and this phenomena is evident following different scales in the figure. At around a few hundred of dilepton invariant mass, Fig. 4.4 exhibits, especially at the low Λ and larger absolute value of K_{Zgg}, the NCSM effect in this distribution deviating from the SM distribution and it increases with M_{ll}.

In Fig. 4.5, we have plotted the total leading-order Drell-Yan cross section σ (in pb) against the LHC collision energy $\sqrt{s}$. The lower curve corresponds to the SM cross section. We find $\sigma = 635(1283)$ pb at $\sqrt{s} = 7(14)$ TeV, respectively. To estimate the total cross section, we have considered the dilepton invariant mass interval $60\text{ GeV} < M_{ll} < 120\text{ GeV}$. To visualize the effect we once again consider a very optimistic values of $\Lambda = 0.6$ TeV and $K_{Zgg} = 0.217$ for the upper curve corresponds to the NCSM cross section. For reference we present the corresponding Drell-Yan cross sections for different machine energy in Table 4.1. For different machine energy between 7 TeV and 14 TeV, the leading order SM and the nmNCSM (for the same reference parameters) cross sections increases from 636 (656)pb to 1283 (1438)pb.

In Fig. 4.6, the nmNCSM Drell-Yan cross section is shown as a function of the NC scale Λ at a fixed machine energy $\sqrt{s} = 7.0$ TeV. Once again dominant production cross section is estimated

$\sqrt{S}$ TeV	$\sigma_{SM}(pb)$ LO, $\mu_f = M_z$	$\sigma_{nmNCSM}(pb)$ LO, $\mu_f = M_z$	$\sigma_{EXP}(pb)$
7.0	636	656	974 ±0.7 (Stat) ±0.7 (Syst)
8.0	731	760	1138 ±8 (Stat)
13.0	1193	1325	
14.0	1283	1438	

Table 4.1: Drell-Yan cross section in the SM, nmNCSM are shown for 60 GeV $<$ M$_{ll}$ $<$ 120 GeV. The experimental data for the same dilepton invariant mass interval are shown. Here we have set the parameters $\Lambda = 0.6$ TeV and $K_{Zgg} = 0.217$ which is optimistic [264].
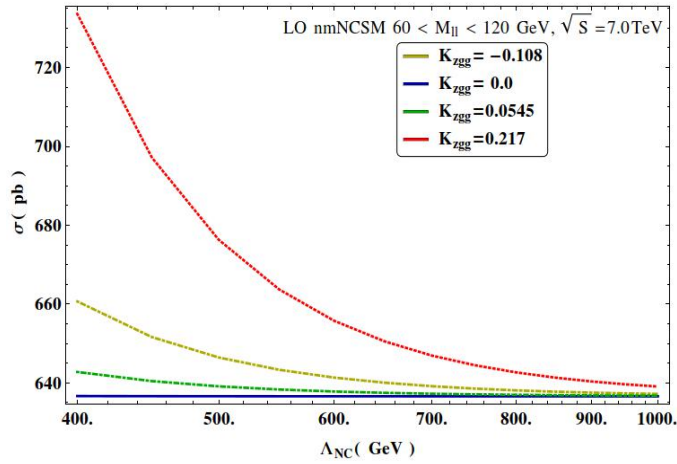
Figure 4.6: The total cross section for $pp \rightarrow (\gamma, Z) \rightarrow l^+l^-$ σ is plotted as a function of the NC scale Λ (GeV) corresponding to $Z = -0.108$, 0.054 and 0.217 and fixed machine energy $\sqrt{s} = 7.0$ TeV.

for the range of invariant mass 60 GeV $<$ M$_{ll}$ $<$ 120 GeV corresponding to different values of the parameter $K_{Zgg} = -0.108$, 0.0, 0.0545 and 0.217. As expected, for a fixed K_{Zgg} coupling the cross section σ decreases as the NC scale Λ increases and finally merges to the SM value at the very high value of Λ. Note that the NCSM contribution to DY process for $K_{Zgg} = 0$ almost equal to the SM value as it receives very small contribution from the quark mediated partonic process and the dominant gluon mediated subprocess is absent due to $K_{Zgg} = 0$ (and $K_{\gamma gg} = 0$). That causes this curve as the lowest (almost) horizontal curve, which is hence independent of the Λ scale. In Table 4.2 we present the leading order cross sections estimated for different $\Lambda = 0.4$, 0.6 and 1.0 TeV corresponding to $K_{Zgg} = 0$, -0.108 and 0.217.

After exploring the additional NC contributions coming towards the Drell-Yan production and

Λ (TeV)	K_{Zgg}	σ_{NCSM} (pb)	Λ (TeV)	K_{Zgg}	σ_{NCSM} (pb)	Λ (TeV)	K_{Zgg}	σ_{NCSM} (pb)
0.4	0.0	637	0.6	0.0	637	1.0	0.0	637
0.4	-0.108	661	0.6	-0.108	641	1.0	-0.108	637
0.4	0.217	734	0.6	0.217	656	1.0	0.217	639

Table 4.2: Drell-Yan cross section $\sigma(pp \rightarrow l^+l^-)$ in nmNCSM scenario for the fixed machine energy $\sqrt{s} = 7.0$ TeV. For $K_{Zgg} = 0$, the partonic subprocess $gg \rightarrow \gamma, Z \rightarrow l^+l^-$ is absent [264].

how different NC parameters can affect such processes, now we would like to point out some of the very characteristic distributions attributed to noncommutativity. Since spacetime noncommutativity essentially breaks the Lorentz invariance, which includes the rotational invariance around beam direction, it can contribute to an anisotropic azimuthal distribution. Angular distributions of the final lepton can thus carry this signature on noncommutativity. Similar feature is noted in many different process earlier related with the NC phenomenology, nevertheless we would like to present this distribution in our context. We show the azimuthal angular distribution for the final lepton in Fig. 4.7. On the left plot this distribution of the azimuthal angle is shown for Drell-Yan events if the noncommutative effect is there. While the anisotropic effect is not much visible here under the considerably large cross section, it would be evident in the right plot where normalized distribution is demonstrated for that same azimuthal angle. This figure is generated corresponding to different scales $\Lambda = 0.6$ TeV and 1 TeV. Also, for each Λ, we have selected $K_{Zgg} = -0.108$ and 0.217, respectively.

From the Fig. 4.7 right plot, we see that the azimuthal distribution of leptons oscillates over ϕ, reaching at their maxima at $\phi = 2.342$ rad and 5.489 rad. The two intermediate minima are located at $\phi = 0.783$ rad and 3.931 rad. Also note that the azimuthal distribution $\frac{d\sigma}{d\phi}$ is completely flat in the SM. A departure from the flat behavior in the NCSM is due to the term $p_4 \Theta p_3 (\sim cos\theta + sin\theta(cos\phi + sin\phi))$ term in the azimuthal distribution which brings ϕ dependence. There still be this feature of azimuthal distribution, even if one deviate from taking the simple form of $\Theta_{\mu\nu}$, however the location of peak positions shift. Such an azimuthal distribution irrespective of peak positions clearly reflects the exclusive nature of spacetime noncommutativity which is rarely to be found in other classes of new physics models and can be tested at LHC.
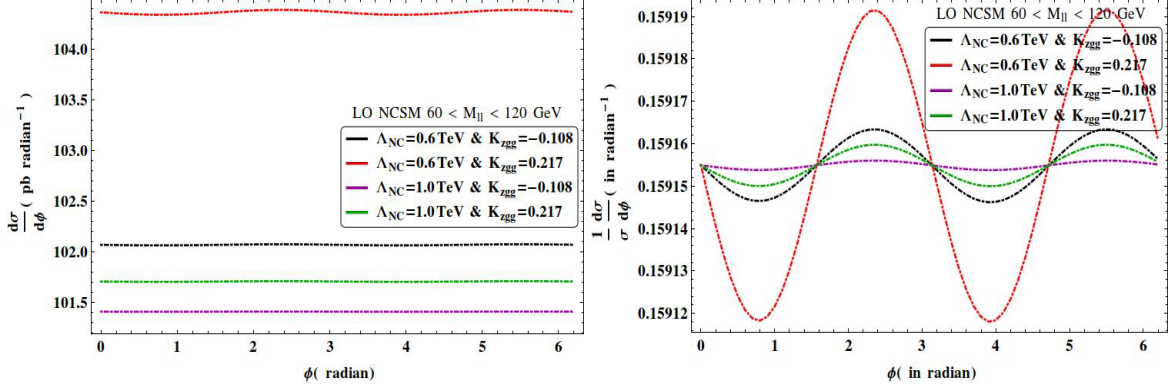
Figure 4.7: $\frac{d\sigma}{d\phi}$ as a function of ϕ for $pp \to (\gamma, Z) \to l^+l^-$ ($l = e, \mu$) for $\Lambda = 0.6$ TeV, 1.0 TeV and $K_{Zgg} = -0.108$ and 0.217, respectively.

4.4 Summary

The idea that spacetime can become noncommutative at high energy has drawn attention following the recent advance in string theory. In this chapter we have explored the NC effect in the Drell-Yan lepton pair production $pp \to (\gamma, Z) \to l^+l^-$ at the Large Hadron Collider. Two new vertices, Zgg and γgg, (absent in the SM) are being found to play a crucial role, giving rise to a new partonic subprocess $gg \xrightarrow{\gamma, Z} l^+l^-$ (absent in the SM). For $\sqrt{s} = 7$ TeV, as the coupling parameter K_{Zgg} (corresponding to the new verices Zgg) changes from -0.108 to 0.217, the cross section σ increases from $637(660)$ pb to $639(734)$ pb corresponding to $\Lambda = 1(0.4)$ TeV. The azimuthal distribution $\frac{d\sigma}{d\phi}$, completely ϕ independent in the SM, deviates substantially in the NCSM. Thus the noncommutative geometry is quite rich in terms of its phenomenological implications, which are worthwhile to explore in the TeV scale Large Hadron Collider.

4.5 Appendix

4.5.1 Feynman rules

The fermion f (quark q and lepton l) coupling to photon and Z bosons, to order $\mathcal{O}(\Theta)$, is given by

$$\gamma f\bar{f} : ieQ_f \left\{ \gamma_\mu + \left[\frac{i}{2} + \left(\frac{P_o\Theta P_i}{8} \right) \right] \left[(P_o\Theta)_\mu (\Delta \not{P}_i) + (\Theta P_i)_\mu (\Delta \not{P}_o) - (P_o\Theta P_i)\gamma_\mu \right] \right\} \quad (4.6)$$

$$Zf\bar{f} : \frac{ieQ_f}{sin(2\theta_W)} \left\{ \gamma_\mu \Gamma_A^-(f) + \left[\frac{i}{2} + \left(\frac{P_o\Theta P_i}{8} \right) \right] \right.$$
$$\left. \left[(P_o\Theta)_\mu (\Delta \not{P}_i)\Gamma_A^-(f) + (\Theta P_i)_\mu (\Delta \not{P}_o)\Gamma_A^-(f) - (P_o\Theta P_i)\gamma_\mu \Gamma_A^-(f) \right] \right\} \quad (4.7)$$

Here we follow the following notation: i: in, o: out and $\Delta \not{P}_{in,out} = \not{P}_{in,out} - m$. Also $\Gamma_A^-(f) = c_V^f - c_A^f \gamma^5$; $\quad c_V^f = I_3^f - 2Q_f \sin^2(\theta_W)$; $\quad c_A^f = I_3^f$. Q_f is the e.m. charge, and I_3^f is the third component of the week isospin of the fermion f (quark(q) or lepton(l)).

The factors θ_3 and ζ_3 arise in $\gamma - g - g$ and $Z - g - g$ and are given by [71, 134],

$$
\begin{aligned}
\theta_3^{\mu\nu\rho}(k_1, k_2, k_3) &= \theta_3[(\mu, k_1), (\nu, k_2), (\rho, k_3)] \\
&= -(k_1 \Theta k_2)[(k_1 - k_2)^\rho \eta^{\mu\nu} + (k_2 - k_3)^\mu \eta^{\nu\rho} + (k_3 - k_1)^\nu \eta^{\rho\mu}] \\
&\quad - \Theta^{\mu\nu}[k_1^\rho(k_2 \cdot k_3) - k_2^\rho(k_1 \cdot k_3)] - \Theta^{\nu\rho}[k_2^\mu(k_3 \cdot k_1) - k_3^\mu(k_2 \cdot k_1)] \\
&\quad - \Theta^{\rho\mu}[k_3^\nu(k_1 \cdot k_2) - k_1^\nu(k_3 \cdot k_2)] + (\Theta k_2)^\mu[\eta^{\nu\rho} k_3^2 - k_3^\nu k_3^\rho] \\
&\quad + (\Theta k_3)^\mu[\eta^{\nu\rho} k_2^2 - k_2^\nu k_2^\rho] + (\Theta k_3)^\nu[\eta^{\mu\rho} k_1^2 - k_1^\mu k_1^\rho] + (\Theta k_1)^\nu[\eta^{\mu\rho} k_3^2 - k_3^\mu k_3^\rho] \\
&\quad + (\Theta k_1)^\rho[\eta^{\mu\nu} k_2^2 - k_2^\mu k_2^\nu] + (\Theta k_2)^\rho[\eta^{\mu\nu} k_1^2 - k_1^\mu k_1^\nu],
\end{aligned} \tag{4.8}
$$

and

$$
\zeta_3 = \frac{1}{3g_3^2} - \frac{1}{6g_4^2} + \frac{1}{6g_5^2} \tag{4.9}
$$

where g_3, g_4 and g_5 are the moduli parameters defined in [134].

4.5.2 Squared-amplitude terms

The amplitude-squared terms for the quark-initiated partonic subprocess $q\bar{q} \to (\gamma, Z) \to l^+ l^-$ from the Feynman diagram 4.2(a),

$$
\overline{|\mathcal{M}_{q,\gamma}|^2} = \left(\frac{AF_1}{3}\right) [(p_1.p_3)(p_2.p_4) + (p_1.p_4)(p_2.p_3)] \tag{4.10}
$$

$$
\begin{aligned}
\overline{|\mathcal{M}_{q,Z}|^2} &= \left(\frac{BF_1}{3}\right)(c_A^{l2} + c_V^{l2})(c_A^{q2} + c_V^{q2}) [(p_1.p_3)(p_2.p_4) + (p_1.p_4)(p_2.p_3)] \\
&\quad + \left(\frac{BF_1}{3}\right) c_A^l c_V^l c_A^q c_V^q [(p_1.p_4)(p_2.p_3) - (p_1.p_3)(p_2.p_4)]
\end{aligned} \tag{4.11}
$$

and

$$
\begin{aligned}
2Re\overline{|\mathcal{M}_{q,\gamma}|^\dagger |\mathcal{M}_{q,Z}|} &= \left(\frac{2CF_1}{3}\right) c_A^l c_A^q [(p_1.p_3)(p_2.p_4) + (p_1.p_4)(p_2.p_3)] \\
&\quad - \left(\frac{2CF_1}{3}\right) c_V^l c_V^q [(p_1.p_4)(p_2.p_3) - (p_1.p_3)(p_2.p_4)]
\end{aligned} \tag{4.12}
$$

95

Here

$$A = \frac{128\pi^2\alpha^2 Q_l^2 Q_q^2}{\hat{s}^2} \quad B = \frac{128\pi^2\alpha^2 Q_l^2 Q_q^2}{Sin^4 2\theta_W \left[(\hat{s}-M_z^2)^2 + (M_Z\Gamma_Z)^2\right]} \quad C = \frac{128\pi^2\alpha^2 Q_l^2 Q_q^2(\hat{s}-M_z^2)}{\hat{s}[(\hat{s}-M_z^2)^2 + M_z^2\Gamma_z^2]}$$

$F_1 = \left[1 + \frac{(P_2\Theta P_1)^2}{4}\right]\left[1 + \frac{(P_4\Theta P_3)^2}{4}\right]$ and $\hat{s} = sx_1x_2$. Note that amplitude-squared terms go as $\mathcal{O}\left(1, \frac{1}{\Lambda_{NC}^2}, \frac{1}{\Lambda_{NC}^4}\right)$, respectively.

For the gluon-initiated partonic subprocess $gg \rightarrow (\gamma, Z) \rightarrow l^+l^-$, the squared-amplitude terms from the Feynman diagram 4.2(b), are given by

$$\overline{|\mathcal{M}_{g,\gamma}|^2} = 4DF_2 \left(p_{3\rho}p_{4\sigma} + p_{3\sigma}p_{4\rho} - \eta_{\rho\sigma}p_3 \cdot p_4\right) \cdot \left(\eta_{\nu\beta}\bar{\theta}_3^{\,\alpha\beta\sigma}\eta_{\alpha\mu}\bar{\theta}_3^{\,\mu\nu\rho}\right) \tag{4.13}$$

Similarly,

$$\overline{|\mathcal{M}_{g,Z}|^2} = 4GF_2(c_A^{l^2} + c_V^{l^2})\left(p_{3\rho}p_{4\sigma} + p_{3\sigma}p_{4\rho} - \eta_{\rho\sigma}p_3 \cdot p_4\right)\left(\eta_{\nu\beta}\bar{\theta}_3^{\,\alpha\beta\sigma}\eta_{\alpha\mu}\bar{\theta}_3^{\,\mu\nu\rho}\right) \tag{4.14}$$

$$2Re\overline{|\mathcal{M}_{g,\gamma}\mathcal{M}_z^\dagger|} = 4HF_2c_V^l\left(p_{3\rho}p_{4\sigma} + p_{3\sigma}p_{4\rho} - \eta_{\rho\sigma}p_3 \cdot p_4\right) \cdot \left(\eta_{\nu\beta}\bar{\theta}_3^{\,\alpha\beta\sigma}\eta_{\alpha\mu}\bar{\theta}_3^{\,\mu\nu\rho}\right) \tag{4.15}$$

Here

$$F_2 = \left[1 + \frac{(P_4\Theta P_3)^2}{4}\right] \quad D = 2\left(\frac{\pi\alpha\sin(2\theta_w)K_{\gamma gg}}{\hat{s}}\right)^2 \quad G = \left[\frac{2\pi^2\alpha^2 k_{zgg}^2}{[(\hat{s}-M_z^2)^2 + M_z^2\Gamma_z^2]}\right]$$

$H = \sin(2\theta_w)K_{\gamma gg}K_{zgg}\left[\frac{4\pi^2\alpha^2}{\hat{s}}\left(\frac{\hat{s}-M_z^2}{[(\hat{s}-M_z^2)^2 + M_z^2\Gamma_z^2]}\right)\right]$.

The quantity $\bar{\theta}_3$ appearing in several squared-amplitude terms, is given by

$$\bar{\theta}_3^{\mu\nu\rho} = -(p_1\Theta p_2)[(p_1 - p_2)^\rho\eta^{\mu\nu} + 2(p_2^\mu\eta^{\nu\rho} - p_1^\nu\eta^{\rho\mu})]$$
$$+ (p_1 \cdot p_2)[\Theta^{\mu\nu}(p_1 - p_2)^\rho - 2((p_2\Theta)^\mu\eta^{\nu\rho} + (p_1\Theta)^\nu\eta^{\mu\rho})] + [(p_2\Theta)^\mu p_1^\nu + (p_1\Theta)^\nu p_2^\mu](p_1 + p_2)^\rho$$

Note that amplitude-squared terms go as $\mathcal{O}\left(\frac{1}{\Lambda_{NC}^4}, \frac{1}{\Lambda_{NC}^8}\right)$, respectively.

In evaluating the matrix element squared, we have used the following orthonormal condition

$$\sum_{\lambda,\lambda'} \epsilon_{\mu'}^{*a'}(p_1, \lambda_1')\epsilon_\mu^a(p_1, \lambda_1) = -\eta_{\mu'\mu}\delta_{a'a} \tag{4.16}$$

$$\sum_{\lambda,\lambda'} \epsilon_\nu^b(p_2, \lambda_2)\epsilon_{\nu'}^{*b'}(p_2, \lambda_2') = -\eta_{\nu'\nu}\delta_{b'b} \tag{4.17}$$

and the color algebra $\sum_{aa'bb'} \delta_{bb'}\delta_{aa'}\delta^{ab}\delta_{a'b'} = \sum_{ab} \delta^{ab}\delta_{ab} = \sum_{a=1}^{8} \delta_{aa} = 8$.

4.5.3 Antisymmetric tensor $\Theta_{\mu\nu}$ and Θ weighted dot product

The antisymmetric tensor $\Theta_{\mu\nu} = \frac{1}{\Lambda^2}c_{\mu\nu}$ has six independent components corresponding to $c_{\mu\nu} = (c_{oi}, c_{ij})$ with $i, j = 1, 2, 3$. Assuming them to be the non vanishing components, we can write them as follows:

$$c_{oi} = \xi_i, \;\; c_{ij} = \epsilon_{ijk}\chi^k \tag{4.18}$$

The NC antisymmetric tensor $\Theta_{\mu\nu}$ is analogous to the electromagnetic(e.m.) field strength tensor $F_{\mu\nu}$ and ξ_i and χ_i are like the electric and magnetic field vectors. Setting $\xi_i = (\vec{E})_i = \frac{1}{\sqrt{3}}$ and $\chi_i = (\vec{B})_i = \frac{1}{\sqrt{3}}$ with $i = 1, 2, 3$ and noting the fact that $\xi_i = -\xi^i$, $\chi_i = -\chi^i$, the normalization condition $\xi_i\xi^j = \frac{1}{3}\delta_i^j$ and $\chi_i\chi^j = \frac{1}{3}\delta_i^j$, we may write $\Theta_{\mu\nu}$ as

$$\Theta_{\mu\nu} = \frac{1}{\sqrt{3}\Lambda^2}\begin{pmatrix} 0 & 1 & 1 & 1 \\ -1 & 0 & -1 & 1 \\ -1 & 1 & 0 & -1 \\ -1 & -1 & 1 & 0 \end{pmatrix} \tag{4.19}$$

Using these, we may write the Θ-weighted dot product as follows:

$$p_2\Theta p_1 = \frac{\hat{s}}{2\sqrt{3}\Lambda^2} \tag{4.20}$$

$$p_4\Theta p_3 = \frac{\hat{s}}{2\sqrt{3}\Lambda^2}\left[cos\theta + sin\theta(cos\phi + sin\phi)\right] \tag{4.21}$$

Chapter 5

Spacetime noncommutativity and $e^+e^- \xrightarrow{\gamma,Z} t\bar{t}$ process at the TeV energy collider

"I am enough of an artist to draw freely upon my imagination. Imagination is more important than knowledge. Knowledge is limited. Imagination encircles the world" - Albert Einstein

5.1 Introduction

The study of top quark pair production and top decay is quite interesting because top quark will not participate in the hadranization process. So it decays into other particles as soon as it produced and also it is more important to study the stability property of the Higgs boson. In ref [274] they have studied the top anomalous couplings which are arises due to CP and parity conserving dimension six operators. It has shown that the unitarity limit on anomalous coupling is $f_{2L(R)} \leq 0.62$ at the effective scale $\Lambda = 1.0$TeV. Tevatron also has strong limits on anomalous coupling, so the upper bound on $f_{2L(R)}$ are of the order of $0.1 - 0.2$. Similarly, parity violating case the upper bound on $f_{2L(R)}$ given as $-0.6(0)$ at $\sqrt{s} = 500$ GeV.

In ref [273] including myself studied top pair forward-backward asymmetry in the context of noncommutative standard model. The forward-backward asymmetry $A_{FB\phi}$ which is zero in the standard model can be as large as 4% for NC scale $\Lambda = 500$ GeV and the NC vector orientation angle $\eta = \pi/2$ at the fixed machine energy $\sqrt{s} = 1.0$ TeV. Assuming that the future TeV linear collider will observe $A_{FB\phi} = \pm 0.01$ we find $\Lambda \geq 750(860)$ GeV corresponding to $\eta = \pi/2$. Similarly, corresponding to polar asymmetry $A_{FBz} = 0.5078$ (which deviates from the standard model prediction by 1%), we find $\Lambda \geq 760$ GeV at the fixed machine energy $\sqrt{s} = 1.0$ TeV for $\eta = \pi/2$.

We study the top quark pair production process in TeV energy electron-positron collider in the non-commutative(NC) spacetime to order $\mathcal{O}(\Theta)$ using the Seiberg-Witten map. We obtain cross section and the azimuthal distribution and investigated their sensitivities on the NC vector $\vec{\Theta}$ with and without considering the effect of earth rotation.

5.2 Methodology

The content of the chapter is as follows. In Sec.5.3, we obtain the cross section and the angular distribution of $e^+e^- \xrightarrow{\gamma,Z} t\bar{t}$ using the order $\mathcal{O}(\Theta)$ Feynman rule. In Sec.5.3.1, we analyze the cross section and the angular distribution for different machine energy and investigate their sensitivities on the NC scale Λ for the three possible cases: Case I: $\Theta_{0i} \neq 0, \Theta_{ij} = 0$ (electric-like NC vector), Case II: $\Theta_{0i} = 0, \Theta_{ij} \neq 0$ (magnetic-like NC vector) and Case III: $\Theta_{0i} \neq 0, \Theta_{ij} \neq 0$ (fully antisymmetric NC vector containing both nonzero electric-like and magnetic-like components). Here we have not considered the effect of earth's rotation into our analysis, which we do consider in the next section. In Sec.5.3.2, we parametrize $\Theta_{\mu\nu}$ in presence of earth's rotation. We construct the time-averaged cross section and azimuthal distribution of $e^+e^- \xrightarrow{\gamma,Z} t\bar{t}$ and investigate their sensitivities on the NC scale Λ and the orientation angle η of the NC vector w.r.t the earth's axis(fixed) of rotation. Finally, in Sec.5.4, we summarize and conclude.

5.3 Process $e^+e^- \xrightarrow{\gamma,Z} t\bar{t}$: Results and Discussion

We investigate the process $e^-(p_1)e^+(p_2) \xrightarrow{\gamma,Z} t(p_3)\bar{t}(p_4)$ in the NCSM. It occurs via the s-channel exchange of γ and Z bosons in the NCSM (like the SM). The corresponding Feynman diagrams are shown below (Fig. 5.1). The Feynman rules for several interaction vertices are shown in Appendix 5.5.1. The scattering amplitudes to $\mathcal{O}(\Theta)$ for the photon(γ) and Z-boson mediated diagrams can be
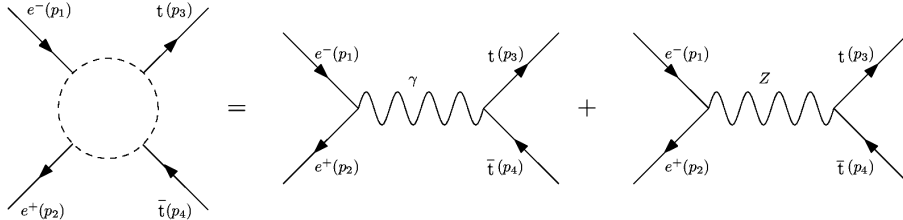
Figure 5.1: *Feynman diagrams for the $e^+e^- \xrightarrow{\gamma,Z} t\bar{t}$ scattering process.*

written as

$$i\mathcal{A}_\gamma = \frac{-8\pi\alpha i}{3s}\left(1+\frac{i}{2}\,p_2\Theta p_1\right)\left(1-\frac{i}{2}\,p_4\Theta p_3\right)[\overline{v}(p_2)\gamma_\mu u(p_1)]\,[\overline{u}(p_3)\gamma^\mu v(p_4)]$$
$$+\frac{8\pi\alpha m_t}{3s}\left(1+\frac{i}{2}\,p_2\Theta p_1\right)[\overline{v}(p_2)\gamma_\mu u(p_1)]\,[\overline{u}(p_3)(p_3\Theta)^\mu v(p_4)] \tag{5.1}$$

and

$$i\mathcal{A}_Z = \frac{4\pi\alpha i}{\sin^2(2\theta_W)s_Z}\left(1+\frac{i}{2}\,p_2\Theta p_1\right)\left[\overline{v}(p_2)\gamma_\mu\Gamma^-_{A_e}u(p_1)\right]$$
$$\times\left[\overline{u}(p_3)\left\{\left(1-\frac{i}{2}\,p_4\Theta p_3\right)\gamma_\mu\Gamma^-_{A_t}-im_t c^t_A\gamma^5(p_3\Theta)^\mu\right\}v(p_4)\right] \tag{5.2}$$

where $s=(p_1+p_2)^2$, $s_Z=s-m_Z^2-im_Z\Gamma_Z$, $\alpha=e^2/4\pi$, $\Gamma^-_{A_f}=c^f_V-c^f_A\gamma^5$ with $c^f_V=T^f_3-2Q_f\sin^2\theta_W$ and $c^f_A=T^f_3$. Here θ_W is the Weinberg angle and f corresponds to SM fermions i.e. $e,\ t,..$ etc. In above m_Z and Γ_Z corresponds to the Z boson mass and its decay width, respectively. The Θ weighted momentum dot products are defined in Appendix 5.5.1. The amplitude square (spin-averaged) can be written as

$$\overline{|\mathcal{A}|^2}(e^+e^-\xrightarrow{\gamma,Z}t\bar{t})=\frac{1}{4}\sum_{spin}|\mathcal{A}|^2=\frac{1}{4}\sum_{spin}\left[|\mathcal{A}_\gamma|^2+|\mathcal{A}_Z|^2+2Re(\mathcal{A}_Z\mathcal{A}^\dagger_\gamma)\right] \tag{5.3}$$

Several terms of Eq. 5.3 are given in Appendix 5.5.3.

5.3.1 Analysis in absence of earth rotation

The spacetime noncommutativity effect enters via the anti-symmetric tensor

$$\Theta_{\mu\nu}=(\Theta_{0i},\Theta_{ij})=\frac{c_{\mu\nu}}{\Lambda^2}=\frac{1}{\Lambda^2}\,(c_{0i},c_{ij})=\frac{1}{\Lambda^2}(\xi_i,\ \epsilon_{ijk}\chi^k)$$

which is a fundamental constant in nature. Here Λ is the spacetime noncommutativity scale. Writing $\xi_i=(\vec{\Theta}_E)_i$ and $\chi_k=(\vec{\Theta}_B)_k$, we first set them as the constant (normalized) vectors $\vec{\Theta}_E=\frac{1}{\sqrt{3}}(\hat{i}+\hat{j}+\hat{k})$ and $\vec{\Theta}_B=\frac{1}{\sqrt{3}}(\hat{i}+\hat{j}+\hat{k})$. They are constant vectors in some preferred direction. We consider three different cases in which the NC tensor is (i) electric-like(i.e. $\xi_i\neq0$ and $\chi_k=0$), (ii) magnetic-like(i.e. $\xi_i=0$ and $\chi_k\neq0$) and fully antisymmetric with $\xi_i\neq0$ and $\chi_k\neq0$, i.e. $\Theta_{\mu\nu}$ has both electric-like and magnetic-like components.

Analysis of space-time and space-space noncommutativity:

In Fig. 5.2, we have plotted the $e^-e^+\to t\bar{t}$ cross section σ (i.e.σ_{ST} for space-time noncommutativity and σ_{SS} for space-space noncommutativity)as a function of the machine energy E_{com} $(=\sqrt{s})$ (GeV) for different Λ values. In Fig. 5.2(a) (left figure), $\sigma_{ST}(e^+e^-\xrightarrow{\gamma,Z}t\bar{t})$ (pb) is shown (note that ST
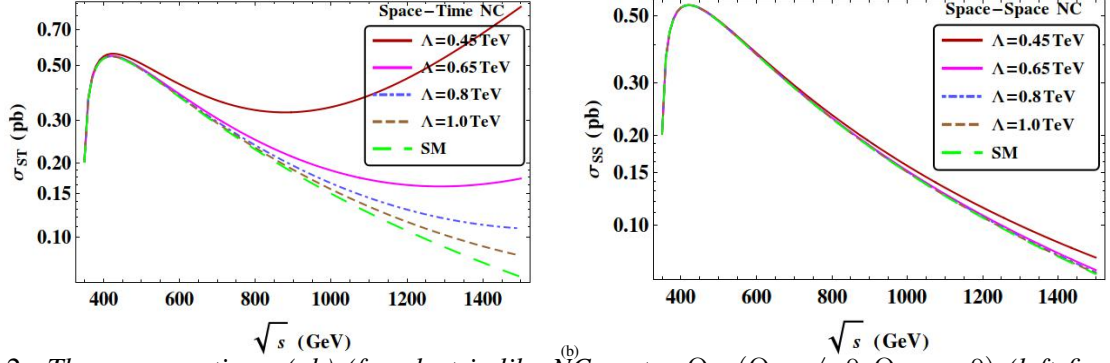
Figure 5.2: *The cross section $\sigma(pb)$ (for electric-like NC vector $\Theta_{\mu\nu}(\Theta_{0i} \neq 0, \Theta_{ij} = 0)$ (left figure) and for magnetic-like NC vector $\Theta_{\mu\nu}(\Theta_{0i} = 0, \Theta_{ij} \neq 0)$ (right figure) is shown against $\sqrt{s}(= E_{com})(GeV)$ for $\Lambda = 0.45, 0.65, 0.8,$ and 1.0 TeV, respectively. The lowest curve corresponds to the standard model curve.*

corresponds to space-time noncommutativity) against E_{com} where the NC vector is electric-like, while in Fig. 5.2(b) (right figure) $\sigma_{SS}(e^+e^- \xrightarrow{\gamma,Z} t\bar{t})$ (pb) is plotted (note that SS corresponds to space-space noncommutativity) against E_{com} where the NC vector is magnetic-like. From the topmost to the to the next to the lowermost curve Λ varies from 0.45 TeV to 1.0 TeV in each Figure. In each figure, the SM curve corresponds to the lowermost curve. On the left figure, we see that σ_{ST} for $\Lambda = 450$ GeV after some value of the machine energy increases. For $\Lambda = 0.45$ TeV, we find that the cross section violates unitarity significantly (a typical problem which arises in the case of the electric-like NC vector) [67]. We find that σ_{ST} deviates from the standard model value quite significantly for the machine energy $E_{com} \geq 1000$ GeV and is found to be less at lower machine energy. We also see that the cross section, at a given machine energy, deviates significantly from the SM value at a smaller Λ value. From Fig. 5.2(b), we see that σ_{SS} decreases with the machine energy for $\Lambda = 450$ GeV i.e. it doesn't have a divergent behaviour as was the case for the electric-like NC vector. Finally, in Fig. 5.3, we have
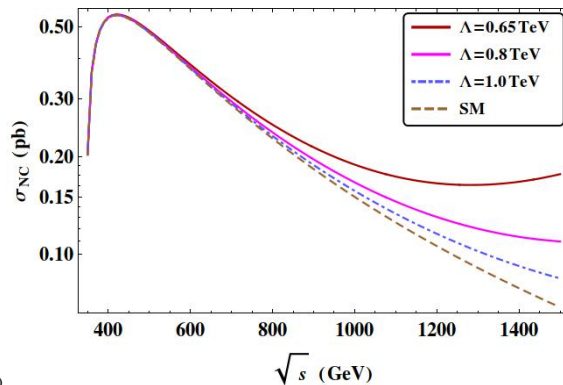
Figure 5.3: *The cross section $\sigma_{NC}(pb)$ is plotted as a function of the machine energy $\sqrt{s}(E_{com})(GeV)$ for the NC scale $\Lambda = 0.65, 0.8$ and 1.0 TeV. The NC tensor contains both electric-like and magnetic-like components. The lowest curve corresponds to the standard model curve.*

shown σ_{NC} as a function of $\sqrt{s}$ with Λ varying from 0.65 TeV to 1.0 TeV. Here the NC tensor $\Theta_{\mu\nu}$

contains both electric-like and magnetic-like components. Also shown is the SM plot in the same figure (the lowermost curve) which is obtained in the $\Lambda \to \infty$ limit. From Fig. 5.3, we find the number of ttbar events $N\ yr^{-1} = 16600\ yr^{-1}$ for the machine energy $E_{com} = 1$ TeV and the LC luminosity $\mathcal{L} = 100\ fb^{-1}$ for the NC scale $\Lambda = 0.8$ TeV. The corresponding SM event is calculated as $15000\ yr^{-1}$. We have seen in above that the dominant contribution to the NCSM cross section follows from the space-time noncommutativity (i.e. when the NC vector is an electric-like vector). We now define two quantities

$$\Delta\sigma_1 = (\sigma_{ST} - \sigma_{SM})/\sigma_{SM}, \;\; \Delta\sigma_2 = (\sigma_{SS} - \sigma_{SM})/\sigma_{SM}$$

and plot them against the machine energy. In Fig. 5.4(a), we have plotted $\Delta\sigma_1$ as a function of the
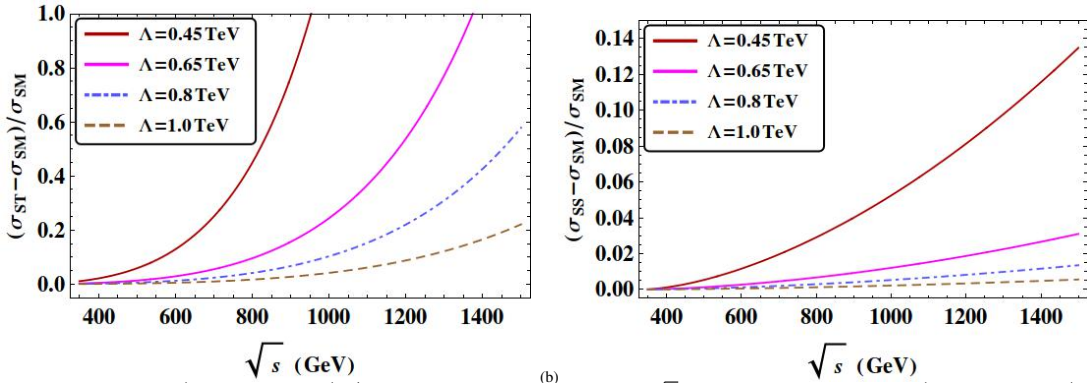
Figure 5.4: *On the left $(\sigma_{ST} - \sigma_{SM})/\sigma_{SM}$ is plotted against $\sqrt{s}$, while on the right $(\sigma_{ST} - \sigma_{SM})/\sigma_{SM}$ is plotted against $\sqrt{s}$ for Λ ranging from 0.45 TeV to 1.0 TeV.*

machine energy $\sqrt{s}$ corresponding to $\Lambda = 0.45,\ 0.65,\ 0.8$ TeV and 1.0 TeV. At $\sqrt{s} = 1.0$ TeV, we find (left figure) that for $\Lambda = 0.45$ TeV, $\sigma_{ST} > 2\sigma_{SM}$ i.e. the difference $(\sigma_{ST} - \sigma_{SM})$ is more than 100% of σ_{SM}. Whereas, for $\Lambda = 0.65$ TeV, the $(\sigma_{ST} - \sigma_{SM}) \sim 20\%$ of σ_{SM}. Assuming that the experimental data will lie within $\sigma_{SM} \pm 0.2\sigma_{SM}$ i.e. $(\sigma_{ST} - \sigma_{SM}) \leq 0.2\sigma_{SM}$, we obtain the bound as $\Lambda \geq 0.65$ TeV. However, the bound obtained in above depends on the machine energy. For $\sqrt{s} = 1.5$ TeV, similarly, assuming that $(\sigma_{ST} - \sigma_{SM}) \leq 0.2\sigma_{SM}$, one finds $\Lambda \geq 1$ TeV. From the right figure, In case II (i.e. Fig. 5.4(b)), we find that $\sigma_{SS} - \sigma_{SM} = 0.01\sigma_{SM}$ i.e. $\Delta\sigma_2 \to 0.01$ at $\Lambda = 0.65$ TeV at $\sqrt{s} = 1.0$ TeV. So, assuming that $(\sigma_{SS} - \sigma_{SM}) \leq 0.02\sigma_{SM}$, one finds $\Lambda \geq 0.65$ TeV at the machine energy $\sqrt{s} = 1.0$ TeV and above.

Azimuthal distribution:

We next study the normalized azimuthal distribution of the top quark pair production. In Fig. 5.5(a)(left), $\frac{1}{\sigma_{ST}} \frac{d\sigma_{ST}}{d\phi}$ (normalized azimuthal distribution for electric-like NC vector) is plotted as a function of ϕ for $\sqrt{s} = 1$ TeV and for different Λ. Note that the height of the peak at the fixed machine energy decreases as Λ
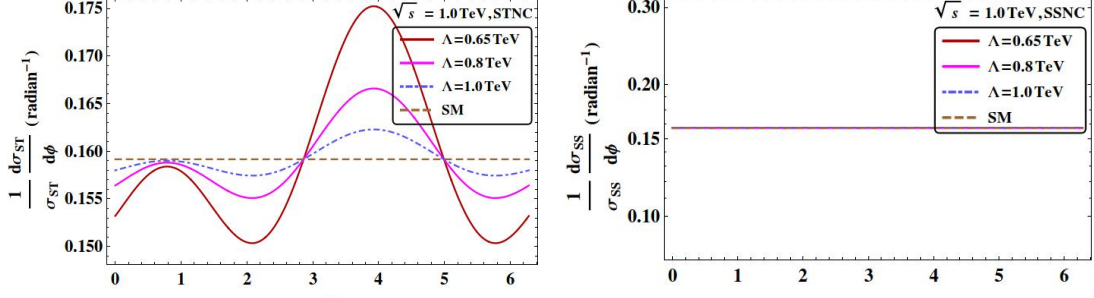
Figure 5.5: *On the left $\frac{1}{\sigma_{ST}}\frac{d\sigma_{ST}}{d\phi}$ is plotted against ϕ, while on the right $\frac{1}{\sigma_{SS}}\frac{d\sigma_{SS}}{d\phi}$ is plotted against ϕ for $\Lambda = 0.65,\ 0.8,\ 1.0$ TeV and the machine energy $E_{com} = 1$ TeV, respectively. In the left figure, the NC tensor is taken as electric-like, whereas for the right figure the NC tensor is magnetic-like. The middle horizontal curve is the SM curve.*
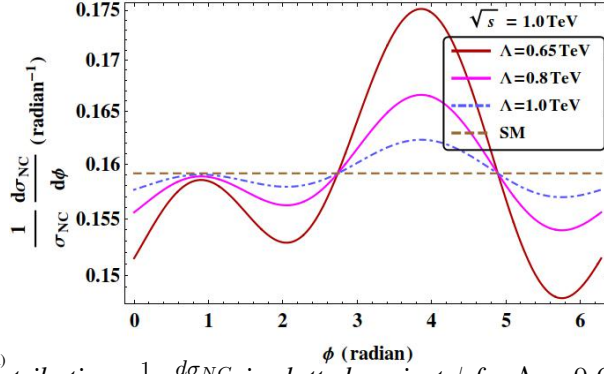
Figure 5.6: *The normalized distribution $\frac{1}{\sigma_{NC}}\frac{d\sigma_{NC}}{d\phi}$ is plotted against ϕ for $\Lambda = 0.65,\ 0.8,\ 1.0$ TeV and the fixed machine energy $E_{com} = 1$ TeV, respectively. Here $\Theta_{\mu\nu}$ contains both electric-like and magnetic-like components. The horizontal curve (in the middle) corresponds to the SM distribution.*

increases. The middle horizontal line is the SM curve. In Fig. 5.5(b) (right), we have shown $\frac{1}{\sigma_{SS}}\frac{d\sigma_{SS}}{d\phi}$ against ϕ for $\Lambda = 0.65$ TeV, 0.8 TeV and 1.0 TeV at $\sqrt{s} = 1.0$ TeV. While the distribution is oscillatory (left figure with electric-like NC vector), it is almost flat (right figure with magnetic-like NC vector) and nearly agrees with the SM value. In Fig. 5.6, $\frac{1}{\sigma_{NC}}\frac{d\sigma_{NC}}{d\phi}$ is plotted against ϕ for $\Lambda = 0.65,\ 0.8$ and 1.0 TeV at $\sqrt{s} = 1$ TeV. The oscillatory behaviour of the distribution with a clear peak at $\phi = 4$ (radian) (found to be absent in most of the BSM scenarios), can serves as the Occam's razor in isolating the spacetime noncommutativity from other class of BSM physics.

5.3.2 Analysis in presence of earth rotation

The electron-positron collision experiment is done on the earth-based laboratory coordinate system which is moving by the earth's rotation. The electric-like and magnetic-like components of $\Theta_{\mu\nu}$ i.e. $\vec{\Theta}_E$ and $\vec{\Theta}_B$ which are fixed vectors in some inertial frame of fixed stars, will also changes with time due to the earth's rotation and we need to take into consideration this time variation of $\Theta_{\mu\nu}$ while
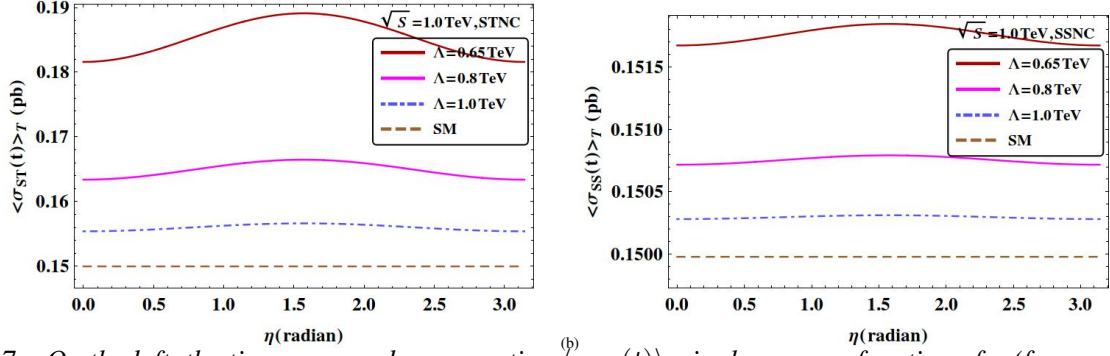
Figure 5.7: *On the left, the time-averaged cross section $\langle\sigma_{ST}(t)\rangle_T$ is shown as a function of η (for an electric-like NC vector), while on the right, $\langle\sigma_{SS}(t)\rangle_T$ is shown as a function of η (for an magnetic-like NC vector) corresponding to $\Lambda = 0.65,\ 0.8$ and 1.0 TeV and the machine energy $E_{com} = 1$ TeV in both cases.*

measuring any NC observables. The time averaged observables are defined in appendix 3.6 while incorporating the effect of earth's rotation.

It is difficult to take the time dependent data. So, one make an estimate of the time-averaged cross section and it's distributions over the period T_{day} and compare those with the experiment. The time averaged observables i.e. the cross section $\langle\sigma(t)\rangle_T$ and the angular distribution $\left(\left\langle\frac{d\sigma(t)}{d\phi}\right\rangle_T\right)$, used in our analysis, are defined in [221, 255, 273]. The cross section $\sigma(=\sigma(\Lambda,\sqrt{s},t))$ and the azimuthal angular distribution are function of time(t). The time(t)-dependence comes through the NC tensor $\Theta_{\mu\nu}(\Theta_{0i},\Theta_{ij})$ which varies with $\zeta = \omega t$. Also the noncommutative angle ξ appears through $\cos(\omega t - \xi)$ or $\sin(\omega t - \xi)$ as the initial phase for time evolution, which however, gets disappeared in the time averaged observables. So the measurement of the time averaged observables gives us an estimate of $\vec{\Theta}_E$ or $\vec{\Theta}_B$ and hence the NC scale Λ and the angle of orientation η of the NC vector.

Time-averaged cross section and angular distribution

We next consider the effect of earth's rotation into our analysis. We plot $\langle\sigma(t)\rangle_T$ against the orientation angle η in the following three cases- Case (I): electric-like NC vector with the orientation angle η, Case (II): magnetic-like NC vector with the orientation angle η and Case (III): $\Theta_{\mu\nu}$ have both electric and magnetic-like components. In either case, the NC vector makes an angle η with the earth's axis of rotation. In Fig. 5.7(a), $\langle\sigma_{ST}(t)\rangle_T$ is shown against η (for electric-like NC vector), while on the right figure $\langle\sigma_{ST}(t)\rangle_T$ is plotted against η(for magnetic-like NC vector), while on the right we have plotted $\langle\sigma_{SS}(t)\rangle_T$ as a function of η (Case II) corresponding to $\Lambda = 0.65,\ 0.8$ and 1.0 TeV at the fixed machine energy $\sqrt{s} = 1.0$ TeV. Note that the height of the maxima decreases with the increase of Λ for a given machine energy. We find that the cross section is maximum at $\eta = \pi/2$ and hence we set $\eta = \pi/2$ in the remaining part of our analysis. In Fig. 5.8, $\langle\sigma(t)\rangle_T$ is plotted against η (Case III) corresponding to $\Lambda = 0.65,\ 0.8$ and 1.0 TeV and $\sqrt{s} = 1.0$ TeV. In Fig. 5.9, on the left, we have shown $\langle\sigma_{ST}(t)\rangle_T$

(a)

Figure 5.8: *The time-averaged cross section $\langle\sigma(t)\rangle_T$ is plotted as a function of η (for the NC vector having both electric-like and magnetic-like components) corresponding to $\Lambda = 0.65,\ 0.8$ and 1.0 TeV and the machine energy $\sqrt{s} = 1$ TeV.*

(b)
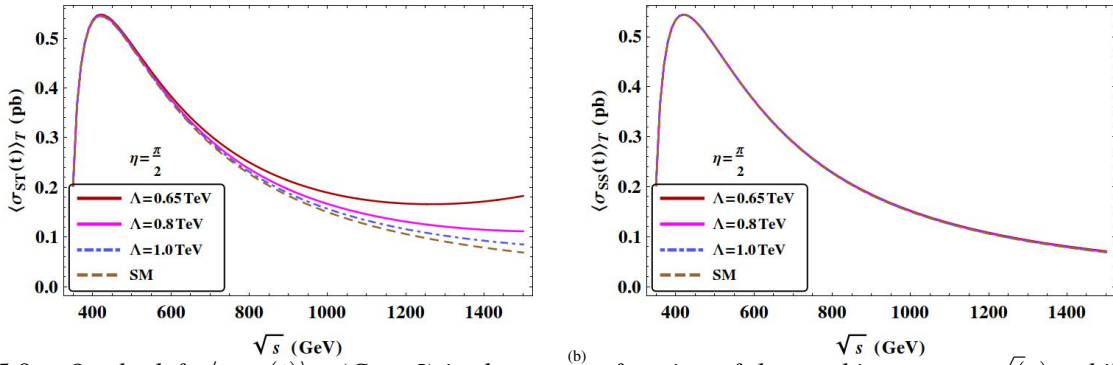
Figure 5.9: *On the left, $\langle\sigma_{ST}(t)\rangle_T$ (Case I) is shown as a function of the machine energy $\sqrt{(s)}$, while on the right, $\langle\sigma_{SS}(t)\rangle_T$ (Case II) is plotted as a function $\sqrt{s}$ corresponding to $\Lambda = 0.65,\ 0.8$ and 1.0 TeV, respectively. The orientation angle η is kept fixed at $\eta = \pi/2$. The lowermost curve corresponds to the SM plot in both Figures.*

against $\sqrt{s}$ (Case I), while on the right, $\langle\sigma_{SS}(t)\rangle_T$ is plotted against $\sqrt{s}$ (Case II) corresponding to $\eta = \pi/2$. From the topmost to the next-to-lowermost curves, Λ increases from $\Lambda = 0.65,\ 0.8$ and 1.0 TeV, respectively. The lowermost curve corresponds to the SM plot (obtained in the limit $\Lambda \to \infty$). On the right side, the curves corresponding to different Λ converges. The magnetic-like NC vector hardly cause any deviation in the cross section from the SM value. In Fig. 5.10, $\langle\sigma_{NC}(t)\rangle_T$ is plotted against $\sqrt{s}$ for $\eta = \pi/2$ and $\Lambda = 0.65,\ 0.8$ and 1.0 TeV, respectively(Case III). We observe that although the deviation from the standard model is small at relatively lower energies, it starts becoming significant at the machine energy $E_{com} \sim 800$ GeV and becomes more prominent with the increase in machine energy. Also we see that at a given machine energy E_{com}, the deviations become larger with smaller value of Λ. We find the number of ttbar events $N\ yr^{-1} = 16680\ yr^{-1}$ for $\Lambda = 0.8$ TeV at $E_{com} = 1$ TeV and the LC luminosity $\mathcal{L} = 100\ fb^{-1}$. The corresponding SM event number will be $15000\ yr^{-1}$.
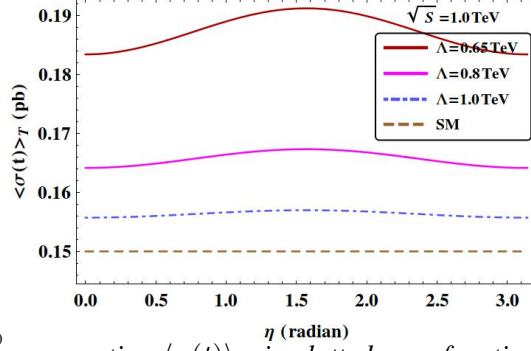
105
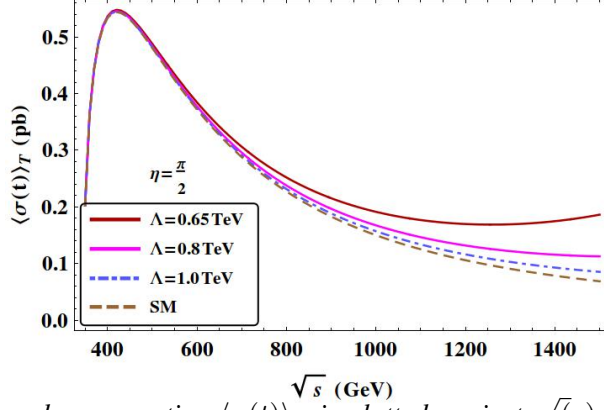
Figure 5.10: *The time-averaged cross section $\langle \sigma(t) \rangle_T$ is plotted against $\sqrt{(s)}$ for the NC vector having both electric-like and magnetic-like components. Λ is chosen to be 0.65, 0.8 and 1.0 TeV and η is set at $\pi/2$. The lowermost curve corresponds to the SM plot which is both time(t) and η independent.*

Normalized azimuthal distribution

As mentioned earlier, the angular distribution of the final state particles can serve as an useful tool in understanding the BSM physics. Since the Lorentz invariance including the rotational invariance
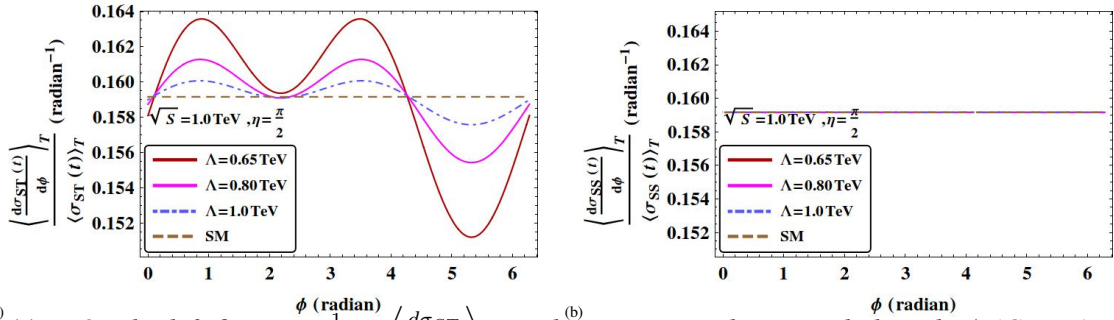
Figure 5.11: *On the left figure $\frac{1}{\langle \sigma_{ST}(t) \rangle} \left\langle \frac{d\sigma_{ST}}{d\phi} \right\rangle_T$ is shown against the azimuthal angle ϕ (Case I), whereas on the right $\frac{1}{\langle \sigma_{SS}(t) \rangle} \left\langle \frac{d\sigma_{SS}(t)}{d\phi} \right\rangle_T$ is plotted against ϕ(Case II) for $\eta = \pi/2$ and $\Lambda = 0.65$, 0.8 and 1.0 TeV, respectively. The horizontal line corresponds to the SM distribution which is time(t) independent.*

around the beam axis is broken by the spacetime noncommutativity which defines a preferred direction, the azimuthal distribution will no longer be isotropic due to its strong dependence on ϕ. This anisotropy observed in the time-averaged azimuthal distribution $\left\langle \frac{d\sigma(t)}{d\phi} \right\rangle_T$ can act as the signature of the space-time noncommutativity, which in most BSM physics is absent. In Fig.5.11(a)(left), $\frac{1}{\langle \sigma_{ST}(t) \rangle} \left\langle \frac{d\sigma_{ST}(t)}{d\phi} \right\rangle_T$ is shown as a function of ϕ for $\eta = \pi/2$ and $\Lambda = 0.65$, 0.8 and 1.0 TeV, while on the right i.e. Fig.5.11(b), $\frac{1}{\langle \sigma_{SS}(t) \rangle} \left\langle \frac{d\sigma_{SS}(t)}{d\phi} \right\rangle_T$ is plotted against ϕ for $\eta = \pi/2$ and the above set of Λ. The machine energy is kept fixed at $E_{com} = 1$ TeV in both cases. One can clearly see the oscillatory behaviour of the azimuthal distribution when the NC vector is electric-like (i.e. Case I), whereas it is completely flat in the case of magnetic-like NC vector, like the usual SM distribution. In Fig.5.12, the normalized $\frac{1}{\langle \sigma(t) \rangle} \left\langle \frac{d\sigma(t)}{d\phi} \right\rangle_T$ is plotted against ϕ at the machine energy $E_{com} = 1$ TeV with $\eta = \pi/2$ and $\Lambda = 0.65$, 0.8 and 1.0 TeV,

106
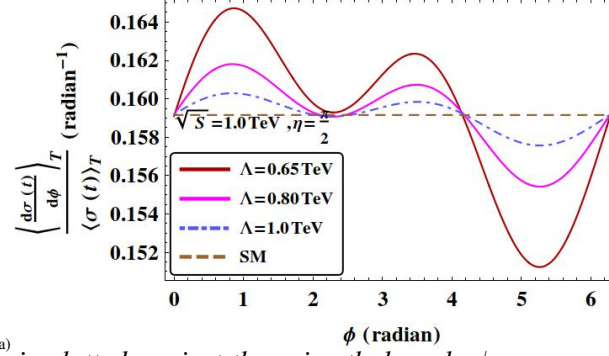
Figure 5.12: $\frac{1}{\langle\sigma(t)\rangle}\left\langle\frac{d\sigma(t)}{d\phi}\right\rangle_T^{(a)}$ *is plotted against the azimuthal angle ϕ corresponding to the orientation angle $\eta = \pi/2$ and the NC scale $\Lambda = 0.65$, 0.8 and 1.0 TeV, respectively. The lowermost curve corresponds to the SM plot which is both t and η independent.*

respectively. The distribution shown several peaks which are located at $\phi = 0.88$ and 3.46 (rad) and dip at $\phi = 5.26$ (rad). The height of the peak decreases as Λ increases, whereas the depth of the dip increases as Λ decreases. The azimuthal distribution which is oscillatory in the NCSM scenario, flat in most BSM scenarios, can act as a Occam's razor in differentiating out the noncommutativity scenario from other class of BSM physics.

Diurnal variation of the cross section

To study the diurnal variation of the cross section over the period of a complete day+night, we now
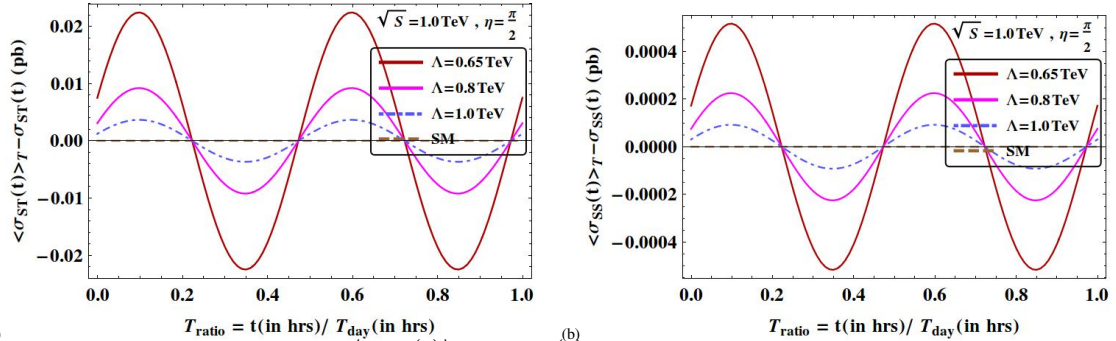
Figure $^{(a)}$5.13: *On the left, $\langle\sigma_{ST}(t)\rangle_T - \sigma(t)$ is plotted against T_{ratio} for $\eta = \pi/2$ (Case I), while on the right $\langle\sigma_{SS}(t)\rangle_T - \sigma(t)$ is plotted against T_{ratio} (Case II) corresponding $\Lambda = 0.65\,\mathrm{TeV(topmost)}, 0.8\,\mathrm{TeV(middle)},\ 1.0\,\mathrm{TeV(lowermost)}$ and for $\eta = \pi/2$. We set $E_{com} = 1.0$ TeV.*

define the quantity $\langle\sigma(t)\rangle_T - \sigma(t)$ and plot it as a function of the normalized time $T_{ratio} = t/T_{day}$ (with t, T_{day} in hrs) corresponding to $\eta = \pi/2$ and $\Lambda = 0.65,\ 0.8$ and 1.0 TeV, respectively. In Fig. 5.13(a), we have plotted $\langle\sigma_{ST}(t)\rangle_T - \sigma(t)$ against T_{ratio} for $\eta = \pi/2$(Case I), whereas in Fig. 5.13(b), we have shown $\langle\sigma_{SS}(t)\rangle_T - \sigma(t)$ against T_{ratio} for $\eta = \pi/2$ (Case II). In Fig. 5.14, $\langle\sigma_{ST}(t)\rangle_T - \sigma(t)$ is plotted as a function of T_{ratio} corresponding to $E_{com} = 1.0$ TeV, $\eta = \pi/2$ and the NC scale $\Lambda = 0.65,\ 0.8$ and 1.0 TeV, respectively (Case III). The machine energy is kept fixed at 1.0 TeV in both cases. Note that the height (the depth) of the peak (the trough) increases with the lowering of Λ for a given machine

107
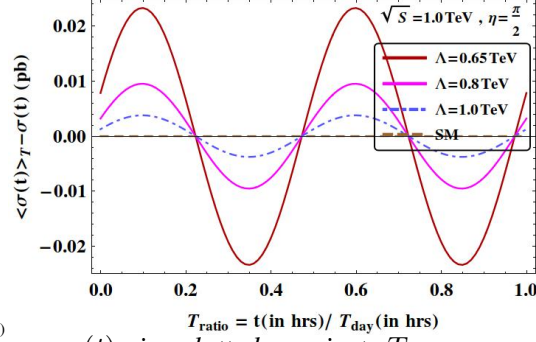
Figure 5.14: $\langle \sigma_{NC}(t) \rangle_T^{(a)} - \sigma(t)$ *is plotted against* T_{ratio} *corresponding to* $\eta = \pi/2$ *and* $\Lambda = 0.65\,\text{TeV}(\text{topmost}),\, 0.8\,\text{TeV}(\text{middle}),\, 1.0\,\text{TeV}(\text{lowermost})$, *respectively. We set* $E_{com} = 1.0\,\text{TeV}$.

energy. Also the pattern of peaks and dips becomes more periodic corresponding to $\eta = \pi/2$. The peak and trough appeared in the cross section at the regular interval of time is a unique feature of the NCSM scenario and found to be absent in other BSM scenarios. Such a time-dependent behaviour of the production cross section can serve as the *Occam's razor* in isolating noncommutative spacetime from other types of New Physics.

5.4   Summary

We study the pair production of the top quark at the TeV energy $e^- e^+$ linear collider in the noncommutative spacetime. We first analyze the process in the absence of earth rotation, with three types i.e. electric-like, magnetic-like and electric+magnetic-like of NC vectors. We found that fo a given value of the NC scale $\Lambda = 0.65$ TeV, the cross section increases with machine energy for a given value in the case when the NC vector is electric-like. At a fixed value of the machine energy, the cross section increases as Λ decreases. The oscillatory behaviour observed in the azimuthal distribution with peaks and dip is unique and can be an useful tool in probing noncommutative spacetime. We have incorporated the effect of earth's rotation into our analysis and constructed time-averaged cross section ($\langle \sigma(t) \rangle$) and angular distribution ($\left\langle \frac{d\sigma(t)}{d\phi} \right\rangle_T$). We investigated their sensitivities on Λ and the orientation angle η of the NC vector. The effect spacetime noncommutativity seems to be most prominent at $\eta = \pi/2$. We find that the maximum effect of spacetime noncommutativity emerges in the case of electric-like NC vector. The total time-averaged cross section is found to increase with the machine energy for $E_{com} \geq 1$ TeV corresponding to $\eta = \pi/2$ and $\Lambda = 0.65$ TeV. The prominent peaks observed in $\frac{1}{\langle \sigma(t) \rangle} \left\langle \frac{d\sigma(t)}{d\phi} \right\rangle_T$ are located at $\phi = 0.88,\, 3.458$ and trough at 5.265 rad for $\Lambda = 0.65,\, 0.8$ and 1.0 TeV and $\eta = \pi/2$ at $E_{com} = 1$ TeV. The height(depth) of the peak(trough) increases with lower Λ value and the pattern of peaks and troughs become more periodic at the orientation angle $\eta = \pi/2$. We find

that at the LC energy $E_{com} = 1$ TeV and the LC luminosity $\mathcal{L} = 100\ fb^{-1}$, the number of ttbar events $N\ yr^{-1} = 16600\ yr^{-1}$ corresponding to $\Lambda = 800$ GeV. The corresponding SM event turns out to be $15000\ yr^{-1}$. Finally, we obtain the diurnal variation of the total cross section over the sidereal day T_{day}. The periodic appearance of peaks and troughs in the diurnal cross section can be searched at the TeV energy colliders.

5.5 Appendix

5.5.1 Feynman rules to order $\mathcal{O}(\Theta)$

The Feynman rule for the $f - \overline{f} - \gamma$ and $f - \overline{f} - Z$ vertices to order $\mathcal{O}(\Theta)$,([208]):

$$\gamma : ieQ_f \left\{ \gamma_\mu + \frac{i}{2} \left[(P_{out}\Theta)_\mu (\slashed{P}_{in} - m) + (\Theta P_{in})_\mu (\slashed{P}_{out} - m) - k_{oi}\gamma_\mu \right] \right\}$$

$$Z : \frac{ie}{sin2\theta_W} \left\{ \gamma_\mu \Gamma^-_{A_f} + \frac{i}{2} \left[(P_{out}\Theta)_\mu (\slashed{P}_{in} - m)\Gamma^-_{A_f} + (\Theta P_{in})_\mu (\slashed{P}_{out} - m)\Gamma^-_{A_f} - k_{oi}\gamma_\mu \Gamma^-_{A_f} \right] \right\}$$

where $\Gamma^-_{A_f} = c^f_V - c^f_A \gamma^5$ with $c^f_V = T^f_3 - 2Q_f sin^2\theta_w$ and $c^f_A = T^f_3$. Here, the flavour $f = e, t$. Also $k_{oi} = P_{out}\Theta P_{in}$. The Θ weighted momentum dot product $k_{oi} = P_{out}\Theta P_{in} = P^\mu_{out}\Theta_{\mu\nu}P^\nu_{in} = -P^\nu_{in}\Theta_{\nu\mu}P^\mu_{out} = -P_{in}\Theta P_{out} = -k_{io}$.

Defining $P_{in} = p_1$, $P_{out} = -p_2$, $P_{in} = -p_4$ and $P_{out} = p_3$, we find the vertices to order $O(\Theta)$

$$\Gamma^{e^-e^+\gamma}_\mu : -ie \left\{ \left(1 + \frac{i}{2}p_2\Theta p_1 \right) \gamma_\mu + \frac{i}{2} \left[(p_1\Theta)_\mu (\slashed{p}_2 - m_e) + (\Theta p_2)_\nu (\slashed{p}_1 - m_e) \right] \right\}$$

$$\Gamma^{\gamma t\bar{t}}_\nu : \frac{2ie}{3} \left\{ \left(1 - \frac{i}{2}p_4\Theta p_3 \right) \gamma_\nu - \frac{i}{2} \left[(p_3\Theta)_\nu (\slashed{p}_4 - m_t) + (\Theta p_4)_\nu (\slashed{P}_3 - m_t) \right] \right\}$$

$$\Gamma^{e^-e^+Z}_\mu : \frac{ie}{sin(2\theta_W)} \left\{ \left(1 + \frac{i}{2}p_2\Theta p_1 \right) \gamma_\mu \Gamma^-_{A_e} + \frac{i}{2} \left[(p_1\Theta)_\mu (\slashed{p}_2 - m_e) + (\Theta p_2)_\mu (\slashed{p}_1 - m_e) \right] \Gamma^-_{A_e} \right\}$$

$$\Gamma^{Zt\bar{t}}_\nu : \frac{ie}{sin(2\theta_W)} \left\{ \left(1 - \frac{i}{2}p_4\Theta p_3 \right) \gamma_\mu \Gamma^-_{A_t} + \frac{i}{2} \left[(p_4\Theta)_\mu (\slashed{p}_3 - m_t) + (\Theta p_3)_\mu (\slashed{p}_4 - m_t) \right] \Gamma^-_{A_t} \right\}$$

5.5.2 Momentum prescriptions and dot products

In center of momentum frame, the 4 incoming and outgoing particles momenta are given by:

$$p_1 = p_{e^-} = \frac{\sqrt{s}}{2} (1, 0, 0, 1) \tag{5.4}$$

$$p_2 = p_{e^+} = \frac{\sqrt{s}}{2} (1, 0, 0, -1) \tag{5.5}$$

$$p_3 = p_t = \frac{\sqrt{s}}{2} \left(1, k' \sin\theta\cos\phi, k'\sin\theta\sin\phi, k'\cos\theta\right) \tag{5.6}$$

$$p_4 = p_{\bar{t}} = \frac{\sqrt{s}}{2} \left(1, -k'\sin\theta\cos\phi, -k'\sin\theta\sin\phi, -k'\cos\theta\right), \tag{5.7}$$

where $k' = \sqrt{1 - \frac{4m_t^2}{s}}$. Here θ is the scattering angle made by the 3-momentum vector p_3 of the outgoing top quark t with the $\hat{k}$ axis (the 3-momentum direction of the incoming electron e^-) and ϕ is the azimuthal angle.

In absence of earth rotation: We note that the constant antisymmetric $\Theta_{\mu\nu}$ tensor, analogous to the field tensor $F_{\mu\nu}$, has 6 independent components: with 3 electric components (Θ_{0i}) and 3 magnetic components (Θ_{ij}) corresponding to

$$\Theta_{\mu\nu} = \frac{1}{\Lambda^2} c_{\mu\nu} = \frac{1}{\Lambda^2}(c_{0i}, c_{ij}) = (\Theta_{0i}, \Theta_{ij}) = (\vec{\Theta}_E, \vec{\Theta}_B)$$

with $i, j = 1, 2, 3$. Assuming all of them are non vanishing they can be written in the form

$$\Theta_{0i} = \frac{1}{\Lambda^2}c_{0i} = \frac{1}{\Lambda^2}\xi_i, \tag{5.8}$$

$$\Theta_{ij} = \frac{1}{\Lambda^2}c_{ij} = \frac{1}{\Lambda^2}\epsilon_{ijk}\chi^k. \tag{5.9}$$

Setting $\xi_i = \frac{1}{\sqrt{3}}$, $\chi_i = \frac{1}{\sqrt{3}}$ with $i = 1, 2, 3$ and the fact that $\chi_i = -\chi^i$, $\xi_i = -\xi^i$, $\xi_i\xi^j = \frac{1}{3}\delta_i^j$ and $\chi_i\chi^j = \frac{1}{3}\delta_i^j$, we find

$$p_2\Theta p_1 = \frac{s}{2\sqrt{3}\Lambda^2}, \tag{5.10}$$

$$p_4\Theta p_3 = \frac{s}{2\sqrt{3}\Lambda^2}\left[\cos\theta + \sin\theta(\cos\phi + \sin\phi)\right]. \tag{5.11}$$

Considering the effect of earth rotation: The antisymmetric NC tensor $\Theta_{\mu\nu} = (\vec{\Theta}_E, \vec{\Theta}_B)$ has six components out of which 3 are electric components of $\vec{\Theta}_E$ and 3 are magnetic components of $\vec{\Theta}_B$.

Finally, the Θ-weighted dot product in the presence of earth rotation can be be written as

$$p_2\Theta p_1 = -\frac{s}{2}\Theta_{Az}^{lab}, \tag{5.12}$$

$$p_4\Theta p_3 = -\frac{s}{2}\left(s_\theta c_\phi \Theta_{Ax}^{lab} + s_\theta s_\phi \Theta_{Ay}^{lab} + c_\theta\Theta_{Az}^{lab}\right). \tag{5.13}$$

where Θ_{Ax}^{lab}, Θ_{Ay}^{lab} and Θ_{Az}^{lab} (with $A = \vec{E}, \vec{B}$) are defined in appendix 3.6.

5.5.3 Amplitude square of the process $e^+e^- \xrightarrow{\gamma, Z} t\bar{t}$

The direct and interference terms of Eq.5.3 are given by

$$\sum_{spin} |\mathcal{A}_\gamma|^2 = \frac{3 \times 64\pi^2\alpha^2}{9s^2} A_{NC} \times Tr\left[(\not{p}_1 + m_e)\gamma_\nu(\not{p}_2 - m_e)\gamma_\mu\right]$$

$$\times\, Tr\left[(p\!\!\!/_4 - m_t)\left(D_{43}\gamma^\mu - i(p_3\Theta)^\nu m_t\right)(p\!\!\!/_3 + m_t)\left(D_{43}^*\gamma^\mu + i(p_3\Theta)^\mu m_t\right)\right] \tag{5.14}$$

$$\sum_{spin}|\mathcal{A}_Z|^2 = \frac{3 \times 16\pi^2\alpha^2}{(Sin2\theta_W)^4}\frac{A_{NC}}{[(s - m_Z^2)^2 + m_Z^2\Gamma_Z^2]} \times Tr\left[(p\!\!\!/_1 + m_e)\gamma_\nu\Gamma_{A_e}^-(p\!\!\!/_2 - m_e)\gamma_\mu\Gamma_{A_e}^-\right]$$

$$\times\, Tr\left[(p\!\!\!/_4 - m_t)\left(D_{43}\gamma^\nu\Gamma_{A_e}^- - im_t c_A^t\gamma^5(p_3\Theta)^\nu\right)(p\!\!\!/_3 + m_t)\left(D_{43}^*\gamma^\mu\Gamma_{A_e}^- - im_t c_A^t\gamma^5(p_3\Theta)^\mu\right)\right]$$

$$\tag{5.15}$$

$$\sum_{spin}2Re(A_Z A_\gamma^\dagger) = -3 \times 2Re\left\{\frac{32\pi^2\alpha^2}{3s(Sin2\theta_W)^2}\frac{A_{NC}}{[s - m_Z^2 - im_Z\Gamma_Z]} \times Tr\left[(p\!\!\!/_1 + m_e)\gamma_\nu\Gamma_{A_e}^-(p\!\!\!/_2 - m_e)\gamma_\mu\right]\right.$$

$$\left.\times\, Tr\left[(p\!\!\!/_4 - m_t)(D_{43}\gamma^\nu\Gamma_{A_e}^- - im_t c_A^t\gamma^5(p_3\Theta)^\nu)(p\!\!\!/_3 + m_t)(D_{43}^*\gamma^\mu + im_t(p_3\Theta)^\mu)\right]\right\}$$

$$\tag{5.16}$$

where 3 is the color factor and $A_{NC} = \left[1 + \frac{1}{4}(p_2\Theta p_1)^2\right]$, $D_{43} = 1 + \frac{i}{2}p_4\Theta p_3$ and $D_{43}^* = 1 - \frac{i}{2}p_4\Theta p_3$.
We have set the electron mass $m_e = 0$ and $m_t = 173.2$ GeV in our analysis

Chapter 6

Conclusions

"I have not failed. I've just found 10,000 ways that won't work"-Thomas A. Edison

Despite the enormous experimental success, the fact that the SM cannot explain several outstanding issues in both theoretical expectations and experimental observations forced us to believe that the SM can at least offer a very good description for low-energy effective theory. To explain those outstanding issues, one needs to think about physics beyond the SM (BSM), which is dubbed as New Physics.

Among the class of BSM models, supersymmetry, extra dimension, space-time noncommutativity has drawn special attention in the high energy physics community. In the TeV scale gravity theory, the strong gravity makes the spacetime noncommutative i.e. $[\hat{x}_\mu, \hat{x}_\nu] = i\Theta_{\mu\nu}$ and it is the scale of non-commutativity Λ $(\Theta^{-1/2})$ that we probe in this thesis. The NC tensor $\Theta_{\mu\nu}$ which breaks the rotational invariance of the cross section about the beam axis, makes the cross section azimuthal (ϕ) dependent and introduces an anisotropy in the azimuthal distribution which can provide the clinching signal of the spacetime noncommutativity in the TeV energy collider.

Limited number of analysis on searching the spacetime noncommutatvity is available in the literature. Most of the existing collider searches of spacetime noncommutativity were made in the context of electron-positron linear collider(LC), while only few were available in the context of currently running LHC. In addition, in most cases the effect of earth rotation was not considered at all, which needs to be taken into account for any serious phenomenological investigation in the noncommutative phenomenology.

The purpose of this thesis work is to widen our understanding of the magnitude of the noncommutative scale Λ by looking at processes both at LHC and LC with and without considering the effect of earth rotation into the analysis. Also the thesis aims to fill up the gap which is due to the lack of spacetime

NC searchs at LHC.

We have investigated the studied the Drell-Yan process at LHC, Higgstrahlung and top quark pair production process at LC and obtained the bound on Λ with and without considering the effect of earth rotation into the analysis. We have demonstrated how the spacetime noncommutativity can be realized in the TeV energy high energy LHC and LC. The thesis consists of five chapters.

In the first chapter, we have reviewed the standard Model of particle physics (e.g. its gauge structure, particle content, symmetry breaking mechanism) and discuss about its limitation. We set the tune for motivation of doing BSM physics and discuss about a few class of new physics models e.g. supersymmetry, extra dimensional models, spacetime noncommutativity etc.

In the second chapter, we have given a brief introduction of noncommutative(NC) geometry, discuss about Weyl-Moyal, Seiberg-Witten and other approaches of spacetime noncommutativity. We briefly addressed the renormalizability issues in the NC models. Finally, we discussed about the construction of minimal NCSM(mNCSM) (in which the standard model vertices gets modified due to spacetime noncommutativity) and non-minimal NCSM(nmNCSM in which besides the minimal NCSM vertices, new couplings e.g. triple neutral gauge boson couplings etc do also arise). Finally, we have given the survey of the noncommutative phenomenology.

In the third chapter, we have studied Higgstrahlung process $e^+e^- \to Zh$ at the TeV energy future linear colliders in the non-minimal NCSM using the Feynman rule to all orders of the noncommutative parameter $\Theta_{\mu\nu}$ while considering the effect of earth rotation.We have found that the optimal collision energy relation which is slightly differs from ref [257], because we have included the $\sqrt{s} = 3.0$ TeV machine energy as well as mass of the Higgs boson $m_H = 125$ GeV. The relation is $\sqrt{s_0} = 7.31164 + 2.50151\Lambda$. One can arrive the conclusion from the table 3.2 to probe the reliable lower value of the Λ which are $\simeq 500$ GeV and $\simeq 1000$ GeV at $\sqrt{s} = 1.5$ TeV and $\sqrt{s} = 3.0$ TeV and the optimal collision energy is $\sqrt{s_0} = 1258.07$ GeV and $\sqrt{s_0} = 2508.82$ GeV respectively.

The diurnal modulation $(\sigma(t) - \langle\sigma\rangle_T)$ vs t/T_{day} graph is found to oscillatory whose amplitude(at a given energy) decreases with the increase in Λ and finally becomes zero in the limit $\Lambda \to \infty$ (Standard Model result). The time-averaged azimuthal distribution $\langle\frac{d\sigma}{d\phi}\rangle_T$ against ϕ for different Λ at different machine energies is found to have a oscillatory behaviour because of the additional terms $p_3\Theta p_4 \sim \frac{s}{\Lambda^2}\left(cos\theta + sin\theta\left(sin\phi + cos\phi\right)\right)$. Note that the distribution is completely flat in the standard model. Such an oscillatory azimuthal distribution, which is found to be absent in most of the BSM models, can be used to single out spacetime noncommutativity from other class of BSM models.

We then did our analysis considering the effect of earth's rotation into the analysis and investigate its

impact on the total cross-section, azimuthal distribution corresponding to the machine energy varying from 0.5 TeV to 3 TeV and the NC scale $\Lambda \geq 0.5$ TeV.

In the fourth chapter, we have investigated the Drell-Yan $pp \to l^+l^-$ ($l = e, \mu$) process in the nm-NCSM at the LHC. We calculate the Drell-Yan production cross section to the first order in $\Theta_{\mu\nu}$. Besides the quark and gluon mediated SM production channels with modified Feynman rules, one needs to take into account for the gluon fusion process the presence of $g - g - \gamma$ and $g - g - Z$ vertices at the tree level. We find some of the characteristic signatures such as oscillatory azimuthal distributions(which is flat in the SM), an outcome of the momentum-dependent effective couplings (which triggers the azimuthal anisotropy through the breaking of the rotational invariance about the beam axis) and explore the noncommutative scale $\Lambda \geq 0.4$ TeV, corresponding to the machine energy($\sqrt{s}$) varying from 7 TeV to 13 TeV. For $\sqrt{s} = 7$ TeV, as the coupling parameter K_{Zgg} (corresponding to the new vertices Zgg) changes from -0.108 to 0.217, the leading order(LO) cross section σ increases from $637(660)$ pb to $639(734)$ pb corresponding to $\Lambda = 1(0.4)$ TeV.

In chapter five, we investigated the pair production of top quark in the noncommutative(NC) spacetime in LC. Using the $\mathcal{O}(\Theta)$ Feynman rule, we obtained the cross section and the azimuthal distribution of the top quark pair production and investigated their sensitivies on the NC vector $\vec{\Theta}$ in the following three cases- Case I: space-time(ST) noncommutativity with $\Theta_{\mu\nu} = \Theta_{0i}$($E$-like NC vector), Case II: space-space(SS) noncommutativity with $\Theta_{\mu\nu} = \Theta_{ij}$ (B-like NC vector) and Case III: space-time and space-space noncommutativity together (NC) with $\Theta_{\mu\nu} = (\Theta_{0i}, \Theta_{ij})$(the NC vector have electric and magnetic components) and the NC scale Λ. In the case of space-space noncommutativity, the fact that $(\sigma_{SS} - \sigma_{SM}) \leq 0.02\sigma_{SM}$, gives rise the lower bound on the NC scale $\Lambda \geq 0.65$ TeV. The azimuthal distribution $\left\langle \frac{d\sigma(t)}{d\phi} \right\rangle_T$ vs ϕ is found to be oscillatory with peaks and troughs corresponding $\eta = \pi/2$ and $\Lambda = 0.65$ TeV at $E_{com} = 1$ TeV in the case of electric-like(Case I) NC vector, whereas flat in the case of magnetic-like NC vector(i.e. Case II). The diurnal (oscillatory) behaviour of the top-quark production cross section over the period of a complete day + night with peaks and troughs corresponding to $\Lambda = 0.65$ TeV and the machine energy $\sqrt{s} = 1$ TeV can be looked at in the future TeV energy colliders.

In this thesis we have made an extensive phenomenological analysis of Seiberg-Witten class of model in present and future colliders. The large η-dependent NC cross-section, time-averaged NC correction, the relative correction and the azimuthal anisotropy in the cross-section can hopefully be found in LHC and LC as the clinching and unmisleadingly clear signal of spacetime noncommutativity.

Future Scope of the Work:

The present thesis, in which we have studied the Higgstrahlung process, top quark pair production at the linear collider and the Drell-Yan process at the Large Hadron Collider in the nocommutative space-time and find Λ, the scale of noncommutativity- is an effort to fill up the gap arised due to the lack of phenomenological searches of spacetime noncommutativity. The azimuthal anisotropy predicted in the cross section and its distribution arising due to the breaking of rotational invariance around the beam axis by the noncommutative vector can undoubtedly be the clear signal and clinching evidence of spacetime noncommutativity. The future direction of the present thesis work:

1. The work done in the context of LHC and LC can further be extended by making the use of helicity amplitude technique to get a better clear picture of noncommutative spacetime at high energy.

2. The detailed analysis of the pair production of W-boson, di-photon and Higgs pair in the non-commutative spacetime can also throw light on the structure of spacetime at high energy.

3. An $U(1)$-extension of the non-minimal NCSM may be a potential contender of a dark matter model and might possibly have several interesting phenomenological consequences. Work in this direction is in progress.

4. The space-time noncommutativity can act as a new source of CP violation, which can be tested in several B meson decays.

Bibliography

[1] Kerson Huang, Fundamental forces of nature:The Story of Gauge Fields, (2007) World Scientific Publishing Co. Pvt. Ltd.

[2] J. Goldstone, Abdus Salam, Steven Weinberg, Broken Symmetries, Phys. Rev. 127, 965-970 (1962).

[3] G. Rajasekaran, Building up the Standard Gauge Model of High Energy Physics,"Gravitation, Gauge Theories and the Early Universe". 185-236 (1989).

[4] Donohue, Golowich, Holstein, Dynamics of the Standard model, Cambridge University Press (1992).

[5] Peter W. Higgs, Broken Symmetries and the Masses of Gauge Bosons, Phys. Rev. Lett. 13, 508-509 (1964).

[6] G. S. Guralnik, C. R. Hagen, T. W. B. Kibble, Global Conservation Laws and Massless Particles, Phys. Rev. Lett. 13, 585-587 (1964).

[7] F. Englert, R. Brout, Broken Symmetry and the Mass of Gauge Vector Mesons, Phys. Rev. Lett. 13, 321-323 (1964).

[8] S. Glashow, The renormalizability of vector meson interactions, Nucl. Phys. 10, 107 (1959).

[9] A. Salam, J. C. Ward, Weak and electromagnetic interactions, Nuovo Cimento. 11, 568-577 (1959).

[10] S. Weinberg, A Model of Leptons, Phys. Rev. Lett. 19, 1264-1266 (1967).

[11] CMS Collaboration S. Chatrchyan et al., Observation of a new boson at a mass of 125 GeV with the CMS experiment at the LHC, Phys. Lett. B 716, 30 (2012).

[12] C. Patrignani et al., (Particle Data Group), Chin. Phys. C, 40, 100001 (2016).

[13] Thomas Blum, Achim Denig, Ivan Logashenko, Eduardo de Rafael, B. Lee Roberts, Thomas Teubner, Graziano Venanzoni, The Muon $(g − 2)$ Theory Value: Present and Future,(2013), arXiv:1311.2198 [hep-ph]

[14] G. Steigman, Primordial Nucleosynthesis in the Precision Cosmology Era, Annual. Rev. Nucl. Part. Sci. 57, 463-491 (2007).

[15] Robert M Wald, Quantum Field Theory in Curved Spacetime and Black Hole Thermodynamics. (1994), University of Chicago Press.

[16] Degrassi, G, S. Di Vita, J. Elias-Miro, J. R. Espinosa, G. F. Giudice, et al., Higgs mass and vacuum stability in the Standard Model at NNLO, JHEP 08, 098 (2012).

[17] K. G. Chetyrkin, M. F. Zoller, Three-loop β functions for top-Yukawa and the Higgs self-interaction in the Standard Model, JHEP 06, 033 (2012).

[18] S. Alekhin, A. Djouadi, S. Moch, The top quark and Higgs boson masses and the stability of the electroweak vacuum, Phys. Lett. B 716, 214 (2012).

[19] M. J. G. Veltman, The Infrared - Ultraviolet Connection, Acta Phys. Polon. B 12, 437 (1981). Abdelhak Djouadi, The Anatomy of Electro-Weak Symmetry Breaking. I: The Higgs boson in the Standard Model, Phys. Rept. 457, 1-216 (2008).

[20] G. L. Fogli, E. Lisi, A. Marrone, G. Scioscia, Super-Kamiokande atmospheric neutrino data, zenith distributions, and three-flavor oscillations, Phys. Rev. D 59, 033001 (1999).

[21] B. Pontecorvo, Inverse beta processes and nonconservation of lepton charge, Zhurnal Eksperimentalnoi i Teoreticheskoi Fiziki. 34, 247 (1957). reproduced and translated in Soviet Physics JETP. 7, 172 (1958).

[22] Z. Maki, M. Nakagawa, S. Sakata,Remarks on the Unified Model of Elementary Particles, Progress of Theoretical Physics. 28, 870 (1962).

[23] M. C. Gonzalez-Garcia, C. Pena-Garay, A. Yu. Smirnov, Zenith angle distributions at Super-Kamiokande and SNO and the solution of the solar neutrino problem, Phys. Rev. D 63, 113004 (2001).

[24] Boris Kayser, F. Gibrat-Debu, F. Perrier, The Physics of massive neutrinos, World Sci. Lect. Notes Phys. 25, 1-117 (1989). G. Rajasekaran, Phenomenology of Neutrino Oscillations, Pramana 55, 19-32 (2000).

[25] John N. Bahcall, M. H. Pinsonneault, Sarbani Basu, Solar Models: Current Epoch and Time Dependences, Neutrinos, and Helioseismological Properties, The Astrophysical Journal, 555, 990-1012 (2001).

[26] S. P. Mikheyev, A. Y. Smirnov, Resonance Amplification of Oscillations in Matter and Spectroscopy of Solar Neutrinos, Sov. J. Nucl. Phys. 42, 913-917 (1985).

[27] L. Wolfenstein, Neutrino Oscillations in Matter, Phys. Rev. D 17, 2369-2374 (1978).

[28] Q. R. Ahmad et al., SNO Collaboration, Direct Evidence for Neutrino Flavor Transformation from Neutral-Current Interactions in the Sudbury Neutrino Observatory, Phys. Rev. Lett. 89, 011301 (2002).

[29] A. J. Bevan et.al., The Physics of the B Factories, Eur. Phys. J. C 74, 3026 (2014).

[30] M. Huschle et.al., Belle Collaboration, Measurement of the branching ratio of $B \to D^* \tau \overline{\nu}_\tau$ relative to $B \to D^* l^- \overline{\nu}_l$ decays with hadronic tagging at Belle, Phys. Rev. D 92, 072014 (2015).

[31] S. Fajfer, J. K Kmenik and I. Nisandzic, On the $B \to D^* \tau \overline{\nu}_\tau$ Sensitivity to New Physics, Phys. Rev. D 85, 094025 (2012).

[32] Capdevila, Bernat, et al. Patterns of New Physics in $b \to s l^+ l^-$ transitions in the light of recent data. arXiv preprint arXiv:1704.05340 (2017)

[33] Edward W. Kolb, Michael S. Turner, The Early Universe, Front. Phys. 69 (1990). H. W. Babcock, The rotation of the Andromeda Nebula, Lick Observatory Bulletin. 19, 41-51 (1939). V. Rubin, Jr. W. K. Ford, Rotation of the Andromeda Nebula from a Spectroscopic Survey of Emission Regions, The Astrophysical Journal. 159, 379 (1970).

[34] Planck Collaboration (P. A. R. Ade (Cardiff U.) et al.), Planck 2015 results. XIII. Cosmological parameters, Astron. Astrophys. A 13, 594 (2016). Carlo Contaldi, Lecture notes for MSc in Particles and Quantum Fields-Particle Cosmology Course, Feb28 2012. Charles L. Bennett et. al., The Cosmic Rosetta Stone, Physics Today 50, 11,32 (1977).

[35] F. Zwicky, Nebulae as Gravitational lenses, Phys. Rev. 51, 290 (1937). D. Walsh, R. J. Carswell, R. J. Weymann, 0957 + 561 A, B: twin quasistellar objects or gravitational lens?, Nature. 279, 381-384 (1979).

[36] Julius Wess, Jonathan Bagger, Supersymmetry and Supergravity, Princeton Series in Physics (1992).

[37] Theodor Kaluza, Zum Unitatsproblem in der Physik, Sitzungsber. Preuss. Akad. Wiss. Berlin. (Math. Phys. 966-972 (1921)).

[38] O. Klein, Quantentheorie und funfdimensionale Relativitatstheorie, Z. Phys. A. 37, 895-906 (1926). O. Klein, The Atomicity of Electricity as a Quantum Theory Law, Nature. 118, 516 (1926).

[39] N. Arkani-Hamed, S. Dimopoulos and G. R. Dvali, The Hierarchy Problem and New Dimensions at a Millimeter, Phys. Lett. B 429, 263 (1998). N. Arkani-Hamed, S. Dimopoulos and G. R. Dvali, Phenomenology, astrophysics, and cosmology of theories with sub millimeter dimensions and TeV scale quantum gravity, Phys. Rev. D 59, 086004 (1999).

[40] T. Han, J. D. Lykken and R. Zhang, On Kaluza-Klein States from Large Extra Dimensions, Phys. Rev. D 59, 105006 (1999).

[41] L. Randall and R. Sundrum, Large Mass Hierarchy from a Small Extra Dimension, Phys. Rev. Lett. 83, 3370 (1999). L. Randall and R.Sundrum, An Alternative to Compactification, Phys. Rev. Lett. 83, 4690 (1999).

[42] W. D. Goldberger and M. B. Wise, Bulk Fields in the Randall-Sundrum Compactification Scenario, Phys. Rev. D 60, 107505 (1999).

[43] C. Csaki, M. Graesser, L. Randall and J. Terning, Cosmology of brane models with radion stabilization, Phys. Rev. D 62, 045015 (2000).

[44] M. L. Graesser, Extra dimensions and the muon anomalous magnetic moment, Phys. Rev. D 61, 074019 (2000).

[45] S. C. Park and H. S. Song, Muon anomalous magnetic moment and the stabilized RandallSundrum scenario, Phys. Lett. B 506, 99 (2001).

[46] K. Cheung, Phenomenology of the radion in the Randall-Sundrum scenario, Phys. Rev. D 63, 056007 (2001).

[47] M. Chaichian, A. Datta, K. Huitu and Z. Yu, Radion and Higgs mixing at the LHC, Phys. Lett. B 524, 161 (2002).

[48] P. K. Das and U. Mahanta, Phys. Lett. 528, 253 (2002), P. K. Das, Phys. Rev. D 72, 055009 (2005), V. H. Satheeshkumar, P. K. Suresh and P. K. Das, AIP Conf. Proc. 939, 258 (2007), P. K. Das, Selvaganapathy J, C. Sharma, T. K. Jha and V Sunil Kumar, Tsallis statistics and the role of a stabilized radion in the supernovae SN1987A cooling, IJMP A28, 1350152 (2013).

[49] Max Born, Werner Heisenberg, and Pascual Jordan. Zur Quantenmechanik II, Z. Phys. 35, 557-615 (1926).

[50] The Physical Principles of the Quantum Theory Werner Heisenberg, Translated by Carl Eckart and F. C Hoyat, Dover Publications, 1949.

[51] Werner Heisenberg and Wolfgang Pauli Zur Quantendynamik der Wellenfelder, Z. Phys. 56, 1-61 (1929).

[52] Werner Heisenberg and Wolfgang Pauli Zur Quantentheorie der Wellenfelder II, Z. Phys. 59, 168-190 (1929).

[53] J. Robert Oppenheimer Note on the Theory of the Interaction of Field and Matter, Phys. Rev. 35, 461-477 (1930).

[54] Lew Landau and Rudolph Peierls Quantenelektrodynamik im Konfigurationsraum, Z. Phys. 62, 188-200 (1930).

[55] Lew Landau and Rudolph Peierls Erweiterung des Unbestimmtheitsprinzips fur die relativistische Quantentheorie, Z. Phys. 69, 56-69 (1931).

[56] Karl von Meyenn, editor. Wolfgang Pauli, Scientific Correspondence, volume II. Springer Verlag (1985).

[57] H. S. Snyder Quantized spacetime, Phys. Rev. 71, 38 (1947).

[58] Snyder H. S, The electromagnetic field in quantized space-time, Phys. Rev. 72, 68-71 (1947).

[59] C. N. Yang, On quantized spacetime, Phys. Rev. 72, 874 (1947).

[60] Sergio Doplicher, Klaus Fredenhagen, and John E. Roberts Space-time quantization induced by classical gravity, Phys. Lett. B 331, 39-44 (1994).

[61] Doplicher S, Fredenhagen K, Roberts J. E, The quantum structure of spacetime at the Planck scale and quantum fields, Comm. Math. Phys. 172, 187-220 (1995).

[62] Thomas Filk, Divergences in a field theory on quantum space, Phys. Lett. B 376, 53-58 (1996).

[63] Jurco B, Schupp P, Wess J, Noncommutative gauge theory for Poisson manifolds, Nucl. Phys. B 584, 784-794 (2000).

[64] Jurco B, Moller L, Schraml S, Schupp P, Wess J, Construction of non-Abelian gauge theories on noncommutative spaces, Eur. Phys. J. C 21, 383-388 (2001).

[65] Aschieri P, Jurco B, Schupp P, Wess J, Non-commutative GUTs, standard model and C, P , T, Nucl. Phys. B 651, 45-70 (2003).

[66] O. Ogievetsky, W. B. Schmidke, J. Wess, and B. Zumino q-deformed Poincare algebra, Commun. Math. Phys. 150, 495-518 (1992).

[67] Seiberg N, Witten E, String theory and noncommutative geometry, JHEP 09, 032 (1999). Seiberg N, Susskind L, Toumbas N, Strings in Background Electric Field, Space/Time Noncommutativity and A New Noncritical String Theory, JHEP 06, 021 (2000).

[68] Minwalla S, Van Raamsdonk M, Seiberg N, Noncommutative perturbative dynamics, JHEP 02, 020 (2000).

[69] Calmet X, Jurco B, Schupp P, Wess J, Wohlgenannt M, The standard model on non-commutative space-time, Eur. Phys. J. C 23, 363-376 (2002).

[70] Melic B, Passek-Kumericki K, Trampetic J, Schupp P, Wohlgenannt M, The standard model on non-commutative space-time: strong interactions included, Eur. Phys. J. C 42, 499-504 (2005).

[71] Melic B, Passek-Kumericki K, Trampetic J, Schupp P, Wohlgenannt M, The standard model on non-commutative space-time: electroweak currents and Higgs sector, Eur. Phys. J. C 42, 483-497 (2005).

[72] N. Cabibbo, Unitary Symmetry and Leptonic Decays, Phys. Rev Lett. 10, 531-533 (1963).

[73] M. Kobayashi, T. Maskawa, CP-Violation in the Renormalizable Theory of Weak Interaction, Progress of Theoretical Physics. 49, 652-657 (1973).

[74] L. Wolfenstein, Parametrization of the Kobayashi-Maskawa Matrix, Phys. Rev. Lett. 51, 1945 (1983).

[75] Sorin Marculescu, Non-commutative extensions of the standard model, 2005, hep-th/0508018.

[76] M. M. Ettefaghi, Singlet particles as cold dark matter in noncommutative space-time, Phys. Rev. D 79, 065022 (2009).

[77] Pascual Jordan, J. von Neumann, Eugene P. Wigner, On an Algebraic generalization of the quantum mechanical formalism, Annals. Math. 35, 29-64 (1934).

[78] A. Connes, Noncommutative geometry, Academic Press, Inc., San Diego, CA, 1994.

[79] A. Connes, Noncommutative geometry and the standard model with neutrino mixing, JHEP 11, 081 (2006).

[80] A. Chamseddine and A. Connes, Universal formula for noncommutative geometry actions: Unification of gravity and the standard model, Phys.Rev.Lett. 77, 4868 (1996).

[81] A. Chamseddine and A. Connes, Why the standard model, J. Geom. Phys. 58, 38 (2008).

[82] Woronowicz, S. L. Compact matrix pseudogroups, Commun. Math. Phys. 111, 613-665 (1987).

[83] Woronowicz, S. L. Tannaka-Krein duality for compact matrix pseudogroups Twisted SU(N) groups, Invent. Math. 93, 35-76 (1988).

[84] Drinfel'd, V. G Hopf algebras and the quantum Yang-Baxter equation, Sov. Math. Dokl. 32, 256-258 (1985).

[85] A. Connes and M. Marcolli, Noncommutative Geometry, Quantum Fields and Motives, American Mathematical Society, Providence, 2008.

[86] A. Chamseddine and A. Connes,Resilience of the spectral standard model, JHEP 09, 104 (2012).

[87] Barrett J.W., Lorentzian version of the noncommutative geometry of the Standard Model of particle physics, J. Math. Phys. 48, 012303 (2007).

[88] J. W. Barrett and R. A. Martins, Non-commutative geometry and the standard model vacuum, J. Math. Phys. 47, 052305 (2006).

[89] R. A. D. Martins, Finite temperature corrections and embedded strings in noncommutative geometry and the standard model with neutrino mixing, J. Math. Phys. 48, 083509 (2007).

[90] T. Krajewski, Classification of finite spectral triples, J. Geom. Phys. 28, 1 (1998).

[91] Christoph A. Stephan, New Scalar Fields in Noncommutative Geometry, Phys.Rev. D 79, 065013 (2013).

[92] J. H. Jureit, T. Krajewski, T. Schucker and C. A. Stephan, On the noncommutative standard model, Acta. Phys. Polon. B 38, 3181 (2007).

[93] Christoph A. Stephan, Noncommutative Geometry in the LHC-Era,Proceedings of he XLVIIIth Rencontres de Moriond EW session, arXiv:1305.3066.

[94] Christoph A. Stephan, A Dark Sector Extension of the Almost-Commutative Standard Model, Int. J. Mod. Phys. A 29, 1450005 (2014).

[95] I. M. Gelfand and M. A. Naimark. On the embedding of normal linear rings into the ring of operators in Hilbert space, Mat. Sbornik. 12, 197 (1943).

[96] Nicolas Franco, Michal Eckstein, Noncommutative geometry Lorentzian structures and causality, arXiv:1409.1480. Review article in "Mathematical Structures of the Universe", eds. M. Eckstein, M. Heller, S. J. Szybka, CC Press 2014.

[97] R. Jackiw. Physical instances of noncommuting coordinates, Nucl. Phys. Proc. Suppl. 108, 30-36 (2002), Gabrielle Magro, Noncommuting Coordinates in the Landau Problem, arXiv:quant-ph/0302001.

[98] P. Aschieri and L. Castellani, Bicovariant calculus on twisted $ISO(N)$, quantum Poincare group and quantum Minkowski space, Int. J. Mod. Phys. A 11, 4513 (1996).

[99] P. Aschieri et al., Noncommutative Spacetimes: Symmetries in Noncommutative Geometry and Field Theory, Lect. Notes Phys. 774 (Springer, Berlin Heidelberg 2009).

[100] X. Calmet, Space-Time Symmetries of Noncommutative Spaces, Phys.Rev. D 71, 085012 (2005).

[101] M. M. Ettefaghi, M. Haghighat., Lorentz Conserving Noncommutative Standard Model, Phys.Rev. D 75, 125002 (2007).

[102] H. Weyl, Quantum mechanics and group theory, Z. Phys. 46, 1 (1927).

[103] Groenewold H. J., On the principles of elementary quantum mechanics, Physica 12, 405-460 (1946).

[104] Madore J, The commutative limit of a matrix geometry, J. Math. Phys. 32, 332-335 (1991).

[105] Madore J, The fuzzy sphere, Classical Quantum Gravity 9, 69-87 (1992).

[106] Lukierski J, Ruegg H, Nowicki A, Tolstoi V. N, q-deformation of Poincare algebra, Phys. Lett. B 264, 331-338 (1991).

[107] Majid S, Ruegg H, Bicrossproduct structure of κ-Poincare group and non-commutative geometry, Phys.Lett. B 334, 348-354 (1994).

[108] Dimitrijevic M, Jonke L, Moller L, Tsouchnika E, Wess J, Wohlgenannt M, Deformed field theory on κ-spacetime, Eur. Phys. J. C 31, 129-138 (2003).

[109] Reshetikhin N, Takhtadzhyan L, Faddeev L, Quantization of Lie groups and Lie algebras, Leningrad Math. J. 1, 193-225 (1990).

[110] Lorek A, Schmidke W. B, Wess J, $SU_q(2)$ covariant R-matrices for reducible representations, Lett. Math. Phys. 31, 279-288 (1994).

[111] J. Novotny, M. Schnabl, Point-splitting Regularization of Composite Operators and Anomalies, Fortschr. Phys. 48, 4, 253-302 (2000).

[112] Sayipjamal Dulat, Kang Li, Landau Problem in Noncommutative Quantum Mechanics, Chin. Phys. C 32, 92-95 (2008).

[113] M. Hayakawa, Perturbative Analysis on Infrared Aspects of Noncommutative QED on R^4, Phys. Lett. B 478, 394-400 (2000).

[114] I. F. Riad, M. M. Sheikh-Jabbari, Noncommutative QED and Anomalous Dipole Moments, JHEP 08, 045(2000).

[115] M. Chaichian, P. Presnajder, M. M. Sheikh-Jabbari, A. Tureanu, Noncommutative Standard Model:Model Building, Eur. Phys. J. C 29, 413-432 (2003).

[116] M. Chaichian, P. Presnajder, M. M. Sheikh-Jabbari, A. Tureanu, Noncommutative Gauge Field Theories: A No-Go Theorem, Phys. Lett. B 526, 132-136 (2002).

[117] B. Jurco, S. Schraml, P. Schupp and J. Wess, Enveloping algebra valued gauge transformations for non-Abelian gauge groups on non-commutative spaces, Eur. Phys. J. C 17, 521 (2000).

[118] J. Trampetic, M. Wohlgenannt, Remarks on the 2nd order Seiberg-Witten maps, Phys. Rev. D 76, 127703 (2007).

[119] G. Barnich, F. Brandt, M. Grigoriev, Local BRST cohomology and Seiberg-Witten maps in noncommutative Yang-Mills theory, Nucl. Phys. B 677, 503-534 (2004).

[120] V. O. Rivelles, Ambiguities in the Seiberg-Witten Map and Emergent Gravity, Class. Quant. Grav. 31, 025011 (2013).

[121] B. Suo, P. Wang, L. Zhao, Ambiguities of the Seiberg-Witten map in the presence of matter field, Commun. Theor. Phys. 37, 571-574 (2002).

[122] Kayhan Ulker, Baris Yapiskan, Seiberg-Witten Maps to All Orders, Phys. Rev. D 77, 065006 (2008).

[123] I. S. Gradshteyn and I. M. Ryzhik, Table of Integrals, Series and Products, Academic Press, Seventh edition, 2007.

[124] R. Horvat, A. Ilakovac, J. Trampetic, J. You, On UV/IR mixing in noncommutative gauge field theories, JHEP 12, 081 (2011).

[125] Yuji Okawa, Hirosi Ooguri, An Exact Solution to Seiberg-Witten Equation of Noncommutative Gauge Theory, Phys. Rev. D 64, 046009 (2001).

[126] Thomas Mehen, Mark B. Wise, Generalized ∗-Products, Wilson Lines and the Solution of the Seiberg-Witten Equations, JHEP 0012, 008 (2000).

[127] Daniel N. Blaschke, Francois Gieres, Erwin Kronberger, Thomas Reis, Manfred Schweda and Rene I.P. Sedmik, Quantum corrections for translation-invariant renormalizable non-commutative ϕ^4 theory, JHEP 11, 074 (2008).

[128] Daniel N. Blaschke, Arnold Rofner, Manfred Schweda, and Rene I.P. Sedmik, One-Loop Calculations for a Translation Invariant Non-Commutative Gauge Model, Eur. Phys. J. C 62, 433 (2009).

[129] Daniel N Blaschke et. al, Translation-invariant models for non-commutative gauge fields J. Phys. A: Math. Theor. 41, 252002(2008).

[130] Harald Grosse and Raimar Wulkenhaar, Renormalisation of ϕ^4 theory on noncommutative $\mathbb{R}^2$ in the matrix base, JHEP 12, 019 (2003).

[131] H. Grosse et F. Vignes-Tourneret, Minimalist translation-invariant non-commutative scalar field theory, J. Noncommut. Geom. 4, 555-576 (2010).

[132] Gurau, Magnen, Rivasseau and Tanasa, A translation-invariant renormalizable non-commutative scalar model, Commun. Math. Phys. 287, 275-290 (2009).

[133] I. Hinchliffe and N. Kersting, CP violation from noncommutative geometry Phys. Rev D 64, 116007 (2001).

[134] W. Behr, N. G. Deshpande, G. Duplancic,P. Schupp, J. Trampetic and J. Wess, The $Z \to \gamma\gamma$, gg Decays in the Noncommutative Standard Model, Eur.Phys.J. C 29, 441 (2003).

[135] G. Duplancic,P. Schupp, J. Trampetic, Comment on triple gauge boson interactions in the non-commutative electroweak sector, Eur. Phys. J. C 32, 141144 (2003).

[136] S. Godfrey, M. A. Doncheski, Signals for Non-Commutative QED in $e\gamma$ and $\gamma\gamma$ Collisions, Phys. Rev. D 65, 015005 (2001).

[137] M. Haghighat, M. M. Ettefaghi, Parton model in Lorentz invariant noncommutative space, Phys. Rev. D 70, 034017 (2004).

[138] A. Devoto, S. DiChiara, W. W. Repko, Noncommutative QED corrections to $e^+e^- \to \gamma\gamma\gamma$ at linear collider energies, Phys. Rev. D 72, 056006 (2005).

[139] X. Calmet, Quantum Electrodynamics on Noncommutative Spacetime, Eur. Phys. J. C 50, 113 (2007).

[140] T. C. Adorno, M. C. Baldiotti, M. Chaichian, D. M. Gitman and A. Tureanu, Dirac Equation in Noncommutative Space for Hydrogen Atom, Phys. Lett. B 682, 235 (2009).

[141] J.-Z. Zhang, Testing Spatial Noncommutativity via Rydberg Atoms, Phys. Rev. Lett. 93, 043002 (2004).

[142] M. Chaichian, A. Demichev, P. Presnajder, M. M. Sheikh-Jabbari, A. Tureanu, Aharonov-Bohm Effect in Noncommutative Spaces, Phys. Lett. B 527, 149 (2002).

[143] M. Chaichian, A. Demichev, P. Presnajder, M.M. Sheikh-Jabbari, A. Tureanu, Quantum Theories on Noncommutative Spaces with Nontrivial Topology: Aharonov-Bohm and Casimir Effects, Nucl. Phys. B 611, 383 (2001).

[144] H. Falomir, J. Gamboa, M. Loewe, F. Méndez, J. C. Rojas, Testing spatial noncommutativiy via the Aharonov-Bohm effect, Phys. Rev. D 66, 045018 (2002).

[145] K. Li, S. Dulat, The AharonovBohm effect in noncommutative quantum mechanics, Eur. Phys. J. C 46, 825 (2006).

[146] B. Mirza, M. Zarei, Noncommutative quantum mechanics and the Aharonov-Casher effect, Eur. Phys. J. C 32, 583 (2004).

[147] K. Li, J.-H. Wang, The topological AC effect on noncommutative phase space, Eur. Phys. J. C 50, (2007) 1007.

[148] B. Mirza, R. Narimani, M. Zarei, Aharonov-Casher effect for spin one particles in a noncommutative space, Eur. Phys. J. C 48, 641 (2006). S. Dulat, K. Li, The AharonovCasher effect for spin-1 particles in non-commutative quantum mechanics, Eur. Phys. J. C 54, 333 (2008).

[149] B. Harms, O. Micu, Noncommutative Quantum Hall Effect and Aharonov-Bohm Effect, J. Phys. A 40, 10337 (2007).

[150] O. F. Dayi, A. Jellal, Hall effect in noncommutative coordinates, J. Math. Phys. 43, 4592 (2002).(Erratum-ibid. 45, 827 (2004)). A. Kokado, T. Okamura, and T. Saito, Noncommutative Phase Space and the Hall Effect , Prog. Theor. Phys. 110, 975 (2003). S. Dulat, K. Li, Quantum Hall effect in noncommutative quantum mechanics, Eur. Phys. J. C 60, 163 (2009).

[151] B. Chakraborty, S. Gangopadhyay, A. Saha, Seiberg-Witten map and Galilean symmetry violation in a non-commutative planar system , Phys. Rev. D 70, 107707 (2004). F. G. Scholtz, B. Chakraborty, S. Gangopadhyay, A. G. Hazra, Dual families of non-commutative quantum systems, Phys. Rev. D 71, 085005 (2005). F. G. Scholtz, B. Chakraborty, S. Gangopadhyay, J. Govaerts, Interactions and non-commutativity in quantum Hall systems, J. Phys. A 38, 9849 (2005).

[152] O. F. Dayi, M. Elbistan, Spin Hall effect in noncommutative coordinates, Phys. Lett. A 373, 1314 (2009).

[153] S. O. Valenzuela, M. Tinkham, Direct electronic measurement of the spin Hall effect, Nature, 442, 176 (2006).

[154] Kai Ma, Sayipjamal Dulat, Spin Hall effect on a noncommutative space, Phys.Rev. A 84, 012104 (2011).

[155] S. Bilmis, M. Deniz, H. B. Li, J. Li, H. Y. Liao, S. T. Lin, V. Singh, H. T. Wong, I. O. Yildirim, Q. Yue, M. Zeyrek, Constraints on Non-Commutative Physics Scale with Neutrino-Electron Scattering, Phys. Rev. D 85, 073011 (2012).

[156] H.B. Li et al.,TEXONO Collaboration, New Limits on Neutrino Magnetic Moments from the Kuo-Sheng Reactor Neutrino Experiment, Phys. Rev. Lett. 90, 131802 (2003); H.T. Wong et al., TEXONO Collaboration, Search of Neutrino Magnetic Moments with a High-Purity Germanium Detector at the Kuo-Sheng Nuclear Power Station, Phys. Rev. D 75, 012001 (2007).

[157] M. Deniz et al.,TEXONO Collaboration, Measurement of Neutrino-Electron Scattering Cross-Section with a CsI(Tl) Scintillating Crystal Array at the Kuo-Sheng Nuclear Power Reactor, Phys. Rev. D 81, 072001 (2010).

[158] L. B. Auerbach et al.,LSND Collaboration, Measurement of electron-neutrino electron elastic scattering, Phys. Rev. D 63, 112001 (2001).

[159] P. Vilain et al.,CHARM-II Collaboration, Measurement of differential cross-sections for muon-neutrino electron scattering, Phys. Lett. B 302, 351 (1993). P. Vilain et al., CHARM-II Collaboration, Precision measurement of electroweak parameters from the scattering of muon-neutrinos on electrons, Phys. Lett. B 335, 246 (1994).

[160] G. Abbiendi et al.,OPAL Collaboration, Test of non-commutative QED in the process $e^+e^- \to \gamma\gamma$ at LEP, Phys. Lett. B 568, 181 (2003).

[161] M.M. Najafabadi,Noncommutative standard model in the top quark sector, Phys. Rev. D 77, 116011 (2008).

[162] P. Schupp, Josip Trampetic, Julius Wess, Georg Raffelt, The photon-neutrino interaction in non-commutative gauge field theory and astrophysical bounds, Eur. Phys. J. C 36, 405 (2004).

[163] M. Haghighat, Bounds on the parameter of noncommutativity from supernova SN1987A, Phys. Rev. D 79, 025011 (2009).

[164] Namit Mahajan, $t \to bW$ in NonCommutative Standard Model, Phys. Rev. D 68, 095001 (2003).

[165] J. L. Hewett, F. J. Petriello, and T. G. Rizzo, Signals for Non-Commutative Interactions at Linear Colliders, Phys. Rev. D 64, 075012 (2001).

[166] M. Buric, D. Latas, V. Radovanovic, and J. Trampetic, Nonzero $Z \to \gamma\gamma$ decays in the renormalizable gauge sector of the noncommutative standard model, Phys. Rev. D 75, 097701 (2007).

[167] X. G. He and X. Q. Li, Probe noncommutative space-time scale using $\gamma\gamma \to Z$ at ILC Phys. Lett. B 64, 28 (2006).

[168] A. Alboteanu, T. Ohl and R. Ruckl, Probing the noncommutative standard model at hadron colliders, Phys. Rev. D 74, 096004 (2006). A. Alboteanu, T. Ohl and R. Ruckl, The Noncommutative standard model at the ILC, Acta Phys. Polon. B 38, 3647 (2007).

[169] J. A. Conley and J. L. Hewett, Effects of the Noncommutative Standard Model in W W scattering, arXiv:0811.4218 [hep-ph]SLAC-PUB-13471 (2008).

[170] P. Mathews, Compton scattering in noncommutative space-time at the NLC, Phys. Rev. D 63, 075007 (2001).

[171] S. Baek et al., Signatures of noncommutative QED at photon colliders, Phys. Rev. D 64, 056001 (2001).

[172] T. Ohl and J. Reuter, Testing the noncommutative standard model at a future photon collider, Phys. Rev. D 70, 076007 (2004).

[173] M. Haghighat and F. Loran, Helium atom spectrum in noncommutative space, Phys. Rev. D 67, 096003 (2003).

[174] M. Chaichian, M.M. Sheikh-Jabbari and A. Tureanu, Hydrogen atom spectrum and the Lamb shift in noncommutative QED, Phys. Rev. Lett. 86, 2716 (2001).

[175] E. O. Iltan, Noncommutative QED and anomalous dipole moments, JHEP 05, 065 (2003).

[176] I. Mocioiu, M. Pospelov and R. Roiban, Limits on the noncommutativity scale, Proceedings of the Second Meeting Bloomington, USA, 15-18 August 2001 arXiv:hep-ph/0110011 (2001).

[177] H. Grosse and Y. Liao, Anomalous C-violating Three Photon Decay of the Neutral Pion in Noncommutative Quantum Electrodynamics, Phys. Lett. B 520, 63 (2001).

[178] H.N. Brown et al.,[Muon g-2 Collaboration], Noncommutative QED and muon anomalous magnetic moment, Phys. Rev. Lett. 86, 2227 (2001). X.J. Wang and M.L. Yan, Precise measurement of the positive muon anomalous magnetic moment, JHEP 03, 047 (2002). N. Kersting, Muon g-2 from noncommutative geometry, Phys. Lett. B 527, 115 (2002).

[179] R. Horvat and J. Trampetic, Constraining spacetime noncommutativity with primordial nucleosynthesis, Phys. Rev. D 79, 087701 (2009).

[180] R. Horvat, D. Kekez and J. Trampetic, Spacetime noncommutativity and ultra-high energy cosmic ray experiments, Phys. Rev. D 83, 065013 (2011).

[181] J. Hewett, F. J. Petriello and T. G. Rizzo, Signals for Noncommutative QED at High Energy e^+e^- colliders, eConf C010630, E3064 (2001).

[182] J. Hewett *et al.* , Signals for Non-Commutative Interactions at Linear Colliders, Phys. Rev. D 64, 075012 (2001), Noncommutativity and unitarity violation in gauge boson scattering, Phys. Rev. D 66, 036001 (2002).

[183] P. Mathews, Compton scattering in noncommutative space-time at the Next Linear Collider, Phys. Rev. D 63, 075007 (2001).

[184] T. G. Rizzo Signals for Noncommutative QED at Future e^+e^- Colliders, Int. J. Mod. Phys. A18, 2797 (2003). M. Hayakawa, Perturbative analysis on infrared and ultraviolet aspects of noncommutative QED on R^4, hep-th/9912167; T. B. Nguyen, The one-loop QED in Noncommutative space, hep-th/0301084;

[185] I. Hinchliffe, N. Kersting and Y. L. Ma, Review of the Phenomenology of Noncommutative Geometry, IJMP, A 19, 179 (2004).

[186] Ana Alboteanu, Thorsten Ohl and Reinhold Rckl, Probing the Noncommutative Standard Model at Hadron Colliders, Phys. Rev. D 74, 096004 (2006).

[187] T. Ohl and C. Speckner, The Noncommutative Standard Model and Polarization in Charged Gauge Boson Production at the LHC, Phys. Rev. D 82, 116011 (2010).

[188] S. Y. Ayazi, S. Esmaeili and M. M. Najafabadu, Single top quark production in t-channel at the LHC in Noncommutative Space-Time Phys. Lett. B 712, 93 (2012).

[189] A. P. Balachandran, T. R. Govindarajan, G. Mangano, A. Pinzul, B. A. Qureshi and S. Vaidya, Statistics and UV-IR mixing with twisted Poincare invariance Phys. Rev. D 75, 045009 (2007).

[190] A. P. Balachandran, Anosh Joseph, Pramod Padmanabhan, Non-Pauli Transitions From Space-time Noncommutativity Phys. Rev. Lett 105, 051601 (2010).

[191] A. Matusis, L. Susskind, and N. Toumbas, The IR/UV connection in the non-commutative gauge theories, JHEP 12, 002 (2000).

[192] A. Bichl, J. Grimstrup, H. Grosse, L. Popp, M. Schweda, and R. Wulkenhaar, Renormalization of the noncommutative photon self-energy to all orders via Seiberg-Witten map,JHEP 13, 0106 (2001).

[193] C. P. Martin, The gauge anomaly and the Seiberg-Witten map,Nucl. Phys. B652, 72 (2003).

[194] Alvarez-Gaume L. and Vazquez-Mozo M. A., General properties of noncommutative field theories, Nucl. Phys. B 668 (2003) 293,Nucl. Phys. B668, 293 (2003).

[195] F. Brandt, C. P. Martin and F. Ruiz Ruiz, Anomaly freedom in Seiberg- Witten noncommutative gauge theories, JHEP 07, 068 (2003).

[196] M. Buric, V. Radovanovic, and J. Trampetic, The one-loop renormalization of the gauge sector in the noncommutative standard model, JHEP 0703, 030 (2007).

[197] Schupp P, You J, UV/IR mixing in noncommutative QED defined bySeiberg-Witten map,JHEP 08, 107 (2008).

[198] Horvat R, Trampetic J, Constraining noncommutative field theories with holography, JHEP 1101, 112 (2011).

[199] R. Horvat, A. Ilakovac, J. Trampetic and J. You, On UV/IR mixing in noncommutative gauge field theories, JHEP 12, 081 (2011).

[200] R. Horvat, A. Ilakovac, P. Schupp, J. Trampetic and J. You, Neutrino propagation in noncommutative spacetimes, JHEP 1204, 108 (2012).

[201] R. Horvat, A. Ilakovac, J. Trampetic and J. You, Self-energies on deformed spacetimes, JHEP 1311, 071 (2013).

[202] J. Trampetic and J. You, Two-Point Functions on Deformed Spacetime, SIGMA 10, 054 (2014).

[203] B. Jarco, L. Moller, S. Schraml, P. Schupp and J. Wess, Construction of non-Abelian gauge theories on noncommutative space Eur. Phys. J, 383 (2001).

[204] T. Mehen and M. B. Wise, Generalized *-products, Wilson lines and the solution of the Seiberg-Witten equations, JHEP 12, 008 (2000).

[205] X. Calmet, B. Jurco, P. Schupp, J. Wess and M. Wohlgenannt, The standard model on noncommutative spacetime. Eur. Phys. J. C 23, 363 (2002).

[206] X. Calmet and M. Wohlgenannt Effective field theories on noncommutative space-time. Phys. Rev. D 68, 025016 (2003).

[207] Abhishodh, P, A, Mitra and Prasanta K. Das, $e^+e^- \to \mu^+\mu^-$ scattering in the Noncommutative standard model, Phys. Rev. D 82, 05020 (2010).

[208] B. Melić, K. P. Kumericki, J. Trampetic, P. Schupp and M. Wohlgenannt The standard model on non-commutative space-time: Electroweak currents and Higgs sector, Eur. Phys. J. C 42, 483 (2005).

[209] B. Melić *et al.* , The standard model on non-commutative space-time: Strong interaction included Eur. Phys. J. C 42, 499 (2005).

[210] W. Behr, N. G. Deshpande, G. Duplancic, P. Schupp, J. Trampetic and J. Wess, The $Z \to \gamma\gamma, gg$ decays in the noncommutative standard model. Eur. Phys. J. C 29, 441 (2003).

[211] P. Aschieri, B. Jurco, P. Schupp and J. Wess Noncommutative GUTs, standard model and C,P,T. Nucl. Phys. B651, 45 (2003).

[212] G. Duplancic, P. Schupp and J. Trampetic, Comment on triple gauge boson interactions in the noncommutative electroweak sector. Eur. Phys. J. C 32, 141 (2003).

[213] M. M. Ettefaghi, M. Haghighat, Lorentz conserving noncommutative standard model, Phys. Rev. D 75, 125002 (2007).

[214] X. Calmet, What are the bounds on space-time non-commutativity?,Eur. Phys. J. C 41, 269 (2005).

[215] X. Calmet and M. Selvaggi,Quantum mechanics on noncommutative spacetime, Phys. Rev. D 74, 037901 (2006).

[216] Horvat R., Ilakovac A., Kekez D., Trampetic J., You J., Forbidden andInvisible Z Boson Decays in Covariant theta-exact Noncommutative Standard Model, J. Phys. G: Nucl. Part. Phys. 41, 055007 (2014).

[217] M. Haghighat *et al.* ,Location and direction dependent effects in collider physics from noncom-mutativity, Phys. Rev. D 82, 016007 (2010).

[218] P. K. Das, N. G. Deshpande and G. Rajasekaran, Polarized Möller and Bhabha scattering in the noncommutative SM Phys. Rev. D 77, 035010 (2008).

[219] S. K. Garg, T. Shrecharan, P. K. Das, N. G. Deshpande and G. Rajasekaran,TeV Scale Implica-tions of Non Commutative Space time in Laboratory Frame with Polarized Beams, JHEP 1107, 24 (2011).

[220] Prasanta K. Das and Abhishodh, P, 126 GeV Higgs boson pair production at the linear collider in the noncommutative space-time, Int. J. Mod. Phys. A27, 1250141 (2012).

[221] Selvaganapathy. J, Prasanta Kr. Das and Partha Konar, Search for associated production of Higgs with Z boson in the noncommutative Standard Model at linear colliders, Int. J. Mod. Phys. A 30, 155015 (2015).

[222] B. Melic *et al.* , Quarkonia decays into two photons induced by the space-time non-commutativity. Phys. Rev. D 72, 054004 (2005).

[223] C. Tamarit and J. Trampetic, Noncommutative fermions and quarkonia decays, Phys. Rev. D 79, 025020 (2009)

[224] B. Melic, K. Passek-Kumericki and J. Trampetic, $K \rightarrow \pi\gamma$ decay and space-time noncommuta-tivity., Phys. Rev. D 72, 057502 (2005)

134

[225] E. O. Iltan, The inclusive $b \rightarrow s\gamma$ decay in the noncommutative standard model, New. J. Phys. 4, 54 (2002).

[226] E. O. Iltan, The form factors existing in the $b \rightarrow sg^*$ decay and possible CP violating effects in the noncommutative standard model, JHEP 11, 029 (2002)

[227] Akofor E, Balachandran A. P, Jo S. G, Joseph A, Quantum fields on the GroenwoldMoyal plane: C, P , T and CP T , JHEP 08, 045 (2007). Namit Mahajan, PCT Theorem in Field Theory on Noncommutative Space, Phys. Lett. B 569, 85-89 (2003).

[228] H. O. Back *et al.* [Borexino Collaboration], "New experimental limits on violations of the Pauli exclusion principle obtained with the Borexino Counting Test Facility," Eur. Phys. J. C 37, 421 (2004).

[229] Y. Suzuki *et al.* [Kamiokande Collaboration], "Study of invisible nucleon decay, N $\rightarrow$ neutrino neutrino anti-neutrino, and a forbidden nuclear transition in the Kamiokande detector," Phys. Lett. B 311, 357 (1993).

[230] A. S. Barabash *et al.*, "Search for anomalous carbon atoms evidence of violation of the Pauli principle during the period of nucleosynthesis," JETP Lett. 68 (1998) 112

[231] R. Arnold *et al.*, "Testing the Pauli exclusion principle with the NEMO-2 detector," Eur. Phys. J. A 6, 361 (1999).

[232] E. Ramberg and G. A. Snow, "A new experimental limit on small violation of the Pauli principle," Phys. Lett. B 238, 438 (1990).

[233] S. Bartalucci *et al.*, "New experimental limit on the Pauli exclusion principle violation by electrons," Phys. Lett. B 641, 18 (2006).

[234] Joseph A, Particle phenomenology on noncommutative spacetime, Phys. Rev. D 79, 096004 (2009).

[235] Gibbons L.K. et al., CP and CP T symmetry tests from the two-pion decays of the neutral kaon with the Fermilab E731 detector, Phys. Rev. D 55, 66256715 (1997).

[236] Angelopoulos A. et al. [CPLEAR collaboration], A determination of the CPT violation parameter Re(δ) from the semileptonic decay of strangeness tagged neutral kaons, Phys. Lett. B 444, 52-60 (1998).

[237] Lai A. et al. [NA48 collaboration], Search for CP violation in $K^0 \rightarrow 3\pi^0$ decays, Phys. Lett. B 610, 165-176 (2005),

[238] Bennett G.W. et al. [Muon (g-2) collaboration], Search for Lorentz and CP T violation effects in muon spin precession, Phys. Rev. Lett. 100, 091602 (2008).

[239] Bailey J. et al. [CERNMainzDaresbury collaboration], Final report on the CERN muon storage ring including the anomalous magnetic moment and the electric dipole moment of the muon, and a direct test of relativistic time dilation, Nuclear Phys. B 150, 1-75 (1979).

[240] Carey R.M. et al., New measurement of the anomalous magnetic moment of the positive muon, Phys. Rev. Lett. 82, 1632-1635 (1999).

[241] Brown H.N. et al. [Muon (g-2) collaboration], Precise measurement of the positive muon anomalous magnetic moment, Phys. Rev. Lett. 86, 2227-2231 (2001).

[242] S. Tizchang, S. Batebi, M. Haghighat, R. Mohammadi, Using an intense laser beam in interaction with muon/electron beam to probe the Noncommutative QED, JHEP, 02, 003 (2017).

[243] M. Zarei, E. Bavarsad, M. Haghighat, R. Mohammadi, I. Motie, Z. Rezaei, Generation of circular polarization of the CMB, Phys. Rev. D 81, 084035 (2010).

[244] http://www.xfel.eu.

[245] C. F. Vulcan, Vulcan glass laser (2010), http://www.clf.rl.ac.uk/Facilities/vulcan/index.htm

[246] Petawatt laser beam, http://laserstars.org/biglasers/pulsed/short/petawatt.html.

[247] The Eli project, [http://www.extreme-light-infraestructure.eu/] and [http://www.eli-beams.eu/].

[248] D. L. Burke et al., Positron Production in Multiphoton Light-by-Light Scattering, Phys. Rev. Lett. 79, 1626 (1997).

[249] P. Schupp, J. Trampetic, J. Wess and G. Raffelt The Photon neutrino interaction in noncommutative gauge field theory and astrophysical bounds. Eur. Phys. J. C 36, 405 (2004).

[250] R. Horvat and J. Trampetic, Constraining spacetime noncommutativity with primordial nucleosynthesis. Phys. Rev. D 79, 087701 (2009).

[251] R. Horvat, D. Kekez and J. Trampetic, Spacetime noncommutativity and ultra-high energy cosmic ray experiments. Phys. Rev. D 83, 065013 (2011).

[252] Arnulf Quadt, Higgs Searches at LEP, arXiv: hep-ex/0207050.

[253] P Teixeira-Dias On behalf of the LEP Higgs working group, Higgs boson searches at LEP , J. Phys: Conf Series, 110, 042030 (2008).

[254] Julien Baglio and Abdelhak Djouadi, Predictions for Higgs production at the Tevatron and the associated uncertainties, JHEP 10, 064 (2010).

[255] Jun. ichi. Kamoshita,Probing Noncommutative Space-Time in the Laboratory Frame, Eur. Phys. J. C 52, 451 (2007).

[256] Prasanta K. Das *et al.* , Neutral Higgs boson pair production at the LC in the Noncommutative Standard Model, Phys. Rev. D 83, 056002 (2011).

[257] W. Wang, F. Tian and Z. M. Sheng, Higgsstrahlung and pair production in e^+e^- collision in the noncommutative standard model, Phys. Rev. D 84, 045012 (2011).

[258] Zheng-Mao Sheng, Yongming Fu and Yu Hai-Bo, Noncommutative QED threshold energy versus Optimum collision energy, Chin. Phys. Lett 22, 561 (2005).

[259] Yongming Fu and Zheng-Mao Sheng, Noncommutative QED corrections to process $e^+e^- \to \mu^+\mu^+\gamma$ at linear collider energies. Phys. Rev. D 75, 065025 (2007)

[260] Yao-Bei Liu et. al., The Higgs-strahlung and double Higgs-strahlung production in the left-right twin Higgs model at the ILC, Eur.Phys. Lett. 81, 31001 (2008), Jinzhong Han et. al., Higgs boson production and decay at e^+e^- colliders as a probe of the Left-Right twin Higgs model, Nucl. Phys. B 896, 200 (2015).

[261] Junjie Cao et. al., Higgs-strahlung production process $e^+e^- \to ZH$ at the future Higgs factory in the Minimal Dilaton Model, JHEP 08, 138 (2014).

[262] Zhaoxia Heng and Haijing Zhou, Higgs-strahlung production process $e^+e^- \to ZH$ at the future Higgs factory in the SM extension with color-octet scalars Chin. J. Phys 54, 308 (2016).

[263] CMS Collaboration, Measurement of the Drell-Yan Cross Section in pp Collisions at $\sqrt{s} = 7$ TeV, JHEP 10, 007 (2011) .

[264] Selvaganapathy. J, P. K. Das and P. Konar, Drell-Yan as an avenue to test noncommutative standard model at large hadron collider Phys. Rev. D 93, 116003 (2016).

[265] Prakash Mathews, Vajravelu Ravindran and Krishnamoorthy Sridhar, NLO-QCD corrections to dilepton production in the Randall-Sundrum model, JHEP 10, 031 (2005).

[266] Prakash Mathews and V. Ravindran, Angular distribution of Drell-Yan process at hadron colliders to NLO-QCD in models of TeV scale gravity, Nucl. Phys. B 753, 1 (2006).

[267] Taushif Ahmed et. al., NNLO QCD corrections to the DrellYan cross section in models of TeV-scale gravity, Eur. Phys. J. C 77, 22 (2017).

[268] R. Frederix et. al., Drell-Yan, ZZ,W^+W^- production in SM and ADD model to NLO+PS accuracy at the LHC, Eur. Phys. J. C 74, 2745 (2014).

[269] Pulak Banerjee et. al., NNLO QCD corrections to production of a spin-2 particle with non-universal couplings in the DY process, arXiv:1710.04184.

[270] J. Fiaschi et. al., Constraining PDFs from neutral current Drell-Yan measurements and effects of resummation in slepton pair production, arXiv: 1805.00842.

[271] Taushif Ahmed et.al., Drell-Yan Production at Threshold to Third Order in QCD, Phys. Rev. Lett. 113, 112002 (2014).

[272] Taushif Ahmed et.al., Rapidity Distributions in Drell-Yan and Higgs Productions at Threshold to Third Order in QCD, Phys. Rev. Lett. 113, 212003 (2014).

[273] Ravi. S. Manohar, Selvaganapathy J and P. K. Das, Probing spacetime noncommutativity in the top quark pair production at e+e- collider, IJMP A 29, 1450156 (2014).

[274] E. Boos, M. Dubinin, M. Sachwitz and H. J. Schreiber, Probe of the Wtb coupling in $t\bar{t}$ pair production at Linear Colliders, Eur. Phys. J. C 16, 269 (2000)

"Even if fate or God doesn't aid, perseverance will pay the wages for one's efforts." - Thirukkural

Curriculum Vitae

Personal Information

Name	Selvaganapathy J
Date of Birth	5th June,1985
Nationality	Indian
Marital Status	Single

Education

Ph.D	Since 2012	BITS PILANI, K K Birla Goa Campus.
M.Sc	$2008 - 2010$	Department of Theoretical Physics, University of Madras, Chennai, Tamilnadu.
B.Sc	$2003 - 2006$	A.S.S Govt Arts College, Tiruttani University of Madras, Tamilnadu.
H.S.C	$2000 - 2002$	Tamilnadu State Board D.R.B.C.C.C Hindu Hr. Sec School, Tiruvallur, Tamilnadu.
S.S.L.C	$1999 - 2000$	Tamilnadu State Board Govt High School, Kakkalur,Tiruvallur, Tamilnadu

List of Publications

1. *Spacetime noncommutativity and $e^+e^- \xrightarrow{\gamma,Z} t\bar{t}$ process at the TeV energy collider.*
   Selvaganapathy J and Prasanta Kr. Das , Submitted to J. Phys. Commun.

2. *q-deformed statistics and the role of a light dark matter fermion in the supernovae SN1987A cooling.*
   Atanu Guha, **Selvaganapathy J** and Prasanta Kr. Das, Phys. Rev. D 95,015001(2017).

3. *Drell-Yan as an avenue to test noncommutative standard model at large hadron collider.*
   Selvaganapathy J, Prasanta Kr. Das and Partha Konar, Phys.Rev.D93:116003(2016).

4. *Search for associated production of Higgs boson with Z boson in the NCSM at linear colliders.*
   Selvaganapathy J, Prasanta Kr. Das and Partha Konar, IJMP A30,1550159(2015).

5. *Probing spacetime noncommutativity in the top quark pair production at e^+e^- collider.*
   Ravi S Manohar, **Selvaganapathy J** and Prasanta Kumar Das, IJMP A29, 1450156 (2014).

6. *Tsallis statistics and role of a stabilized radion in supernovae SN1987A Cooling.*

   Prasanta Kumar Das, **Selvaganapathy J**, C.Sharma, T.K.Jha and V.SunilKumar,IJMP A28,1350152 (2013).

List of Schools/Workshops/Conferences attended

1. WHEPP XV (Workshop on High Energy Physics Phenomenology XV - 2017) held at IISER Bhopal, during December 14 - 23, 2017

2. "CANDLES OF DARKNESS" discussion meeting on "Dark matter and search for physics beyond the Standard Model" held at ICTS-TIFR, Bangalore: 5-9 June, 2017.

3. XXII DAE-BRNS High Energy Physics Symposium, held at the University of Delhi (DU): Dec 12- Dec 16, 2016.

4. 9th International Workshop on the CKM Unitarity Triangle (CKM 2016) to be held at the Tata Institute of Fundamental Research (TIFR), Mumbai, India: Nov 28 Dec 3, 2016.

5. Indo-US bilateral workshop on "Understanding the Origin of the Invisible Sector: From Neutrinos to Dark Matter and Dark Energy held at the University of Hyderabad : November 16-18, 2016.

6. SERC Main School in Theoretical High Energy Physics in Bits-Pilani, K K Birla Goa campus: Dec 20, 2014 to Jan 8, 2015.

7. XXI DAE-BRNS HEP Symposium in IIT Guwahati: 8-12 Dec 2014.

8. Sangam @ HRI 2014 Workshop in HRI Allahabad: 24-29 March 2014.

9. Higgstop 2013 Workshop in Bits-Pilani, K K Birla Goa campus : 25-27 Feb, 2013.

<div align="center">**Curriculum Vitae**</div>

Personal Information

Name	Prasanta Kumar Das
Affiliation	BITS Pilani University, Goa campus
Designation	Associate Professor
Nationality	Indian
Phone & Email	0832-2580-448, pdas@goa.bits-pilani.ac.in
Personal webpage	http://universe.bits-pilani.ac.in/goa/pdas/profile

Education

Post Doc	$2005-2007$	Institute of Mathematical Science, Chennai.
Post Doc	$2004-2005$	CYCU, Chung-Li, Taiwan, ROC.
Post Doc	$2002-2004$	Harish-Chandra Research Institute, Allahabad.
Ph.D	$1996-2002$	Indian Institute of Technology, Kanpur.
M.Sc	$1993-1995$	Science College, University of Calcutta.
B.Sc	$1990-1995$	R.B.C College, University of Calcutta.

Research Interests

Dr. Prasanta Kumar Das works works in the area of Astrophysics and High Energy Physics Phenomenology which works in the interface of particle physics experiments with the theoretical physics and model building. His primary interest is in looking for the signatures of beyond the standard model physics (dubbed as New Physics) at high energy colliders and in astrophysics. He is interested in models of noncommutative geometry, extra dimension, supersymmetry among the class of BSM models.

List of Publications

1. *q-deformed statistics and the role of a light dark matter fermion in the supernovae SN1987A cooling"*, Atanu Guha, Selvaganapathy J and **Prasanta Kumar Das**, Phys. Rev. D 95,015001(2017).

2. *Drell-Yan as an avenue to test noncommutative standard model at large hadron collider*, Selvaganapathy J, **Prasanta Kumar Das** and Partha Konar, Phys.Rev.D93:116003(2016).

3. *Search for associated production of Higgs boson with Z boson in the NCSM at linear colliders*, Selvaganapathy J, **Prasanta Kumar Das** and Partha Konar, IJMP A30,1550159(2015).

4. *Probing spacetime noncommutativity in the top quark pair production at e^+e^- collider*, Ravi S Manohar, Selvaganapathy J and **Prasanta Kumar Das**, IJMP A29, 1450156 (2014).

5. *Tsallis statistics and role of a stabilized radion in supernovae SN1987A Cooling*, **Prasanta Kumar Das**, Selvaganapathy J, C.Sharma, T.K.Jha and V.SunilKumar,IJMP A28,1350152 (2013).

6. *126 GeV Higgs boson pair production at the Linear Collider in the noncommutative spacetime*, **Prasanta Kumar Das**(BITS-Pilani, Goa), Abhishodh Prakash (SUNY, Stonybrook, USA), IJMP A28,135004 (2013).

<div align="center">**Curriculum Vitae**</div>

Personal Information

Name	Partha Konar
Affiliation	Physical Research Laboratory, Ahmedabad
Designation	Associate Professor
Nationality	Indian
Phone & Email	079-2631-4479 , konar@prl.res.in
Personal webpage	http://www.prl.res.in/~konar

Education

Post Doc	$2007 - 2010$	University of Florida, USA.
Post Doc	$2005 - 2007$	University of Karlsruhe, Germany.
Post Doc	$2004 - 2005$	TIFR, Mumbai.
Ph.D	$1998 - 2004$	Harish-Chandra Research Institute, Allahabad.
M.Sc & B. Sc		Visva-Bharati University.

Research Insterests Dr. Partha Konar's research interests are broadly in the area of High Energy Physics (HEP) phenomenology, which works in the interface of particle physics experiments with the theoretical physics and model building. Privileged being in an era of successful and active stage of Large Hadron Collider (LHC), almost all his analysis are done considering the detectors at the LHC, covering physics beyond the standard model and their collider signatures; in particular, electroweak symmetry breaking, class of supersymmetry and theories with extra-dimensions.

List of Publications

1. *Drell-Yan as an avenue to test noncommutative standard model at large hadron collider*, Selvaganapathy J, Prasanta Kumar Das and **Partha Konar**, Phys.Rev. D93:116003(2016).

2. *Heavy neutrino @NLO at the LHC and beyond*, A. Das, **Partha Konar** and S. Majhi, JHEP 1606, 019 (2016).

3. *Compressed SUSY with 125 GeV Higgs*, J. Dutta,**Partha Konar**, S. Mondal, B. Mukhopadhyaya and S. K. Rai, JHEP 1601, 051 (2016).

4. *Reconstruct semi-invisible tau from Higgs*, **Partha Konar** and A. K. Swain, Phys.Lett. B757, 211 (2016).

5. *Mass reconstruction with M2 at LHC*, **Partha Konar** *et al.* , Phys.Rev. D93, 015021(2016).

6. *Search for associated production of Higgs boson with Z boson in the NCSM at linear colliders*, Selvaganapathy J, Prasanta Kumar Das and **Partha Konar**, IJMP A30,1550159(2015).